2010, VOLUME 4

PROGRESS IN PHYSICS

"All scientists shall have the right to present their scientific research results, in whole or in part, at relevant scientific conferences, and to publish the same in printed scientific journals, electronic archives, and any other media." — Declaration of Academic Freedom, Article 8

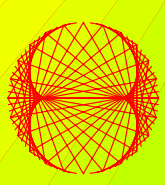

ISSN 1555-5534

The Journal on Advanced Studies in Theoretical and Experimental Physics, including Related Themes from Mathematics

PROGRESS IN PHYSICS

A quarterly issue scientific journal, registered with the Library of Congress (DC, USA). This journal is peer reviewed and included in the abstracting and indexing coverage of: Mathematical Reviews and MathSciNet (AMS, USA), DOAJ of Lund University (Sweden), Zentralblatt MATH (Germany), Scientific Commons of the University of St. Gallen (Switzerland), Open-J-Gate (India), Referativnyi Zhurnal VINITI (Russia), etc.

To order printed issues of this journal, contact the Editors. Electronic version of this journal can be downloaded free of charge:
http://www.ptep-online.com

This journal is powered by LaTeX

A variety of books can be downloaded free from the Digital Library of Science:
http://www.gallup.unm.edu/~smarandache

ISSN: 1555-5534 (print)
ISSN: 1555-5615 (online)

Standard Address Number: 297-5092
Printed in the United States of America

OCTOBER 2010 **VOLUME 4**

CONTENTS

Information for Authors and Subscribers

Progress in Physics has been created for publications on advanced studies in theoretical and experimental physics, including related themes from mathematics and astronomy. All submitted papers should be professional, in good English, containing a brief review of a problem and obtained results.

All submissions should be designed in LaTeX format using *Progress in Physics* template. This template can be downloaded from *Progress in Physics* home page http://www.ptep-online.com. Abstract and the necessary information about author(s) should be included into the papers. To submit a paper, mail the file(s) to the Editor-in-Chief.

All submitted papers should be as brief as possible. We accept brief papers, no larger than 8 typeset journal pages. Short articles are preferable. Large papers can be considered in exceptional cases to the section *Special Reports* intended for such publications in the journal. Letters related to the publications in the journal or to the events among the science community can be applied to the section *Letters to Progress in Physics*.

All that has been accepted for the online issue of *Progress in Physics* is printed in the paper version of the journal. To order printed issues, contact the Editors.

This journal is non-commercial, academic edition. It is printed from private donations. (Look for the current author fee in the online version of the journal.)

Formation of Singlet Fermion Pairs in the Dilute Gas of Boson-Fermion Mixture

Vahan Minasyan and Valentin Samoilov
Scientific Center of Applied Research, JINR, Dubna, 141980, Russia
E-mails: mvahan@scar.jinr.ru; scar@off-serv.jinr.ru

We argue the formation of a free neutron spinless pairs in a liquid helium -dilute neutron gas mixture. We show that the term, of the interaction between the excitations of the Bose gas and the density modes of the neutron, meditate an attractive interaction via the neutron modes, which in turn leads to a bound state on a spinless neutron pair. Due to presented theoretical approach, we prove that the electron pairs in superconductivity could be discovered by Frölich earlier then it was made by the Cooper.

1 Introduction

In 1938, the connection between the ideal Bose gas and superfluidity in helium was first made by London [1]. The ideal Bose gas undergoes a phase transition at sufficiently low temperatures to a condition in which the zero-momentum quantum state is occupied by a finite fraction of the atoms. This momentum-condensed phase was postulated by London to represent the superfluid component of liquid ^{4}He. With this hypothesis, the beginnings of a two- fluid hydrodynamic model of superfluids was developed by Landau [2] where he predicted the notation of a collective excitations so- called phonons and rotons.

The microscopic theory most widely- adopted was first described by Bogoliubov [3], who considered a model of a non-ideal Bose-gas at the absolute zero of temperature. In 1974, Bishop [4] examined the one-particle excitation spectrum at the condensation temperature T_c.

The dispersion curve of superfluid helium excitations has been measured accurately as a function of momentum [5]. At the lambda transition, these experiments show a sharp peak inelastic whose neutron scattering intensity is defined by the energy of the single particle excitations, and there is appearing a broad component in the inelastic neutron scattering intensity, at higher momenta. To explain the appearance of a broad component in the inelastic neutron scattering intensity, the authors of papers [6–7] proposed the presence of collective modes in superfluid liquid ^{4}He, represented a density excitations. Thus the collective modes are represent as density quasiparticles [8]. Such density excitations and density quasiparticles appear because of the remaining density operator term that describes atoms above the condensate, a term which was neglected by Bogoliubov [3].

Previously, the authors of ref [9] discovered that, at the lambda transition, there was scattering between atoms of the superfluid liquid helium, which is confirmed by the calculation of the dependence of the critical temperature on the interaction parameter, here the scattering length. On other hand, as we have noted, there are two types of excitation in superfluid helium at lambda transition point [5]. This means it is necessary to revise the conditions that determine the Bose-Einstein condensation in the superfluid liquid helium. Obviously, the peak inelastic neutron scattering intensity is connected with the registration of neutron modes in a neutron-spectrometer which, in turn, defines the nature of the excitations. So we may conclude that the registration of single neutron modes or neutron pair modes occurs at the lambda transition, from the neutron-spectrometer.

In this letter, we proposed new model for Bose-gas by extending the concept of a broken Bose-symmetry law for bosons in the condensate within applying the Penrose-Onsager definition of the Bose condensation [10]. After, we show that the interaction term between Boson modes and Fermion density modes is meditated by an effective attractive interaction between the Fermion modes, which in turn determines a bound state of singlet Fermion pair in a superfluid Bose liquid- Fermion gas mixture.

We investigate the problem of superconductivity presented by Frölich [11]. Hence, we also remark the theory of superconductivity, presented by Bardeen, Cooper and Schrieffer [12], and by Bogoliubov [13] (BCSB). They asserted that the Frölich effective attractive potential between electrons leads to shaping of two electrons with opposite spins around Fermi level into the Cooper pairs [14]. However, we demonstrate the term of the interaction between electrons and ions of lattice meditates the existence of the Frölich singlet electron pairs.

2 New model of a superfluid liquid helium

First, we present new model of a dilute Bose gas with strongly interactions between the atoms, to describe the superfluid liquid helium. This model considers a system of N identical interacting atoms via S-wave scattering. These atoms, as spinless Bose-particles, have a mass m and are confined to a box of volume V. The main part of the Hamiltonian of such system is expressed in the second quantization form as:

$$\hat{H}_a = \sum_{\vec{p}\neq 0} \frac{p^2}{2m} \hat{a}^+_{\vec{p}} \hat{a}_{\vec{p}} + \frac{1}{2V} \sum_{\vec{p}\neq 0} U_{\vec{p}} \hat{\varrho}_{\vec{p}} \hat{\varrho}^+_{\vec{p}} . \qquad (1)$$

Here $\hat{a}^+_{\vec{p}}$ and $\hat{a}_{\vec{p}}$ are, respectively, the "creation" and "annihilation" operators of a free atoms with momentum $\vec{p}$; $U_{\vec{p}}$ is the Fourier transform of a S-wave pseudopotential in the

momentum space:

$$U_{\vec{p}} = \frac{4\pi d\hbar^2}{m}\,, \tag{2}$$

where d is the scattering amplitude; and the Fourier component of the density operator presents as

$$\hat{\varrho}_{\vec{p}} = \sum_{\vec{p}_1} \hat{a}^+_{\vec{p}_1-\vec{p}}\,\hat{a}_{\vec{p}_1}\,. \tag{3}$$

According to the Bogoliubov theory [3], it is necessary to separate the atoms in the condensate from those atoms filling states above the condensate. In this respect, the operators $\hat{a}_0$ and $\hat{a}^+_0$ are replaced by c-numbers $\hat{a}_0 = \hat{a}^+_0 = \sqrt{N_0}$ within the approximation of the presence of a macroscopic number of condensate atoms $N_0 \gg 1$. This assumption leads to a broken Bose-symmetry law for atoms in the condensate state. To extend the concept of a broken Bose-symmetry law for bosons in the condensate, we apply the Penrose-Onsager definition of Bose condensation [10]:

$$\lim_{N_0,N\to\infty} \frac{N_0}{N} = const. \tag{4}$$

This reasoning is a very important factor in the microscopic investigation of the model non-ideal Bose gas because the presence of a macroscopic number of atoms in the condensate means new excitations in the model Bose-gas for superfluid liquid helium:

$$\frac{N_{\vec{p}\neq 0}}{N_0} = \alpha \ll 1\,,$$

where $N_{\vec{p}\neq 0}$ is the occupation number of atoms in the quantum levels above the condensate; α is the small number. Obviously, conservation of the total number of atoms suggests that the number of the Bose-condensed atoms N_0 essentially deviates from the total number N:

$$N_0 + \sum_{\vec{p}\neq 0} N_{\vec{p}\neq 0} = N\,,$$

which is satisfied for the present model. In this context,

$$\alpha = \frac{N - N_0}{N_0 \sum_{\vec{p}\neq 0} 1} \to 0\,,$$

where $\sum_{\vec{p}\neq 0} 1 \to \infty$.

For futher calculations, we replace the initial assumptions of our model by the approximation

$$\lim_{N_0\to\infty} \frac{N_{\vec{p}}}{N_0} \approx \delta_{\vec{p},0} \tag{5}$$

The next step is to find the property of operators $\frac{\hat{a}^+_{\vec{p}_1-\vec{p}}}{\sqrt{N_0}}$, $\frac{\hat{a}_{\vec{p}_1-\vec{p}}}{\sqrt{N_0}}$ by applying (5). Obviously,

$$\lim_{N_0\to\infty} \frac{\hat{a}^+_{\vec{p}_1-\vec{p}}}{\sqrt{N_0}} = \delta_{\vec{p}_1,\vec{p}} \tag{6}$$

and

$$\lim_{N_0\to\infty} \frac{\hat{a}_{\vec{p}_1-\vec{p}}}{\sqrt{N_0}} = \delta_{\vec{p}_1,\vec{p}}\,. \tag{7}$$

Excluding the term $\vec{p}_1 = 0$, the density operators of bosons $\hat{\varrho}_{\vec{p}}$ and $\hat{\varrho}^+_{\vec{p}}$ take the following forms:

$$\hat{\varrho}_{\vec{p}} = \sqrt{N_0}\,\left(\hat{a}^+_{-\vec{p}} + \sqrt{2}\,\hat{c}_{\vec{p}}\right) \tag{8}$$

and

$$\hat{\varrho}^+_{\vec{p}} = \sqrt{N_0}\,\left(\hat{a}_{-\vec{p}} + \sqrt{2}\,\hat{c}^+_{\vec{p}}\right) \tag{9}$$

where $\hat{c}_{\vec{p}}$ and $\hat{c}^+_{\vec{p}}$ are, respectively, the Bose-operators of density-quasiparticles presented in reference [8], which in turn are the Bose-operators of bosons used in expressions (6) and (7):

$$\hat{c}_{\vec{p}} = \frac{1}{\sqrt{2N_0}} \sum_{\vec{p}_1\neq 0} \hat{a}^+_{\vec{p}_1-\vec{p}}\,\hat{a}_{\vec{p}_1} = \frac{1}{\sqrt{2}} \sum_{\vec{p}_1\neq 0} \delta_{\vec{p}_1,\vec{p}}\,\hat{a}_{\vec{p}_1} = \frac{\hat{a}_{\vec{p}}}{\sqrt{2}} \tag{10}$$

and

$$\hat{c}^+_{\vec{p}} = \frac{1}{\sqrt{2N_0}} \sum_{\vec{p}_1\neq 0} \hat{a}^+_{\vec{p}_1}\,\hat{a}_{\vec{p}_1-\vec{p}} = \frac{1}{\sqrt{2}} \sum_{\vec{p}_1\neq 0} \delta_{\vec{p}_1,\vec{p}}\,\hat{a}^+_{\vec{p}_1} = \frac{\hat{a}^+_{\vec{p}}}{\sqrt{2}}\,. \tag{11}$$

Thus, we reach to the density operators of atoms $\hat{\varrho}_{\vec{p}}$ and $\hat{\varrho}^+_{\vec{p}}$, presented by Bogoliubov [3], at approximation $\frac{N_0}{N}$=$const$, which describes the gas of atoms ^{4}He with strongly interaction via S-wave scattering:

$$\hat{\varrho}_{\vec{p}} = \sqrt{N_0}\,\left(\hat{a}^+_{-\vec{p}} + \hat{a}_{\vec{p}}\right) \tag{12}$$

and

$$\hat{\varrho}^+_{\vec{p}} = \sqrt{N_0}\,\left(\hat{a}_{-\vec{p}} + \hat{a}^+_{\vec{p}}\right) \tag{13}$$

which shows that the density quasiparticles are absent.

The identical picture is observed in the case of the density excitations, as predicted by Glyde, Griffin and Stirling [5–7] proposing $\hat{\varrho}_{\vec{p}}$ in the following form:

$$\hat{\varrho}_{\vec{p}} = \sqrt{N_0}\,\left(\hat{a}^+_{-\vec{p}} + \hat{a}_{\vec{p}} + \tilde{\varrho}_{\vec{p}}\right) \tag{14}$$

where terms involving $\vec{p}_1 \neq 0$ and , $\vec{p}_1 \neq \vec{p}$ are written separately; and the operator $\tilde{\varrho}_{\vec{p}}$ describes the density-excitations:

$$\tilde{\varrho}_{\vec{p}} = \frac{1}{\sqrt{N_0}} \sum_{\vec{p}_1\neq 0,\vec{p}_1\neq\vec{p}} \hat{a}^+_{\vec{p}_1-\vec{p}}\,\hat{a}_{\vec{p}_1}\,. \tag{15}$$

After inserting (6) and (7) into (15), the term, representing the density-excitations vanishes because $\tilde{\varrho}_{\vec{p}} = 0$.

Consequently, the Hamiltonian of system, presented in (1) with also (12) and (13), represents an extension of the Bogoliubov Hamiltonian, with the approximation $\frac{N_0}{N} = const$, which in turn does not depend on the actual amplitude of interaction. In the case of strongly interacting atoms, the Hamiltonian takes the following form:

$$\hat{H}_a = \sum_{\vec{p}\neq 0} \left(\frac{p^2}{2m} + mv^2\right) \hat{a}^+_{\vec{p}}\,\hat{a}_{\vec{p}} + \frac{mv^2}{2} \sum_{\vec{p}\neq 0} \left(\hat{a}^+_{-\vec{p}}\,\hat{a}^+_{\vec{p}} + \hat{a}_{\vec{p}}\,\hat{a}_{-\vec{p}}\right), \tag{16}$$

where $v = \sqrt{\frac{U_{\vec{r}} N_0}{mV}} = \sqrt{\frac{4\pi d\hbar^2 N_0}{m^2 V}}$ is the velocity of sound in the Bose gas, and which depends on the density atoms in the condensate $\frac{N_0}{V}$.

For the evolution of the energy level, it is a necessary to diagonalize the Hamiltonian $\hat{H}_a$ which is accomplished by introduction of the Bose-operators $\hat{b}^+_{\vec{p}}$ and $\hat{b}_{\vec{p}}$ by using of the Bogoliubov linear transformation [3]:

$$\hat{a}_{\vec{p}} = \frac{\hat{b}_{\vec{p}} + L_{\vec{p}}\,\hat{b}^+_{-\vec{p}}}{\sqrt{1 - L^2_{\vec{p}}}}\,, \tag{17}$$

where $L_{\vec{p}}$ is the unknown real symmetrical function of a momentum $\vec{p}$.

Substitution of (17) into (16) leads to

$$\hat{H}_a = \sum_{\vec{p}} \varepsilon_{\vec{p}}\,\hat{b}^+_{\vec{p}}\,\hat{b}_{\vec{p}} \tag{18}$$

hence we infer that $\hat{b}^+_{\vec{p}}$ and $\hat{b}_{\vec{p}}$ are the "creation" and "annihilation" operators of a Bogoliubov quasiparticles with energy:

$$\varepsilon_{\vec{p}} = \left[\left(\frac{p^2}{2m}\right)^2 + p^2 v^2\right]^{1/2}. \tag{19}$$

In this context, the real symmetrical function $L_{\vec{p}}$ of a momentum $\vec{p}$ is found

$$L^2_{\vec{p}} = \frac{\frac{p^2}{2m} + mv^2 - \varepsilon_{\vec{p}}}{\frac{p^2}{2m} + mv^2 + \varepsilon_{\vec{p}}}\,. \tag{20}$$

As is well known, the strong interaction between the helium atoms is very important and reduces the condensate fraction to 10 percent or $\frac{N_0}{N} = 0.1$ [5], at absolute zero. However, as we suggest, our model of dilute Bose gas may be valuable in describing thermodynamic properties of superfluid liquid helium, because the S-wave scattering between two atoms, with coordinates $\vec{r}_1$ and $\vec{r}_2$ in coordinate space, is represented by the repulsive potential delta-function $U_{\vec{r}} = \frac{4\pi d\hbar^2 \delta_{\vec{r}}}{m}$ from $\vec{r} = \vec{r}_1 - \vec{r}_2$. The model presented works on the condensed fraction $\frac{N_0}{N} \ll 1$ and differs from the Bogoliubov model where $\frac{N_0}{N} \approx 1$.

3 Formation singlet spinless neutron pairs

We now attempt to describe the thermodynamic property of a helium liquid-neutron gas mixture. In this context, we consider a neutron gas as an ideal Fermi gas consisting of n free neutrons with mass m_n which interact with N interacting atoms of a superfluid liquid helium. The helium-neutron mixture is confined in a box of volume V. The Hamiltonian of a considering system $\hat{H}_{a,n}$ consists of the term of the Hamiltonian of Bogoliubov excitations $\hat{H}_a$ in (18) and the term of the Hamiltonian of an ideal Fermi neutron gas as well as the term of interaction between the density of the Bogoliubov excitations and the density of the neutron modes:

$$\begin{aligned}\hat{H}_{a,n} &= \textstyle\sum_{\vec{p},\sigma} \frac{p^2}{2m_n}\,\hat{a}^+_{\vec{p},\sigma}\,\hat{a}_{\vec{p},\sigma} + \\ &+ \sum_{\vec{p}} \varepsilon_{\vec{p}}\,\hat{b}^+_{\vec{p}}\,\hat{b}_{\vec{p}} + \frac{1}{2V}\sum_{\vec{p}\neq 0} U_0\,\hat{\varrho}_{\vec{p}}\,\hat{\varrho}_{-\vec{p},n}\,,\end{aligned} \tag{21}$$

where $\hat{a}^+_{\vec{p},\sigma}$ and $\hat{a}_{\vec{p},\sigma}$ are, respectively, the operators of creation and annihilation for free neutron with momentum $\vec{p}$, by the value of its spin z-component $\sigma = {}^+_- \frac{1}{2}$; U_0 is the Fourier transform of the repulsive interaction between the density of the Bogoliubov excitations and the density modes of the neutrons:

$$U_0 = \frac{4\pi d_0 \hbar^2}{\mu}\,, \tag{22}$$

where d_0 is the scattering amplitude between a helium atoms and neutrons; $\mu = \frac{m \cdot m_n}{m + m_n}$ is the relative mass.

Hence, we note that the Fermi operators $\hat{a}^+_{\vec{p},\sigma}$ and $\hat{a}_{\vec{p},\sigma}$ satisfy to the Fermi commutation relations $[\cdots]_+$ as:

$$\left[\hat{a}_{\vec{p},\sigma},\ \hat{a}^+_{\vec{p}',\sigma'}\right]_+ = \delta_{\vec{p},\vec{p}'}\ \delta_{\sigma,\sigma'}\,, \tag{23}$$

$$[\hat{a}_{\vec{p},\sigma}, \hat{a}_{\vec{p}',\sigma'}]_+ = 0\,, \tag{24}$$

$$[\hat{a}^+_{\vec{p},\sigma}, \hat{a}^+_{\vec{p}',\sigma'}]_+ = 0\,. \tag{25}$$

The density operator of neutrons with spin σ in momentum $\vec{p}$ is defined as

$$\hat{\varrho}_{\vec{p},n} = \sum_{\vec{p}_1,\sigma} \hat{a}^+_{\vec{p}_1-\vec{p},\sigma}\,\hat{a}_{\vec{p}_1,\sigma}\,, \tag{26}$$

where $\hat{\varrho}^+_{\vec{p},n} = \hat{\varrho}_{-\vec{p},n}$.

The operator of total number of neutrons is

$$\sum_{\vec{p},\sigma} \hat{a}^+_{\vec{p},\sigma}\,\hat{a}_{\vec{p},\sigma} = \hat{n}; \tag{27}$$

on other hand, the density operator, in the term of the Bogoliubov quasiparticles $\hat{\varrho}_{\vec{p}}$ included in (21), is expressed by following form, to application (17) into (12):

$$\hat{\varrho}_{\vec{p}} = \sqrt{N_0}\,\sqrt{\frac{1 + L_{\vec{p}}}{1 - L_{\vec{p}}}}\left(\hat{b}^+_{-\vec{p}} + \hat{b}_{\vec{p}}\right). \tag{28}$$

Hence, we note that the Bose- operator $\hat{b}_{\vec{p}}$ commutates with the Fermi operator $\hat{a}_{\vec{p},\sigma}$ because the Bogoliubov excitations and neutrons are an independent.

Now, inserting of a value of operator $\hat{\varrho}_{\vec{p}}$ from (28) into (21), which in turn leads to reducing the Hamiltonian of system $\hat{H}_{a,n}$:

$$\begin{aligned}\hat{H}_{a,n} &= \textstyle\sum_{\vec{p},\sigma} \frac{p^2}{2m_n}\,\hat{a}^+_{\vec{p},\sigma}\,\hat{a}_{\vec{p},\sigma} + \sum_{\vec{p}} \varepsilon_{\vec{p}}\,\hat{b}^+_{\vec{p}}\,\hat{b}_{\vec{p}} + \\ &+ \frac{U_0\sqrt{N_0}}{2V}\sum_{\vec{p}} \sqrt{\frac{1 + L_{\vec{p}}}{1 - L_{\vec{p}}}}\left(\hat{b}^+_{-\vec{p}} + \hat{b}_{\vec{p}}\right)\hat{\varrho}_{-\vec{p},n}\,.\end{aligned} \tag{29}$$

Hence, we note that the Hamiltonian of system $\hat{H}_{a,n}$ in (29) is a similar to the Hamiltonian of system an electron gas-phonon gas mixture which was proposed by Frölich at solving of the problem superconductivity (please, see the Equation (16) in Frölich, *Proc. Roy. Soc. A*, 1952, v.215, 291–291 in the reference [11]), contains a subtle error in the term of the interaction between the density of phonon modes and the density of electron modes which represents a third term in right side of Equation (16) in [11] because the later is described by two sums, one from which goes by the wave vector $\vec{w}$ but other sum goes by the wave vector $\vec{k}$. This fact contradicts to the definition of the density operator of the electron modes $\hat{\varrho}_{\vec{w}}$ (please, see the Equation (12) in [11]) which in turn already contains the sum by the wave vector $\vec{k}$, and therefore, it is not a necessary to take into account so-called twice summations from $\vec{k}$ and $\vec{w}$ for describing of the term of the interaction between the density of phonon modes and the density of electron modes Thus, in the case of the Frölich, the sum must be taken only by wave vector w, due to definition of the density operator of electron modes with the momentum of phonon $\vec{w}$.

To allocate anomalous term in the Hamiltonian of system $\hat{H}_{a,n}$, which denotes by third term in right side in (29), we apply the Frölich approach [11] which allows to do a canonical transformation for the operator $\hat{H}_{a,n}$ within introducing an operator $\tilde{H}$:

$$\tilde{H} = \exp\left(\hat{S}^{+}\right)\ \hat{H}_{a,n} \exp\left(\hat{S}\right), \tag{30}$$

which is decayed by following terms:

$$\begin{aligned} \tilde{H} &= \exp\left(\hat{S}^{+}\right)\ \hat{H}_{a,n} \exp\left(\hat{S}\right) = \\ &= \hat{H}_{a,n} - \left[\hat{S}, \hat{H}_{a,n}\right] + \frac{1}{2}\left[\hat{S}, \left[\hat{S}, \hat{H}_{a,n}\right]\right] - \cdots , \end{aligned} \tag{31}$$

where the operators represent as:

$$\hat{S}^{+} = \sum_{\vec{p}} \hat{Sp} \tag{32}$$

and

$$\hat{S} = \sum_{\vec{p}} \hat{Sp} \tag{33}$$

and satisfy to a condition $\hat{S}^{+} = -\hat{S}$.

In this respect, we assume that

$$\hat{Sp} = A_{\vec{p}}\left(\hat{\varrho}_{\vec{p},n}\hat{b}_{\vec{p}} - \hat{\varrho}^{+}_{\vec{p},n}\hat{b}^{+}_{\vec{p}}\right), \tag{34}$$

where $A_{\vec{p}}$ is the unknown real symmetrical function from a momentum $\vec{p}$. In this context, at application $\hat{Sp}$ from (34) to (33) with taking into account $\hat{\varrho}^{+}_{-\vec{p},n} = \hat{\varrho}_{\vec{p},n}$, then we obtain

$$\hat{S} = \sum_{\vec{p}} \hat{Sp} = \sum_{\vec{p}} A_{\vec{p}}\,\hat{\varrho}_{\vec{p},n}\left(\hat{b}_{=\vec{p}} - \hat{b}^{+}_{\vec{p}}\right). \tag{35}$$

In analogy manner, at $\hat{\varrho}^{+}_{-\vec{p},n} = \hat{\varrho}_{\vec{p},n}$, we have

$$\begin{aligned} \hat{S}^{+} &= \textstyle\sum_{\vec{p}} \hat{Sp} = \sum_{\vec{p}} A_{\vec{p}}\,\hat{\varrho}^{+}_{\vec{p},n}\left(\hat{b}^{+}_{\vec{p}} - \hat{b}_{-\vec{p}}\right) = \\ &= -\sum_{\vec{p}} A_{\vec{p}}\,\hat{\varrho}_{\vec{p},n}\left(\hat{b}_{-\vec{p}} - \hat{b}^{+}_{\vec{p}}\right). \end{aligned} \tag{36}$$

To find $A_{\vec{p}}$, we substitute (29), (35) and (36) into (31). Then,

$$\begin{aligned} \left[\hat{S}, \hat{H_{a,n}}\right] &= \tfrac{1}{V}\textstyle\sum_{\vec{p}} A_{\vec{p}}\, U_0 \sqrt{N_0}\sqrt{\frac{1+L_{\vec{p}}}{1-L_{\vec{p}}}}\,\hat{\varrho}_{\vec{p},n}\hat{\varrho}_{-\vec{p},n} + \\ &+ \sum_{\vec{p}} A_{\vec{p}}\,\varepsilon_{\vec{p}}\left(\hat{b}^{+}_{\vec{p}} + \hat{b}_{-\vec{p}}\right)\hat{\varrho}_{-\vec{p},n}, \end{aligned} \tag{37}$$

$$\frac{1}{2}\left[\hat{S}, \left[\hat{S}, \hat{H}_{a,n}\right]\right] = \sum_{\vec{p}} A^{2}_{\vec{p}}\,\varepsilon_{\vec{p}}\,\varrho_{\vec{p},n}\,\hat{\varrho}_{-\vec{p},n} \tag{38}$$

and $[\hat{S}, [\hat{S}, [\hat{S}, \hat{H}_{a,n}]]] = 0$ within application a Bose commutation relations as $[\varrho_{\vec{p}_1,n}, \hat{\varrho}_{\vec{p}_2,n}] = 0$ and $[\hat{a}^{+}_{\vec{p}_1,\sigma}\hat{a}_{\vec{p}_1,\sigma}, \hat{\varrho}_{\vec{p}_2,n}] = 0$.

Thus, the form of new operator $\tilde{H}$ in (31) takes a following form:

$$\begin{aligned} \tilde{H} &= \textstyle\sum_{\vec{p}} \varepsilon_{\vec{p}}\,\hat{b}^{+}_{\vec{p}}\,\hat{b}_{\vec{p}} + \sum_{\vec{p},\sigma} \frac{p^2}{2m_n}\,\hat{a}^{+}_{\vec{p},\sigma}\,\hat{a}_{\vec{p},\sigma} + \\ &+ \frac{1}{2V}\sum_{\vec{p}} U_0\sqrt{N_0}\sqrt{\frac{1+L_{\vec{p}}}{1-L_{\vec{p}}}}\left(\hat{b}^{+}_{-\vec{p}} + \hat{b}_{\vec{p}}\right)\hat{\varrho}_{-\vec{p},n} - \\ &- \sum_{\vec{p}} A_{\vec{p}}\,\varepsilon_{\vec{p}}\left(\hat{b}^{+}_{-\vec{p}} + \hat{b}_{\vec{p}}\right)\hat{\varrho}_{-\vec{p},n} + \sum_{\vec{p}} A^{2}_{\vec{p}}\,\varepsilon_{\vec{p}}\,\hat{\varrho}_{\vec{p},n}\,\hat{\varrho}_{-\vec{p},n} - \\ &- \frac{1}{V}\sum_{\vec{p}} A_{\vec{p}} U_0\sqrt{N_0}\sqrt{\frac{1+L_{\vec{p}}}{1-L_{\vec{p}}}}\,\hat{\varrho}_{\vec{p},n}\,\hat{\varrho}_{-\vec{p},n}\,. \end{aligned} \tag{39}$$

The transformation of the term of the interaction between the density of the Bogoliubov modes and the density neutron modes is made by removing of a second and fifth terms in right side of (39) which leads to obtaining of a quantity for $A_{\vec{p}}$:

$$A_{\vec{p}} = \frac{U_0\sqrt{N_0}}{2\varepsilon_{\vec{p}}V}\sqrt{\frac{1+L_{\vec{p}}}{1-L_{\vec{p}}}}\,. \tag{40}$$

In this respect, we reach to reducing of the new Hamiltonian of system (39):

$$\begin{aligned} \tilde{H} &= \textstyle\sum_{\vec{p}}\,\varepsilon_{\vec{p}}\,\hat{b}^{+}_{\vec{p}}\,\hat{b}_{\vec{p}} + \sum_{\vec{p},\sigma}\frac{p^2}{2m_n}\,\hat{a}^{+}_{\vec{p},\sigma}\hat{a}_{\vec{p},\sigma} - \\ &- \frac{1}{V}\sum_{\vec{p}} A_{\vec{p}} U_0\sqrt{N_0}\sqrt{\frac{1+L_{\vec{p}}}{1-L_{\vec{p}}}}\,\hat{\varrho}_{\vec{p},n}\,\hat{\varrho}_{-\vec{p},n} + \\ &+ \sum_{\vec{p}} A^{2}_{\vec{p}}\,\varepsilon_{\vec{p}}\,\hat{\varrho}_{\vec{p},n}\,\hat{\varrho}_{-\vec{p},n}\,. \end{aligned} \tag{41}$$

As result, the new form of Hamiltonian system takes a following form:

$$\tilde{H} = \sum_{\vec{p}}\varepsilon_{\vec{p}}\,\hat{b}^{+}_{\vec{p}}\,\hat{b}_{\vec{p}} + \hat{H}_n\,, \tag{42}$$

where $\hat{H}_n$ is the effective Hamiltonian of a neutron gas which contains an effective interaction between neutron modes:

$$\hat{H}_n = \sum_{\vec{p},\sigma} \frac{p^2}{2m_n} \hat{a}^+_{\vec{p},\sigma} \hat{a}_{\vec{p},\sigma} + \frac{1}{2V} \sum_{\vec{p}} V_{\vec{p}} \hat{\varrho}_{\vec{p},n} \hat{\varrho}_{-\vec{p},n} , \qquad (43)$$

where $V_{\vec{p}}$ is the effective potential of the interaction between neutron modes which takes a following form at substituting a value of $A_{\vec{p}}$ from (40) into (41):

$$\begin{aligned} V_{\vec{p}} &= -2A_{\vec{p}} U_0 \sqrt{N_0} \sqrt{\tfrac{1+L_{\vec{p}}}{1-L_{\vec{p}}}} + 2A^2_{\vec{p}} \varepsilon_{\vec{p}} V = \\ &= -\frac{U_0^2 N_0 \left(1 + L_{\vec{p}}\right)}{V\varepsilon_{\vec{p}} \left(1 - L_{\vec{p}}\right)} . \end{aligned} \qquad (44)$$

In this letter, we consider following cases:

1. At low momenta atoms of a helium $p \ll 2mv$, the Bogoliunov's quasiparticles in (19) represent as the phonons with energy $\varepsilon_{\vec{p}} \approx pv$ which in turn defines a value $L^2_{\vec{p}} \approx \frac{1-\frac{p}{mv}}{1+\frac{p}{mv}} \approx \left(1 - \frac{p}{mv}\right)^2$ in (20) or $L_{\vec{p}} \approx 1 - \frac{p}{mv}$. In this context, the effective potential between neutron modes takes a following form:

$$V_{\vec{p}} \approx -\frac{2mU_0^2 N_0}{Vp^2} = -\frac{4\pi\hbar^2 e_1^2}{p^2} . \qquad (45)$$

The value e_1 is the effective charge, at a small momenta of atoms:

$$e_1 = \frac{U_0}{\hbar} \sqrt{\frac{mN_0}{2V\pi}} .$$

2. At high momenta atoms of a helium $p \gg 2mv$, we obtain $\varepsilon_{\vec{p}} \approx \frac{p^2}{2m} + mv^2$ in (19) which in turn defines $L_{\vec{p}} \approx 0$ in (20). Then, the effective potential between neutron modes presents as:

$$V_{\vec{p}} \approx -\frac{mU_0^2 N_0}{Vp^2} = -\frac{4\pi\hbar^2 e_2^2}{p^2} , \qquad (46)$$

where e_2 is the effective charge, at high momenta of atoms:

$$e_2 = \frac{U_0}{2\hbar} \sqrt{\frac{mN_0}{V\pi}} .$$

Consequently, in both cases, the effective scattering between two neutrons is presented in the coordinate space by a following form:

$$V(\vec{r}) = \frac{1}{V} \sum_{\vec{p}} V_{\vec{p}} \, e^{i\frac{\vec{p}\vec{r}}{\hbar}} = -\frac{e_*^2}{r} , \qquad (47)$$

where $e_* = e_1$, at small momenta of atoms; and $e_* = e_2$, at high momenta.

The term of the interaction between two neutrons $V(\vec{r})$ in the coordinate space mediates the attractive Coulomb interaction between two charged particles with mass of neutron m_n, having the opposite effective charges e_* and $-e_*$, which together create a neutral system. Indeed, the effective Hamiltonian of a neutron gas in (43) is rewrite down in the space of coordinate by following form:

$$\hat{H}_n = \sum_{i=1}^{\frac{n}{2}} \hat{H}_i = -\frac{\hbar^2}{2m_n} \sum_{i=1}^{n} \Delta_i - \sum_{i<j} \frac{e_*^2}{\mid \vec{r}_i - \vec{r}_j \mid} , \qquad (48)$$

where $\hat{H}_i$ is the Hamiltonian of system consisting two neutron with opposite spin which have a coordinates $\vec{r}_i$ and $\vec{r}_j$:

$$\hat{H}_i = -\frac{\hbar^2}{2m_n} \Delta_i - \frac{\hbar^2}{2m_n} \Delta_j - \frac{e_*^2}{\mid \vec{r}_i - \vec{r}_j \mid} . \qquad (49)$$

The transformation of considering coordinate system to the relative coordinate $\vec{r} = \vec{r}_i - \vec{r}_j$ and the coordinate of center mass $\vec{R} = \frac{\vec{r}_i + \vec{r}_j}{2}$, we have

$$\hat{H}_i = -\frac{\hbar^2}{4m_n} \Delta_R - \frac{\hbar^2}{m_n} \Delta_r - \frac{e_*^2}{r} . \qquad (50)$$

In analogy of the problem Hydrogen atom, two neutrons with opposite spins is bound as a spinless neutron pair with binding energy:

$$E_n = -\frac{m_n e_*^4}{4\hbar^2 n^2} = -\frac{const}{n^2} \left(\frac{N_0}{V}\right)^2 , \qquad (51)$$

where n is the main quantum number which determines a bound state on a neutron pair, at $const > 0$.

Thus, a spinless neutron pair with mass $m_0 = 2m_n$ is created in a helium liquid-dilute neutron gas mixture.

4 Formation of the Frölich electron pairs in superconductivity

We now attempt to describe the thermodynamic property of the model a phonon-electron gas mixture confined in a box of volume V. In this context, we consider an electron gas consisting of n free electrons with mass m_e which interact with phonon modes of lattice by constancy interaction [11]. The Frölich Hamiltonian has a following form:

$$\hat{H} = \hat{H}_0 + \hat{H}_1 + \hat{H}_2 \qquad (52)$$

with

$$\hat{H}_0 = \sum_{\vec{k},\sigma} \varepsilon_{\vec{k}} \hat{d}^+_{\vec{k},\sigma} \hat{d}_{\vec{k},\sigma} , \qquad (53)$$

$$\hat{H}_1 = \sum_{\vec{w}} \hbar w s \, \hat{b}^+_{\vec{w}} \hat{b}_{\vec{w}} , \qquad (54)$$

$$\hat{H}_2 = i \sum_{\vec{w}} D_w \left(\hat{b}_{\vec{w}} \hat{\varrho}^+_{\vec{w}} - \hat{b}^+_{\vec{w}} \hat{\varrho}_{\vec{w}}\right), \qquad (55)$$

where $\hat{d}^+_{\vec{k},\sigma}$ and $\hat{d}_{\vec{k},\sigma}$ are, respectively, the Fermi operators of creation and annihilation for free electron with wave-vector

$\vec{k}$ and energy $\varepsilon_{\vec{k}} = \frac{\hbar^2 k^2}{2m_e}$, by the value of its spin z-component $\sigma = {}^{+}_{-}\frac{1}{2}$; s is the velocity of phonon; $\hat{b}^{+}_{\vec{w},\sigma}$ and $\hat{b}_{\vec{w},\sigma}$ are, respectively, the Bose operators of creation and annihilation for free phonon with wave-vector $\vec{w}$ and energy$\hbar ws$; D_w is the constant of the interaction between the density of the phonon excitations and the density modes of the electrons which equals to $D_w = \sqrt{\frac{\alpha\hbar ws}{V}}$ (where $\alpha = \frac{C^{"2}}{2Ms^2\frac{n}{V}}$ is the constant characterizing of the metal; $C^{"}$ is the constant of the interaction; M is the mass of ion); $\hat{\varrho}_{\vec{w}}$ is the density operator of the electron modes with wave vector $\vec{w}$ which is defined as:

$$\hat{\varrho}_{\vec{w}} = \sum_{\vec{k},\sigma} \hat{d}^{+}_{\vec{k}-\vec{w},\sigma}\hat{d}_{\vec{k},\sigma} \tag{56}$$

and

$$\hat{\varrho}^{+}_{\vec{w}} = \sum_{\vec{k},\sigma} \hat{d}^{+}_{\vec{k},\sigma}\hat{d}_{\vec{k}-\vec{w},\sigma}\,, \tag{57}$$

where $\hat{\varrho}^{+}_{\vec{w}} = \hat{\varrho}_{-\vec{w}}$.

Hence, we note that the Fermi operators $\hat{d}^{+}_{\vec{k},\sigma}$ and $\hat{d}_{\vec{k},\sigma}$ satisfy to the Fermi commutation relations $[\cdots]_+$ presented in above for neutrons (23–25).

Obviously, the Bose- operator $\hat{b}_{\vec{w}}$ commutates with the Fermi operator $\hat{d}_{\vec{k},\sigma}$ because phonon excitations and electron modes are an independent.

Now, we introduce new transformation of the Bose-operators of phonon modes $\hat{b}^{+}_{\vec{w}}$ and $\hat{b}_{\vec{w}}$ by the new Bose - operators of phonon excitations $\hat{c}^{+}_{\vec{w}}$ and $\hat{c}_{\vec{w}}$ which help us to remove an anomalous term:

$$\hat{b}_{\vec{w}} = -i\hat{c}_{\vec{w}} \tag{58}$$

and

$$\hat{b}^{+}_{\vec{w}} = i\hat{c}^{+}_{\vec{w}}\,. \tag{59}$$

Then, $\hat{H}_1$ in (56) and $\hat{H}_2$ in (57) take following forms:

$$\hat{H}_1 = \sum_{\vec{w}} \hbar ws\,\hat{c}^{+}_{\vec{w}}\hat{c}_{\vec{w}}\,, \tag{60}$$

$$\hat{H}_2 = \sum_{\vec{w}} D_w\left(\hat{c}_{\vec{w}}\,\hat{\varrho}^{+}_{\vec{w}} + \hat{c}^{+}_{\vec{w}}\,\hat{\varrho}_{\vec{w}}\right) = \sum_{\vec{w}} D_w\,\hat{\varrho}_{\vec{w}}\left(\hat{c}_{\vec{w}} + \hat{c}^{+}_{\vec{w}}\right). \tag{61}$$

To allocate anomalous term in the Hamiltonian of system $\hat{H}$ in (54), presented by the term in (63), we use of the canonical transformation for the operator $\hat{H}$ presented by formulae (30). Due to this approach, we obtain new form for operator Hamiltonian $\tilde{H}$:

$$\tilde{H} = \sum_{\vec{w}} \hbar ws\,\hat{b}^{+}_{\vec{w}}\,\hat{b}_{\vec{w}} + \hat{H}_e\,, \tag{62}$$

where

$$\hat{H}_e = \sum_{\vec{k},\sigma} \varepsilon_{\vec{k}}\,\hat{d}^{+}_{\vec{k},\sigma}\hat{d}_{\vec{k},\sigma} + \frac{1}{2V}\sum_{\vec{w}} V_{\vec{w}}\,\hat{\varrho}_{\vec{w}}\,\hat{\varrho}_{-\vec{w}}\,, \tag{63}$$

hence $V_{\vec{w}}$ is the effective potential of the interaction between electron modes, which at taking into account $D_w = \sqrt{\frac{\alpha\hbar ws}{V}}$, has the form:

$$V_{\vec{w}} = -\frac{2D_w^2 V}{\hbar ws} = -2\alpha\,. \tag{64}$$

Consequently, the effective scattering between two electrons in the coordinate space takes a following form:

$$V(\vec{r}) = \frac{1}{V}\sum_{\vec{w}} V_{\vec{w}}\,e^{i\vec{w}\vec{r}} = -2\alpha\delta(\vec{r}) \tag{65}$$

at using of $\frac{1}{V}\sum_{\vec{w}} e^{i\vec{w}\vec{r}} = \delta(\vec{r})$.

Using of the relative coordinate $\vec{r} = \vec{r}_i - \vec{r}_j$ and the coordinate of center mass $\vec{R} = \frac{\vec{r}_i+\vec{r}_j}{2}$, we reach to the Hamiltonian of system consisting two electron with opposite spins:

$$\hat{H}_i = -\frac{\hbar^2}{4m_e}\Delta_R - \frac{\hbar^2}{m_e}\Delta_r + V(\vec{r})\,. \tag{66}$$

To find the binding energy $E < 0$ of electron pair, we search the solution of the Schrödinger equation with introduction of wave function $\psi(\vec{r})$:

$$\hat{H}_i\,\psi_s(\vec{r}) = E\psi_s(\vec{r})\,.$$

In this respect, we have a following equation

$$-\frac{\hbar^2}{m_e}\Delta_r\psi_s(\vec{r}) + V(\vec{r})\,\psi_s(\vec{r}) = E\psi(\vec{r}) \tag{67}$$

which may determine the binding energy $E < 0$ of electron pair, if we claim that the condition $\frac{p_f d}{\hbar} \ll 1$ always is fulfilled. This reasoning implies that the effective scattering between two electrons is presented by the coordinate space:

$$V(\vec{r}) = \frac{1}{V}\sum_{\vec{w}} V_{\vec{w}}\,e^{i\vec{w}\vec{r}} = 4\pi\int_0^{w_f} V_{\vec{w}}\,w^2\,\frac{\sin(wr)}{wr}\,dw\,, \tag{68}$$

where we introduce a following approximation as $\frac{sin(wr)}{wr} \approx 1 - \frac{w^2r^2}{6}$ at conditions $w \le w_f$ and $w_f d \ll 1$ ($w_f = \left(\frac{3\pi^2 n}{V}\right)^{\frac{1}{3}}$ is the Fermi wave number). The later condition defines a state for distance r between two neighboring electrons which is a very small $r \ll \frac{1}{w_f} = \left(\frac{V}{3\pi^2 n}\right)^{\frac{1}{3}}$ where $\frac{4\pi w_f^3}{3} = \frac{n}{2V}$. Then,

$$V(\vec{r}) \approx -\frac{\alpha n}{V} + \alpha\left(\frac{n}{V}\right)^{\frac{5}{3}}\,r^2. \tag{69}$$

Thus, the effective interaction between electron modes $V(\vec{r}) = -2\alpha\delta(\vec{r})$, presented in (65) is replaced by a screening effective scattering presented by (69). This approximation means that there is an appearance of a screening character in the effective scattering because one depends on the density electron modes. Now, denoting $E = E_s$, and then, we arrive

to an important equation for finding a binding energy E_s of singlet electron pair:

$$\left[-\frac{\hbar^2}{m_e}\Delta_r - \frac{n\alpha}{V} + \alpha\left(\frac{n}{V}\right)^{\frac{5}{3}} r^2\right]\psi_s(r) = E_s\,\psi_s(r)\,, \qquad (70)$$

which we may rewrite down as:

$$\frac{d^2\psi_s(r)}{dr^2} + \left(\lambda - \theta^2 r^2\right)\psi_s(r) = 0\,, \qquad (71)$$

where we take $\theta = -\sqrt{\frac{m_e\alpha}{\hbar^2}\left(\frac{n}{V}\right)^{\frac{5}{3}}}$, and $\lambda = \frac{m_e E_s}{\hbar^2} - \frac{\alpha m_e n}{\hbar^2 V}$.

Now, introducing the wave function $\psi_s(r)$ via the Chebishev-Hermit function $H_s(it)$ from an imaginary number as argument it [15] (where i is the imaginary one; t is the real number; $s = 0; 1; 2; \ldots$), the equation (71) has a following solution:

$$\psi_s(\vec{r}) = e^{-\theta\cdot r^2} H_s\left(\sqrt{\theta}\, r\right),$$

where

$$H_s(it) = i^s e^{-t^2}\,\frac{d^s e^{t^2}}{dt^s}$$

at $\theta < 0$, where

$$\lambda = \theta\left(s + \frac{1}{2}\right).$$

Consequently, the quantity of the binding energy E_s of electron pair with mass $m_0 = 2m_e$ takes a following form:

$$E_s = -\sqrt{\frac{\alpha\hbar^2}{m_e}\left(\frac{n}{V}\right)^{\frac{5}{3}}}\left(s + \frac{1}{2}\right) + \frac{\alpha n}{V} < 0 \qquad (72)$$

at $s = 0; 1; 2; \ldots$.

The normal state of electron pair corresponds to quantity $s = 0$ which defines maximal binding energy of electron pair:

$$E_0 = -\sqrt{\frac{\alpha\hbar^2}{m_e}\left(\frac{n}{V}\right)^{\frac{5}{3}}} + \frac{\alpha n}{V} < 0\,. \qquad (73)$$

This fact implies that the formation of the superconducting phase in superconductor is appeared by condition for density of metal $\frac{n}{V}$:

$$\frac{n}{V} > \left(\frac{C^2 m_e}{2Ms^2\hbar^2}\right)^{\frac{3}{2}}.$$

At choosing $C \approx 10$ eV [11]; $M \approx 5{\times}10^{-26}$ kg; $s \approx 3{\times}10^3$ m, we may estimate density of electron $\frac{n}{V} > 10^{27}$ m^{-3} which may represent as superconductor.

Acknowledgements

We thank Professor Marshall Stoneham for help with the English.

Submitted on April 12, 2010 / Accepted on April 19, 2010

References

1. London F. *Nature*, 1938, v. 141, 643.
2. Landau L. *Journal of Physics (USSR)*, 1941, v. 5, 77.
3. Bogoliubov N.N. On the theory of superfludity. *Journal of Physics (USSR)*, 1947, v. 11, 23.
4. Bishop R.F. *J. Low Temp. Physics*, 1974, v. 15, 601.
5. Blagoveshchenskii N.N. et al. *Physical Review B*, 1994, v. 50, 16550.
6. Glyde H.R., Griffin A. *Physical Review Letters*, 1990, v. 65, 1454.
7. Stirling W.G.,Griffin A., Glyde H.R. *Physical Review B*, 1990, v. 41, 4224.
8. Minasyan V.N. et al. *Physical Review Letters*, 2003, v. 90, 235301.
9. Morawetz K. et al. *Physical Review B*, 2007, v. 76, 075116.
10. Penrose O., Onsager L. *Physical Review*, 1956, v. 104, 576.
11. Frölich H. *Proc. Roy. Soc.*, 1952, v. A215, 576.
12. Bardeen J., Cooper L.N., and Schrieffer J.R. *Physical Review*, 1957, v. 108, 1175.
13. Bogoliubov N.N. *Nuovo Cimento*, 1958, v. 7, 794.
14. Cooper L.N. *Physical Review*, 1956, v. 104, 1189.
15. Lavrentiev N.A. and Shabat B.V. Methods of the theory of a function of a complex variable. Nauka, Moscow, 1972.

Dispersion of Own Frequency of Ion-Dipole by Supersonic Transverse Wave in Solid

Vahan Minasyan and Valentin Samoilov
Scientific Center of Applied Research, JINR, Dubna, 141980, Russia
E-mails: mvahan@scar.jinr.ru; scar@off-serv.jinr.ru

First, we predict an existence of transverse electromagnetic field formed by supersonic transverse wave in solid. This electromagnetic wave acquires frequency and speed of sound, and it propagates along of direction propagation of supersonic wave. We also show that own frequency of ion-dipole depends on frequency of supersonic transverse wave.

1 Introduction

In our latest paper [1], we investigated the light diffraction by supersonic longitudinal waves in crystal. In this respect, we predicted an existence of transverse electromagnetic field created by supersonic longitudinal waves in solid. This electromagnetic wave with frequency of ultrasonic field is moved by speed of supersonic field toward to direction propagation of sound. There was shown that the average Poynting vector of superposition field involves the intensities of the transverse electromagnetic and the optical fields which form the intensity of light diffraction. We considered a model of solid as lattice of ions and gas of free electrons. Each ion of lattice coupled with a point of lattice knot by spring, creating of ion dipole. The knots of lattice define a position dynamical equilibrium of each ion which is vibrated by own frequency Ω_0. Hence, we may argue that the presented new model of solid leads to the same results which may obtain for solid by one dimensional model of single atomic crystal representing as model of continuum elastic medium which is described by chain of ions [2]. The vibration of ion occurs near position of equilibrium corresponding to minimum of potential energy (harmonic approximation of nearing neighbors).

Thus, the existence of transverse electromagnetic field is an important factor for correction so called the Raman-Nath theory [3] and the theory of photo-elastic linear effect [4] which were based on a concept that acoustic wave generates a periodical distribution of refractive index in the coordinate-time space.

In this letter, we attempt to investigate a property of solid by under action of supersonic transverse wave. In this context, we find dispersion law for own frequency of ion-dipole which depends on frequency of supersonic transverse wave.

2 Formation of transverse electromagnetic field

Let's consider the coupled ions with points of lattice knots. These ions are vibrated by own frequency Ω_0 into ion-dipoles. We note that ion-dipole is differ from electron-ion dipole which was discussed within elementary dispersion theory [5]. Hence, we assume that property of springs of ion dipole and ion-electron one are the same. This assumption allows us to obtain a connection between own frequencies of electron ω_0 and ion Ω_0 by condition $\Omega_0 = \sqrt{\frac{q}{M}} = \omega_0 \sqrt{\frac{m}{M}}$ where q is the rigidity of spring; m is the mass of electron.

By under action of transverse acoustic wave, there is an appearance of vector displacement $\vec{u}$ of each ions in solid.

Consider the propagation of an ultrasonic transverse plane traveling wave in cubic crystal. Due to laws of elastic field for solid [6], the vector displacement $\vec{u}$ satisfies to condition which defines property of transverse supersonic field

$$\operatorname{div} \vec{u} = 0 \tag{1}$$

and is defined by wave-equation

$$\nabla^2 \vec{u} - \frac{1}{c_t^2} \frac{d^2 \vec{u}}{dt^2} = 0 , \tag{2}$$

where c_t is the velocity of a transverse ultrasonic wave which is determined by elastic coefficients.

The simple solution of (2) in respect to $\vec{u}$ has a following form

$$\vec{u} = \vec{u}_0 \sin (Kx + \Omega t) , \tag{3}$$

where $\vec{u}_0$ is the amplitude of vector displacement; $K = \frac{\Omega \sqrt{\varepsilon}}{c}$ is the wave number of transverse electromagnetic wave.

Thus each ion acquires the dipole moment of ion $\vec{p} = -e\vec{u}$. Now, we may argue that there is a presence of transverse electromagnetic field with vector of electric field $\vec{E}$ due to displacement of ion:

$$M \frac{d^2 \vec{u}}{dt^2} + q\vec{u} = -e\vec{E} , \tag{4}$$

where $\vec{E}$ is the vector electric field which is induced by transverse ultrasonic wave; M is the mass of ion; the second term $q\vec{u}$ in left part represents as changing of quasi-elastic force which acts on ion.

Using of the operation div of the both part of (4) together with (1), we obtain a condition for Transverse electromagnetic wave

$$\operatorname{div} \vec{E} = 0 . \tag{5}$$

Now, substituting solution $\vec{u}$ from (3) in (4), we find the vector transverse electric wave

$$\vec{E} = \vec{E}_0 \sin (Kx + \Omega t) , \tag{6}$$

where

$$\vec{E}_0 = \frac{M\left(\Omega_0^2 - \Omega^2\right)\vec{u}_0}{e} \tag{7}$$

is the amplitude of transverse electric field which acts on ion into ion dipole.

The ion dipole acquires a polarizability α, which is determined via total dipole moment:

$$\vec{P} = N\alpha\vec{E}\,. \tag{8}$$

where N is the concentration of ion dipoles.

In the presented theory, the vector electric induction $\vec{D}$ is determined as

$$\vec{D} = 4\pi\vec{P} + \vec{E}\,, \tag{9}$$

and

$$\vec{D} = \varepsilon\vec{E}\,, \tag{10}$$

where $\vec{P}$=$N_0\vec{p}$ is the total polarization created by ion-dipoles.

It is easy to find the dielectric respond ε of acoustic medium which takes a following form

$$\varepsilon = 1 + 4\pi N\alpha = 1 + \frac{4\pi N e^2}{M\left(\Omega_0^2 - \Omega^2\right)}\,, \tag{11}$$

This formulae is also obtained by model of ions chain [2].

The dielectric respond ε of acoustic medium is similar to optical one, therefore,

$$\sqrt{\varepsilon} = \frac{c}{c_t}\,, \tag{12}$$

where c is the velocity of electromagnetic wave in vacuum.

Thus, we found that transverse electric wave with frequency Ω is propagated by velocity c_t of ultrasonic transverse wave in the direction OX.

Furthermore, we present the Maxwell equations for electromagnetic field in acoustic medium with a magnetic permittivity $\mu = 1$:

$$\operatorname{curl}\vec{E} + \frac{1}{c}\frac{d\vec{H}}{dt} = 0\,, \tag{13}$$

$$\operatorname{curl}\vec{H} - \frac{1}{c}\frac{d\vec{D}}{dt} = 0\,, \tag{14}$$

$$\operatorname{div}\vec{H} = 0\,, \tag{15}$$

$$\operatorname{div}\vec{D} = 0 \tag{16}$$

where $\vec{E} = \vec{E}(\vec{r}, t)$ and $\vec{H} = \vec{H}(\vec{r}, t)$ are the vectors of local electric and magnetic fields in acoustic medium; $\vec{D} = \vec{D}(\vec{r}, t)$ is the local electric induction in the coordinate-time space; $\vec{r}$ is the coordinate; t is the current time in space-time coordinate system.

We search a solution of Maxwell equations by introducing the vectors of magnetic and electric fields by following way

$$\vec{H} = \operatorname{curl}\vec{A}\,, \tag{17}$$

where

$$\vec{E} = -\frac{d\vec{A}}{cdt}\,, \tag{18}$$

where $\vec{A}$ is the vector potential of electromagnetic wave.

After simple calculation, we reach to following equation for vector potential $\vec{A}$ of transverse electromagnetic field

$$\nabla^2\vec{A} - \frac{\varepsilon}{c^2}\frac{d^2\vec{A}}{dt^2} = 0 \tag{19}$$

with condition of plane transverse wave

$$\operatorname{div}\vec{A} = 0\,. \tag{20}$$

The solution of (24) and (25) may present by plane transverse wave with frequency Ω which is moved by speed c_t along of direction of unit vector $\vec{s}$:

$$\vec{A} = \vec{A}_0\cos\left(Kx + \Omega t\right)\,, \tag{21}$$

and

$$\vec{A}\cdot\vec{s} = 0\,, \tag{22}$$

where $K = \frac{\Omega\sqrt{\varepsilon}}{c}$ is the wave number of transverse electromagnetic wave; $\vec{s}$ is the unit vector in direction of wave normal; $\vec{A}_0$ is the vector amplitude of vector potential. In turn, at comparting (23) and (6), we may argue that the vector of wave normal $\vec{s}$ is directed along of axis OX ($\vec{s} = \vec{e}_x$), because the vector electric transverse wave $\vec{E}$ takes a form presented in (6):

$$\vec{E} = \vec{E}_0\sin\left(Kx + \Omega t\right)\,, \tag{23}$$

where

$$\vec{E}_0 = \frac{\Omega\vec{A}_0}{c}\,.$$

To find a connection between vector amplitude of electric field $\vec{E}_0$ and vector amplitude of acoustic field $\vec{u}_0$, we use of the law conservation energy. The average density energy w_a of ultrasonic wave is transformed by one w_t of transverse electromagnetic radiation. In turn, there is a condition $w_a = w_t$ where Thus,

$$\begin{aligned} w_a &= MN\Omega^2u_0^2\lim_{T\to\infty}\tfrac{1}{2T}\int_{-T}^{T}\cos^2\left(Kx + \Omega t\right)dt = \\ &= \frac{MN\Omega^2u_0^2}{2}\,, \end{aligned} \tag{24}$$

In analogy manner,

$$w_t = \frac{\varepsilon}{4\pi}\,E_0^2\lim_{T\to\infty}\frac{1}{2T}\int_{-T}^{T}\sin^2\left(Kx + \Omega t\right)dt = \frac{\varepsilon}{8\pi}\,E_0^2\,. \tag{25}$$

Thus, at comparing (24) and (25), we arrive to an important expression which leads to foundation of dispersion law for own frequency of ion-dipole:

$$\frac{\varepsilon}{4\pi}\,E_0^2 = MN\Omega^2u_0^2\,, \tag{26}$$

where introducing meanings of $\vec{E}_0$ and ε from (7) and (11) into Eq.(26), we obtain a dispersion equation:

$$\left(\Omega_0^2 - \Omega^2\right)^2 + 2\Omega_p^2\left(\Omega_0^2 - \Omega^2\right) - \Omega_p^2\Omega^2 = 0\,, \qquad (27)$$

where $\Omega_p = \sqrt{\frac{4\pi N e^2}{M}} = \omega_p\sqrt{\frac{m}{M}}$ is the classic plasmon frequency of ion but ω_p is the plasmon frequency of electron. For solid $\omega_p \sim 10^{16}$ s^{-1}, therefore, at $\sqrt{\frac{m}{M}} \sim 10^{-2}$), it follows $\Omega_p \sim 10^{14}$ s^{-1}.

The solution of Eq.(27) in regard to own frequency of ion Ω_0 take following forms:

1. At $\Omega_0 \geqslant \Omega$

$$\Omega_0 = \sqrt{\Omega^2 - \Omega_p^2 + \sqrt{\Omega_p^4 + \Omega_p^2\Omega^2}}\,. \qquad (28)$$

2. At $\Omega_0 \leqslant \Omega$

$$\Omega_0 = \sqrt{\Omega^2 - \Omega_p^2 - \sqrt{\Omega_p^4 + \Omega_p^2\Omega^2}}\,. \qquad (29)$$

Now, consider following solutions of above presented equations:

1. At $\Omega \ll \Omega_p$, $\Omega_0 \geqslant \Omega$, we obtain $\Omega_0 \approx \sqrt{\frac{3}{2}}\Omega$ but at $\Omega_0 \leqslant \Omega$, it follows $\Omega_0 \approx \sqrt{\frac{1}{2}}\Omega$. This condition implies that we may consider model of solid as ideal gas of atoms at smaller Ω. 2. At $\Omega \gg \Omega_p$, $\Omega_0 \geqslant \Omega$ we obtain $\Omega_0 \approx \Omega + \frac{\Omega_p}{2}$ but at $\Omega_0 \leqslant \Omega$, it follows that $\Omega_0 \approx \Omega - \frac{\Omega_p}{2}$. 3. At $\Omega \approx \Omega_p$, $\Omega_0 \approx 2^{\frac{1}{4}}\Omega_p$.

In conclusion, we may note that the action of ultrasonic transverse wave in solid leads to new property as determination of own frequency of ion-dipole. This fact is useful because in the case of action of ultrasonic longitudinal wave in solid, the own frequency of ion-dipole can not be determined. However, knowledge of value of own frequency of ion-dipole allows us to calculate the intensity of sound by formulae (26) (at known meaning of intensity of transverse electromagnetic field excited by ultrasonic longitudinal wave in solid). In turn, it determines the resonance frequency ω_0 of optical light in solid because $\omega_0 = \Omega_0\sqrt{\frac{M}{m}}$ due to condition that the rigidity of spring is the same for ion-dipole and electron-ion dipole. Thus, the action of ultrasonic transverse wave on solid may change an optical property of solid.

Submitted on April 12, 2010 / Accepted on April 19, 2010

References

1. Minasyan V.N. and Samoilov V.N. The intensity of the light diffraction by supersonic longitudinal waves in solid. *Progress in Physics*, 2010, v. 2, 63.
2. Vonsovsky S.V. and Kasnelson M.N. Quantum physics of solid. Nauka, Moscow, 1983.
3. Raman C.V., Nath N.S.N. *Proc. Indian. Acad. Sci.*, 1935, v. 2, 406.
4. Estermann R. and Wannier G. *Helv. Phys. Acta*, 1936, v. 9, 520; Pockels F. Lehrduch der Kristalloptic. Leipzig, 1906.
5. Born M. and Wolf E. Principles of optics. Pergamon Press, Oxford, 1964.
6. Landau L.D. and Lifshiz E.M. Theory of elasticity. (Theoretical Physics, v. 11), Nauka, Moscow, 2003.

Predictions of High Energy Experimental Results

Eliahu Comay

Charactell Ltd., PO Box 39019, Tel-Aviv, 61390, Israel. E-mail: elicomay@post.tau.ac.il

Eight predictions of high energy experimental results are presented. The predictions contain the Σ^+ charge radius and results of two kinds of experiments using energetic pionic beams. In addition, predictions of the failure to find the following objects are presented: glueballs, pentaquarks, Strange Quark Matter, magnetic monopoles searched by their direct interaction with charges and the Higgs boson. The first seven predictions rely on the Regular Charge-Monopole Theory and the last one relies on mathematical inconsistencies of the Higgs Lagrangian density.

1 Introduction

A person who studies a well established physical theory becomes acquainted with its mathematical structure and with results of key experiments that are consistent with it. Here one generally does not pay much attention to the historical order of the development of theory and experiment. The situation is different in the case of a theory which has not yet passed the test of time. In the case of such a theory, one generally compares its conclusions with already known experimental results. However, in this situation, experiments that have not yet been performed play a specific role and one is generally inclined to be convinced of the theory's merits, if it predicts successfully experimental results that are obtained later.

This work describes eight predictions of high energy experimental results. All but one of the predictions rely on the Regular Charge-Monopole Theory (RCMT) [1, 2] and on its application to hadronic structure and processes [3]. From this point of view, the prediction of the failure to find a genuine Higgs boson makes an exception, because it relies on the inherently problematic structure of the Higgs Lagrangian density [4]. Some of the predictions refer to experiments that have not yet been carried out, whereas others refer to experiments that are performed for decades and failed to detect special objects. The second set contains the search for a monopole by means of its direct interaction with charge, glueballs, pentaquarks, nuggets of Strange Quark Matter (SQM) and the Higgs boson. In spite of a long list of experimental attempts that have ended in vain, searches for these objects still continue. The predictions made herein state that genuine particles of these kinds will not be found.

The second section presents a detailed phenomenological calculation that yields a prediction of the charge radius of the Σ^+ baryon. This outcome is higher than that of a QCD based prediction that has been published recently [5]. All other predictions are derived briefly or have already been published elsewhere. The third section contains a list of short descriptions of each of these predictions. Concluding remarks are included in the last section.

2 The Σ^+ charge radius

The prediction of the Σ^+ charge radius relies on phenomenological estimates of expectation value of spatial variables of baryonic quarks. Here the RCMT indicates a similarity between electrons in an atom and quarks in a baryons [3]. Appropriate phenomenological assumptions are explained and it is shown how their application yields the required prediction of the Σ^+ charge radius. The procedure used herein relies on the currently known data of the proton, the neutron and the Σ^- baryons [6]. The π and the k meson data are used as a justification for the calculations.

Particle	Mass (MeV)	$\langle \rho r^2 \rangle$	$\langle r \rangle$	Error
p	938.3	0.766	0.875	
n	939.6	−0.116		
Σ^-	1197.4	−0.61	0.78	0.15
π^+	139.6	0.452	0.672	
k^+	493.7	0.314	0.56	

Table 1: Known mean square charge radius ($\langle \rho r^2 \rangle$) and charge radius ($\langle r \rangle$) of hadrons.

Table 1 contains the presently known data of the mean square charge radius ($\langle \rho r^2 \rangle$) and of the corresponding charge radius of several hadrons, written in units of *fm*.

Remarks: *The experimental error refers to* $\langle \rho r^2 \rangle$. *Here the error of the* Σ^- *data is much larger than that of the other baryons. Therefore, only the* Σ^- *error is mentioned. The* π^- *and* k^- *are antiparticles of their respective positively charged counterparts and have the same spatial data.*

The three valence quarks of baryons make an important contribution to the quantities described in Table 1. Beside these quarks, it is well known that pairs of $\bar{q}q$ are found in baryons. The graphs of Fig. 1 describe the distribution of quarks and antiquarks in the proton. Two physically important properties of the proton (and of all other baryons) are inferred from the data of Fig. 1.

A. Antiquarks (namely, additional $\bar{q}q$ pairs) are explicitly seen in baryons and their probability is not negligible.

B. The x-width of antiquarks is much smaller than that of quarks. This property also proves that the Fermi motion of antiquarks is much smaller than that of quarks. Using the Heisenberg uncertainty principle, one finds that,

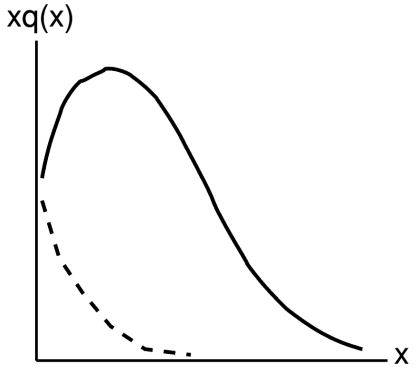

Fig. 1: The quantity $xq(x)$ is describes qualitatively as a function of x ($q(x)$ denotes quark/antiquark distribution, respectively). The solid line represents quarks and the broken line represents antiquarks. (The original accurate figure can be found on [7, see p. 281]).

> in a baryon, the volume of antiquarks is much larger than that of quarks.

These conclusions are called below Property A and Property B, respectively.

Property B is consistent with the RCMT hadronic model [3]. Indeed, in this model baryons have a core. The model assigns three positive monopole units to the baryonic core and one negative monopole unit to every quark. Now, by analogy with the electronic structure of atoms, one infers that, at the inner baryonic region, the potential of the baryonic core is not completely screened by quarks. For this reason, antiquarks, whose monopole unit has the same sign as that of the baryonic core, are pushed out to the baryonic external region and are enclosed inside a larger volume. (Property B is not discussed in QCD textbooks.)

An evaluation of experimental data of the proton indicates that the u, d quark flavors make the dominant contribution to the $\bar{q}q$ pairs and that, in the proton, the ratio between the probability of these kinds of quarks is [8]

$$\frac{\langle \bar{d} \rangle}{\langle \bar{u} \rangle} \simeq 3/2. \tag{1}$$

This ratio is used later in this work. Obviously, isospin symmetry shows that this ratio is reversed for the neutron. The excess of the additional $\bar{d}d$ quark pairs in the proton is consistent with the Pauli exclusion principle, which RCMT ascribes to the spin-1/2 quarks. Indeed, a proton contains uud valence quarks. Hence, it is energetically easier to add a $\bar{d}d$ pair than a $\bar{u}u$ pair.

The following assumption relies on Property A of Fig. 1.

I. It is assumed that, on the average, a baryon contains one additional $\bar{q}q$ pair. Thus, in the discussion carried out below, baryons contain four quarks and one antiquark. In particular, a proton contains an additional 0.6 $\bar{d}d$ fraction of a pair and 0.4 $\bar{u}u$ fraction of a pair. Isospin symmetry indicates that for a neutron, the corresponding quantities are reversed.

The calculation of the baryonic *charge radius* is not very sensitive to the accuracy of Assumption I. Indeed, each member of a $\bar{q}q$ has an opposite electric charge and their contributions partially cancel each other. Moreover, the ud quarks carry charge of opposite sign. This property further reduces the effect of the additional pairs. The discussion of the neutron data, which is carried out later, illustrates these issues.

The baryonic mean square charge radius is obtained below as a sum of the contribution of the baryon's individual quarks. Thus, the following notation is used for a quark q and a baryon b

$$R^2(q_i, b) \equiv \int r^2 \psi_i^\dagger \psi_i \, d^3x, \tag{2}$$

where $\psi_i^\dagger \psi_i$ represents the single particle density of a q_i quark. (Below, ψ is not used explicitly, and the value of $R^2(q, b)$ is derived phenomenologically from the data of Table 1.) Thus, $R^2(u, p)$ denotes the value of (2) for one of the proton's u quarks. Analogous expressions are used for other quark flavors and for other baryons. It follows that the contribution of each quark to the baryonic *mean square charge radius* is obtained as a product $QR^2(q, b)$, where Q denotes the charge of the respective quark. Relying on isospin symmetry, one defines Assumption II:

$$R^2(u, p) = R^2(d, p) = R^2(u, n) = R^2(d, n) \equiv R^2, \tag{3}$$

where the last symbol is used for simplifying the notation.

As explained above, both the data depicted in Fig. 1 and the RCMT model of hadrons [3], indicate that the volume of baryonic antiquarks is larger than that of the corresponding quarks (herein called Property B). Therefore, by analogy of (3), the following definition is used for the proton/neutron antiquarks

$$R^2(\bar{u}, p) = R^2(\bar{d}, p) = R^2(\bar{u}, n) = R^2(\bar{d}, n) = \lambda R^2, \tag{4}$$

where $\lambda > 1$ is a numerical parameter.

The foregoing arguments and the data of Table 1 enable one to equate the experimental value of the proton's mean square charge radius with the quantities defined above

$$0.766 = 2\,\frac{2}{3}R^2 - \frac{1}{3}R^2 - 0.4\,(\lambda - 1)\,\frac{2}{3}R^2 + 0.6\,(\lambda - 1)\,\frac{1}{3}R^2 =$$
$$= R^2 - 0.2\,(\lambda - 1)\,\frac{1}{3}R^2. \tag{5}$$

The terms on the right hand side of the first line of (5) are defined as follows. The first term represents the contribution of the two uu valence quarks; the second term is for the single d quark; the third term is for the $\bar{u}u$ pair; the last term is for the $\bar{d}d$ pair.

An analogous treatment is applied to the neutron and the result is

$$-0.116 = \frac{2}{3}R^2 - 2\,\frac{1}{3}R^2 - 0.6\,(\lambda - 1)\,\frac{2}{3}R^2 + 0.4\,(\lambda - 1)\,\frac{1}{3}R^2 =$$
$$= -0.8\,(\lambda - 1)\,\frac{1}{3}R^2. \tag{6}$$

Here one sees once again the merits of the RCMT model of hadrons [3]. Thus, the fact that the proton's antiquarks volume is larger than that of its quarks means that $\lambda > 1$, as seen in (4). Obviously, the final result of (6) proves that this relation is mandatory for explaining the *sign* of the experimental value of the neutron's mean square charge radius. It is also evident that the contribution of the quark-antiquark pair to R^2 is small.

The neutron relation (6) enables the removal of the λ parameter from (5). Thus, one finds that

$$R^2 = 0.766 + 0.116/4 = 0.795. \tag{7}$$

This value of R^2 will be used in the derivation of the prediction for the charge radius of the Σ^+ baryon.

Let us turn to the Σ^- baryon whose valence quarks are dds. The u, d quarks of the previous discussion are regarded as particles having (practically) the same mass and a different electric charge. This is the underlying basis of isospin symmetry. It is also agreed that the s quark is heavier. Indeed, the following data support this statement. Thus, the experimental mass difference (in MeV) of the k, π mesons is [6]

$$M(k^+) - M(\pi^+) = 493.7 - 139.6 = 354.1 \tag{8}$$

and the difference between the isospin average of the $\Sigma^{\pm}$ and the nucleons is

$$\frac{1}{2}\left(M(\Sigma^+) + M(\Sigma^-) - M(p) - M(n)\right) = \\ = \frac{1}{2}(1197.4 + 1189.4 - 938.3 - 939.6) = 254.5. \tag{9}$$

In each of the previous relations, the mass difference between two hadrons, where an s quark replaces a u (or d) quark is positive. This outcome indicates that the s quark is indeed heavier than the u quark.

The RCMT model of baryons and mesons [3] is analogous to the atomic structure of electrons and to the positronium, respectively. The results of (8) and (9) show that replacing a u (or d) quark by an s quark in a nucleon yields more binding energy than doing it in a pion. This outcome is consistent with the RCMT model. Indeed, in a meson, an s quark is attracted just by the field of one antiquark that carries *one* monopole unit. On the other hand, in a nucleon, the s quark is attracted by the baryonic core that carries *three* monopole units. Like in the atomic case, the field of the core is not completely screened by the other quarks. (A QCD explanation of this phenomenon is certainly less obvious.)

Let us turn to the problem of the s quark single particle radial distribution. Thus, if a u (or d) quark is replaced by the heavier s quark, then the s quark mean radius will be smaller than that of the u quark. This conclusion is supported both by the mass dependence of the radial function of a Dirac solution of the Hydrogen atom (see [9, see p. 55] and by a comparison of the experimental k and π radii of Table 1. For this reason, it is defined here that

$$R^2(s, \Sigma^-) = \eta R^2, \tag{10}$$

where $0 < \eta < 1$ is a yet undefined parameter.

By analogy with the case of atomic electrons, one should expect that the negative monopole of the s quark, which is closer to the core, partially *screens* the potential of the positive monopole at the baryonic core. Therefore, one may expect a somewhat larger size for the d quarks of the Σ^- baryon

$$R^2(d, \Sigma^-) = \xi R^2, \tag{11}$$

where $\xi > 1$ is another undefined parameter.

Like the neutron, whose valence quarks are udd, the Σ^- valence quarks dds contains a pair of d quarks. Hence, it is assumed here that the contribution of a quark-antiquark pair to the Σ^- mean square charge radius is the same as that of the neutron (6). (As shown above, the contribution of this effect is relatively small, and the final result is not sensitive to a small change of this quantity.) Taking the experimental value of the Σ^- from Table 1, one uses (6), (7), (10), and (11) and writes the following relation for the two undetermined parameters ξ, η

$$-0.61 \pm \delta = -2\,\frac{1}{3}\,0.795\,\xi - \frac{1}{3}\,0.795\,\eta - 0.116, \tag{12}$$

where δ is related to the error assigned to the measurement of the mean square charge radius of the Σ^- baryon (see Table 1).

Taking into account the constraint on ξ, η, one finds that relation (12) does not hold for $\delta = 0$. Table 2 describes some pairs of values of the parameters ξ, η and their relation to δ. It is shown below how each pair of the ξ, η parameters of Table 2 yields a prediction of the Σ^+ mean square charge radius.

The Σ^+ baryon contains the uus valence quarks and it is the isospin counterpart of the Σ^- baryon. Hence, the spatial properties of its u quarks are the same as those of the d quarks of the Σ^- baryon. Also the s quark of these baryons is assumed to have the same spatial properties. The small effect of the quark-antiquark pairs is equated to that of the proton, because both have a pair of uu valence quarks. Thus, the phenomenological formula for the mean square charge radius of the Σ^+ baryon is

$$R^2(\Sigma^+) = 2\,\frac{2}{3}\,0.795\,\xi - \frac{1}{3}\,0.795\,\eta - 0.029, \tag{13}$$

where $R^2(b)$ denotes the mean square charge radius of the baryon b. Substituting the values of each pair of the parameters ξ, η into (13), one obtains a predictions for $R^2(\Sigma^+)$. It is clear from the details of the discussion presented above that a prediction of $R^2(\Sigma^+)$ must carry the estimated experimental error of the mean square charge radius of the Σ^- baryon *and*

δ	ξ	η
−15	1.0	0.43
−15	1.05	0.33
−15	1.1	0.23
−10	1.12	0.0
−5	1.03	0.0

Table 2: Several values of ξ and η of (12).

the uncertainties of the assumptions used herein. Thus, the final prediction is given (in fm^2):

$$0.85 \leqslant R^2(\Sigma^+) \leqslant 1.17. \quad (14)$$

The prediction for the charge radius (in fm) is

$$0.91 \leqslant R(\Sigma^+) \leqslant 1.12. \quad (15)$$

The range of these predictions is higher than that of a QCD dependent prediction which has been published recently [5].

3 The other seven high energy predictions

This section presents seven predictions of high energy experimental results.

- High Energy pion beams exist. Thus, in principle, the experiment described here can be performed in the near future. The RCMT basis for a prediction of the elastic $\pi - \pi$ cross section is explained. Unlike protons (see [10] and references therein), pions are characterized by a pair of quark-antiquark and *they do not have inner quark shells*. Moreover, in a deep inelastic $e - p$ experiment, the electron collides with one quark at a time. This property should also hold for the quark-quark interaction in a $\pi-\pi$ collision. Therefore, relying on RCMT, where quarks carry one monopole unit, the $\pi - \pi$ elastic cross section is analogous to the elastic cross section of colliding charges. It is well known that this cross section decreases with the increase of the collision energy (see chapter 6 of [7]).

  Prediction: Unlike the proton case, where the elastic cross section increases for collision energy which is greater than that of point C of Fig. 2, a decrease of the elastic cross section is predicted for a $\pi - \pi$ scattering. Hence, its graph will not increase for energies which are not too close to a resonance. In particular, no similar effect like the rise of the $p - p$ cross section on the right hand side of point C will be found in a $\pi - \pi$ collision. By the same token, for a very high energy $\pi - \pi$ scattering, the ratio of the elastic cross section to the total cross section will be much smaller then that of the $p - p$ cross section of Fig. 2, which is about 1/6.

- The problem of the portion of the pion's momentum carried by quarks. The deep inelastic $e - p$ scattering data are used for calculating the relative portion of the proton's momentum carried by quarks, as seen in a frame where the proton's momentum is very very large. It turns out that for a proton, the overall quarks' portion is about one half of the total momentum. The RCMT proves that baryons have a core and that this is the reason for the effect. Mesons are characterized as a bound $\bar{q}q$ pair and they *do not have a core*. This is the basis for the following prediction:

  Unlike the proton case, it is predicted that an analogous experiment of deep inelastic $e - \pi$ scattering will prove that in this case the pion's quarks carry all (or nearly all) the pion's momentum.

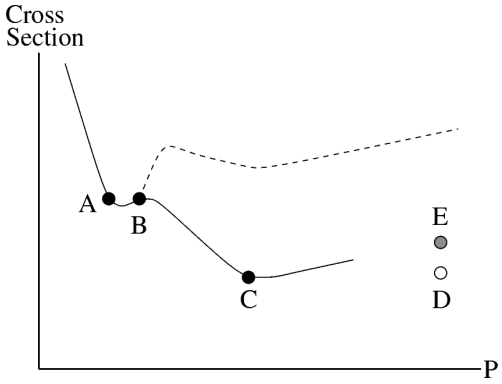

Fig. 2: A qualitative description of the pre-LHC proton-proton cross section versus the laboratory momentum P. Axes are drawn in a logarithmic scale. The solid line denotes the elastic cross section and the broken line denotes the total cross section. (The accurate figure can be found in [6].)

- Several decades ago, claims concerning the existence of glueballs have been published by QCD supporters (see [11], p. 100). RCMT describes the strong interactions as interactions between monopoles that satisfy the RCMT equations of motion. Here, no gluon exist. A fortiori, a genuine glueball does not exist. On April 14, 2010, Wikipedia says that glueballs "have (as of 2009) so far not been observed and identified with certainty."

- Several decades ago, claims concerning the existence of pentaquarks have been published by QCD supporters [12, 13]. Pentaquarks are supposed to be strongly bound states of a baryon and a meson. RCMT clearly contradicts the existence of these kinds of objects. Indeed, like nucleons, all hadrons are neutral with respect to monopoles. Hence, like the nuclear force, a hadron-hadron interaction has residual features. In a deuteron the proton-neutron binding energy is about 2.2 MeV. Let us compare this value to what is expected for a baryon-meson binding energy. For each flavor, the lightest meson, which is the best candidate for assembling a pentaquark, is a spin-0 particle, which resembles a noble gas. Hence, the binding energy of a nucleon with this kind of meson should be even smaller

than the 2.2 MeV binding energy of the deuteron. For this reason, strongly bound pentaquarks should not exist. Experimental results are consistent with this theoretical conclusion [14].

- Several decades ago, claims concerning the existence of SQM have been published by QCD supporters [15]. RCMT clearly contradicts the existence of this kind of matter. Indeed, an SQM is a nugget of Λ baryons. Now the mass of a Λ baryon is greater than the nucleon mass by more than 170 MeV. On the other hand, the Λ binding energy in an SQM should be similar to the nucleon binding energy in a nucleus, which is about 8 MeV per nucleon. This very large difference between energy values proves that the SQM is unstable and will disintegrate like a free Λ. Experimental results are consistent with this theoretical conclusion [16].
- RCMT proves that there is no *direct* charge-monopole interaction. Radiation fields (namely, real photons) interact with charges *and* with monopoles. As of today, experimental attempts to detect monopoles rely on a direct interaction of the monopole fields with charges of the measuring device. As stated above, such an interaction does not exist. Hence, no genuine monopole will be detected. This prediction has been made about 25 years ago [17]. In spite of a very long search, all attempts to detect monopoles have ended in vain [6, see p. 1209]. Monopole search continues [18].
- A genuine Higgs boson will not be found. For a theoretical discussion, see the first four sections of [4]. This conclusion relies on inherent inconsistencies of the Higgs Lagrangian density.

4 Concluding remarks

A physical theory is tested by its consistency with experimental results that belong to the theory's domain of validity. A second kind of test is the demand that the examined theory has a solid mathematical structure. However, one does not really think that a theory having an erroneous mathematical structure can fit all experimental data. Therefore, one may argue that a test of the theory's mathematical structure plays an auxiliary role. On the other hand, an analysis of the mathematical structure can provide convincing arguments for disqualifying incorrect theories. The present work concentrates on the examination of the fit of high energy theories to the data.

In undertaking this task, one realizes that the historical order of formulating the theory's predictions and carrying out the required experiments bears no fundamental meaning. Thus, at this point, one may state that making a prediction that is later found to be successful is *at least* as good as deriving a theoretical result that fits a known measurement. This is certainly an incomplete description of the problem. Indeed, many predictions depend on numerical value of adjustable parameters that yield the required quantity. Therefore, in the case of a theory that is not fully established, a successful prediction that is *later* confirmed by measurement provides a significantly better support for it. This aspect is one of the motivations for writing the present work which contains eight different predictions. Let us wait and see what will come out of the experimental work.

Submitted on April 19, 2010 / Accepted on April 23, 2010

References

1. Comay E. Axiomatic deduction of equations of motion in Classical Electrodynamics. *Nuovo Cimento B*, 1984, v. 80, 159–168.
2. Comay E. Charges, Monopoles and duality relations. *Nuovo Cimento B*, 1995, v. 110, 1347–1356.
3. Comay E. A regular theory of magnetic monopoles and its implications. In: *Has the Last Word Been Said on Classical Electrodynamics?* Editors: Chubykalo A., Onoochin V., Espinoza A.R. and Smirnov-Rueda R. Rinton Press, Paramus (NJ), 2004.
4. Comay E. Physical consequences of mathematical principles. *Prog. in Phys.*, 2009, v. 4, 91–98.
5. Wang P., Leinweber D. B., Thomas A. W. and Young R. D. Chiral extrapolation of octet-baryon charge radii. *Phys. Rev. D*, 2009, v. 79, 094001-1–094001-12.
6. Amsler C. et al. Review of particle physics. *Phys. Lett. B*, 2008, v. 667, 1–1340.
7. Perkins D. H. Introduction to high energy physics. Addison-Wesley, Menlo Park (CA), 1987.
8. Alberg M. Parton distributions in hadrons. *Prog. Part. Nucl. Phys.*, 2008, v. 61, 140–146.
9. Bjorken J. D. and Drell S. D. Relativistic quantum mechanics. McGraw-Hill, New York, 1964.
10. Comay E. On the significance of the upcoming large hadron collider proton-proton cross section data. *Prog. in Phys.*, 2010 v. 2, 56–59.
11. Frauenfelder H. and Henley E. M. Subatomic physics. Prentice Hall, Englewood Cliffs, 1991.
12. Gignoux C., Silvestre-Brac B. and Richard J.M. Possibility of stable multiquark baryons. *Phys. Lett.*, 1987, v. 193, 323–326.
13. Lipkin H.J. New possibilities for exotic hadrons — anticharmed strange baryons. *Phys. Lett.*, 1987, v. 195, 484–488.
14. Whole C.G. (in the 2009 report of PDG). See: http://pdg.lbl.gov/2009/reviews/rpp2009-rev-pentaquarks.pdf
15. Witten E. Cosmic separation of phases. *Phys. Rev. D*, 1984, v. 30, 272–285.
16. Han K. et al. Search for stable strange quark matter in Lunar soil. *Phys. Rev. Lett.*, 2009, v.103, 092302-1–092302-4.
17. Comay E. Will magnetic monopoles be detected in our instruments? *Lett. Nuovo Cimento*, 1985, v. 43, 150–152.
18. A monopole search is planned to be carried out at the LHC. See: http://cdsweb.cern.ch/record/1243082

Neutrosophic Diagram and Classes of Neutrosophic Paradoxes or to the Outer-Limits of Science

Florentin Smarandache

Department of Mathematics, University of New Mexico, Gallup, NM 87301, USA. E-mail: smarand@unm.edu

These paradoxes are called "neutrosophic" since they are based on indeterminacy (or neutrality, i.e. neither true nor false), which is the third component in neutrosophic logic. We generalize the Venn diagram to a Neutrosophic Diagram, which deals with vague, inexact, ambiguous, illdefined ideas, statements, notions, entities with unclear borders. We define the neutrosophic truth table and introduce two neutrosophic operators (neuterization and antonymization operators) give many classes of neutrosophic paradoxes.

1 Introduction to the neutrosophics

Let <*A*> be an idea, or proposition, statement, attribute, theory, event, concept, entity, and <*non A*> what is not <*A*>.

Let <*anti A*> be the opposite of <*A*>. We have introduced a new notation [1998], <*neut A*>, which is neither <*A*> nor <*anti A*> but in between. <*neut A*> is related with <*A*> and <*anti A*>.

Let's see an example for vague (not exact) concepts: if <*A*> is *"tall"* (an attribute), then <*anti A*> is *"short"*, and <*neut A*> is *"medium"*, while <*non A*> is *"not tall"* (which can be *"medium or short"*). Similarly for other <*A*>, <*neut A*>, <*anti A*> such as: <*good*>, <*so so*>, <*bad*>, or <*perfect*>, <*average*>, <*imperfect*>, or <*high*>, <*medium*>, <*small*>, or respectively <*possible*>, <*sometimes possible and other times impossible*>, <*impossible*>, etc.

Now, let's take an exact concept / statement: if <*A*> is the statement "1 + 1 = 2 *in base* 10" , then <*anti A*> is "1 + 1 ≠ 2 *in base* 10", while <*neut A*> is undefined (doesn't exist) since it is not possible to have a statement in between "1 + 1 = 2 *in base* 10" and "1 + 1 ≠ 2 *in base* 10" because in base 10 we have 1+1 is either equal to 2 or 1+1 is different from 2. <*non A*> coincides with <*anti A*> in this case, <*non A*> is "1 + 1 ≠ 2 *in base* 10".

Neutrosophy is a theory the author developed since 1995 as a generalization of dialectics. This theory considers every notion or idea <*A*> together with its opposite or negation <*anti A*>, and the spectrum of "neutralities" in between them and related to them, noted by <*neut A*>.

The Neutrosophy is a new branch of philosophy which studies the origin, nature, and scope of neutralities, as well as their interactions with different ideational spectra.

Its Fundamental Thesis:
Any idea <*A*> is *T*% true, *I*% indeterminate (i.e. neither true nor false, but neutral, unknown), and *F*% false.

Its Fundamental Theory:
Every idea <*A*> tends to be neutralized, diminished, balanced by <*non A*> ideas (not only by <*anti A*> as Hegel asserted) — as a state of equilibrium.

In between <*A*> and <*anti A*> there may be a continuous spectrum of particular <*neut A*> ideas, which can balance <*A*> and <*anti A*>.

To neuter an idea one must discover all its three sides: of sense (truth), of nonsense (falsity), and of undecidability (indeterminacy) — then reverse/combine them. Afterwards, the idea will be classified as neutrality.

There exists a *Principle of Attraction* not only between the opposites <*A*> and <*anti A*> (as in dialectics), but also between them and their neutralities <*neut A*> related to them, since <*neut A*> contributes to the *Completeness of Knowledge*.

Hence, neutrosophy is based not only on analysis of oppositional propositions as dialectic does, but on analysis of these contradictions together with the neutralities related to them.

Neutrosophy was extended to Neutrosophic Logic, Neutrosophic Set, Neutrosophic Probability and Neutrosophic Statistics, which are used in technical applications.

In the *Neutrosophic Logic* (which is a generalization of fuzzy logic, especially of intuitionistic fuzzy logic) every logical variable x is described by an ordered triple $x = (T, I, F)$, where T is the degree of truth, F is the degree of falsehood, and I the degree of indeterminacy (or neutrality, i.e. neither true nor false, but vague, unknown, imprecise), with T, I, F standard or non-standard subsets of the non-standard unit interval $]^{-}0, 1^{+}[$. In addition, these values may vary over time, space, hidden parameters, etc.

Neutrosophic Probability (as a generalization of the classical probability and imprecise probability) studies the chance that a particular event <*A*> will occur, where that chance is represented by three coordinates (variables): *T*% chance the event will occur, *I*% indeterminate (unknown) chance, and *F*% chance the event will not occur.

Neutrosophic Statistics is the analysis of neutrosophic probabilistic events.

Neutrosophic Set (as a generalization of the fuzzy set, and especially of intuitionistic fuzzy set) is a set such that an element belongs to the set with a neutrosophic probability,

i.e. T degree of appurtenance (membership) to the set, I degree of indeterminacy (unknown if it is appurtenance or non-appurtenance to the set), and F degree of non-appurtenance (non-membership) to the set.

There exist, for each particular idea: PRO parameters, CONTRA parameters, and NEUTER parameters which influence the above values.

Indeterminacy results from any hazard which may occur, from unknown parameters, or from new arising conditions. This resulted from practice.

2 Applications of neutrosophics

Neutrosophic logic/set/probability/statistics are useful in artificial intelligence, neural networks, evolutionary programming, neutrosophic dynamic systems, and quantum mechanics.

3 Examples of neutrosophy used in Arabic philosophy (F. Smarandache and S. Osman)

- While Avicenna promotes the idea that the world is contingent if it is necessitated by its causes, Averroes rejects it, and both of them are right from their point of view.

  Hence <*A*> and <*anti A*> have common parts.
- Islamic dialectical theology (*kalam*) promoting creationism was connected by Avicenna in an extraordinary way with the opposite Aristotelian-Neoplatonic tradition.

  Actually a lot of work by Avicenna falls into the frame of neutrosophy.
- Averroes's religious judges (*qadis*) can be connected with atheists' believes.
- al-Farabi's metaphysics and general theory of emanation vs. al-Ghazali's Sufi writings and mystical treatises [we may think about a coherence of al-Ghazali's "Incoherence of the Incoherence" book].
- al-Kindi's combination of Koranic doctrines with Greek philosophy.
- Islamic Neoplatonism + Western Neoplatonism.
- Ibn−Khaldun's statements in his theory on the cyclic sequence of civilizations, says that:

  Luxury leads to the raising of civilization (because the people seek for comforts of life) but also Luxury leads to the decay of civilization (because its correlation with the corruption of ethics).
- On the other hand, there's the method of absent−by−present syllogism in jurisprudence, in which we find the same principles and laws of neutrosophy.
- In fact, we can also function a lot of Arabic aphorisms, maxims, Koranic miracles (Ayat Al- Qur'an) and Sunna of the prophet, to support the theory of neutrosophy.

Take the colloquial proverb that "The continuance of state is impossible" too, or "Everything, if it's increased over its extreme, it will turn over to its opposite"!

4 The Venn diagram

In a Venn diagram we have with respect to a universal set U the following:

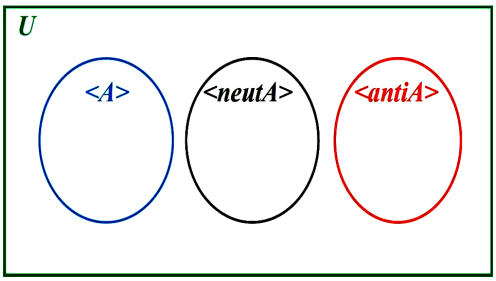

Fig. 1: Venn diagram

Therefore, there are no common parts amongst <*A*>, <*neut A*>, and <*anti A*>, and all three of them are (completely) contained by the universal set U. Also, all borders of these sets <*A*>, <*neut A*>, <*anti A*>, and U are clear, exact. All these four sets are well−defined.

While <*neut A*> means neutralities related to <*A*> and <*anti A*>, what is outside of <*A*> U <*neut A*> U <*anti A*> but inside of U are other neutralities, not related to <*A*> or to <*anti A*>.

Given <*A*>, there are two types of neutralities: those related to <*A*> (and implicitly related to <*anti A*>), and those not related to <*A*> (and implicitly not related to <*anti A*>)

5 The neutrosophic diagram, as extension of the Venn diagram

Yet, for ambiguous, vague, not-well-known (or even unknown) imprecise ideas / notions / statements / entities with unclear frontiers amongst them the below relationships may occur because between an approximate idea noted by <*A*> and its opposite <*anti A*> and their neutralities <*neut A*> there are not clear delimitations, not clear borders to distinguish amongst what is <*A*> and what is not <*A*>. There are buffer zones in between <*A*> and <*anti A*> and <*neut A*>, and an element x from a buffer zone between <*A*> and <*anti A*> may or may not belong to both <*A*> and <*anti A*> simultaneously. And similarly for an element y in a buffer zone between <*A*> and <*neut A*>, or an element z in the buffer zone between <*neut A*> and <*anti A*>. We may have a buffer zone where the confusion of appurtenance to <*A*>, or to <*neut A*>, or to <*anti A*> is so high, that we can consider that an element w belongs to all of them simultaneously (or to none of them simultaneously).

We say that all four sets <*A*>, <*neut A*>, <*anti A*>, and the neutrosophic universal set U are illdefined, inexact, unknown (especially if we deal with predictions; for example

if <*A*> is a statement with some degree of chance of occurring, with another degree of change of not occurring, plus an unknown part). In the general case, none of the sets <*A*>, <*neut A*>, <*anti A*>, <*non A*> are completely included in *U*, and neither *U* is completely known; for example, if *U* is the neutrosophic universal set of some specific given events, what about an unexpected event that might belong to *U*? That's why an approximate *U* (with vague borders) leaves room for expecting the unexpected.

The *Neutrosophic Diagram* in the general case is the following (Fig. 2): the borders of <*A*>, <*anti A*>, and <*neut A*> are dotted since they are unclear.

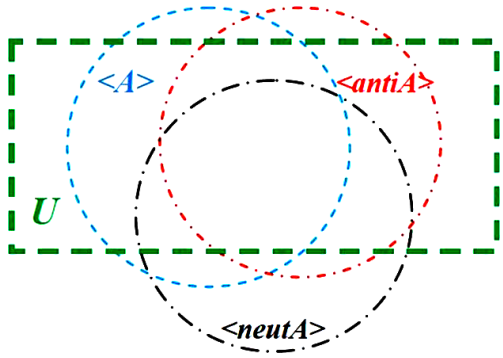

Fig. 2: Neutrosophic Diagram

Similarly, the border of the neutrosophic universal set *U* is dotted, meaning also unclear, so *U* may not completely contain <*A*>, nor <*neut A*> or <*anti A*>, but *U* "approximately" contains each of them. Therefore, there are elements in <*A*> that may not belong to *U*, and the same thing for <*neut A*> and <*anti A*>. Or elements, in the most ambiguous case, there may be elements in <*A*> and in <*neut A*> and in <*anti A*> which are not contained in the universal set *U*.

Even the neutrosophic universal set is ambiguous, vague, and with unclear borders.

Of course, the intersections amongst <*A*>, <*neut A*>, <*anti A*>, and *U* may be smaller or bigger or even empty depending on each particular case.

See below an example of a particular neutrosophic diagram (Fig. 3), when some intersections are contained by the neutrosophic universal set:

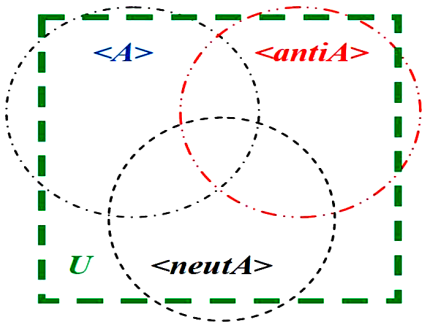

Fig. 3: Example of a particular neutrosophic diagram

A neutrosophic diagram is different from a Venn diagram since the borders in a neutrosophic diagram are vague. When all borders are exact and all intersections among <*A*>, <*neut A*>, and <*anti A*> are empty, and all <*A*>, <*neut A*>, and <*anti A*> are included in the neutrosophic universal set *U*, then the neutrosophic diagram becomes a Venn diagram.

The neutrosophic diagram, which complies with the neutrosophic logic and neutrosophic set, is an extension of the Venn diagram.

6 Classes of neutrosophic paradoxes

The below classes of neutrosophic paradoxes are not simply word puzzles. They may look absurd or unreal from the classical logic and classical set theory perspective. If <*A*> is a precise / exact idea, with well-defined borders that delimit it from others, then of course the below relationships do not occur.

But let <*A*> be a vague, imprecise, ambiguous, not-well-known, not-clear-boundary entity, <*non A*> means what is not <*A*>, and <*anti A*> means the opposite of <*A*>. <*neut A*> means the neutralities related to <*A*> and <*anti A*>, neutralities which are in between them.

When <*A*>, <*neut A*>,<*anti A*>,<*non A*>, *U* are uncertain, imprecise, they may be selfcontradictory. Also, there are cases when the distinction between a set and its elements is not clear.

Although these neutrosophic paradoxes are based on "pathological sets" (those whose properties are considered atypically counterintuitive), they are not referring to the theory of Meinongian objects (*Gegenstandstheorie*) such as round squares, unicorns, etc. Neutrosophic paradoxes are not reported to objects, but to vague, imprecise, unclear ideas or predictions or approximate notions or attributes from our everyday life.

7 Neutrosophic operators

Let's introduce for the first time two new Neutrosophic Operators:

1. An operator that "neuterizes" an idea. To **neuterize** [*neuter+ize*, transitive verb; from the Latin word *neuter* = neutral, in neither side], $\mathfrak{n}(.)$, means to map an entity to its neutral part. [We use the Segoe Print for "*n*(.)".]
   "To neuterize" is different from "to neutralize" [from the French word *neutraliser*] which means to declare a territory neutral in war, or to make ineffective an enemy, or to destroy an enemy.
   $\boldsymbol{n}$(<*A*>) = <*neut A*>. By definition $\mathfrak{n}$(<*neut A*>) = <*neut A*>.
   For example, if <*A*> is "tall", then $\boldsymbol{n}(tall) = medium$, also $\boldsymbol{n}(short) = medium$, $\boldsymbol{n}(medium) = medium$.
   But if <*A*> is "1 + 1 = 2 *in base* 10" then $\mathfrak{n}$(<1 + 1 = 2 *in base* 10>) is undefined (does not exist), and similarly $\mathfrak{n}$(<1 + 1 ≠ 2 *in base* 10>) is undefined.

2. And an operator that "antonymizes" an idea. **To antonymize** [*antonym+ize*, transitive verb; from the Greek work *antōnymia* = instead of, opposite], $\mathfrak{a}(.)$, means to map an entity to its opposite. [We use the Segoe Print for $\mathfrak{a}(.)$] $\mathfrak{a}(<A>) = <anti\ A>$.

   For example, if $<A>$ is "*tall*", then $\mathfrak{a}(tall) = short$, also $\mathfrak{a}(short) = tall$, and $\mathfrak{a}(medium) = tall\ or\ short$.

   But if $<A>$ is "$1 + 1 = 2\ in\ base\ 10$" then $\mathfrak{a}(<1 + 1 = 2\ in\ base\ 10>) = <1+1 \neq 2\ in\ base\ 10>$ and reciprocally $\mathfrak{a}(<1 + 1 \neq 2\ in\ base\ 10>) = <1 + 1 = 2\ in\ base\ 10>$.

The classical operator for *negation / complement* in logics respectively in set theory, "*to negate*" ($\neg$), which is equivalent in neutrosophy with the operator " *to nonize*" (i.e. to *non+ize*) or *nonization* (i.e. *non+ization*), means to map an idea to its neutral or to its opposite (a union of the previous two neutrosophic operators: *neuterization and antonymization*):
$\neg<A> = <non\ A> = <neut\ A> \cup <anti\ A> = \mathfrak{n}(<A>) \cup \mathfrak{a}(<A>)$.

Neutrosophic Paradoxes result from the following *neutrosophic logic / set connectives* following all apparently impossibilities or semi-impossibilities of neutrosophically connecting $<A>$, $<anti\ A>$, $<neut\ A>$, $<non\ A>$, and the neutrosophic universal set U.

8 Neutrosophic truth tables

For $<A>$ = "*tall*":

$<A>$	$\mathfrak{a}(<A>)$	$\mathfrak{n}(<A>)$	$\neg<A>$
tall	short	medium	short or medium
medium	short or tall	medium	short or tall
short	tall	medium	tall or medium

To remark that $\boldsymbol{n}(<medium>) \triangleq medium$. If $<A> = tall$, then $<neut\ A> = medium$, and $<neut(neut\ A)> = <neut\ A>$, or $\boldsymbol{n}(<\boldsymbol{n}(<A>)>) = n(<A>)$.

For $<A>$ = "$1 + 1 = 2\ in\ base\ 10$" we have $<anti\ A> = <non\ A>$ = "$1 + 1 \neq 2\ in\ base\ 10$", while $<neut\ A>$ is undefined (N/A) — whence the neutrosophic truth table becomes:

$<A>$	$\boldsymbol{a}(<A>)$	$\boldsymbol{n}(<A>)$	$\neg<A>$
True	False	N/A	False
False	True	N/A	True

In the case when a statement is given by its neutrosophic logic components $<A> = (T, I, F)$, i.e. $<A>$ is $T\%$ true, $I\%$ indeterminate, and $F\%$ false, then the neutrosophic truth table depends on the defined neutrosophic operators for each application.

9 Neutrosophic operators and classes of neutrosophic paradoxes

a) **Complement/Negation**
$\neg<A> \neq <non\ A>$ and reciprocally $\neg<non\ A> \neq <A>$.
$\neg(\neg<A>) \neq <A>$
$\neg(\neg<anti\ A>) \neq <anti\ A>$
$\neg(\neg<non\ A>) \neq <non\ A>$
$\neg(\neg<neut\ A>) \neq <neut\ A>$
$\neg(\neg U) \neq U$, where $U$is the neutrosophic universal set. $\neg(\neg<\varnothing>) \neq <\varnothing>$, where $<\varnothing>$ is the neutrosophic empty set.

b) **Neuterization**
$\boldsymbol{n}(<A>) \neq <neut\ A>$
$\boldsymbol{n}(<anti\ A>) \neq <neut\ A>$
$\boldsymbol{n}(<non\ A>) \neq <neut\ A>$
$\boldsymbol{n}(\boldsymbol{n}(<A>)) \neq <A>$

c) **Antonymization**
$\boldsymbol{a}(<A>) \neq <anti\ A>$
$\boldsymbol{a}(<anti\ A>) \neq <A>$
$\boldsymbol{a}(<non\ A>) \neq <A>$
$\boldsymbol{a}(\boldsymbol{a}(<A>)) \neq <A>$

d) **Intersection/Conjunction**
$<A> \cap <non\ A> \neq \varnothing$ (neutrosophic empty set) [symbolically $(\exists x)(x \in A \wedge x \in \neg A)$],
or even more $<A> \cap <anti\ A> \neq \varnothing$ [symbolically $(\exists x)(x \in A \wedge x \in \boldsymbol{a}(A))$],
similarly $<A> \cap <neut\ A> \neq \varnothing$ and $<anti\ A> \cap <neut\ A> \neq \varnothing$,
up to $<A> \cap <neut\ A> \cap <anti\ A> \neq \varnothing$.
The symbolic notations will be in a similar way.
This is *Neutrosophic Transdisciplinarity*, which means to find common features to uncommon entities.
For examples:
There are things which are good and bad in the same time.
There are things which are good and bad and medium in the same time (because from one point of view they may be god, from other point of view they may be bad, and from a third point of view they may be medium).

e) **Union / Weak Disjunction**
$<A> \cup <neut\ A> \cup <anti\ A> \neq U$.
$<anti\ A> \cup <neut\ A> \neq <non\ A>$.
Etc.

f) **Inclusion/Conditional**
$<A> \subset <anti\ A>$
$(\forall x)(x \in A \rightarrow x \in \boldsymbol{a}(A))$
All is $<anti\ A>$, the $<A>$ too.
All *good* things are also *bad*.
All is *imperfect*, the *perfect* too.

$<anti\ A> \subset <A>$
$(\forall x)(x \in \boldsymbol{a}(A) \rightarrow x \in A)$
All is $<A>$, the $<anti\ A>$ too.
All *bad* things have something *good* in them [this is rather a fuzzy paradox].
All is *perfect* things are *imperfect* in some degree.

$<non\ A> \subset <A>$
$(\forall x)(x \in \neg A \rightarrow x \in A)$
All is $<A>$, the $<non\ A>$ too.
All *bad* things have something *good* and something *medium* in them [this is a neutrosophic paradox, since it is based on good, bad, and medium].
All is *perfect* things have some *imperfectness* and *mediocrity* in them at some degree.
$<A> \subset <neut\ A>$
$(\forall x)(x \in A \rightarrow x \in \boldsymbol{n}(A))$
All is $<neutA>$, the $<A>$ too.

$<non\ A> \subset <neutA>$ [partial neutrosophic paradox of inclusion]
$(\forall x)(x \in \neg A \rightarrow x \in \boldsymbol{n}(A))$
All is $<neutA>$, the $<non\ A>$ too.
$<non\ A> \subset <antiA>$ [partial neutrosophic paradox of inclusion]
$(\forall x)(x \in \neg A \rightarrow x \in \boldsymbol{a}(A))$
All is $<antiA>$, the $<non\ A>$ too.
$<antiA> \subset <neut\ A>$
$(\forall \mathtt{x})(\mathtt{x} \in \boldsymbol{a}(A) \rightarrow \mathtt{x} \in \boldsymbol{n}(\mathtt{A}))$
All is $<neut\ A>$, the $<anti\ A>$ too.
$<A> \cup <anti\ A> \subset <neut\ A>$
$(\forall \mathtt{x})((x \in \mathtt{A} \vee \mathtt{x} \in \boldsymbol{a}(\mathtt{A})) \rightarrow \mathtt{x} \in \boldsymbol{n}(\mathtt{A}))$
All is $<neutA>$, the $<A>$ and $<antiA>$ too.

Paradoxes of some Neutrosophic Arguments
$<A> \Rightarrow <B>$
$<B> \Rightarrow <anti\ A>$
$\therefore <A> \Rightarrow <anti\ A>$
Example: too much work produces sickness; sickness produces less work (absences from work, low efficiency); therefore, too much work implies less work (this is a *Law of Self-Equilibrium*).
$<A> \Rightarrow <B>$
$<B> \Rightarrow <non\ A>$
$\therefore <A> \Rightarrow <non\ A>$

$<A> \Rightarrow <B>$
$<B> \Rightarrow <neut\ A>$
$\therefore <A> \Rightarrow <neut\ A>$

g) **Equality/Biconditional**
Unequal Equalities
$<A> \neq <A>$
which symbolically becomes $(\exists x)(x \in \neg A \leftrightarrow x \notin \neg A)$ or even stronger inequality $(\forall x)(x \in \neg A \leftrightarrow x \notin \neg A)$.
Nothing is $<A>$, nor even $<A>$.
$<anti\ A> \neq <anti\ A>$
which symbolically becomes $(\exists x)(x \in A \leftrightarrow x \notin A)$ or even stronger inequality $(\forall x)(x \in A \leftrightarrow x \notin A)$.

$<neut\ A> \neq <neut\ A>$
which symbolically becomes $(\exists x)(x \in \upsilon A \leftrightarrow x \notin \upsilon A)$ or even stronger inequality $(\forall x)(x \in \upsilon A \leftrightarrow x \notin \upsilon A)$.

$<non\ A> \neq <non\ A>$
which symbolically becomes $(\exists x)(x \in \neg A \leftrightarrow x \notin \neg A)$ or even stronger inequality $(\forall x)(x \in \neg A \leftrightarrow x \notin \neg A)$.

Equal Inequalities
$<A> = <anti\ A>$
$(\forall x)(x \in A \leftrightarrow x \in \boldsymbol{a}(A))$
All is $<A>$, the $<anti\ A>$ too; and reciprocally, all is $<anti\ A>$, the $<A>$ too. Or, both combined implications give: All is $<A>$ is equivalent to all is $<anti\ A>$.

And so on:
$<A> = <neut\ A>$
$<anti\ A> = <neut\ A>$
$<non\ A> = <A>$

Dilations and Absorptions
$<anti\ A> = <non\ A>$,
which means that $<anti\ A>$ is dilated to its neutrosophic superset $<non\ A>$, or $<non\ A>$ is absorbed to its neutrosophic subset $<anti\ A>$.
Similarly for:
$<neut\ A> = <non\ A>$
$<A> = U$
$<neut\ A> = U$
$<anti\ A> = U$
$<non\ A> = U$

h) Combinations of the previous single neutrosophic operator equalities and/or inequalities, resulting in more neutrosophic operators involved in the same expression.
For examples:
$<neut\ A> \cap (<A> \cup <anti\ A>) \neq \varnothing$ [two neutrosophic operators].
$<A> \cup <anti\ A> \neq \neg <neut\ A>$ and reciprocally $\neg(<A> \cup <anti\ A>) \neq <neut\ A>$.
$<A> \cup <neut\ A> \neq \neg <anti\ A>$ and reciprocally.
$\neg(<A> \cup <neut\ A> \cup <anti\ A>) \neq \varnothing$ and reciprocally.
Etc.

i) We can also take into consideration other logical connectors, such as strong disjunction (we previously used the *weak disjunction*), *Shaffer's connector, Peirce's connector*, and extend them to the neutrosophic form.

j) We may substitute $<A>$ by some entities, attributes, statements, ideas and get nice neutrosophic paradoxes, but not all substitutions will work properly.

10 Some particular paradoxes

Quantum Semi-Paradox
Let's go back to 1931 Schrödinger's paper. Saul Youssef writes (flipping a *quantum coin*) in arXiv.org at quant-ph/9509004:

> "The situation before the observation could be described by the distribution (1/2,1/2) and after observing heads our description would be adjusted to (1,0). The problem is, what would you say to a student who then asks: "Yes, but what causes (1/2,1/2) to evolve into (1,0)? How does it happen?"

It is interesting. Actually we can say the same for any probability different from 1: If at the beginning, the probability of a quantum event, P(*quantum event*) = p, with $0<p<1$, and if later the event occurs, we get to P(*quantum event*) = 1; but if the event does not occur, then we get P(*quantum event*) = 0, so still a kind of contradiction.

Torture's paradox

An innocent person P, who is tortured, would say to the torturer T whatever the torturer wants to hear, even if P doesn't know anything.

So, T would receive incorrect information that will work against him/her. Thus, the torture returns against the torturer.

Paradoxist psychological behavior

Instead of being afraid of something, say <*A*>, try to be afraid of its opposite <*anti A*>, and thus− because of your fear − you'll end up with the <*anti*<*anti A*>>, which is <*A*>.

Paradoxically, *negative publicity* attracts better than positive one (enemies of those who do negative publicity against you will sympathize with you and become your friends).

Paradoxistically [word coming etymologically from *paradoxism, paradoxist*], to be in opposition is more poetical and interesting than being opportunistic.

At a sportive, literary, or scientific competition, or in a war, to be on the side of the weaker is more challenging but on the edge of chaos and, as in Complex Adoptive System, more potential to higher creation.

Law of Self-Equilibrium

(Already cited above at the Neutrosophic Inclusion/Conditional Paradoxes) <*A*> → <*B*> and <*B*> → <*anti A*>, therefore <*A*> → <*anti A*> !

Example: too much work produces sickness; sickness produces less work (absences from work, low efficiency); therefore, too much work implies less work.

Submitted on April 25, 2010 / Accepted on April 30, 2010

References

1. Weisstein E.W. Smarandache paradox. *CRC Concise Enciclopedia of Mathematics*, CRC Press, Boca Raton, FL, 1998, 1661.
2. Begay A. The Smarandache Semantic Paradox. *Humanistic Mathematics Network Journal*, Harvey Mudd College, Claremont (CA), 1998, no. 17, 48.
3. Greenstein C.H. Dictionary of logical terms and symbols. Van Nostrand Reinhold Co., 1978.
4. Devaraj Ramasamy. Florentin Smarandache set up the paradoxist literary movement. In *Parnassus of World Poets 1994*, Madras, India, September 1994.
5. Dale J. Logic: the semantics of existence and nonexistence. Berlin, de Gruyter, 1996.
6. Le C.T. The Smarandache class of paradoxes. *Bulletin of the Transylvania University of Brasov*, New Series, Series B, 1994, v.1(36), 7–8.
7. Le C.T. The Smarandache class of paradoxes. *Bulletin of Pure and Applied Sciences E*, 1995, v.14(2), 109–110.
8. Le C.T. The most paradoxist mathematician of the world: Florentin Smarandache. *Bulletin of Pure and Applied Sciences E*, 1996, v.15(1), 81–100.
9. Le C.T. The Smarandache class of paradoxes. *Journal of Indian Academy of Mathematics*, 1996, v.18, no.1, 53–55.
10. Le C.T. The Smarandache class of paradoxes (mathematical poem). In: Bunner H.C. An anthology in memoriam. Bristol Banner Books, Bristol (IN), 1996, 94.
11. Le C.T. Clasa de paradoxuri Smarandache. *Tempus*, 1994, anul III, no.2(5), 4.
12. Mitroiescu I. The Smarandache class of paradoxes applied in computer sciences. *Abstracts of Papers Presented to the American Mathematical Society*, 1995, v.16, no.3, issue 101, 651.
13. Mitroiescu I. The Smarandache class of paradoxes. *The Mathematical Gazette*, 1995, v.79, no.484, 125.
14. Popescu M. A model of the Smarandache paradoxist geometry. *Abstracts of Papers Presented to the American Mathematical Society*, 1996, v.17, no.1, issue 103, 265.
15. Smarandache F. Neutrosophy. Neutrosophic probability, set, and logic. American Research Press, Rehoboth (NM), 1998; Republished in 2000, 2003, 2005 as Smarandache F. A unifying field in logics: neutrosophic logic. Neutrosophy, neutrosophic set, neutrosophic probability and statistics. American Research Press, Rehoboth (NM).
16. Smarandache F. Mixed non-Euclidean geometries. Arhivele Statului, Filiala Vâlcea, Rm. Vâlcea, 1969.
17. Smarandache F., Osman S. Neutrosophy in Arabic philosophy. Renaissance High Press (Ann Arbor), 2007.
18. Smarandache F. Mathematical fancies and paradoxes. *The Eugene Strens Memorial on Intuitive and Recreational Mathematics and its History*, University of Calgary, Alberta, Canada, 27 July — 2 August, 1986.
19. Tilton H.B. Smarandache's paradoxes. *Math Power*, Tucson (AZ), 1996, v.2, no.9, 1–2.

Five Paradoxes and a General Question on Time Traveling

Florentin Smarandache

Department of Mathematics, University of New Mexico, Gallup, NM 87301, USA. E-mail: smarand@unm.edu

These are five paradoxes on time traveling, which come from Neutrosophy and Neutrosophic Logics applied to the theory of relativity.

1 Traveling to the past

Joe40, who is 40 years old, travels 10 years back to the past when he was 30 years old. He meets himself when he was 30 years old, let's call this Joe30.

Joe40 kills Joe30.

If so, we mean if Joe died at age 30 (because Joe30 was killed), how could he live up to age 40?

2 Traveling to the future

Joe30, who is 30 years old, travels 10 years in the future and meats himself when he will be 40 years old, let's call him Joe40.

Joe40 kills Joe30.

At what age did Joe die, at 30 or 40?

If Joe30 died, then Joe40 would not exist.

3 Traveling pregnant woman

a) A 3-month pregnant woman, Jane3, travels 6 months to the future where she gives birth to a child Johnny3.
b) Then she returns with the child back, and after 1 month she travels 5 months to the future exactly at the same time as before.

Then how is it possible to have at exactly the same time two different situations: first only the pregnant woman, and second the pregnant woman and her child?

4 Traveling in the past before birth

Joe30, who is 30 years old, travels 40 years in the past, therefore 10 years before he was born.

How is it possible for him to be in the time when he did not exist?

5 Traveling in the future after death

Joe30, who is 30 years old, travels 40 years in the future, 10 years after his death. He has died when he was 60 years old, as Joe60.

How is it possible for him to be in the time when he did not exist any longer?

6 A general question about time traveling

When traveling say 50 years in the past [let's say from year 2010 to year 1960] or 50 years in the future [respectively from year 2010 to year 2060], how long does the traveling itself last?

If it's an instantaneous traveling in the past, is the time traveler jumping from year 2010 directly to year 1960, or is he continuously passing through all years in between 2010 and 1960? Similar question for traveling in the future.

If the traveling lasts longer say, a few units (seconds, minutes, etc.) of time, where will be the traveler at the second unit or third unit of time? I mean, suppose it takes 5 seconds to travel from year 2010 back to year 1960; then in the 1st second is he in year 2000, in the 2nd second in year 1990, in the 3rd second in year 1980, in the 4st second in year 1970, and in the 5st second in year 1960? So, his speed is 10 years per second?

Similar question for traveling in the future.

Submitted on April 25, 2010 / Accepted on April 30, 2010

References

1. Weisstein E.W. Smarandache paradox. *CRC Concise Enciclopedia of Mathematics*, CRC Press, Boca Raton, FL, 1998, 1661.
2. Smarandache F. Neutrosophy. Neutrosophic probability, set, and logic. American Research Press, Rehoboth (NM), 1998; Republished in 2000, 2003, 2005 as Smarandache F. A unifying field in logics: neutrosophic logic. Neutrosophy, neutrosophic set, neutrosophic probability and statistics. American Research Press, Rehoboth (NM).
3. Smarandache F. Mixed non-Euclidean geometries. Arhivele Statului, Filiala Vâlcea, Rm. Vâlcea, 1969.
4. Smarandache F. Mathematical fancies and paradoxes. *The Eugene Strens Memorial on Intuitive and Recreational Mathematics and its History*, University of Calgary, Alberta, Canada, 27 July — 2 August, 1986.

Do the Uncertainty Relations Really have Crucial Significances for Physics?

Spiridon Dumitru

Department of Physics (retired), Transilvania University, B-dul Eroilor 29, 500036 Braşov, Romania
E-mail: s.dumitru42@yahoo.com

It is proved the falsity of idea that the Uncertainty Relations (UR) have crucial significances for physics. Additionally one argues for the necesity of an UR-disconnected quantum philosophy.

1 Introduction

The Uncertainty Relations (UR) enjoy a considerable popularity, due in a large measure to the so called Conventional (Copenhagen) Interpretation of UR (CIUR). The mentioned popularity is frequently associated with the idea (which persist so far) that UR have crucial significances for physics (for a list of relevant references see [1–3]). The itemization of the alluded idea can be done through the following more known Assertions (***A***):

• $\boldsymbol{A}_1$: In an experimental reading the UR are crucial symbols for measurement characteristics regarding Quantum Mechanics (QM) in contrast with non-quantum Classical Physics (CP). The pointed characteristics view two aspects: (i) the so called "observer effect" (i.e. the perturbative influence of "observation"/measuring devices on the investigated system), and (ii) the measurement errors (uncertainties). Both of the alluded aspects are presumed to be absolutely notable and unavoidable in QM contexts respectively entirely negligible and avoidable in CP situations. ■

• $\boldsymbol{A}_2$: From a theoretical viewpoint UR are essential distinction elements between the theoretical frameworks of QM and CP. This in sense of the supposition that mathematically UR appear only in QM pictures and have not analogues in the CP representations. ■

• $\boldsymbol{A}_3$: In both experimental and theoretical acceptions the UR are in an indissoluble connection with the description of uncertainties (errors) specific for Quantum Measurements (QMS). ■

• $\boldsymbol{A}_4$: As an esential piece of UR, the Planck's constant $\hbar$, is appreciated to be exclusively a symbol of quanticity (i.e. a signature of QM comparatively with CP), without any kind of analogue in CP. ■

• $\boldsymbol{A}_5$: UR entail [4] the existence of some "impossibility" (or "limitative") principles in foundational physics. ■

• $\boldsymbol{A}_6$: UR are regarded [5] as expression of *"the most important principle of the twentieth century physics"*. ■

To a certain extent the verity of the idea itemized by assertions $\boldsymbol{A}_1 - \boldsymbol{A}_6$ depends on the entire truth of CIUR. That is why in the next section we present briefly the CIUR untruths which trouble the mentioned verity. Subsequently, in Section 3, we point out a lot of Observations (***O***) which invalidate completely and irrefutably the items $\boldsymbol{A}_1 - \boldsymbol{A}_6$. The respective invalidation suggests a substitution of UR-subordinate quantum philosophy with an UR-disconnected conception. Such a suggestion is consolidated by some additional Comments (***C***) given in Section 4. So, in Section 5, we can conclude our considerations with: (i) a definitely negative answer to the inquired idea, respecively (ii) a pleading for a new quantum philosophy. Such conclusions argue for the Dirac's intuitional guess about the non-survival of UR in the physics of future.

2 Shortly on the CIUR untruths

In its essence the CIUR doctrine was established and disseminated by the founders and subsequent partisans of Copenhagen School in QM. The story started from the wish to give out an unique and generic interpretation for the thought-experimental (*te*) formula

$$\Delta_{te}A \cdot \Delta_{te}B \geqslant \hbar \tag{1}$$

(A and B being conjugated observables) respectively for the QM theoretical formula

$$\Delta_{\psi}A \cdot \Delta_{\psi}B \geqslant \frac{1}{2}\left|\left\langle\left[\hat{A},\hat{B}\right]\right\rangle_{\psi}\right| \tag{2}$$

(where the notations are the usual ones from usual QM — see also [3]). Both the above two kind of formulas are known as UR.

The alluded doctrine remains a widely adopted conception which, in various manners, dominates to this day the questions regarding the foundation and interpretation of QM. However, as a rule, a minute survey of the truths-versus-untruths regarding its substance was (and still is) underestimated in the main stream of publications (see the literature mentioned in [1, 2]). This in spite of the early known opinions like [6]: *"the idea that there are defects in the foundations of orthodox quantum theory is unquestionable present in the conscience of many physicists"*.

A survey of the mentioned kind was approached by us in the report [3] as well as in its precursor papers [7–15] and preprints [16]. Our approaches, summarized in [3], disclose the fact that each of all basic elements (presumptions) of CIUR are troubled by a number of insurmountable shortcomings (unthruths). For that reason we believe that CIUR must be wholly abandoned as a wrong construction which, in its substance, has no noticeable value for physics. The disclosures from [3] were carried out by an entire class of well

argued remarks ($\boldsymbol{R}$). From the mentioned class we compile here only the following ones:

• $\boldsymbol{R}_a$: Formula (1) is mere provisional fiction without any durable physical significance. This because it has only a transitory/temporary character, founded on old resolution criteria from optics (introduced by Abe and Rayleigh). But the respective criteria were surpassed by the so called super-resolution techniques worked out in modern experimental physics.
Then, instead of CIUR formula (1), it is possible to imagine some "improved relations" (founded on some super-resolution thought-experiments) able to invalidate in its very essence the respective formula. ■

• $\boldsymbol{R}_b$: From a theoretical perspective the formula (2) is only a minor and deficient piece, resulting from the genuine Cauchy-Schwarz relation

$$\Delta_\psi A \cdot \Delta_\psi B \geqslant \left|\left(\delta_\psi \hat{A}\,\psi, \delta_\psi \hat{B}\,\psi\right)\right| \tag{3}$$

written in terms of usual QM notations (see [3]).
As regards their physical significance the formulas (2) and (3) are nothing but simple (second order) fluctuations relations from the same family with the similar ones [3, 7–9, 12, 15] from the statistical CP. ■

• $\boldsymbol{R}_c$: In a true approach the formulas (1) and (2) as well as their "improvised adjustments" have no connection with the description of QMS. ■

• $\boldsymbol{R}_d$: The Planck's constant $\hbar$ besides its well-known quanticity significance is endowed also [3, 12] with the quality of generic indicator for quantum randomness (stochasticity) — i.e. for the random characteristics of QM observables. Through such a quality $\hbar$ has [3, 12] an authentic analogue in statistical CP. The respective analogue is the Boltzmann's constant k_B which is an authentic generic indicator for thermal randomness. Note that, physically, the randomness of an observable is manifested through its fluctuations [3, 7–9, 12, 15]. ■

• $\boldsymbol{R}_e$: The formula (2) is not applicable for the pair of (conjugated) observables $t - E$ (time-energy). In other words [3] a particularization of (2) in the form

$$\Delta_\psi t \cdot \Delta_\psi E \geqslant \frac{\hbar}{2} \tag{4}$$

gives in fact a wrong relation. This because in usual QM the time t is a deterministic variable but not a random one. Consequently for any QM situation one finds the expressions $\Delta_\psi t \equiv 0$ respectively $\Delta_\psi E = a\ finite\ quantity$.
Note that in a correct mathematical-theoretical approach for the $t-E$ case it is valid only the Cauchy Schwarz formula (3), which degenerate into trivial relation $0 = 0$. ■

Starting from the above remarks $\boldsymbol{R}_a$–$\boldsymbol{R}_e$ in the next section we add an entire group of Observations ($\boldsymbol{O}$) able to give a just estimation of correctness regarding the assertions $\boldsymbol{A}_1 - \boldsymbol{A}_6$.

3 The falsity of assertions $\boldsymbol{A}_1 - \boldsymbol{A}_6$

The above announced estimation can be obtained only if the mentioned remarks are supplemented with some other notable elements. By such a supplementation one obtains a panoramic view which can be reported through the whole group of the following Observations ($\boldsymbol{O}$) :

• $\boldsymbol{O}_1$: The remark $\boldsymbol{R}_a$, noted in previous section, shows irrefutably the falsity of the assertion $\boldsymbol{A}_1$. The same falsity is argued by the fact that the referred "observer effect" and corresponding measuring uncertainties can be noticeable not only in QMS but also in some CP measurements (e.g. [17] in electronics or in thermodynamics) ■

• $\boldsymbol{O}_2$: On the other hand the remark $\boldsymbol{R}_b$ points out the evident untruth of the assertion $\boldsymbol{A}_2$. ■

• $\boldsymbol{O}_3$: Furthermore the triplet of remarks $\boldsymbol{R}_a - \boldsymbol{R}_c$ infringes the essence of the assertion $\boldsymbol{A}_3$. ■

• $\boldsymbol{O}_4$: The exclusiveness feature of Planck's constant $\hbar$, asserted by $\boldsymbol{A}_4$, is evidently contradicted by the remark $\boldsymbol{R}_d$. ■

• $\boldsymbol{O}_5$: Assertion $\boldsymbol{A}_5$ was reinforced and disseminated recently [4] thrugh the topic:

> *"What role do 'impossibility' principles or other limits (e.g., sub-lightspeed signaling,* ***Heisenberg uncertainty****, cosmic censorship, the second law of thermodynamics, the holographic principle,* ***computational limits****, etc.) play in foundational physics and cosmology?"*.

Affiliated oneself with the quoted topic the assertion $\boldsymbol{A}_5$ implies two readings: (i) one which hints at Measuring Limits (ML), respectively (ii) another associated with the so called "Computational Limits" (CL). ■

• $\boldsymbol{O}_6$: In the reading connected with ML the assertion $\boldsymbol{A}_5$ presumes that the QMS accuracies can not surpass "Heisenberg uncertainties" (1) and (2). Such a presumption is perpetuated until these days through sentences like: *"The uncertainty principle of quantum mechanics places a fundamental limitation on what we can know"* [18].
Now is easy to see that the above noted remarks $\boldsymbol{R}_a$ and $\boldsymbol{R}_c$ reveal beyond doubt the weakness of such a presumption. Of course that, as a rule, for various branches of physics (even of CP nature such are [17] those from electronics or thermodynamics), the existence of some specific ML is a reality. The respective existence is subordinate to certain genuine elements such are the accuracy of experimental devices and the competence of the theoretical approaches. But note that as it results from the alluded remarks the formulas (1) and (2) have nothing to do with the evaluation or description of the ML (non-performances or uncertainties) regarding QMS. ■

• $\boldsymbol{O}_7$: The reading which associate the UR with CL sems to refer mainly to the Bremermann's limit (i.e. to the maximum computational speed of a self-contained system in the universe) [19, 20]. But it is easy to see from [19, 20] that the aludded association is builded in fact on the wrong relations (1) and (4) written for the observables pair $t - E$. Conse-

quently such an association has not any real value for appreciation of UR significance as CL. Add here the remark that, nevertheless, the search [20] for finding the ultimate physical limits of computations remains a subject worthy to be investigated. This because, certainly, that what is ultimately permissible in practical computational progresses depends on what are the ultimate possibilities of real physical artifacts (experiences). However, from our viewpoint, appraisals of the alluded possibilities do not require any appeal to the relations (1, 2, 4). ■

• $\boldsymbol{O}_8$: For a true judgment regarding the validity of assertion $\boldsymbol{A}_6$ can be taken into account the following aspects:

(i) In its essence $\boldsymbol{A}_6$ prove oneself to be nothing but an unjustifiable distortion of the real truths. Such a proof results directly from the above remarks $\boldsymbol{R}_a - \boldsymbol{R}_c$. According to the alluded remarks in reality the UR (1) and (2) are mere provisional fictions respectively minor (and restricted) QM relations. So it results that, in the main, UR are insignificant things comparatively with the true important principles of the 20th century physics (such are the ones regarding *Noether's theorem*, *mass-energy equivalence*, *partricle-wave duality* or *nuclear fission*).

(ii) It is wrongly to promote the assertion $\boldsymbol{A}_6$ based on the existent publishing situation where, in the mainstream of QM text-books, the UR (1) and/or (2) are amalgamated with the basic quantum concepts. The wrongness is revealed by the fact that the alluded situation was created through an unjustified perpetuance of the writing style done by the CIUR partisans.

(iii) The assertion $\boldsymbol{A}_6$ must be not confused with the history confirmed remark [21] : *UR "are probably the most controverted formulae in the whole of the theoretical physics"*. With more justice the respective remark has to be regarded as accentuating the weakness of concerned assertion.

Together the three above noted aspects give enough reasons for an incontestable incrimination of the assertion under dicussion. ■

The here detailed observations $\boldsymbol{O}_1 - \boldsymbol{O}_8$ assure sufficient solid arguments in order to prove the indubitable incorrectness for each of the assertions $\boldsymbol{A}_1 - \boldsymbol{A}_6$ and, consequently, the falsity of the idea that UR really have crucial significances for physics. But the alluded proof conflicts with the UR-subordinate quantum philosophy in which the interpretational questions of QM and debates about QMS description are indissolubly associated with the formulas (1) and/or (2). The true (and deep) nature of the respective conflict suggests directly the necesity of improvements by substituting the alluded philosophy with another UR-disconnected conception.

Of course that the before-mentioned substitution necessitates further well argued reconsiderations, able to gain the support of mainstream scientific communities and publications. Note that, in one way or other, elements of the UR-subordinate philosophy are present in almost all current QM interpretations [22]. We think that among the possible multitude of elements belonging to the alluded reconsiderations can be included the additional group of comments from the next section.

4 Some additional comments

The Comments ($\boldsymbol{C}$) from the foregoing announced group, able to suggest also improvements in quantum philosophy, are the following ones:

• $\boldsymbol{C}_1$: Firstly we note that the substance of above presented remarks $\boldsymbol{R}_a - \boldsymbol{R}_b$ respectively observations $\boldsymbol{O}_1 - \boldsymbol{O}_3$ can be fortified by means of the following three our views:

(i) In its bare and lucrative framework, the usual QM offers solely theoretical models for own characteristics of the investigated systems (microparticles of atomic size).

(ii) In the alluded framework QM has no connection with a natural depiction of QMS.

(iii) The description of QMS is an autonomous subject, investigable in addition to the bare theoretical structure of usual QM.

We think that, to a certain extent, our above views find some support in the Bell's remark [23]: *"the word (**measurement**) has had such a damaging efect on the discussions that ... it should be banned altogether in quantum mechanics"*. (It happened that, in a letter [24], J.S.Bell comunicated us early the essence of the alluded remark together with a short his personal agreement with our incipient opinions about UR and QMS). ■

• $\boldsymbol{C}_2$: In its substance the view (i) from $\boldsymbol{C}_1$ regards the bare QM as being nothing but an abstract (mathematical) modeling of the properties specific to the atomic-size sytems (microparticles). For a given system the main elements of the alluded modeling are the wave functions ψ_α, respectively the quantum operators $\hat{A}_j$. On the one hand ψ_α describes the probabilistic situation of the system in α state. Mathematically ψ_α is nothing but the solution of the corresponding Schrodinger equation. On the other hand each of the operators $\hat{A}_j$ ($j = 1, 2, \ldots, n$) is a generalised radom variable associated to a specific observable A_j (e.g. coordinate, momentum, angular momentum or energy) of the system. Then in a probabilistic sense the global characterization of the observables A_j is given by the expected parameters:
(i) the mean values $\left\langle A_j \right\rangle_\psi = \left(\psi, \hat{A}_j \psi\right)$ wherre $\psi \equiv \psi_\alpha$ while (f, g) denotes the scalar product of functions f and g,
(ii) the $(r + s)$-order correlations

$$\mathrm{K}_\psi(i, j; r, s) = \left(\left(\delta_\psi \hat{A}_i\right)^r \psi, \left(\delta_\psi \hat{A}_j\right)^s \psi\right),$$

with $\delta_\psi \hat{A}_j = \hat{A}_j - \left\langle A_j \right\rangle_\psi$ and $r + s \geqslant 2$.
So the definitions of parameters $\langle A_a \rangle_\psi$ and $\mathrm{K}_\psi(i, j; r, s)$ appeal to the usual notations from QM texts (see [3, 25, 26]). ■

• $\boldsymbol{C}_3$: The before mentioned QM entities are completely similar with the known things from statistical CP (such are the phenomenological theory of fluctuations [27, 28] respectively the classical statistical mechanics [29, 30]). So the wave functions ψ_α correspond to the probability distributions w_α while the operators $\hat{A}_j$ are alike the macroscopic random observables $\mathbb{A}_j$. Moreover the QM probabilistc expected parameters $\langle A_a \rangle_\psi$ and $\mathrm{K}_\psi(i, j; r, s)$ are entirely analogous with the mean values respectively the second and higher order fluctuations correlations regarding the macroscopic observables $\mathbb{A}_j$ [3, 7–10, 12, 15, 27–31] ■

• $\boldsymbol{C}_4$: It is interesting to complete the above comment with the following annotations. Undoubtedly that, mathematically, the QM observables have innate characteristics of random variables. But similar characteristics one finds also in the case of statistical CP observables. Then it is surprisingly that the two kinds of random observables (from QM and CP) in their connection with the problem of measurements are approached differently by the same authors [25, 29] or teams [26, 30]. Namely the alluded problem is totally neglected in the case of CP observables [29, 30], respectively it is regarded as a capital question for QM observables [25, 26]. Note that the mentioned differentiation is not justified [25, 26, 29, 30] by any physical argument. We think that, as regard the description of their measurements, the two kinds of random observables must be approached in similar manners.
In the context of above annotations it is interesting to mention the following very recent statement [32]: *"To our best current knowledge the measurement process in quantum mechanics is non-deterministic"*. The inner nature of the mentioned statement strengthens our appreciation [3] that a measurement of a (random) quantum observable must be understood not as a single trial (which give a unique value) but as a statistical sampling (which yields a spectrum of values). Certainly that in such an understanding the concept of "wave function collapse" [33] becomes an obsolete thing. ■

• $\boldsymbol{C}_5$: A credible tentative in approaching similarly the description of measurements regarding random observables from both QM and CP was promoted by us in [3, 34]. Our approach was done according the views (ii) and (iii) noted in the above comment $\boldsymbol{C}_1$. Mainly the respective approach aims to obtain a well argued (and consequently credible) description of QMS. So, in papers [3, 34], a QMS was depicted as a distortion of the information about the measured system. For a given system the respective distortion is described (modeled) as a process which change linearly the probability density and current (given in terms of wave function) but preserve the mathematical expressions of QM operators regarded as generalised random variables. Note that an analogous description of measurements concerning the random observables from CP was done by us formerly in [35]. ■

• $\boldsymbol{C}_6$: Other open question of quantum philosophy regards the deterministic subjacency of QM randomness. The question, of great interest [36], aims to clarify if the respective randomness has an irreducible nature or otherwise it derives from the existence of some subjacent hidden variables of deterministic essence. Then it appears as a notable aspect the fact that, in so reputable report [36] about the alluded question, the possible involvement of UR (1) and/or (2) is completely omited. Such a remarkable omission show clearly that the UR (1) and/or (2) do not present any interest for one of the most thought-provoking subject regarding quantum philosophy. ■

• $\boldsymbol{C}_7$: Here is the place to refer comparatively to the deterministic subjacency regarding CP kind of randomness. The respective kind is associated (both theoretically and experimentally) with a class of subjacent deterministic variables, specific to the molecular and atomic motions [27–30]. The important feature of the alluded CP subjacency is the fact that it does not annul at all the corresponding randomness. Namely the respective deterministic subjacency do not revoke at all the random entities such are the probability distributions w_α and macroscopic observables $\mathbb{A}_j$, mentioned above in $\boldsymbol{C}_3$. The respective entities keep the essence of the CP randomness revealed physically through the corresponding global fluctuations of macroscopic observables.
We think that the noted classical feature must be taken as a reference element in managing the discussions regarding the deterministic subjacency of QM (i.e. the question of hidden variables — versus — QM randomness) and, generally speaking, the renovation of quantum philosophy. More exactly it is of direct interest to see if the existence of hidden variables removes or keeps the QM randomness incorporated within the wave functions ψ_α and operators $\hat{A}_j$. We dare to believe that the alluded QM randomness will persist, even if the existence of some subjacent hidden variables would be evidenced (first of all experimentally). ■

• $\boldsymbol{C}_8$: Now some other words about the question of "impossibility" principles in foundational physics, discussed above in observations $\boldsymbol{O}_5 - \boldsymbol{O}_7$. The respective principles were mentioned in connection with questions like: ' What is Ultimately Possible in Physics?' (see [4]). To a deeper analysis the alluded connection calls attention to 'the frontier of knowledge'. In scrutinizing the respective frontier it was acknowledged recently [32] that: *"Despite long efforts, no* ***progress*** *has been made...* for *... the understanding of quantum mechanics, in particular its measurement process and interpretation"*. What is most important in our opinion is the fact that, in reality, for the sought ***"progress"*** the UR (1) and (2) are of no interest or utility. ■

By ending this section it is easy to see that the here added comments $\boldsymbol{C}_1 - \boldsymbol{C}_8$ give supports to the before suggested proposal for a UR-disconnected quantum philosophy.

5 Conclusions

A survey, in Section 3, of the observations $\boldsymbol{O}_1 - \boldsymbol{O}_8$ discloses that ***in fact the UR (1) and (2) have not any crucial significance for physics***. Additionally, in Section 4, an examination of the comments $\boldsymbol{C}_1 - \boldsymbol{C}_8$ provides supporting elements for a UR-disconnected quantum philosophy.

So we give forth a class of solid arguments which come to advocate and consolidate the Dirac's intuitional guess [37] that: ***"uncertainty relations in their present form will not survive in the physics of future"***.

Submitted on May 04, 2010 / Accepted on May 05, 2010

References

1. Auletta G. Foundations and interpretation of Quantum Mechanics. World Scientific, Singapore, 2000.
2. Cabello A. Bibliographic guide to the foundations of quantum mechanics and quantum information. arXiv: quant-ph/0012089.
3. Dumitru S. Reconsideration of the Uncertainty Relations and Quantum Measurements. *Progress in Physics*, v.2, 2008, 50–68.
4. The pretext of A_5 is comprised in a topic circulated through the web page of "*FQXi 2009 Essay Contest: What's Ultimately Possible in Physics? (Introduction)*", promoted by Foundational Questions Institute (FQXi). The respective page was disponible during the Spring 2009 but is now closed However the home one of FQXi is: http://www.fqxi.org/community. But note that the before mentioned topic is entirely quoted by us above in observation O_5 from Section 3.
5. Martens H. Uncertainty Principle, *Ph.D. Thesis*. Tehnical University, Eidhoven, 1991.
6. Piron C. What is wrong in Orthodox Quantum Theory. *Lect. Notes. Phys.*, Springer, v.153, 1982, 179–182.
7. Dumitru S. Fluctuations and Thermodynamic Inequalities. *Physica Scripta*, v.10, 1974, 101–103.
8. Dumitru S. Uncertainty relations or correlation relations? *Epistemological Letters*, Issue 15, 1977, 1–78.
9. Dumitru S. Fluctuations but not uncertainities deconspiration of some confusions. In: *Recent Advances in Statistical Physics*, ed. by B. Datta and M. Dutta, World Scientific, Singapore, 1987, 122–151.
10. Dumitru S. $L_z - \varphi$ uncertainty relation versus torsion pendulum example and the failure of a vision. *Revue Roumaine de Physique*, v.33, 1988, 11–45.
11. Dumitru S. Compatibility versus commutativity — the intriguing Ccse of angular momentum-azimuthal angle. In: *Symmetries and Algebraic Structures in Physics — Proceedings of the XVIII International Colloquium on Group Theoretical Methods in Physics*, Moscow, 4–9 June, 1990, ed.by V.V.Dodonov and V.I.Manko, Nova Science Publishers, Commack, N.Y., 1991, 243–246.
12. Dumitru S. The Planck and Boltzmann constants as similar generic indicators of stochasticity: some conceptual implications of quantum-nonquantum analogies. *Physics Essays*, v.6, 1993, 5–20.
13. Dumitru S., Verriest E.I. Behaviour patterns of observables in quantum-classical limit. *Int. J. Theor. Physics*, v.34, 1995, 1785–1790.
14. Dumitru S. A possible general approach regarding the conformability of angular observables with the mathematical rules of Quantum Mechanics. *Progress in Physics* v.1, 2008, 25–30.
15. Dumitru S., Boer A. Fluctuations in the presence of fields — phenomenological Gaussian approximation and a class of thermodynamic inequalities. *Phys. Rev. E*, v.64, 2001, 021108.
16. Dumitru S. The preprints deposited in E-Print Libraries at: (i) the Cornell University arXiv and CERN Library (CDS CERN).
17. *Wikipedia*, Observer effect (physics), http://en.wikipedia.org/wiki/Observer_effect_(physics); Dated: May 04, 2010.
18. Gleiser M. Unification and the limits of knowledge. Preprint of Foundational Questions Institute, http://www.fqxi.org/community/essay/winners/2009.1#Gleiser
19. Bremermann H.J. Optimization through evolution and recombination. In: *Self-Organizing systems*, ed. M.C. Yovitts et al., Spartan Books, Washington, DC, 1962, 93–106.
20. Lloyd S. Ultimate physical limits to computation. *Nature*, v.406, 2000, 1047–1054.
21. Bunge M. Interpretation of Heisenberg's Inequalities. In: *Denken und Umdenken (zu Werk und Werkung von Werner Heisenberg)*, ed. by H. Pfepfer, Piper R., Munchen, 1977.
22. Ismael J. Quantum Mechanics. In: *The Stanford Encyclopedia of Philosophy*, Edward N. Zalta (ed.), Winter 2009 Edition.
23. Bell J.S. Against "measurement". *Physics World*, v.3, 1990, 33–40. Reprinted also in some books containing J.S.Bell's writings.
24. A letter to the present author from J.S.Bell, dated 1985, Jan 29: arXiv: quant-ph/0004013.
25. Schwabl F. Quantum Mecanics. 2nd rev. ed., Springer, Berlin, 1995.
26. Cohen-Tannoudji C., Diu B., Laloe F. Quantum Mechanics, vol. I, II. J. Wiley, 1977.
27. Munster A. Statistical thermodynamics, vol. I. Springer, Berlin, 1969.
28. Landau L., Lifchitz E. Physique statistique. Mir, Moscou, 1984.
29. Schwabl F. Statistical mechanics. Springer, Berlin, 2002.
30. Diu B., Guthmann C., Lederer D., Roulet B. Elements de physique statistique. Herman, Paris, 1989.
31. Boer A., Dumitru S. Higher order correlations in the presence of fields. *Phys. Rev. E*, v.66, 2002, 046116.
32. Hossenfelder S. At the frontier of knowledge. arXiv: physics.pop-ph/1001.3538.
33. Ghirardi G. Collapse theories. In: *The Stanford Encyclopedia of Philosophy*, Edward N. Zalta (ed.), Fall 2008 Edition.
34. Dumitru S., Boer A. On the measurements regarding random observables. *Rom. Journ. Phys.*, v.53, 2008, 1111–1116.
35. Dumitru S. Phenomenological theory of recorded fluctuations. *Phys. Lett. A*, v.48, 1974, 109-110.
36. Genovese M. Research on Hidden Variable Theories: a review of recent progresses. *Phys. Rep.*, v.413, 2005, 319–396; arXiv: quant-ph/0701071.
37. Dirac P.A.M. The evolution of physicist's picture of nature. *Scientific American*, v.208, May 1963, 45–53.

Lunar Laser Ranging Test of the Invariance of c: a Correction

Ulrich E. Bruchholz

Wurzen, Germany. E-mail: Ulrich.Bruchholz@t-online.de; http://www.bruchholz-acoustics.de

In the APOLLO test, a speed of light was found, which seemingly supports a Galileian addition theorem of velocities [1]. However, the reported difference of 200 ± 10 m/s is based on a simple error. The correct evaluation of this test leads to the known value of c within the given precision. This correction does not mean an impossibility of detecting spatial anisotropies or gravitational waves.

The Apache Point Lunar Laser-ranging Operation (APOLLO) provides a possibility of directly testing the invariance of light speed [1, 2]. Gezari [1] reported a difference of 200 ± 10 m/s to the known value ($c = 299,792,458$ m/s according to [1]), which is in accordance with the speed of the observatory on the earth to the retro-reflector on the moon. That would support rather a Galileian addition theorem of velocities than the local invariance of light speed. Let us follow up the path of light, Figure 1.

The way from the Apache Point Observatory (APO) to the retro-reflector and back to APO assumed by Gezari (see also Figure 2 in [1]) is $D_{LB} + D_{BR}$ (dotted lines). Gezari [1] wrote:

> Note that the Earth and Moon are moving together as a binary system at ∼30 km/s in that frame, as the Earth orbits the Sun, and relative to each other at much smaller speeds of order ∼10 m/s due to the eccentricity of the lunar orbit.

This "much smaller speed" may be the vertical speed of the moon relative to the earth. However, the moon moves irregularly in the used frame. This motion is not straight-line, that means, there is no relativity of motion between earth and moon. Therefore, we have to consider the horizontal speed (speed of revolution) of $v_{hor} \approx 1$ km/s. In the test constellation, the moon covers smaller distances parallel to the earth than the earth itself, Figure 1. It is false to set a unitary velocity of the "binary system" of ∼ 30 km/s. If we define a "binary system" with power (what is an unfortunate step), this unitary velocity becomes here smaller.

Therefore, the path of light from APO to retro-reflector is shorter than assumed by Gezari. It is now D'_{LB} (full line), because the earth takes another position in the chosen frame at launch, see Figure 1. — The elapsed time $t_{LB} + t_{BR}$ was measured correctly but the calculation of the light speed gave a false (greater) value. As well, the way back via D_{BR} does not differ from that reported by Gezari. With it, the difference of the path of light is (Figure 1)

$$D_{LB} - D'_{LB} \approx \Delta l \cos\theta \tag{1}$$

with

$$\Delta l = v_{hor}\, t_{LB}\, \sin\theta\,, \tag{2}$$

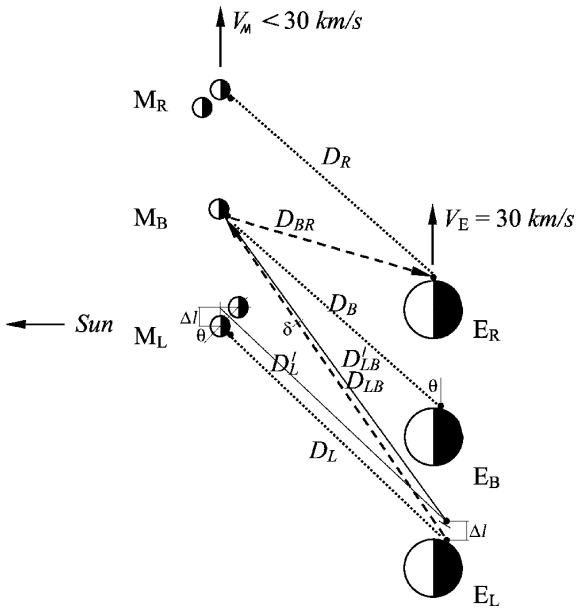

Fig. 1: Corrected path of light.

i.e.

$$D_{LB} - D'_{LB} \approx \frac{1}{2}\, v_{hor}\, t_{LB}\, \sin 2\theta\,, \tag{3}$$

with the numerical values

$$D_{LB} - D'_{LB} < \frac{1}{2}\ \text{km/s} \times 1.3\ \text{s} \approx 650\ \text{m}\,. \tag{4}$$

This difference becomes maximal with $\theta = 45°$.

The reported value of the light speed c has to be corrected for a difference (with the ratio of path difference to whole path)

$$\Delta c < \frac{300000\ \text{km/s} \times 650\ \text{m}}{780000\ \text{km}} \approx 250\ \text{m/s}\,. \tag{5}$$

We get the reported difference of 200 m/s for $\theta = 27°$ and for $\theta = 63°$. That means a coincidence within a tolerance of ±20%. — Thus, we have to take this result as negative regarding a verification of a violation of *local* invariance of c.

This from now on negative result does *not* rule out the possible existence of spatial anisotropies, as dependences of stochastic processes on direction [3] or measurements with

gas interferometers [2] demonstrate. The observed effects like anisotropic light speed in gas could be based on anisotropic material properties, which come from anisotropic metrics. The reason is explained in [4]:

The universal (according to author's opinion) field equations as quoted in [4, 5] (Eq. (1),(2),(3) in [5]) involve 10 independent equations for 14 components of metrics and electromagnetic vector potential. If one considers only gravitation, that become 6 independent equations for 10 components of metrics. This means, four components of metrics are ambiguous *in first order*. Since our existence is time-like, these ambiguous components are space-like. For example in central-symmetric and time-independent solutions, vertical metric (first order) results according to

$$\gamma_{(vert)} = +\frac{\kappa\, m}{4\pi\, r}\,, \tag{6}$$

which comes from Eq. (35) in [4], during horizontal metrics can have any value, i.e. Eq. (35) in [4] is correct only for $\gamma_{(vert)}$. On the earth is $\gamma_{(vert)} \approx 1.5{\times}10^{-9}$, but $\gamma_{(hor)}$ could be just zero. — An upgrade APOLLO equipment could be suited for direct detection of such differences in metrics, if exist.

Submitted on March 01, 2010 / Accepted on May 14, 2010

References

1. Gezari D.Y. Lunar laser ranging test of the invariance of c. arXiv: 0912.3934
2. Cahill R.T. Lunar laser-ranging detection of light-speed anisotropy and gravitational waves. *Progress in Physics*, 2010, v. 2, 31–35.
3. Shnoll S.E., Rubinstein I.A., Vedenkin N.N. "The arrow of time" in the experiments in which alpha-activity was measured using collimators directed at East and West. *Progress in Physics*, 2010, v. 1, 26–29.
4. Bruchholz U.E. Key notes on a geometric theory of fields. *Progress in Physics*, 2009, v. 2, 107–113.
5. Bruchholz U.E. Geometry of space-time. *Progress in Physics*, 2009, v. 4, 65-66.

Demonstrating Gravitational Repulsion

Pieter Cornelius Wagener

Department of Physics, Nelson Mandela Metropolitan University, Port Elizabeth, South Africa
E-mail: Pieter.Wagener@nmmu.ac.za

In previous papers we showed that a classical model of gravitation explains present gravitational phenomena. This paper deals with gravitational repulsion and it shows how it manifests in black holes and particle pair production. We also suggest a laboratory experiment to demonstrate gravitational repulsion.

1 Introduction

In previous papers [1–5] we showed that a Lagrangian

$$L = -m_0(c^2 + v^2)\exp R/r, \tag{1}$$

where

m_0 = *gravitational rest mass* of a test body moving at velocity $\mathbf{v}$ in the vicinity of a massive, central body of mass M,
γ = $1/\sqrt{1 - v^2/c^2}$,
R = $2GM/c^2$ is the Schwarzschild radius of the central body.

gives rise to the following conservation equations:

$$E = mc^2 e^{R/r} = \text{total energy} = \text{constant}, \tag{2}$$
$$\mathbf{L} = e^{R/r}\mathbf{M}, \tag{3}$$
$$L = \text{magnitude of } \mathbf{L} = \text{constant}, \tag{4}$$
$$L_z = M_z e^{R/r} = e^{R/r} m_0 r^2 \sin^2\theta\dot{\phi}, \tag{5}$$
$$= z \text{ component of } \mathbf{L} = \text{constant},$$

where

$$m = m_0/\gamma^2, \tag{6}$$

is a *variable gravitational mass* and

$$\mathbf{M} = (\mathbf{r} \times m_0\mathbf{v}), \tag{7}$$

is the total angular momentum of the test body. Eqs. (3) and (4) are amendments to the equations in the previous articles.

The above equations give rise to equations of motion that satisfy all tests for present gravitational phenomena.

2 Gravitational repulsion

Eq. (2) shows that gravitational repulsion occurs between bodies when their masses m are increased by converting radiation energy into mass. This conversion occurs according to the photoelectric effect,

$$h\nu \to mc^2. \tag{8}$$

This is the reverse of what occurs during nuclear fission.

In a previous paper [4, §3] we proposed that this accounts for the start of the Big Bang as well as the accelerating expansion of the universe. We now consider other effects.

2.1 Black holes

With black holes the reverse of repulsion occurs. According to (2) and (6) matter is converted into radiation energy ($v \to c$) as $r \to 0$. Conversely, as radiation is converted into mass, matter should be expelled from a black hole. This phenomenon has been observed [6].

In this regard our model of a black hole differs from that of general relativity (GR) in that our model does not approach a mathematical singularity as $r \to 0$, whereas GR does approach one as $r \to R$.

2.2 Pair production

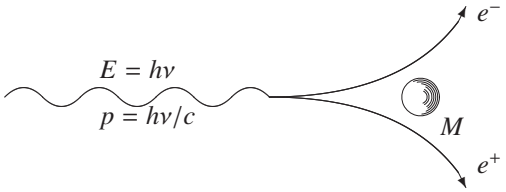

Fig. 1: A high-energy gamma ray passing near matter can create an electron-positron pair.

In pair production a gamma ray converts into a positron and an electron, with both particles moving away from one another. Pair production only occurs in the presence of a heavy mass. The explanation for the required presence of the mass is generally given in texts as:

> The process as we have assumed it to occur is impossible. This is because energy and momentum cannot simultaneously be conserved in free space in this process. ...
>
> However, if the high-energy gamma ray passes near a very heavy particle, then the heavy particle can soak up all the momentum without carrying away a significant amount of energy [7, §5.6].

We aver that the explanation is contrived. The last sentence is too inexact for a rigorous mathematical formulation. Although we do not submit a formulation at this stage, we suggest that repulsion occurs between the particles and the heavy mass.

2.3 Laboratory demonstration

It should be possible to demonstrate gravitational repulsion in a laboratory. A suggestion on how to do this is provided by Jennison and Drinkwater [8]. Their experiment was not designed to demonstrate gravitational repulsion, but to demonstrate how the properties of mass, or inertia, are simulated by phase-locked standing waves in a microwave transmitter/receiver system mounted on a frictionless air track. It should be possible to modify their experiment to show that gravitational repulsion would occur if the frequencies of the standing waves were increased. As a prototype we propose a modification of their experimental setup as depicted in Fig. 2. Two microwave transmitters/receivers lock a standing wave of frequency ν near a large mass M. Increasing the frequency of the standing wave should push it away from M.

From (2) and (8) an increase of $\Delta\nu$ will cause a separation of the microwave system from M equal to

$$\Delta r = A/(B - \ln h\Delta\nu), \tag{9}$$

where A, B are constants.

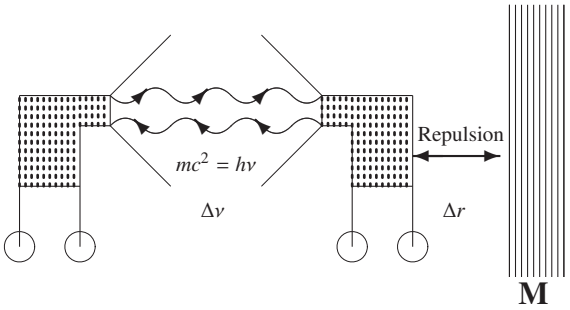

Fig. 2: Repulsion of a trapped wave. Repulsion $\Delta r = A/(B - \ln \Delta mc^2)$ where A, B = constant and $\Delta m = h\Delta\nu/c^2$.

The repulsive effect can also be measured by a sensitive gravimeter placed between M and the standing wave system.

Setting up the above experiment could be cumbersome on a macro scale. The author is investigating demonstrating the repulsive effect at nano scales.

3 Conclusion

The success of the proposed theory to explain present gravitational phenomena supports the above proposal to demonstrate gravitational repulsion.

Submitted on April 28, 2010 / Accepted on May 17, 2010

References

1. Wagener P.C. A classical model of gravitation. *Progress in Physics*, v.3, 2008, 21–23.
2. Wagener P.C. A unified theory of interaction: gravitation and electrodynamics. *Progress in Physics*, v.4, 2008, 3–9.
3. Wagener P.C. A unified theory of interaction: gravitation, electrodynamics and the strong force. *Progress in Physics*, v.1, 2009, 33–35.
4. Wagener P.C. Experimental verification of a classical model of gravitation. *Progress in Physics*, v.3, 2009, 24–26.
5. Wagener P.C. From inspired guess to physical theory: finding a theory of gravitation. *Progress in Physics*, v.1, 2010, 11–14.
6. Elbaz D., Jahnke K., Pantin E., Le Borgne D. and Letawe G. Quasar induced galaxy formation: a new paradigm? *Astronomy & Astrophysics*, v.507, 2009, 1359–1374.
7. Ashby N. and Miller S.C. Principles of Modern Physics. Holden-Day, 1970.
8. Jennison R.C. and Drinkwater A.J. An approach to the understanding of inertia from the physics of the experimental method. *J. Phys. A. Math. Gen.*, v.10, 1977, 167–179.

The Relativity Principle: Space and Time and the Planck Vacuum

William C. Daywitt

National Institute for Standards and Technology (retired), Boulder, Colorado, USA.
E-mail: wcdaywitt@earthlink.net

This short paper examines the Relativity Principle in light of the emerging Planck Vacuum (PV) theory and shows that Special and General Relativity are based physically on the Relativity Principle and the dynamics of the PV.

The idea that absolute motion through space is undetectable has been around for a long time, spanning the work of Galileo and Newton, and the Special and General theories of Relativity [1]. The Relativity Principle asserts that the cosmos is so constituted that it is impossible to detect absolute motion by any type of experiment whatsoever, or in more modern terms, that the equations of physics must be fundamentally covariant [2]. It is important to note, however, that this principle *does not* imply that a fundamental reference frame does not exist. In fact, the following discussion indicates that there may be a hierarchy of reference frames that are hidden from our view.

The PV theory views the cosmos as consisting of an omnipresent, negative-energy, degenerate collection of Planck particles known as the PV; *and* free space which is the void of classical physics [3]. Uniformly spread throughout this free space is the quantum vacuum [4] which consists of an omnipresent field of virtual photons and massive virtual particles whose source is the PV [5]. The free-space vacuum state is not empty, but as Davies puts it, "[this living vacuum] holds the key to a full understanding of the forces of nature" [6, p.104]. How the PV and free space manage to coexist is not known, but the equations of modern physics strongly suggest that some type of active vacuum state does indeed exist, when Newton's gravitational constant, Planck's constant, and the fine structure constant are replaced by their more fundamental counterparts

$$G = \frac{e_*^2}{m_*^2} \qquad \hbar = \frac{e_*^2}{c} \qquad \alpha = \frac{e^2}{e_*^2} \tag{1}$$

in those equations. The universality of this suggestion can be seen by combining the relationships in (1) to yield the string of equalities

$$m_*^2 G = c\hbar = \frac{e^2}{\alpha} \tag{2}$$

where e_* and m_* are the charge and mass of the Planck particles making up the PV. These equations imply that gravitational physics ($m_*^2 G$), quantum physics ($c\hbar$), and electromagnetics (e^2/α) belong to a *single physics*, and their arrangement in the string suggests the central position occupied by the quantum theory in uniting mass and charge. The latter suggestion is realized in the equality between the two particle forces that perturb the PV

$$\frac{mc^2}{r} = \frac{e_*^2}{r^2} \qquad \text{at } r = r_c \tag{3}$$

leading to the particle's Compton radius $r_c\,(= e_*^2/mc^2)$ [3], where mc^2/r and e_*^2/r^2 are the curvature force (a gravitational force) and the polarization force (an electrical force) the particle exerts on the PV. That mc^2/r is a gravitational type of force can be seen from Newton's expression for the gravitational force between two masses m and M separated by a distance r

$$\frac{mMG}{r^2} = \frac{(mc^2/r)(Mc^2/r)}{(m_*c^2/r_*)} \tag{4}$$

where $c^4/G = m_*c^2/r_*$ is used to remove G from the left side of the equation. The ratios mc^2/r and Mc^2/r are the curvature forces the masses m and M exert on the PV, while $m_*c^2/r_* = e_*^2/r_*^2$ is the maximum force sustainable by the PV. One of the e_*s in the product e_*^2 comes from the charge on the free particle and the other represents the charge on the individual Planck particles within the PV.

The reaction of the PV to the uniform motion of a free charge is such that an iterative process taking place between 'the magnetic and Faraday fields produced by the PV' and the charge results in the well known relativistic electric and magnetic fields commonly ascribed to the charge as a single entity [3, Sec. 4]. Since these magnetic and Faraday fields emerge from the PV, it is reasonable to suggest that the Maxwell equations themselves must owe their existence to a perturbed PV. If it is then assumed that the tensor forms of the Maxwell equations are *the* covariant equations for electromagnetics, the corresponding coordinate transformation that leaves these equations covariant is the coordinate transformation that satisfies the Relativity Principle. This will be the Lorentz transformation assuming the result is unique. With this transformation in hand, the constancy of the speed of light can be deduced and the Michelson-Morley experiments [7] satisfied. From that point on relativistic kinematics can be derived in the usual way [2, p.9]. Special Relativity is now based on (1) relativity and (2) the dynamics of the PV state, rather than the standard postulates including (1) relativity and (2) the constancy of the speed of light. In this PV formulation of Special Relativity the constancy of the speed of light is a *derived* result, not a postulate.

The presence of the PV in the kinematic picture causes a mix-up in the classical position and time coordinates (r, t), resulting in the differential interval

$$ds^2 = c^2dt^2 - dr^2 \tag{5}$$

between the two events in spacetime at (r, t) and $(r+dr, t+dt)$. However, with the PV in the picture: the mixing of space and time is no longer the mystery that it is in the pre-PV formalism where the equations in (1) are unknown; and (r, t) is still just the bookkeeping entry it is in pre-relativistic physics.

The mixing of coordinates and time in Special Relativity is necessarily carried over into the equations of General Relativity to insure covariance of those equations. But now the effects of a mass perturbing the PV show up in the equations. For a point mass the force perturbation is mc^2/r and the resulting differential-interval equation is the Schwarzschild line element [8]

$$ds^2 = (1 - 2n_r)\, c^2dt^2 - \frac{dr^2}{(1 - 2n_r)} \tag{6}$$

where

$$n_r \equiv \frac{mc^2/r}{m_*c^2/r_*} \tag{7}$$

is the relative curvature force the mass m exerts on the PV. If there were no perturbing mass ($m = 0$), the line element would reduce to that of the Special Relativity result in (5) as it should.

Expressing the Einstein field equation in the following way [9]

$$G_{\mu\nu} = \frac{8\pi G}{c^4}\, T_{\mu\nu} \qquad \rightarrow \qquad \frac{G_{\mu\nu}/6}{1/r_*^2} = \frac{T_{\mu\nu}}{\rho_*} \tag{8}$$

shows that it, and those equations like (6) that follow from it, owe their existence to the PV as implied by the presence of the Planck-particle Compton radius r_* $(= e_*^2/m_*c^2)$ and the energy density

$$\rho_* = \frac{m_*c^2}{4\pi r_*^3/3} = \frac{e_*^2/r_*}{4\pi r_*^3/3} \tag{9}$$

in the final equation of (8). The ratio $1/r_*^2$ in (8) is the Gaussian curvature of a spherical volume of the PV equal to $4\pi r_*^3/3$.

Although it is accepted knowledge that absolute motion through free space is undetectable, such motion is clearly suggested by the equations of modern physics as seen above. The assumed existence of the PV implies that extra-free-space (XFS) reference frames must exist, at least those reference frames that describe the dynamics taking place within the PV for example. From this point it is easy to speculate that some XFS frames might be associated with levels of reality more fundamental than both the free-space and the PV frames. Thus the picture emerges of a cosmos possibly occupied by successive sets of XFS reference frames, in addition to the free-space frames in which we live, that belong to deeper levels of reality yet to be discovered.

The coexistence of the free-space and PV reference frames on top of each other is easily seen in equation (4), where the Newtonian force on the LHS belongs to the free-space frame and the three PV-curvature forces on the RHS to the PV reference frame. The reference frame for both sides of equations (5) through (9) is the PV reference frame. The presence of the PV frame in the equations indicates that, although it may be impossible to detect an absolute frame experimentally, there is abundant evidence that at least XFS reference frames do exist.

Finally, it is worth noting that there may exist only one reference frame (the absolute frame) in which there are successively more complicated states of existence figuratively "piled on top of each other like the skins of an onion" with the free-space state at the top of the pile.

Submitted on May 11, 2010 / Accepted on May 17, 2010

References

1. Møller C. The Theory of Relativity. Oxford Clarendon Press, First Addition, NY, Toronto, London, . . . , 1952–1962.
2. Leighton R.B. Principles of modern physics. McGraw-Hill Book Co., NY, Toronto, London, 1959.
3. Daywitt W.C. The Planck vacuum. *Progress in Physics*, v. 1, 2009, 20.
4. Milonni P.W. The quantum vacuum — an introduction to Quantum Electrodynamics. Academic Press, New York, 1994.
5. Daywitt W.C. The source of the quantum vacuum. *Progress in Physics*, v. 1, 2009, 27.
6. Davies P. Superforce — the search for a Grand Unified Theory of Nature. Simon and Schuster, New York, 1984.
7. Michelson A.A., Morley E.W. Relative motion of earth and luminiferous ether. *Silliman J.*, v. 34, 1887, 333, 427.
8. Daywitt W.C. The Planck vacuum and the Schwarzschild metrics. *Progress in Physics*, v. 3, 2009, 30.
9. Daywitt W.C. Limits to the validity of the Einstein field equations and General Relativity from the viewpoint of the negative-energy Planck vacuum state. *Progress in Physics*, v. 3, 2009, 27.

Finding the Fine Structure of the Solutions of Complicate Logical Probabilistic Problems by the Frequent Distributions

Anatoly V. Belyakov
E-mail: belyakov.lih@gmail.com

The Author suggests that frequent distributions can be applied to the modelling the influences of stochastically perturbing factors onto physical processes and situations, in order to look for most probable numerical values of the parameters of the complicate systems. In this deal, very visual spectra of the particularly undetermined complex problems have been obtained. These spectra allows to predict the probabilistic behaviour of the system.

Normal distribution, also known as the Gauss distribution, is a distribution of the probabilities ruling physical quantities and any other parameters in general, if the parameters are affected by a large number of purely stochastic processes. The normal distribution plays a highly important rôle in many fields of knowledge and activity of the Mankind. This is because of all distributions, which may be met in the Nature, the most frequent is the normal distribution. In particular, the normal distribution sets up the law of the Brownian motion — the fluctuations of Brownian particles being affected by the probabilistically perturbing factors such as the heat motion of molecules. In these fluctuations, the consecutive changes of the particles' location are independent from the last events in them, and their any current location can be assumed to be the initially start-point.

As an example of another sort, a simplest situation of the theory of games can be provided. In this example, an initially rate S_0 increases proportionally to the progression coefficient q_1 with a probability of p_1, or decreases proportionally the progression coefficient q_2 with a probability of p_2. As is obvious, the pair of these numerical values are connected to each other here: these are the current and past values connected as $S_{i+1} = S_i\, q_i$.

However in the core of this problem, the examples are a manifestation of the same situation, because S_0 can be meant as any parameter under consideration in a process being affected by perturbing factors.

It is clear that, having duration of the process unbounded, the numerical value of the parameter S_0 will vary near an average value, then filling, step-by-step, the arc of the normal distribution.

The current value S_i should return back to this average value each time after a number of the steps passed in the ways of different lengthes under stochastic alternating q_1 and q_2. Therefore, concerning the parameters of the perturbing effects in the perturbation series, the set of the current numerical values of the parameters is different in the cases of both sequent and parallel observations. Thus, it seems that there should not be "spectra" or "non-uniformities" in the Gauss arc. On the other hand, the Gauss distribution is a particular case of more complicate distributions, where the smooth form of the Gauss distribution is only an idealisation of those. Because some numerical values can meet each other in the series of the observations, the frequent distribution* of the *sum of all numerical values registered in many series* manifests the preferred numerical values of S_i thus producing by this its own specific spectrum.

Note that the discrete nature of normal distributions was experimentally discovered in different physical processes in already the 1950's by S. E. Shnoll [1].

Figures 1–3 show examples of the frequent spectra which came from the normal distributions being affected by two, three, and four perturbing factors (the progression coefficients q_i). The ordinate axis shows the number of coincident numerical values. The axis of abscissas shows the current values of S_i in doles of the initially value. These numerical values were given, for more simple and convenient comparing the histograms, in the same interval of abscissas from 0.0001 to 10000, while the initially parameters were assumed to be such that the axis of the distribution crosses the initially sum S_0. The diagrams were obtained by summing 500 series of 500 steps in each (so the common number of the values is $500 \times 500 = 250000$). The relative length of the current interval q was assumed 10^{-6} of the current value S_i. The algorithmic language C++ was used in the calculation.

This is a fragment of a computer program

```
for ( int t = 1; t < 500; t ++ )   {
double  Si = 1;
for ( int u = 1; u < 500; u ++ )   {

if ( a >=  b && a >= c ) {qi = q1 ; goto nn ; }
if ( b >=  a && b >= c ) {qi = q2 ; goto nn ; }
if ( c >=  a && c >= b ) {qi = q3 ; goto nn ; }
nn:    Si = Si*qi ;
if ( Si < 10000 && Si > 0.0001 )
i++ ,  m[ i ] = Si ;               }
                                   }
```

*Frequent distributions provide a possibility for bonding the probability of the appearance of numerical values of a function in the area where it exists. That is, the frequent distributions show the reproducibility of numerical values of the function due to allowed varying its arguments. There is a ready-to-use function "frequency" in MS Excel; any other software can be applied as well.

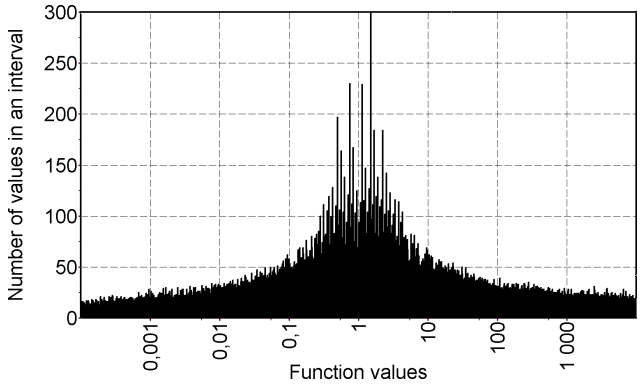

Fig. 1: Frequent distribution obtained with $q_1 = 1.5$, $q_2 = 0.5$, $p_1 = 0.555$, $p_2 = 0.444$; number of steps in the series is 500, number of the series is 500; number of the numerical values in the scale 190,000 (of those, nonzero intervals are 8,000).

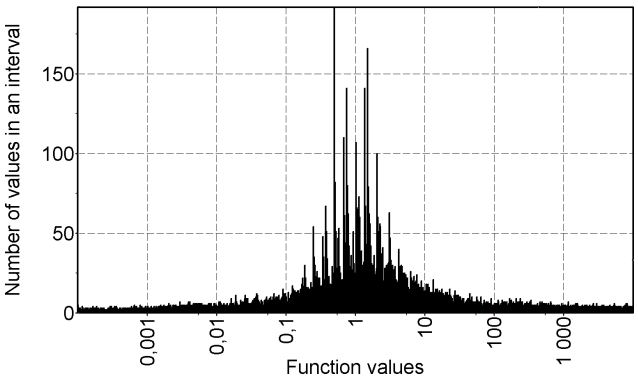

Fig. 2: Frequent distribution obtained with $q_1 = 1.5$, $q_2 = 0.5$, $q_3 = 1.37$, $p_1 = 0.333$, $p_2 = 0.333$, $p_3 = 0.333$; number of the steps in the series is 500, number of the series is 500; number of the numerical values in the scale is 180,000 (of those, nonzero intervals are 62,000).

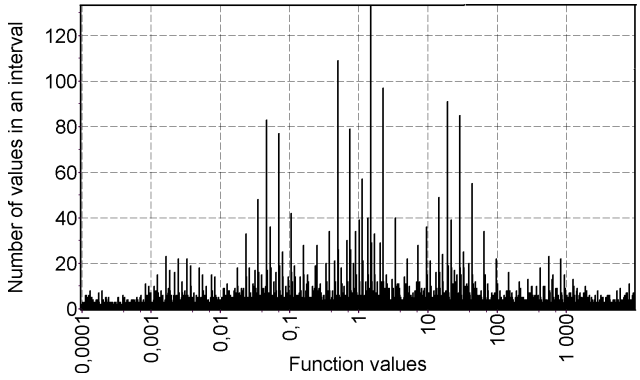

Fig. 3: Frequent distribution obtained with $q_1 = 1.5$, $q_2 = 0.5$, $q_3 = 19.3$, $q_4 = 0.047$, $p_1 = 0.294$, $p_2 = 0.235$, $p_3 = 0.235$, $p_4 = 0.235$; number of the steps in the series is 500, number of the series is 500; number of the numerical values in the scale is 67,000 (of those, nonzero intervals are 28,000).

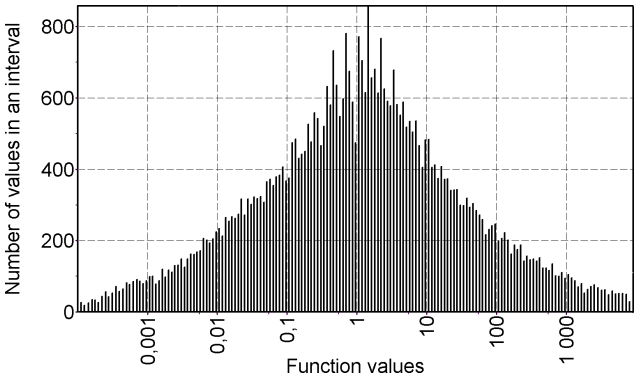

Fig. 4: Frequent distribution obtained with $g = 0.1$ from the current numerical value S_i; here $q_1 = 1.5$, $q_2 = 0.5$, $p_1 = 0.555$, $p_2 = 0.444$; number of the steps in the series is 100, number of the series is 500; number of the numerical values in the scale is 48,000 (of those, nonzero intervals are 173).

modelling the change of the parameter S_i and the set of a massive data of S_i, in look for the frequent distributions obtained due to three perturbing factors q_1, q_2, q_3. Here a, b, c are prime numbers which stochastically change (the computer program contains a function which generates random numbers), in each single cycle of the observation, along the intervals whose length is proportional to their probabilities p_1, p_2, p_3.

The graphs manifest that fact that, in the common background of the numerical values of the current parameters, there is only minor number of those whose probability exceeds the average value in many times. Besides that, the exceeding numerical values depend on the numerical values of the progression coefficients, but are independent from the length of the series (the number of the steps). Increasing the number of the perturbing factors does not make the non-uniform distribution more smooth, as it should be expected. Contrary, the non-uniformity of the distribution increases: in this process the allowed current values S_i occupy more square of the graph, while their number in the given section of the axis x decreases. Therefore a small probability of that the current values S_i will valuable shift from their average positions appear due to the appearance of the long chains of the co-multipliers which have the progression coefficients larger (or lesser) than unit. If the progression coefficients differ valuable from each other, the histogram manifest distributions of high orders (see Figure 3).

Consider an ultimate case where all perturbing factors, i.e. the progression coefficients q_i, differ from each other by the numerical values, and there is not their coinciding numerical values in the series. This situation can easy be modelled, if setting up in the computer program that the progression coefficients have a connexion with the counters of the cycles t and u, or that they are varied by any other method. In this case, in a limit, the amplitude of the numerical values in the histogram will never exceed unit, nowhere, while the *frequent non-uniformity* will still remain in the distribution. Therefore, even if extending the length of the unit interval, the same dis-

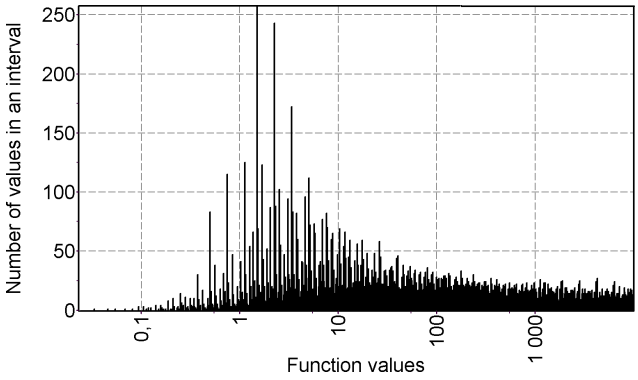

Fig. 5: Non-symmetric frequent distribution obtained according to the data of Fig. 2; number of the numerical values in the scale is 22,000 (of those, nonzero intervals are 2,400).

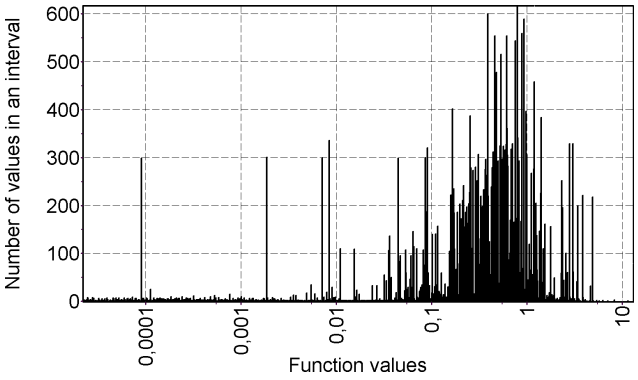

Fig. 6: Frequent distribution of the solutions of the quadratic equation $x^2 - 2Bx + C = 0$ with $q_1 = 1.33$, $q_2 = 0.71$, $q_3 = 1.33$, $q_4 = 0.71$; here $p_1 = p_2 = p_3 = p_4 = 0.25$; number of the steps in the series is 300, number of the series is 300; number of nonzero intervals is 16,000. All geometric coefficients of the progression are independent from each other.

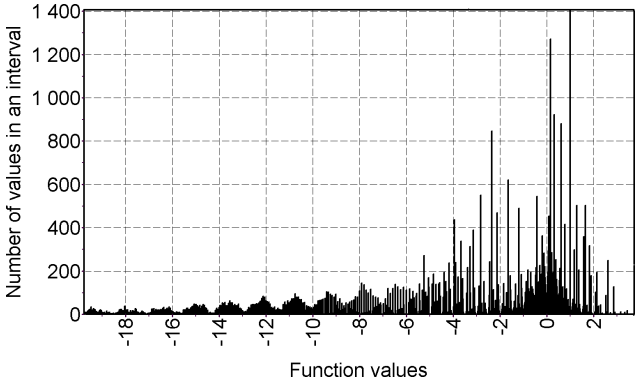

Fig. 7: Frequent distribution of the solutions of the quadratic equation $x2 - 2Bx + C = 0$ with $q_1 = 0.71$, $q_2 = -0.71$, $q_3 = 0.71$, $q_4 = -0.71$; here $p_1 = p_2 = p_3 = p_4 = 0.25$; number of the steps in the series is 250, number of the series is 250, number of nonzero intervals is 1,800. All arithmetic coefficients of the progression are independent from each other.

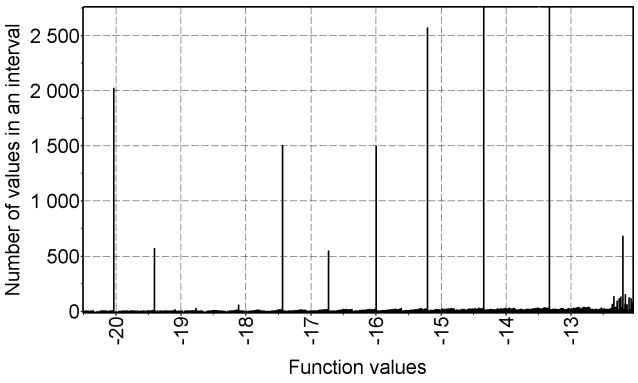

Fig. 8: Frequent distribution of the solutions of the quadratic equation $x2 - 2Bx + C = 0$ with $q_1 = 0.127$, $q_2 = 1.13$; $p_1 = 0.465$, $p_2 = 0.535$; number of the steps in the series is 500, number of the series is 10,000; number of the numerical values in the scale is 27,000, number of nonzero intervals is 1,350. All arithmetic coefficients of the progression are dependent on each other.

tribution takes the amplitudal discrete shape again. Finally, under truncating the number of the intervals (this, generally speaking, means analysis of the given process with a lower precision), the graph takes a shape of almost the smooth normal distribution (see Figure 4).

It is possible to suppose that the discreteness of normal distributions (and, as is obvious, any other distributions as well) is their core property originated from that the rational numbers are distributed with different density along the axis of numbers [2, 3].

Shapes of the histograms depend on specific parameters; they may be very spectacular. So, in the bit of the computer program that was given above, each perturbing factor realizes itself independent from the others. If however, for instance in the first condition, one replaces the logical "and" with the logical "or", the distribution changes its shape very much (see Figure 5).

So forth, Figures 6–9 show illustrative examples of the versions of the frequent distributions of one of the solutions of a quadratic equation $x^2 - 2Bx + C = 0$, where we see iterrationally correcting two parameters B and C whose initially numerical values are units.

In the example shown in Figure 6, the progression coefficients are geometric, and are independent from each other. The parameter B is under a correction by the coefficients q_1 and q_2, while the parameter C is under a symmetrical correction by the coefficients q_3 and q_4. Specific to the graph is that, somewhere left from the main distribution, in the background of many dense numerical values whose probabilities are very small, a small number of the numerical values having a very high probability appear (they experience a shift to the side of small numerical values of the function).

In the other examples shown in Figures 7 and 8, the progression coefficients are arithmetic. In the distribution shown

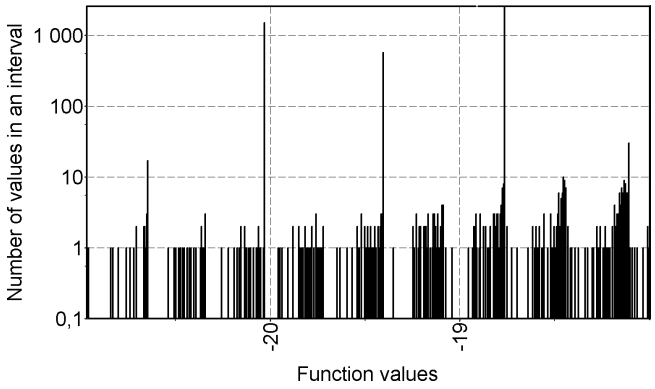

Fig. 9: A fragment of the frequent distrinution according to the data of Fig. 8; number of the numerical values in the scale is 5,300 (of those, nonzero intervals are 220).

in Figure 7, four progression coefficients are present; they are symmetric. The histogram is built by a set of the Gauss arcs of the first, second, and higher orders which fill the side of negative numerical values. The distance between the arcs, and their shape depend on the numerical value of the progression coefficients. In Figure 8, we give a part of the quadratic function distribution in the region of negative numerical values of its solutions taken under two coefficients q_1 and q_2, where the parameters B and C are additionally connected to each other, and their correction is produced commonly for them. The respective bit of the algorithm has the form:

```
for ( int t = 1; t < 10000; t ++ )      {
double  B  =  C = 1;
for ( int u = 1; u < 500; u ++ )        {

if ( a >=  b )   B = B + q1 , C = C - sqrt(q2) ;
if ( b >=  a )   C = C + q2 , B = B -  q1 ;
if ( B*B - C > 0 )
Si =  B - sqrt ( B*B - C ) ;
i++ ,  m[ i ] = Si ;                    }
                                        }
```

Here, as well as in the example shown in Figure 7 (but with more obvious visibility), that fact is manifested that the overwhelming number of the numerical values, i.e. the probable solutions of the function obtained under the variation of the parameters B and C, have an infinitesimally small probability in the scale, while the probability of the solutions is concentrated in a very small number of the solutions where it thus is very high. In the fragment of the histogram taken in a semi-logarithmic scale (Figure 9), is is clearly seen that the peaks of the maxima "grow up" from the frequent concentrations of the numerical values of the functions in the axis x. Should this mean that, in the case of similar distributions of a macroscopic system having an arbitrary number of solutions (degrees of freedom), the macroscopic system under a specific set of the parameters acting in it can be in selected special discrete (quantum) states, i.e. the system can have discrete solutions?

It is absolutely obvious that, first, such maximally probable solutions are mostly interested in processes and phenomena we study. Finding these solutions by some other methods that the method given above would be very complicate. Of course, in formulating algorithms for similar problems (obtaining the massive of the required values and their distribution by the algorithm) it is expedient to introduce reasonable limitations on the intervals of the parameters, their relations, etc., in order to excluse some extra calculations non-useful in the problems.

The simple examples we considered here show that the logical mathematical models similar to those we considered can contain actually unbounded number (with a limit provided by the computer techniques only) of both stochastic influences (the parameters q_i) and the conditions of their appearance (the logical and other relations between the coefficients q_i and also the parameters of the system). In the same way, very complicate complex influences of very different stochastic factors affecting any processes we study (not only physical processes) can be modelled if their formalization is possible. Moreover, it is probably we can set up the probabilistic system or process to be into a small number of stable states, which are necessary to our needs in the problem, by respective choice of the parameters affecting it.

Concerning the Brownian motion as a particular case of normal distributions, it can be also analysed if we know the spectrum of the factors perturbing it (the dole of each factor in their common sum, and the goal of each factor into the commonly perturbing influence). Concentration of the Brownian molecules and their momentum can be such factors in the problem.

Generalizing all that has been presented in this paper, I would like to say that frequent distributions provide a possibility for bonding the reaction of different parameters of a complicate system being affected by stochastic factors of the surrounding world, and also finding most probable states of the system thus predicting its behaviour. Having any problem, both those of physics, industry, economics, game, and others where numerous parameters are unknown, non-sufficiently determined, or are affected by stochastic changes, the method that presented in the paper leads to a spectrum of the most probable solutions of the problem.

Submitted on April 24, 2010 / Accepted on May 17, 2010

References

1. Shnoll S. E. Cosmic physical factors in random processes. Svenska fysikarkivet, Stockholm, 2009, 388 pages.
2. Dombrowski K. I. *Bulletin of Soviet Atron. Geodesical Society*, 1956, no. 17(24), 46–50.
3. Dombrowski K. I. Rational numbers distribution and resonance. *Progress in Physics*, 2005, v.1, 65–67.

On the Necessity of Using Element No.155 in the Chemical Physical Calculations: Again on the Upper Limit in the Periodic Table of Elements

Albert Khazan
E-mail: albkhazan@gmail.com

It is shown how the properties of different elements of the Periodic System of Elements can be obtained using the properties of the theoretically predicted heaviest element No.155 (it draws the upper principal limit of the Table, behind which stable elements cannot exist). It is suggested how the properties of element No.155 can be used in the synthesis of superheavy elements. An analysis of nuclear reactions is also produced on the same basis.

1 Introduction

At the present time, we know about 20 lists of chemical elements (representing their most important properties such as atomic mass and radius, density, temperatures of melting and boiling, energy of ionization, etc.), which were suggested by their authors as periodic tables of the elements. These data were however obtained for, mainly, stable isotopes and numerous other radioactive isotopes that makes further interpolation of these properties onto superheavy elements quite complicate.

This is most important for planning further experiments whose task is synthesis new superheavy elements which approach to the recently predicted heaviest element No.155, whose atomic mass is 411.66 (the upper limit of elements in Mendeleev's Table of Elements behind which stable elements cannot exist). Thus, using the parameters of element 155 in the analysis of other elements, we will see in this paper how the properties of the elements behave with increasing their number in the Table.

2 Some peculiarities of the dependency between atomic mass of the elements and their numbers in the Table of Elements

Consider the dependency between atomic mass of the elements and their number in the Table of Elements. This dependency is well known in science and industry and is presented as numerous lists and tables. As is seen in Fig. 1, this dependency is well described by the exponential equation of the line of the trend. However, if we take more attention to this figure, we find numerous areas which destroy the common picture. Approximately smooth line continues from the origin of coordinates to almost the end of Period 6 (No.83, 208.98, Bismuth). This is the last stable isotope, after whom all elements of the Table have an artificial (radioactive) origin, except of Thorium (No.90, 232.038), Protactinium (No.91, 231.036) and Uranium (No.92, 238.029). This is their order in the family of actinides. Period of half-decay of these natural elements consists many thousand years. It is easy to find in the figure that valuable deviations from the line of the trend are present in the region from Bismuth to element 104, then to element 119 where the deviations from the line of the trend are high (especially — in the region of the already synthesized superheavy elements 104–118).

This is seen more obvious in Fig. 2, where the absolute deviations of the atomic masses are presented. These are deviations between the data of the Table of elements and the result obtained after the equation

$$y = 1.6143\, x^{1.0981}, \qquad R^2 = 0.9969, \tag{1}$$

where y is the atomic mass, while x is the number in the Table of Elements.

It should be noted that mass number is an integer equal to the common number of nucleons in the nucleus. Mass number of an isotope is equal to the numerical value of its mass, measured in atomic mass units (a.m.u.) and approximated to a near integer. A difference between the mass numbers of different isotopes of the same element is due to the different number of neutrons in their nuclei.

It is seen in the figure that this difference does not exceed 4 a.m.u. in the first five periods and in lanthanides. This tendency still remain upto Bismuth after whom the deviations of actinides experience a positive shift: this means that the numerical values of the atomic masses presented in the Periodic Table are overstated for the region.

Then, after actinides, a region of the atomic masses of the elements of Period 7 (elements 104–118) is located. These elements were obtained as a result of nuclear reactions. As is seen, all deviations in this region are negative: this can mean a large deficiency of the numerical values of the atomic masses obtained in the nuclear synthesis producing these elements, incorrect calculations, or a lack of neutrons in the nuclei. All these in common resulted large deviations of the atomic masses upto 10–12 a.m.u.

Look at Fig. 1 and Fig. 2 again. Section of the line of the trend in the interval No.119–155 is manifested in Fig. 1 as a very straight line without any deviation, while the same section in Fig. 2 manifests deviations from 0.63 to 1.28. Once we get a ratio of the difference between the table and calculated numerical values of the atomic masses to the respective a.m.u., we obtain Fig. 3 which shows the respective de-

viations in percents. As is seen in the figure, most valuable deviations are located in the left side (upto the first 20 numbers). This is because the respective elements of the Table of Elements bear small atomic masses under high difference of a.m.u., i.e. the larger numerator results the larger ratio. It is necessary to note that the results presented in this figure are within 3–5%. Most lower results are located in the scale from element 104 to element 118: according to our calculation, the deviations are only 0.2–0.3% there.

In order to exclude any influence of our calculations onto the creation of the line of the trend, we study the dependency "atomic mass — number in the Table" in the scale from element 1 to element 118 according to the equation

$$y = 1.6153\, x^{1.0979}, \qquad R^2 = 0.9966. \tag{2}$$

As a result we obtain that the general shape of the deviations and their numerical values are actually the same as the results obtained due to equation (1). So forth, the next particular equations were taken under analysis:

$$\text{elements 1–54:} \quad y = 1.6255\, x^{1.0948}, \quad R^2 = 0.9922, \tag{3}$$

$$\text{elements 55–118:} \quad y = 1.8793\, x^{1.0643}, \quad R^2 = 0.9954, \tag{4}$$

$$\text{elements 119–155:} \quad y = 1.5962\, x^{1.1009}, \quad R^2 = 1.0\,. \tag{5}$$

These sections gave no any substantial change to the previous: the ultimate high difference of the deviations taken in 3 points of 120 was 0.7% for element 111, 0.95% for element 118, and 1.5% for element 57.

3 Why one third of the elements of the Table of Elements is taken into square brackets?

94 chemical elements of 118 already known elements are natural substances (contents of several of them consists, however, of only traces). Rest 24 superheavy elements were obtained artificially as a result of nuclear reactions. Atomic mass of an element in Table of Elements is presented by the average atomic mass of all stable isotopes of the element with taking their content in the lithosphere. This average mass is presented in each cell of the Table, and is used in calculations.

If an elements has not stable isotopes, it is taken into square brackets that means the atomic mass of most long living isotope or the specific isotope contents. There are 35 such elements. Of those 35, elements from 93 to 118 are actinides and artificially synthesized superheavy elements. Hence, one third of 118 elements (known in science at the present time) bears undetermined atomic masses.

Fig. 4 shows common number of isotopes of all elements of the Table of Elements. Location of all elements can be described by the equation of parabola with a high coefficient of real approximation. As is seen, the descending branch of the parabola manifest that fact that the heavier element in the Table (the larger is its number) the lesser number of its isotopes. This tendency lads to decreasing the number of isotopes upto 1 at element 118.

4 Synthesis of superheavy elements and the upper limit of the Periodic Table

Because number of the isotopes reduces to 1 in the end of Period 7, the possibility of Period 8 and Period 9 (each consisting of 50 elements) in the Table of Elements suggested earlier by Seaborg and Goldanskii [1, 2] seems non-real. At the same time, Seaborg suggested a possibility of the synthesis of a "magic nucleus" consisting of 114 protons and 184 neutrons: according to his suggestion, this nucleus should be the centre of a large "island of stability" in the sea of spontaneous decay. Goldanskii told that the "isthmus of stability" may be a region where isotopes of the elements bearing nuclear charges 114, 126, and even 164 may be located. Flerov [3], when analysed studies on the synthesis of superheavy elements, claimed that the elements should give us a possibility for answering the question: are the elements bearing nuclear charges 100–110 located at the real end of the Table of Elements, or more heavy nuclei exist in the Nature? There are many studies of the conditions of nuclear reactions. For instance, in already 1966, Strutinski [4] theoretically predicted a valuable increase of stability of nuclei near the "magic numbers" $Z = 114$ and $N = 184$. His calculation was based on the shell model of nucleus (this model won Nobel Prize in physics in 1963 [5, 6, 7]).

In 1973, Oganesyan in Dubna (Russia) and a group of German scientists in Darmstadt (Germany) first used cold synthesis, where the "magic nuclei" were used as both a target and bombing particles [8]. In 1973, Oganesyan claimed that elements with atomic numbers 160 and, maybe, 170, are hypothetically possible. However only two years later, he claimed that the properties of an element with number 400 and bearing 900 neutrons in its nucleus were theoretically discussed [9].

In addition to the indeterminacy of atomic masses in the synthesis of superheavy elements, Oganesyan also told, in his papers, that we do not know limits in the Table of Elements behind whom superheavy elements cannot exist. According to his own words, "the question about limits of the existence of the elements should be addressed to nuclear physics" [10]. A few years later, in 2005, Oganesyan claimed "this question is still open: where is the limit of chemical elements?" [11]. In 2006, in his interview to *Moscow News*, he set up the questions again: "is a limit there?" and "how many elements can exist?". So forth, he tells in the interview: "We use modelling instead a theory. Each models approaches this system in a form of those known to us in analogy to the macroscopic world. However we still do not understand what is nuclear substance. Thus the question asked about a limit of the Periodic System is still open for discussion" [12].

In January 20–21, 2009, in Dubna, the international symposium celebrating the 175th birthday of Dmitri Mendeleev set up the question about limits of the Table of Elements, and the complete number of elements in it again. Some-

one suggested even a possibility of the synthesis of elements with numbers 150–200 [13]. However a few weeks later, in February 09, at a press-conference in Moscow, the participants claimed that "at present the scientists discuss a theoretical possibility of extending Mendeleev's Periodic Table upto **150 elements**" [14].

In April 07, 2010, the world press claimed about the end of an experiment in which element 117 was synthesized (this experiment continued from July 27, 2009, until February 28, 2010). During these seven months, the experimentalists registered six cases where nuclei of the new element were born. This experiment was also based on the supposition that there is an "island of stability" near an element bearing parameters $Z = 114$ and $N = 184$. Lifespan of this island should be a few million years. However this target was not reached in the experiment. The research group of experimentalists in Dubna prepares next experiments which target synthesis of element 119 and element 120 [15].

In this connexion it is interesting those words said by Sigurd Hofman (the GSI Helmholtz Centre for Heavy Ion Research, Darmstadt), where he claimed about filling the Table of Elements upto its end in the close time. According to his opinion, atomic nuclei heavier than No.126 cannot exist, because they should have not the shell effect [16].

5 Discussion of the results

1. The considered dependency of atomic masses of the elements on their numbers in the Table of Elements cannot answer the question "where is the upper limit of the Table".

Despite the coefficient of the line of the trend is very close to unit, it is easy to see that there are large deviations of the data, especially starting from the numbers of actinides and then so forth. Because all actinides bear similar chemical properties, selecting a segregate element in this group is quite complicate task. Besides, the possibility of different isotopic content in samples of the elements leads to a large deviation of the calculated atomic masses from the atomic masses given by the Table of Elements. This is related to one third part of all elements of the Table.

2. Next elements to actinides, i.e. a group of elements 104–118, were synthesized as a result of nuclear reactions, in a very small portions (only segregate atoms were produced). The way how the elements were produced makes a problem in the identification of them, and the large deviations of the data of the Table of Elements from the line of the trend. Hence, atomic masses attributed to these numbers in the Table of Elements, are determined very approximate. The line of the trend, which includes element 155, gives a possibility to exclude the deviations of the atomic masses.

3. Section 4 gave a survey of opinions on the structure of the Table of Elements, its limits, superheavy elements (their synthesis and the products of the synthesis), the search for an "island of stability", and the technical troubles with the nuclear reactions.

Many questions could be removed from discussion, if my recommendations suggested in [17], where I suggested the last (heaviest) element of the Table of Elements as a reference point in the nuclear reactions, would be taken into account. This survey manifests that the quantum mechanical approach does not answer the most important question: **where is the limit of the Periodic Table of Elements?** Only our theory gives a clear answer to this question, commencing in the **pioneering paper of 2005**, where the **hyperbolic law** — a new fundamental law discovered in the Table of Elements — was first claimed. This theory was never set up under a substantially criticism.

It should be noted that the word "discovery" is regularly used in the press when telling on the synthesis of a new element. This is incorrect in the core, because "discovery" should mean finding new dependencies, phenomena, or properties, while the synthesis of a new element is something like an invention in the field of industry, where new materials are under development.

4. Taking all that has been said above, I suggest to IUPAC that they should produce a legal decision about the use of element 155, bearing atomic mass 411.66, as a reference point in the synthesis of new superheavy elements, and as an instrument correcting their atomic masses determined according to the Table of Elements.

My theory I used in the calculations differs, in principle, from the calculations produced by the quantum mechanical methods, which were regularly used for calculations of the stability of elements. The theory was already approved with the element Rhodium that verified all theoretical conclusions produced in the framework of the theory with high precision to within thousandth doles of percent. Therefore there is no a reason for omiting the theory from scientific consideration.

6 Conclusions

Having all that has been said above as a base, I suggest an open discussion of the study **Upper Limit in Mendeleev's Periodic Table — Element No.155** at scientific forums with participation of the following scientific organizations:

— International Union of Pure and Applied Chemistry (IUPAC);

— International Council for Science (ICSU);

— American Physical Society (APS).

This step should allow to give a correct identification to the chemical elements and substances, and also to plan new reactions of nuclear reactions with a well predicted result. In this deal, financial spends on the experimental research in nuclear reactions could be substantially truncated, because the result would be well predicted by the theory. The experimental studies of nuclear reactions could be continued as a verification of the theory, and aiming the increase of the experimental techniques. Thus, according to the last data of the

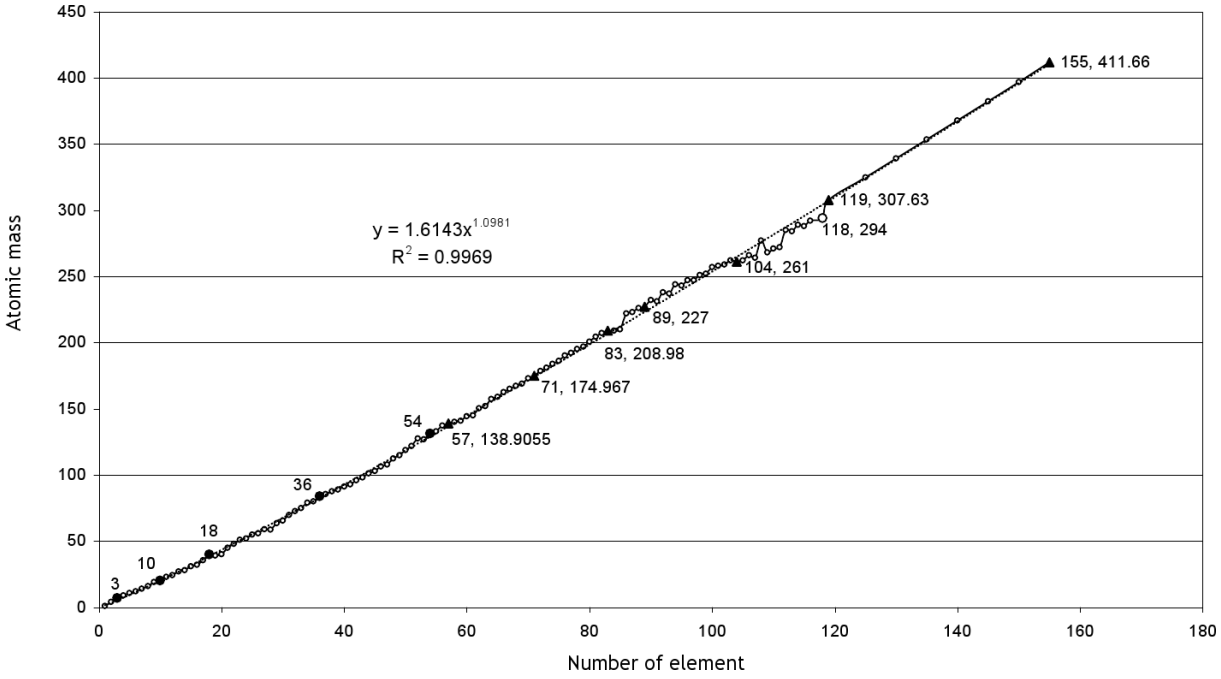

Fig. 1: Dependency between the atomic mass of the elements and their number in the Table of Elements (including element 155).

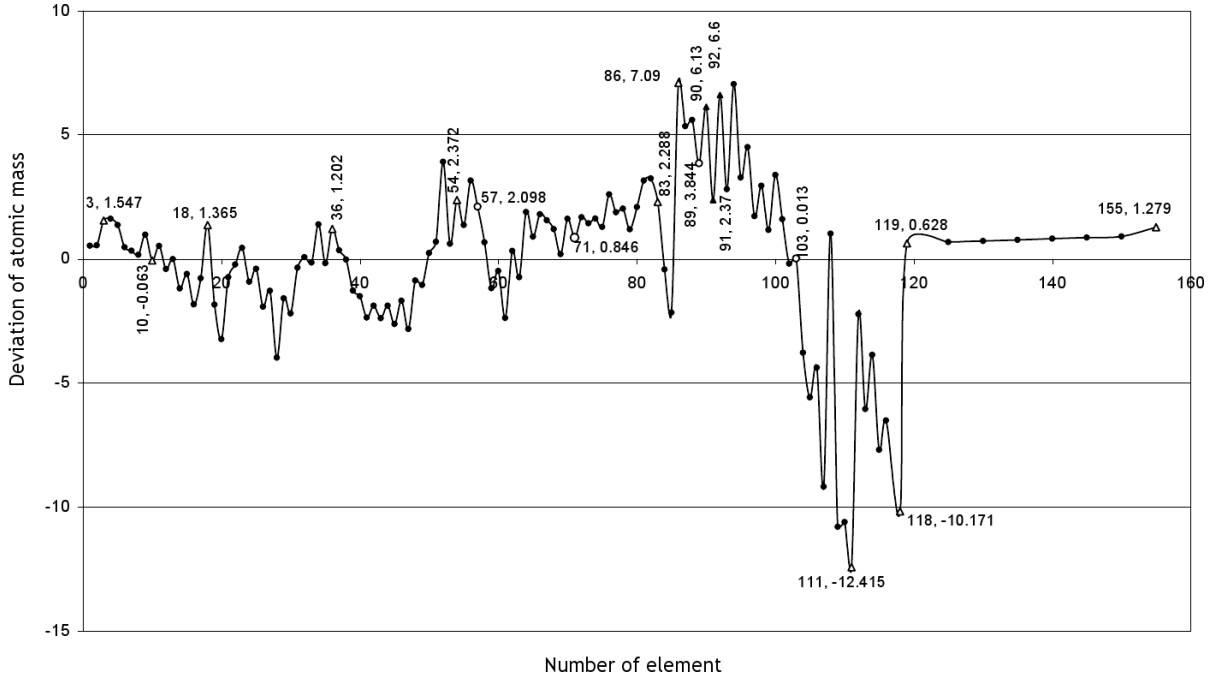

Fig. 2: Absolute deviations of atomic masses of the elements from the line of the trend (including element 155).

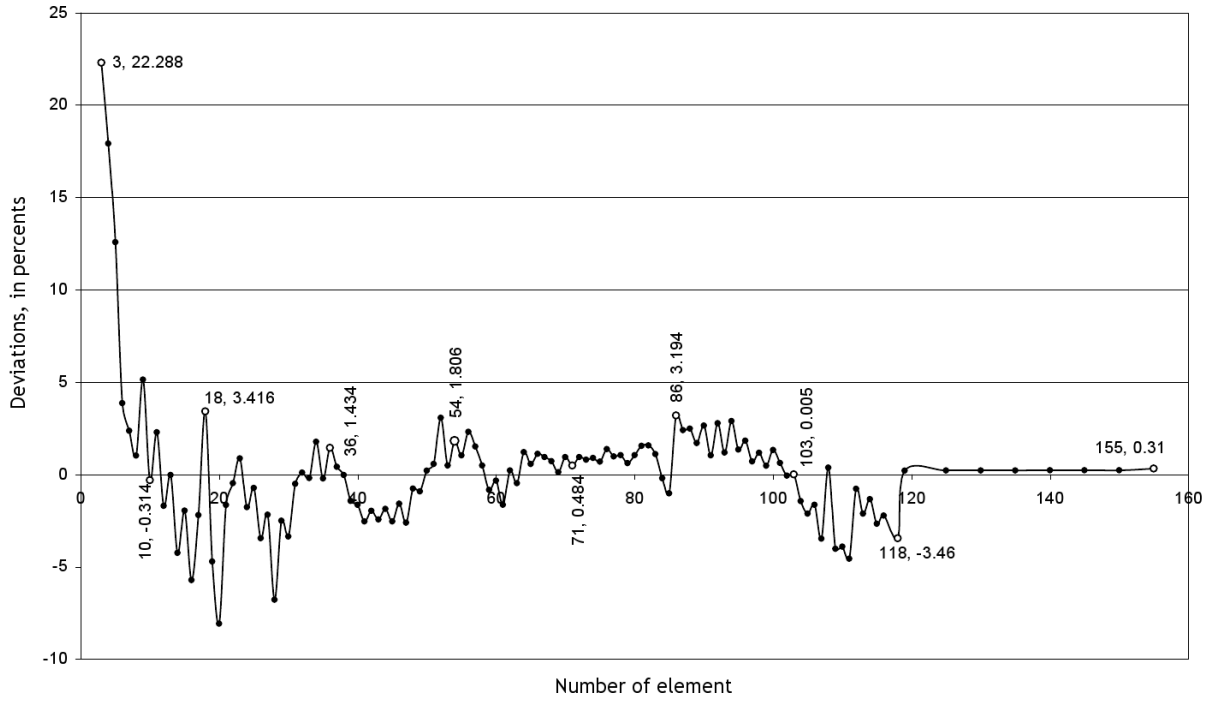

Fig. 3: Relative deviation of the atomic masses from the line of the trend, in percents.

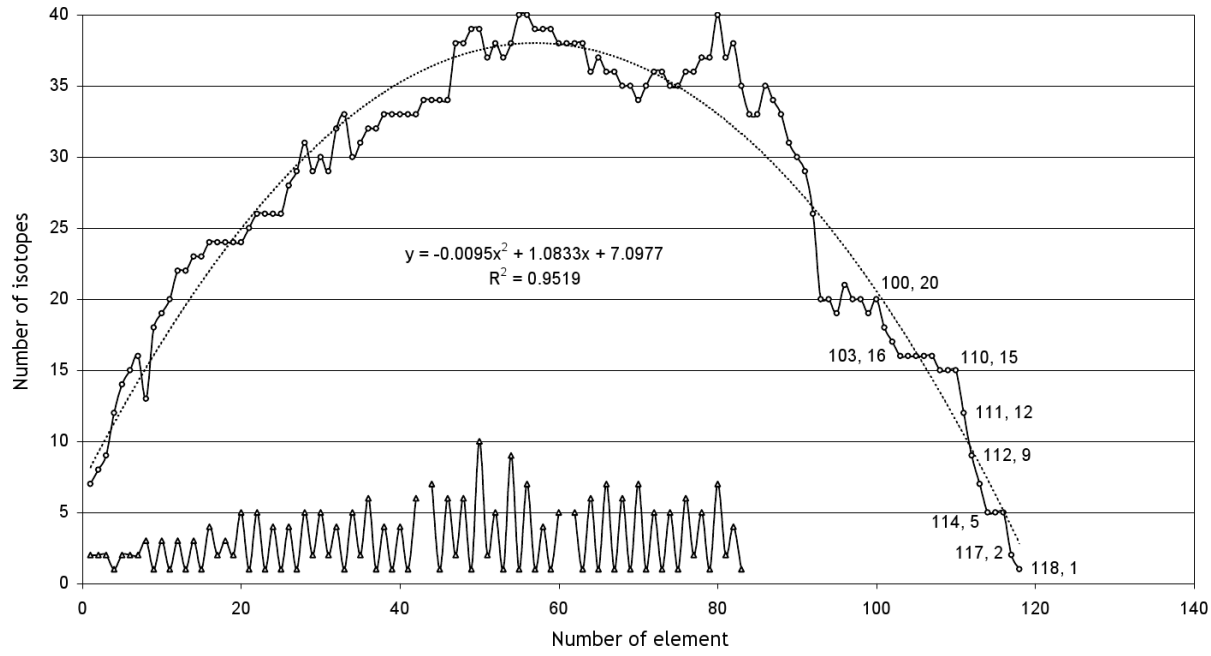

Fig. 4: Dependency between the number of the isotopes (3180) and the number of element in the Table of Elements. Location of the stable isotopes (256) is also shown. The data of Brookhaven National Laboratory, National Nuclear Data Center.

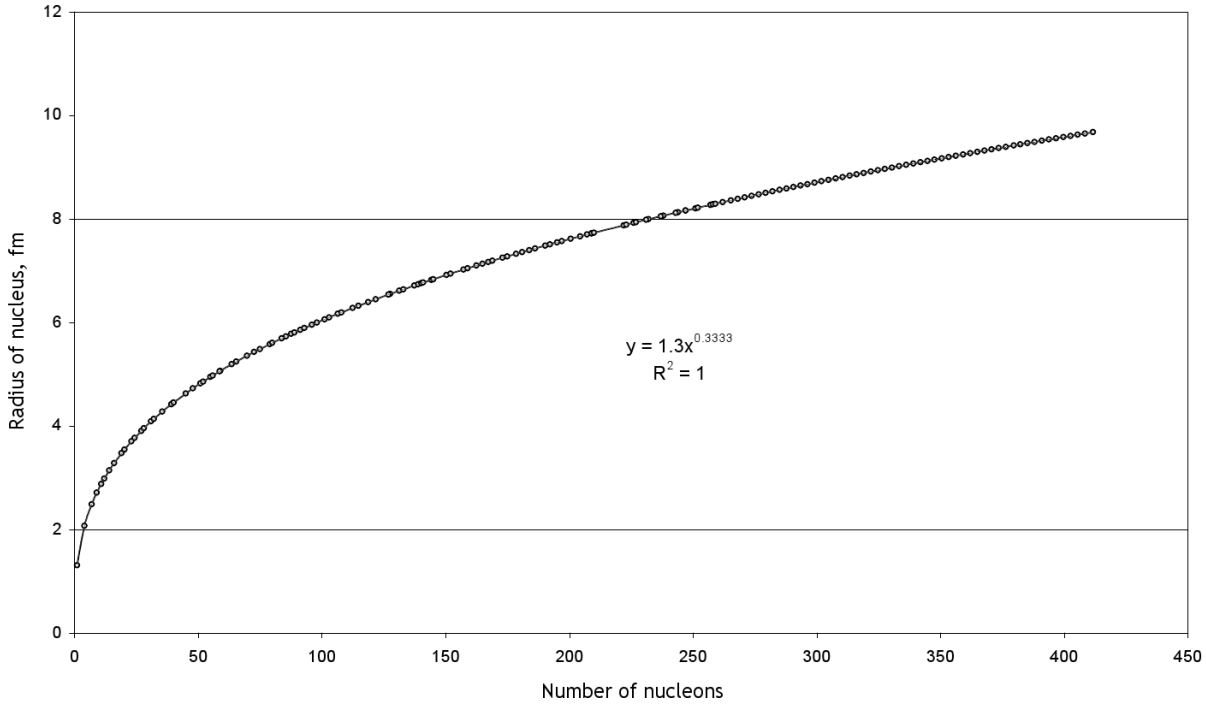

Fig. 5: Empirical dependency between the radius of the nuceus (fm) and the number of the nucleons.

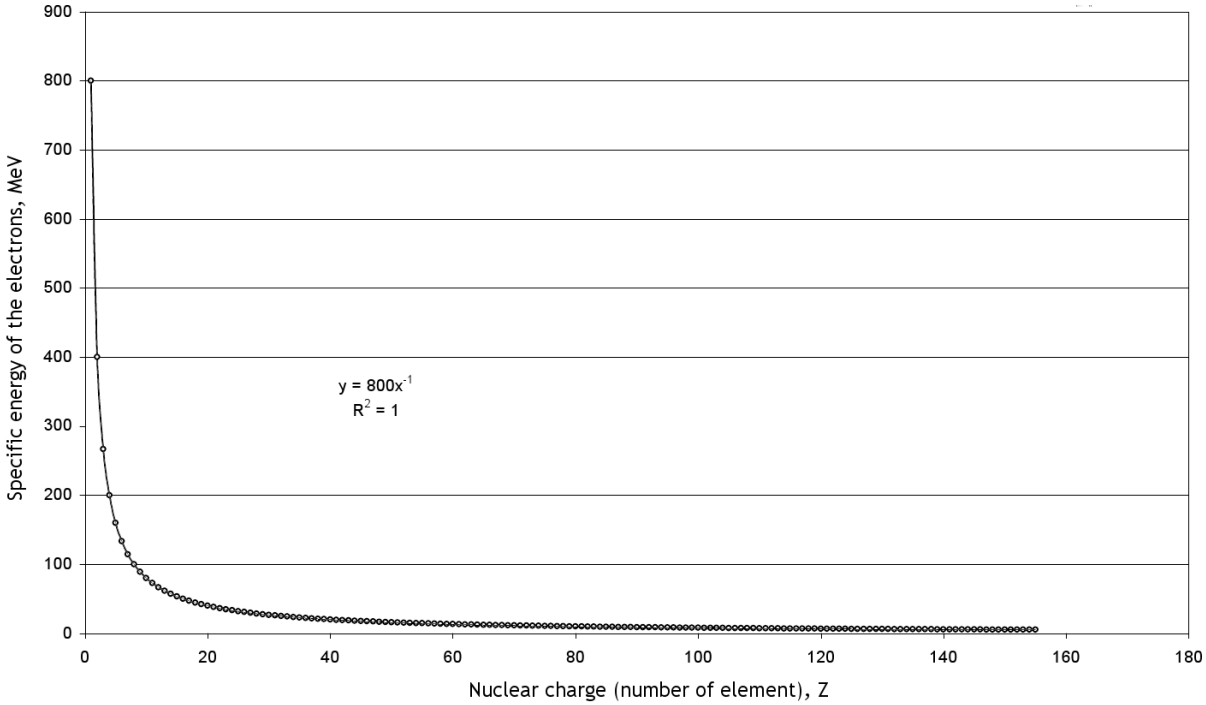

Fig. 6: Dependency beween the critical energy of the electrons and the nuclear charge, according to formula $T = 800/Z$.

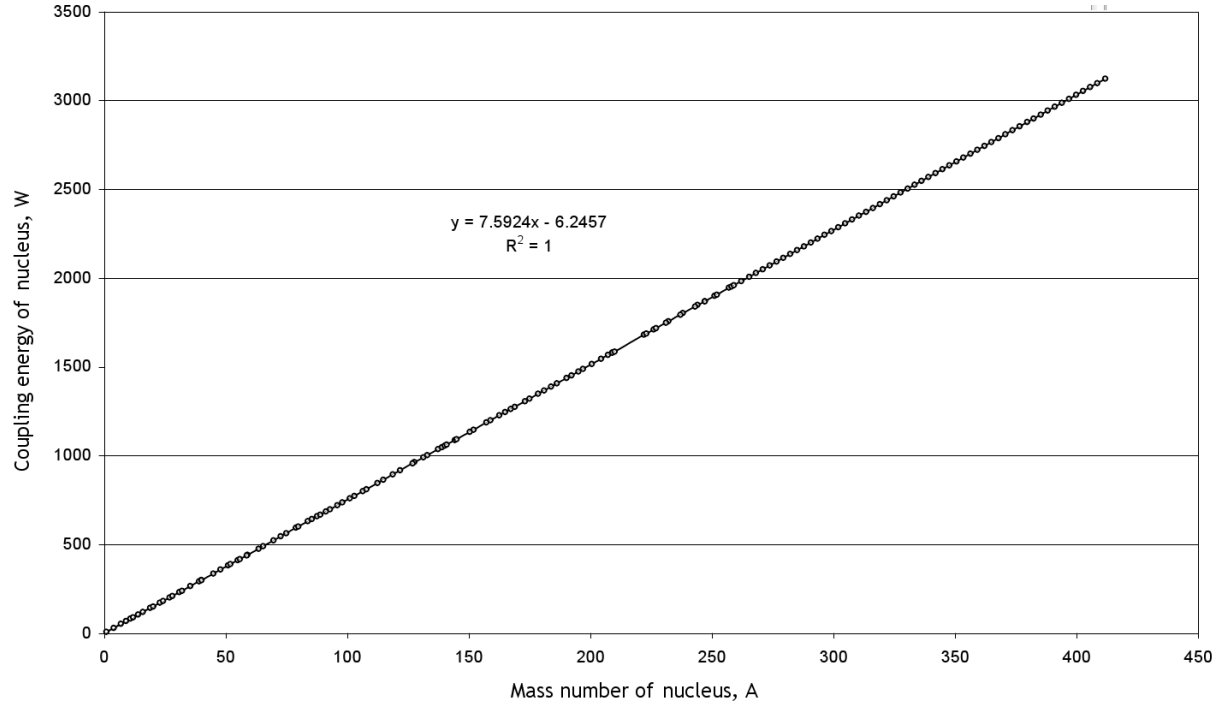

Fig. 7: Dependency between the coupling energy of the nuclei and the mass number (number of nucleons).

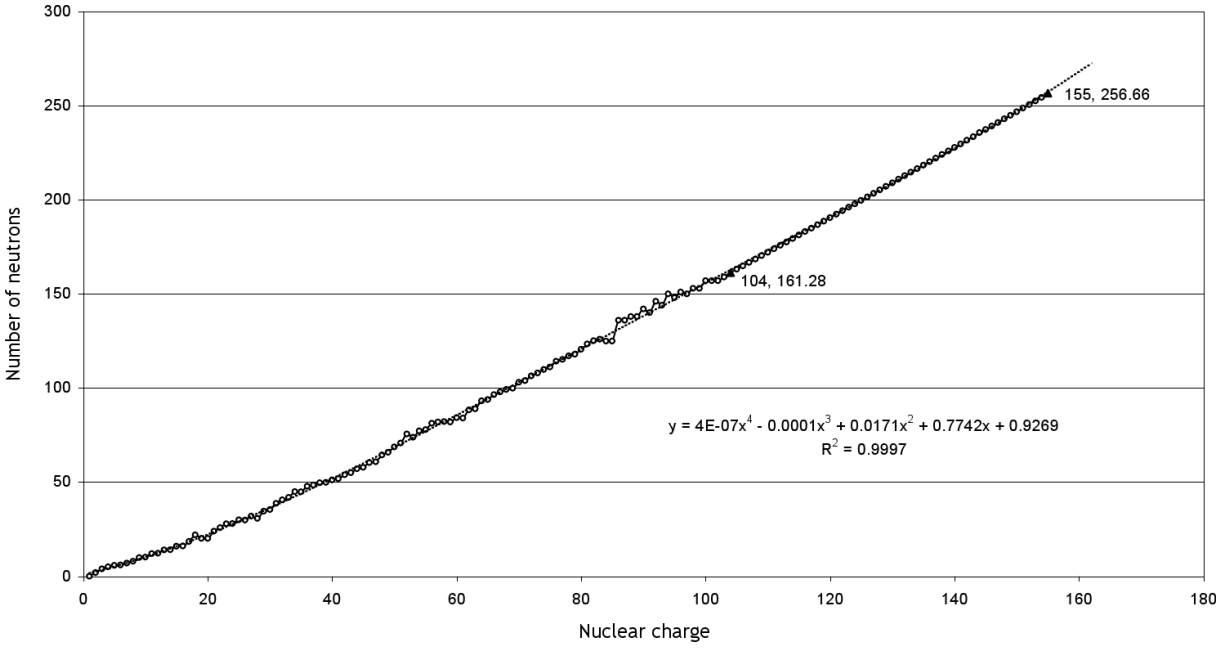

Fig. 8: Dependency between the number of neutrons and the number of protons in the atomic mass, for all elements of the Table of Elements. Our calculation data are given beginning from element 104.

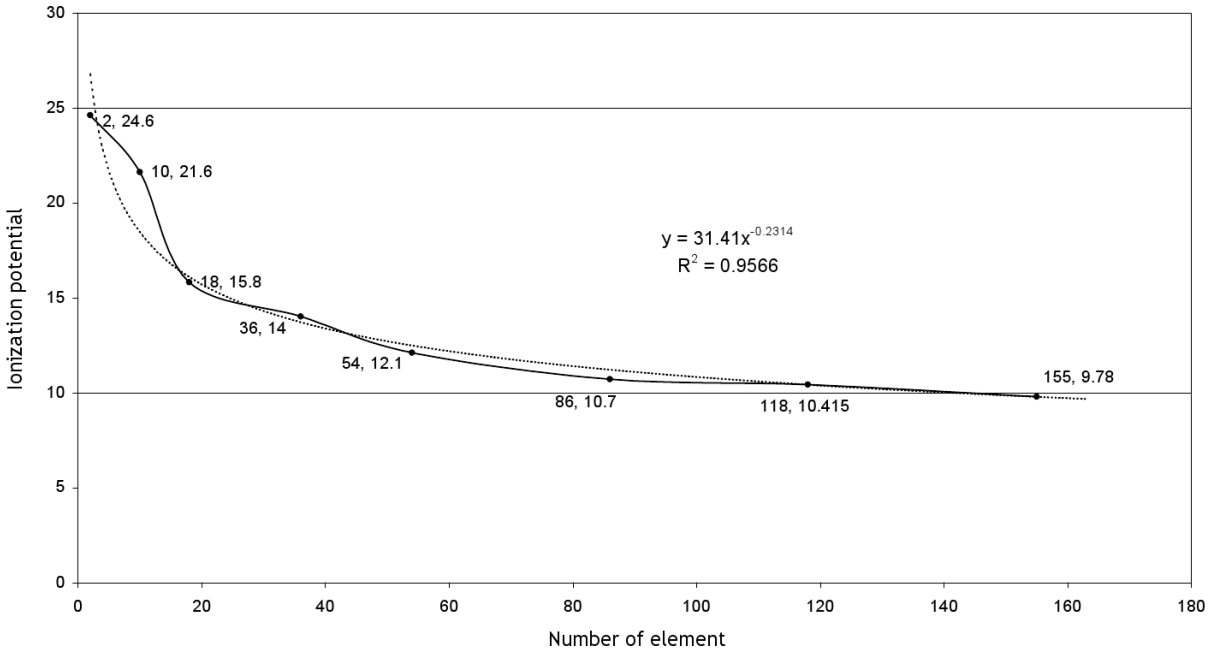

Fig. 9: Dependency between the ionization potential and the number of the elements (nuclear charge), for the neutral atoms of the elements ending the periods of the Table of Elements (including calculated element 118 and element 155).

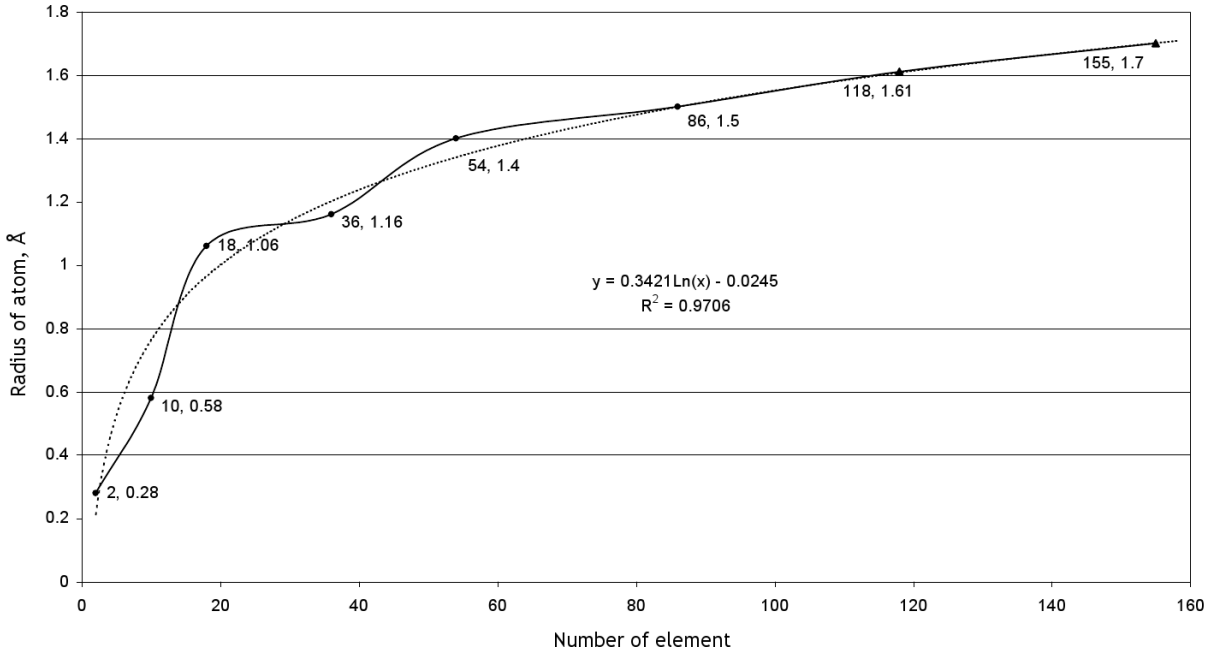

Fig. 10: Dependency between the atomic radius and the number of the elements in all periods of the Table of Elements, including the calculated elements No.188 in Period 7 and No.155 in Period 8.

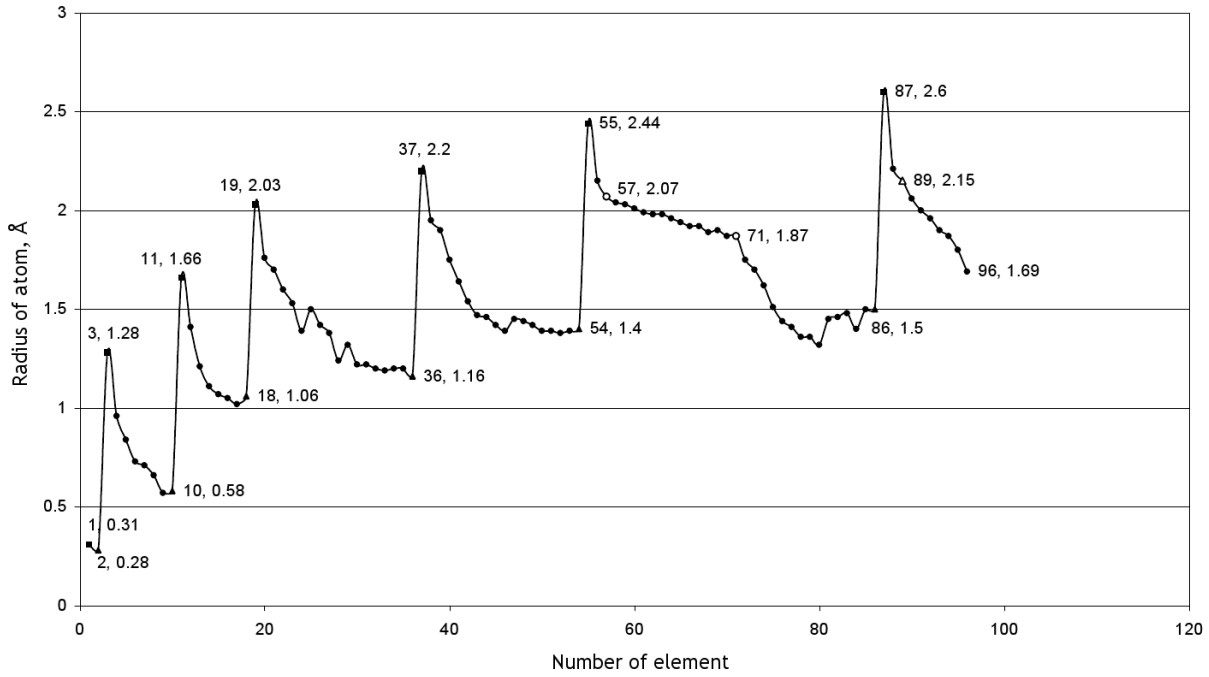

Fig. 11: Change of the numerical value of the atomic radius in each period with increasing number in the Table of Elements.

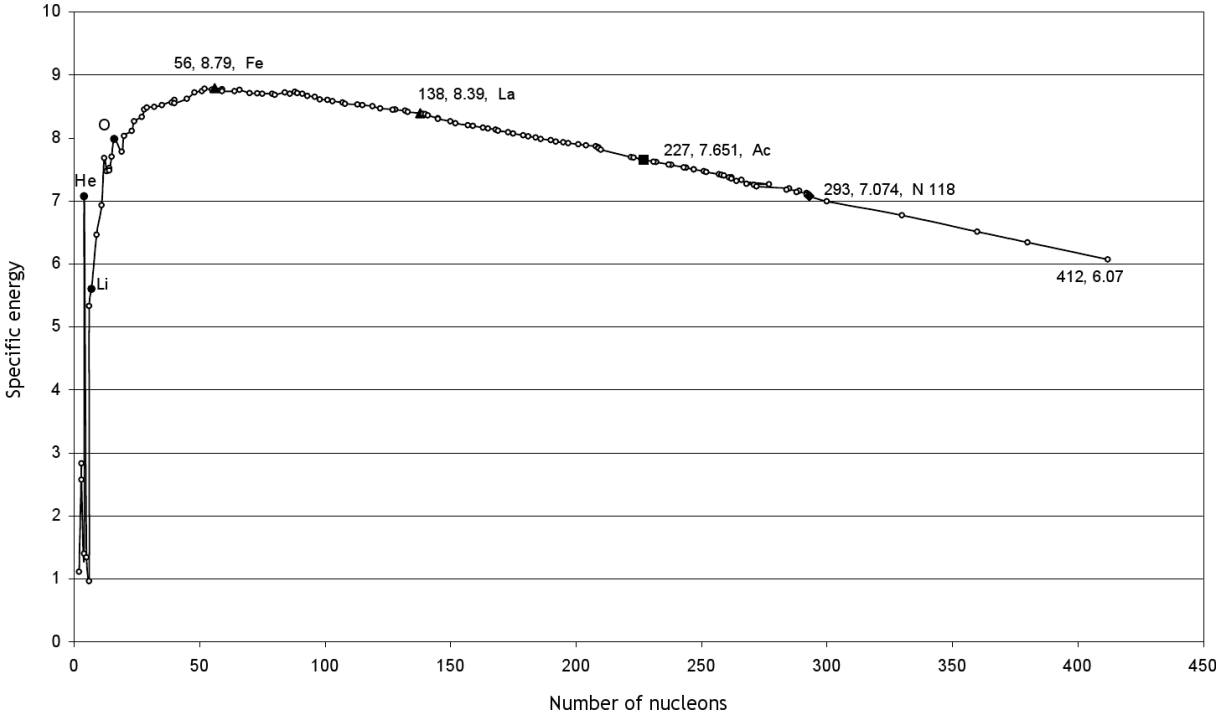

Fig. 12: Dependency between the specific energy of ther coupling in an atomic nuclei and the number of the nucleons in it.

List of Chemical Elements (on April 08, 2010), Ununseptium (No.117) bears atomic mass [295], while atomic mass of Ununoctium (No.118) is [294]. According to the calculation, produced in the framework of my theory, these quantities should be 301.95 and 304.79 respectively.

As was shown the theoretical studies according to the theory, and its comparing to the experimental data, the element bearing number 155 and atomic mass 411.66 a.m.u. answers all conditions necessary for including it into the Periodic Table of Elements.

Appendix I

As was already noted above, we took much attention to the dependency between atomic mass of the elements and their number in the Table of Elements. It was shown that the line of the trend continued upto No.155 provides obtaining very correct results. In verification of this fact, additional dependencies concerning the last element No.155 were studied [18].

Fig. 5 shows an empirical dependency between the radius of a nucleus and the number of nucleons in it (mass number). This graph manifests that this dependency is true upto element 155: the arc has the same shape without deviation along all its length.

Fig. 6 shows an arc, which manifests critical energies of the electrons for all elements of the Table of Elements, including No.155. A critical is that energy with whom energy loss for ionization and radiation become equal to each other. Formula for the critical energy is $T_{\text{crit}} = 800/Z$, where Z is the charge the nucleus (in units of the charge of the electron). As is seen from the graph, this formula is applicable to all elements of the Table of Elements.

Fig. 7 gives calculations of the coupling energy in nuclei. This graph shows that minimally energy required for destruction of the nucleus into its nucleons. It is seen, from the graph, that this dependency is strictly straight along all Table of Elements, including element 155.

Dependency between the number of the neutrons and the charge of the nucleus is shown in Fig. 8. As is seen, equation of the line of the trend describes, with a high level of probability ($R^2 = 0.9997$), the polynomial of the fourth order presented in the graph. This equation covers a large region along the axis x, from element 1 upto element 155 including. This dependency was also calculated, in order to compare it with the previous result, for a truncated region of the protons from element 1 upto element 104:

$$Y = 4E - 0.7x^4 + 2E - 0.5x^3 + 0.007x^2 + \\ + 1.0014x - 0.2176, \quad (6)$$

where $R^2 = 0.999$.

As is seen, certainty the level of the approximation differs only in 0.0007 from the previous. This manifests that fact that this dependency is as well true for the elements heavier than No.104, including element 155.

Appendix II

At the present time there are many versions of the periodic tables of elements, where each cell contains a property of a respective element (such as atomic radius, volume, density, first ionization potential, etc.). This information can also be obtained from the regular lists of the properties of chemical elements. This information has, however, a substantially lack: most data end in the beginning or the middle of Period 7.

Here we target continuing the list of numerous properties of the elements upto element 155, and also the compatibility of the properties with the reference data.

Fig. 9 shows a dependency between the ionization potential of the neutral atoms of the elements and the change of their nuclei. Each point corresponds to the last element of the period, from Period 1 to Period 6. The end of Period 7 and that of Period 8 were calculated according to the equation of the trend. As is seen, the points corresponding element 118 and element 155 are completely correlated with the initially data.

An important characteristic of atomic nucleus is the numerical value of its radius (see Fig. 10). This graph was created on the basis of the reference data known at the present time. This dependency between the atomic radius and the number of the last element in the period was created for all periods of the Table of Elements where it was possible. Coordinates of the points for Period 7 and Period 8 were calculated according to the equation of the line of the trend. As is easy to see, even the point of Period 6 meets the calculated data in complete.

Fig. 11 shows how the atomic radii change from period to period and inside each period of the Table of Elements (i.e. in the columns of the Table from up to down, and along the horizontal line). The upper maxima represent the beginning of the periods, while the lower points represent their ends. It should be noted that in lanthanides, which are No.57–No.71, a linear dependency between the radius and the number is observed. Further study of the correlation shows that there is a change of the linearity upto No.80 (Mercury). Another very interesting detail is that fact that, in the transfer from the alkaline to the alkaline earth elements, a valuable lowering the numerical values of the radii (for 0.3Å on the average) is observed in the periods.

In the calculations of nuclear reactions, the information about the stability of the nuclei as the systems consisting of protons and neutrons has a valuable maning. The forces joining the partcles altogether are known as nuclear forces; they exceed the forces of electrostatic and gravitational interactions in many orders.

The "resistance" of a nucleus can be bond by their coupling energy which shows the energy required for destroying the nucleus into its consisting nucleons (their number in the nucleus is equal to the mass number A expressed in atomic units of mass, a.m.u.). It is known that the sum of the masses

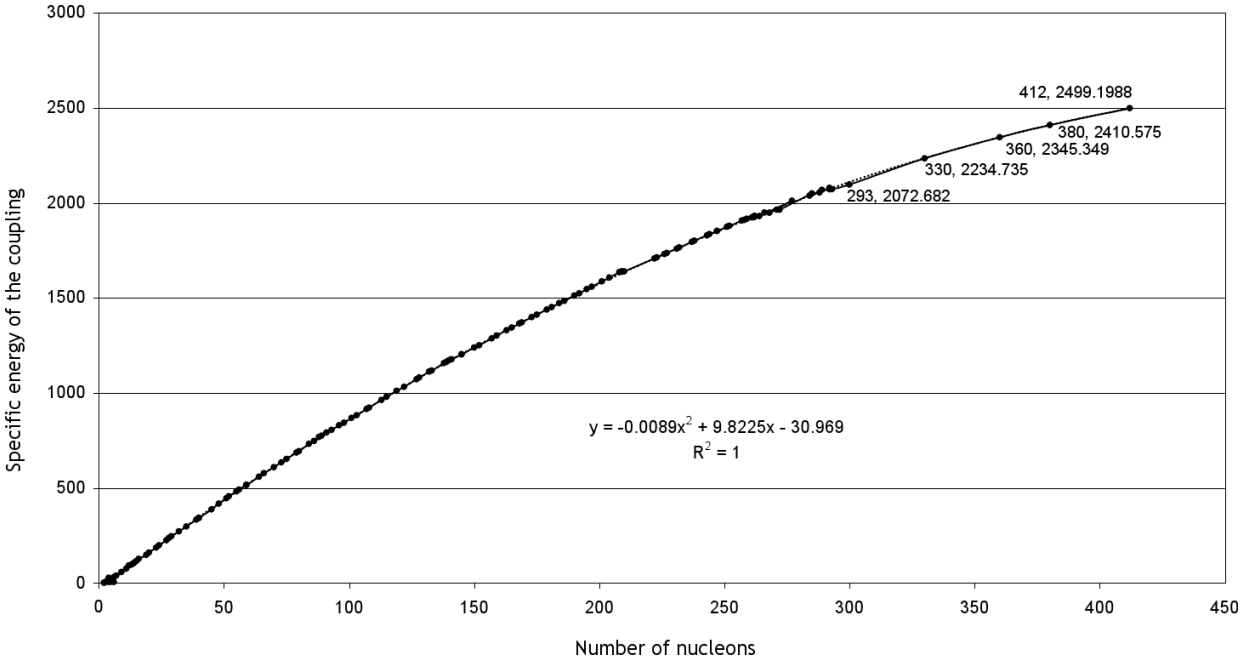

Fig. 13: Dependency between the specific energy of ther coupling in an atomic nuclei and the number of the nucleons in it.

of the free nucleons is already larger than the mass of the nucleus they consist. The difference of the masses is known as the mass defect, according to which Einstein's formula $E = \Delta mc^2$ gives a possibility for calculating the coupling energy of the nucleus, thus the specific energy in it per one nucleon.

Fig. 12 shows an arc, created according to the table data, which manifests the dependency between the specific energy of the coupling in a nucleus and the number of nucleons in it [19]. The left side of the graph shows several isotopes of Hydrogen and the nucleus of several light elements, which bear close numerical values of the specific energy of the coupling and, thus, a large deviation of the data. The arc become more smooth with increasing the number of the nucleons. The maximum is reached in a region of $A = 50$–60, then the falls slow down. The main advantage of this graph is that we produced the calculation beyond element 118 (at which the table data ended): we showed that the results of our calculation *completely meet* the table data known from the reference literature. Decreasing the specific energy of the coupling in the region of heavy nuclei is explained by increasing the number of protons that leads to increasing the Coulomb forces thus the need of additional neutrons apprears.

This is well manifested in Fig. 13. The arc described by the quadratic three-term equation has the numerical value of real approximation $R^2 = 1$. In the region of the nuclei consisting about 120 nucleons, this dependency is actually linear. Then this dependency transforms into an arc of a very large curvature radius. Data bofore the point of the nuclear charge 118 (203, 2072.582) were taken from the previous Fig. 12, then the calculation was produced on the basis of the coordinaters of the suggested last element No.155. As is seen, the arc approaches the horizontal location, where the number of nucleons in a nucleus is not affected by its coupling energy. Accordimng to our calculation, this happens in a region of the coordinates (530, 2670) — (550, 2673) — (600, 2659). This is the ultimate high energy of the coupling of nuclei. If a nucleus has a higher coupling energy, is becomes instable: even a small external influence is needed in order to destry it.

Therefore, Oganesyan's claim that the theoretical physicists discuss the properties of an element with number 400 and bearing 900 neutrons in its nucleus [9] has not any ground or reason.

Submitted on May 01, 2010 / Accepted on May 21, 2010

References

1. Seaborg G.T. and Bloom J.L. The synthetic elements, *Scientific American*, 1969, v.220, no.4, 56.
2. Goldanskii V.I. About connections nuclear and chemical physics. *Progress in Physical Sciences*, 1976, v.118, issue 2.
3. Flerov G.N., Druin Z.A., and Pleve A.A. Stability of heavy nucleus and borders of Periodic System of elements. *Uspekhi Fizicheskikh Nauk*, 1970, v.100, no.11, 45–92.
4. Penionzhkevich Yu.E. Physics of exotics of nucleus. *Soros' Educational Journal*, 1995, 1.
5. Goeppert-Mayer M. Nuclear shell structure. In: *Modern Physics for the Engineer*, McGraw Hill, 1961, 40.
6. Goeppert-Mayer M., Jensen J.H.D. Elementary theory of nuclear of shell. Foreign Literature, Moscow, 1958.
7. Eisenbood L. and Wigner E.P. Structure of the nucleus. Foreign Literature, Moscow, 1959.

8. Oganesyan Yu. New area of the nucleus stability. *Herald of Russian Academy of Sci.*, 2001, v.71, no.7, 590–599.
9. Oganesyan Yu. Superheavy race. Flerov Laboratory, JINR, Dubna, Russia, Atomium 1 [5], 2003. http://flerovlab.jinr.ru/linkc/flerov/atomium/atomium_ogan.html
10. Scientific medium. *Literaturnaya Gazeta*, May 8–14, 2002, no.18–19 (5877), *in Russian*.
11. Oganesyan Yu. Islands of the stability. *Scientific American Russian Edition*, 2005, no.3.
12. Oganesyan Yu. We revive elements of the timeless of the creation of the world. *Moscow News*, December 15, 2006.
13. Mendeleev's year began in Dubna. Weekly of the United Institute of the Nucleus Research (UINR), February 06, 2009, no.5 (3944) *in Russian*; http://wwwinfo.jinr.ru/j̃inrmag/win/2009/5/me5.htm
14. The scientists try to extend Mendeleev's Table upto 150 elements. *Izvestiya*, February 09, 2009 *in Russian*; http://www.izvestia.ru/news/20/news197601/index.html
15. Prehistory of the synthesis of the 117th of the element. *Nezavisimaya Gazeta*, April 14, 2010 *in Russian*; http://www.ng.ru/science/2010-04-14/15_117th.html
16. *RIA News*, Science and Technologies, August 03, 2009 *in Russian*; http://rian.ru/science/20090803/179595691.html
17. Khazan A. Upper limit of the Periodic Table and synthesis of superheavy elements. *Progress in Physics*, 2007, v.2, 104–109.
18. Ishanov B.S., Kebin E.I. Nuclear physics on-line. Physics of nuclei and particles. XX century. Moscow, Moscow University Press, 2000.
19. Audi G., Wapstra A.H., and Thibault C. The AME2003 anomic mass evaluation (II). Tables, graphs, and references. *Nuclear Physics A*, 2003, v.729, 337–676.

An Experimental Proposal for Demonstration of Macroscopic Quantum Effects

Raymond Jensen

Department of Mathematics and Informatics, Trine University, Angola, Indiana, USA. E-mail: rjensen@allmail.net

An experiment is proposed, whose purpose is to determine whether quantum indeterminism can be observed on a truly macroscopic scale. The experiment involves using a double-slit plate or interferometer and a macroscopic mechanical switch. The objective is to determine whether or not the switch can take on an indeterminate state.

1 Introduction

Since the founding of quantum theory in the last century, there has been the question of what limit, if any, there is to the quantum effects which may be observed, in terms of size or number of particles of a system under observation. By *quantum effects*, it is meant in particular, phenomena such as entanglement or indeterminism. The most famous gedankenexperiment in quantum theory, *Schrödingers cat*, concerns this *macroscopic* question. This *cat paradox* argument was used by Schrödinger to ridicule the Copenhagen interpretation of quantum theory. [1]. Another well-known paradox was that of Einstein, Podolsky and Rosen [2] commonly referred to as the *EPR paradox*. This gedankenexperiment was also an attempt to discredit the Copenhagen interpretation, but for a different reason than that of the cat paradox.

Regrettably, there are few known experiments that demonstrate whither the macroscopic question, unlike with the EPR paradox. A recent experiment [3] has shown that quantum effects *i.e.* entanglement, can occur between systems of $O(10^{12})$ particles. Although these results are encouraging, such a system can hardly be termed macroscopic in spite of the title of the article in which it appears. Here, we consider a *macroscopic* system to be one clearly visible to the naked eye and in the solid state, such as Schrödingers cat. Another experiment, of Schmidt [4], seems to demonstrate that bits on a computer disk, even printouts of ones and zeros concealed in an envelope, take on indeterminate states. However, the desire remains for further proof of macroscopic quantum effects, in particular, absent of paranormal phenomena and resulting complications [5]. Perhaps the reason that evidence of macroscopic quantum effects is so few and far between is because macroscopic analogs to experiments such as the double-slit experiment are difficult to design. One cannot simply shoot cats through a double slit and expect to see an interference pattern!

Instead of shooting Schrödingers cat through the double slit, suppose the cat is kept in its box, but a large double slit plate is also placed inside the box. Things are arranged so that the cat in the alive state obstructs one slit, and the cat in the dead state obstructs the other. All in the box is concealed from the observer and also, many cats would need to be used. See Figure 1. Now the question arises: will an interference pattern be observed on the screen if individual photons are transmitted through the double slit and box, one by one? If interference is observed, would this indicate that the cats were in an alive-dead state? The answer is in the affirmative; for if the cats were each definitely either alive or dead when the photons passed through, then no interference pattern should be observed.

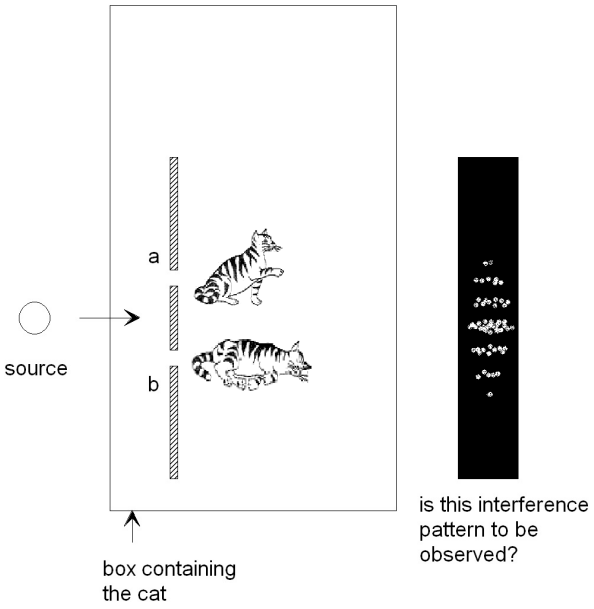

Fig. 1: An experiment with Schrödingers cat and a double slit. The experiment is designed so that if the cat is in the alive state, it obstructs slit **a** and if the cat is in the dead state it obstructs slit **b**. Many cats are needed for the experiment. If the cats remain unobserved and individual photons are transmitted through the double-slit and box, the question is: would an interference pattern be observed on the screen, and further, does this signify that the cats were in a superposition of alive and dead states?

In the next section, a more realizable (and cat-friendly) experimental set-up than the previous is proposed. This experiment will aid in answering the question of macroscopic indeterminism, as the accompanying calculations show. Although the set-up is quite simple by todays standards, it is not the intention of the author, a theorist, to carry out the experiment. Rather, it is hoped that an experimentalist is willing to carry out the necessary work.

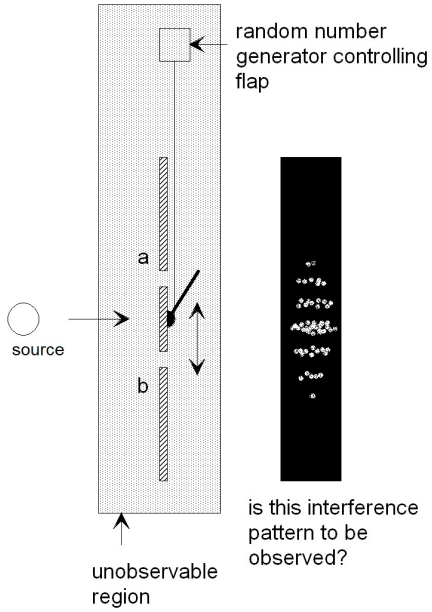

Fig. 2: The apparatus in Figure 1 is now modified so that a flap takes the place of Schrödingers cat. The flap position is controlled by an indeterministic random number generator, in order to put the flap in an indeterminate state with regard to which slit it covers. If measures are taken to destroy information about the flaps position before the photons reach the screen, the individual photons passing through the double slit apparatus should build up an interference pattern on the screen.

2 Double-slit experiment

Consider a set-up with a double slit, as in Figure 2. The difference between this set-up and the previous is that a flap takes the place of the cat. The flap covers either one slit or the other, and alternates between the two positions, controlled by a random-number generator.

The random number generator, flap and double-slit are concealed from the observer. The random number generator should be of the indeterministic type such as the one developed by Stipčević and Rogina [6]. The purpose of this is to put the flap into an indeterminate state. The set-up in Figure 2 is similar to one proposed by Mandel [7] which was carried out by Sillitto and Wykes [8]. However in that experiment, photons were *not* transmitted individually. So it is likely that the experiment was *not* free of photon-photon interference, whereas in the experiment under consideration here, such interference must be eliminated. Also, it is unclear if the electro-optic shutter used in that experiment could be said to be in an indeterminate state or to even be a mechanical macroscopic object.

Assuming that the flap in Figure 2 can be put into an indeterminate state, the flap can be represented by the equation

$$|\psi\rangle = \frac{1}{\sqrt{2}}\Big(|\mathbf{a}_f\rangle + |\mathbf{b}_f\rangle\Big), \qquad (1)$$

where $|\mathbf{a}_f\rangle$, $|\mathbf{b}_f\rangle$ are the basis states representing the flap f covering slits **a** and **b**, respectively. Now if a single photon p passes through the double-slit, say it passes through slit **b**, then the flap must be covering slit **a**, and *vice versa*. Thus, each photon passing through the double-slit is entangled together with the flap, and the flap-photon entangled state is:

$$|\psi\rangle = \frac{1}{\sqrt{2}}\Big(|\mathbf{a}_f\rangle|\mathbf{b}_p\rangle + |\mathbf{b}_f\rangle|\mathbf{a}_p\rangle\Big), \qquad (2)$$

where $|\mathbf{a}_p\rangle$, $|\mathbf{b}_p\rangle$ are the basis states for photon p. Equation (2) indicates that each photon passing through the double-slit takes on an indeterminate state with regards to which slit it passes through. Individual photons in the state (2) will build up an interference pattern if certain precautions are taken. Rather than using equation (2) to calculate the pattern which results from the set-up in Figure 2, we look at a variation of this experiment, for which it is easier to calculate interference. The apparatus is shown in Figure 3, in the next section.

3 Mach-Zehnder interferometer experiment

The set-up in Figure 3 essentially involves the same experiment as that shown in Figure 2, except that the isolated photons traverse a Mach-Zehnder interferometer (MZ) instead of a double-slit, and a moveable mirror (rm) replaces the flap. The rotation of the mirror rm switches the photon trajectory between two possible paths through MZ. The two different configurations are shown in the figure, top and bottom. Similar to the previous experiment, rm is to be put into an indeterminate state by controlling it with an indeterministic random number generator concealed from the observer (not shown in figure), and isolated photons can only be allowed to enter MZ through a gate. Further, position information of rm must be destroyed before each time a photon reaches the detectors. After such precautions are taken, the photons should each take an indeterminate path through MZ. Interference patterns of photon counts *vs.* relative length or phase between paths, the same observed by Aspect, Grangier and Roger [9] will then be seen. We next calculate these interference patterns.

Suppose first, rm is in the down position (upper diagram in Figure 3). This causes the photon to take the lower (–) path through MZ. Conversely, if the mirror is in the up position (lower diagram in Figure 3), the photon will take the upper (+) path through MZ. If rm can be prepared in an indeterminate state between up and down positions, then what results is the following entangled state between photon and mirror [*cf.* equation (2)]:

$$|\psi\rangle = \frac{1}{\sqrt{2}}\left(|\text{rm up}\rangle|+\rangle + |\text{rm down}\rangle|-\rangle\right), \qquad (3)$$

where $|\text{rm up}\rangle$, $|\text{rm down}\rangle$ are the two possible basis states for the moveable mirror rm and $|+\rangle$, $|-\rangle$ are the resultant basis states of the photon traversing MZ.

Let ϕ be the phase shift between arms of MZ, due to the presence of a phase shifter, or to a variation in the arms relative lengths. Using the rotation transformation equations

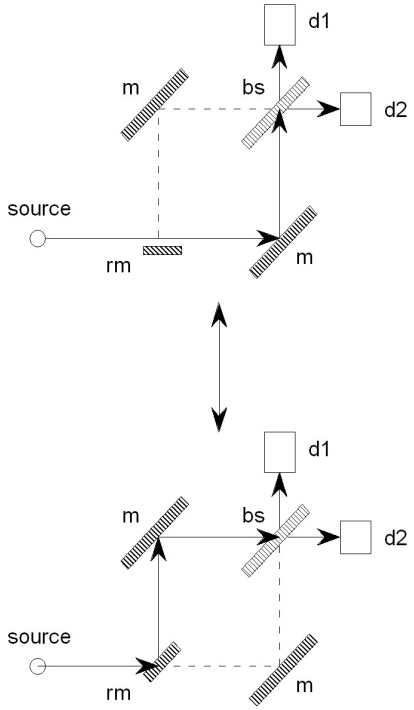

Fig. 3: A Mach-Zehnder (MZ) interferometer instead of the double slit of Figure 2. The moveable mirror rm acts as the former flap. The devices labeled m are fixed mirrors, bs, a beam splitter and d1, d2 are detectors. When rm is in the horizontal (down) position as at top, the photon takes the lower (–) path of mz (solid line with arrows). When rm is in the 45-degree position (up) as at bottom, then the photon takes the upper (+) path. If rm can take on an indeterminate state between these two configurations, then the photon paths will also be indeterminate, and thus interference patterns will result in d1 and d2, as variations of photon counts *vs.* relative length or phase ϕ between the two paths.

$|+\rangle = \sin\phi|\mathrm{d1}\rangle + \cos\phi|\mathrm{d2}\rangle$, $|-\rangle = \cos\phi|\mathrm{d1}\rangle - \sin\phi|\mathrm{d2}\rangle$ to put state (3) into the basis $|\mathrm{d1}\rangle$, $|\mathrm{d2}\rangle$ of the detectors, we obtain:

$$|\psi\rangle = \frac{1}{\sqrt{2}}\left(\sin\phi|\mathrm{rm\ up}\rangle|\mathrm{d1}\rangle + \cos\phi|\mathrm{rm\ up}\rangle|\mathrm{d2}\rangle + \right. \\ \left. + \cos\phi|\mathrm{rm\ down}\rangle|\mathrm{d1}\rangle - \sin\phi|\mathrm{rm\ down}\rangle|\mathrm{d2}\rangle\right). \quad (4)$$

If rm is successfully put into an indeterminate state, then the detector probabilities will be, using equation (4):

$$p\,(\mathrm{d1}) = |<\mathrm{rm\ up}, \mathrm{d1}|\psi\rangle + <\mathrm{rm\ down}, \mathrm{d1}|\psi\rangle|^2 = \\ = \frac{1}{2}\,(1+\sin 2\phi) \quad (5)$$

and

$$p(\mathrm{d2}) = \frac{1}{2}\,(1-\sin 2\phi)\,. \quad (6)$$

That is, interference fringes will be observed as oppositely-modulated signal intensity ($\propto$ probability) as a function of relative phase ϕ. These interference patterns; *i.e.* the interference patterns predicted by equations (5) and (6) are the same observed by Aspect and co-workers [9] using a similar set-up.

On the other hand, if rm remains in a *determinate* state, then *no* interference fringes will be observed; *i.e.* the signal intensity *vs.* phase-shift ϕ will be flat:

$$p\,(\mathrm{d1}) = |<\mathrm{rm\ up}, \mathrm{d1}|\psi\rangle|^2 + |<\mathrm{rm\ down}, \mathrm{d1}|\psi\rangle|^2 = \frac{1}{2} \quad (7)$$

and

$$p\,(\mathrm{d2}) = \frac{1}{2}\,. \quad (8)$$

Thus we have that: *the interference patterns* (5), (6) *result if and only if rm is in an indeterminate state. Presence of the interference patterns* (5), (6) *is therefore proof of macroscopic indeterminism, since the moveable mirror rm is a macroscopic object.*

It is emphasized again that it is important for the experimenter to take care that any information about the position of moveable mirror rm during the experiment is destroyed. This means that the random number generator should reset rm after each time an individual photon exits MZ, prior to the photon reaching detectors d1 or d2; otherwise in principle at least, the experimenter could discover which path the photon passed through, by uncovering rm. In that case, *no* interference [*i.e.* equations (7) and (8)] will be observed. Additional time to allow resetting rm can be obtained by placing d1 and d2 at some distance beyond the half-silvered mirror bs.

The experimental set-up of Figure 3 is similar to one proposed by Žukowski *et al.* [10], except that they propose to use a pair of electro-optical switches (one for each arm of MZ), instead of a moveable mirror before the arms. This is because the object of their proposal is to demonstrate whether or not the individual photons traverse MZ using both paths when the photon wave packet is cut in two using the switches as it passes though MZ. Their aim is to determine which of several interpretations of quantum theory is correct [11]. The purpose of that experiment is *not* to determine if the electro-optical switches take on an indeterminate state, even if again, such switches could be called mechanical and macroscopic.

4 Conclusion

An experiment involving individual photons passing through a double-slit plate or Mach-Zehnder interferometer apparatus has been proposed. Rather than keep both paths in the plate or apparatus open at all times however, one path or the other is kept closed by a macroscopic mechanical switch, controlled by an indeterministic device. The purpose of this is to determine whether the macroscopic switch can take on an indeterminate state: such indeterminism is detectible, dependent on whether an interference pattern results.

Acknowledgements

Thanks to C. Dumitrescu, who alerted the author to the third reference.

Submitted on June 21, 2010 / Accepted on June 25, 2010

References

1. Trimmer J. The present situation in Quantum Mechanics: a translation of Schrödingers Cat Paradox paper. *Proc. Am. Phil. Soc.*, 1980, v. 124, 323–338.
2. Einstein A., Podolsky B., Rosen N. Can quantum-mechanical description of physical reality be considered complete? *Phys. Rev.*, 1935, v. 47, 777–780.
3. Julsgaard B., Kozhekin A., Polzik E. Experimental long-lived entanglement of two macroscopic objects. *Nature*, 2001, v. 413, 400–403.
4. Schmidt H. Observation of a psychokinetic effect under highly controlled conditions. *J. Parapsychol.*, 1993, v. 57, 351–372.
5. Stapp H. Theoretical model of a purported empirical violation of the predictions of quantum theory. *Phys. Rev. A*, 1994, v. 50, 18–22.
6. Stipčević M., Rogina M. Quantum random number generator based on photonic emission in semiconductors. *Rev. Sci. Instr.*, 2007, v. 78, 45104.
7. Mandel L. On the possibility of observing interference effects with light beams divided by a shutter. *J. Opt. Soc. Am.*, 1959, v. 49, 931–932.
8. Sillitto R., Wykes C. An interference experiment with light beams modulated in anti-phase by an electro-optic shutter. *Phys. Lett. A*, 1972, v. 39, 333–334.
9. Grangier P., Roger G., Aspect A. Experimental evidence for a photon anticirrelation effect on a beam splitter: a new light on single-photon interferences. *Europhysics Lett.*, 1986, v. 1 (4), 173–179.
10. Žukowski M., Posiewnik A., Pykacz J. Interference in the double-slit experiment with only one slit open at a time. *Phys. Lett. A*, 1989, v. 135 (8,9), 411–416.
11. Posiewnik A., Pykacz J. Double-slit experiment, Copenhagen, neo-Copenhagen and stochastic interpretation of Quantum Mechanics. *Phys. Lett. A*, 1988, v. 128 (1,2), 5–8.

Gravitational Spectral Shift Exterior to the Sun, Earth and the Other Oblate Spheroidal Planets

Chifu Ebenezer Ndikilar*, Adam Usman†, and Osita C. Meludu†

*Department of Physics, Gombe State University, P.M.B 127, Gombe, Nigeria
†Department of Physics, Federal University of Technology, Yola, Adamawa State, Nigeria
E-mails: ebenechifu@yahoo.com; aausman@yahoo.co.uk; ocmeludu@yahoo.co.uk

Here, we use our new metric tensor exterior to homogeneous oblate spheroidal mass distributions to study gravitational spectral shift of light in the vicinity of the Sun, Earth and other oblate spheroidal planets. It turns out most profoundly that, this experimentally verified phenomenon holds good in the gravitational field exterior to an oblate spheroid using our approach. In approximate gravitational fields, our obtained theoretical value for the Pound-Rebka experiment on gravitational spectra shift along the equator of the Earth (2.578×10^{-15}) agrees satisfactorily with the experimental value of 2.45×10^{-15}. We also predict theoretical values for the Pound-Rebka experiment on the surface (along the equator) of the Sun and other oblate spheroidal planets.

1 Introduction

According to the General Theory of Gravitation, the rate of a clock is slowed down when it is in the vicinity of a large gravitating mass. Since the characteristic frequencies of atomic transitions are, in effect, clocks, one has the result that the frequency of such a transition occurring, say, on the surface of the Sun, should be lowered by comparison with a similar transition observed in a terrestrial laboratory. This manifests itself as a gravitational red shift in the wavelengths of spectral lines [1]. It has been experimentally and astrophysically observed that there is an increase in the frequency of light (photon) when the source or emitter is further away from the body than the receiver. The frequency of light will increase (shifting visible light towards the blue end of the spectrum) as it moves to lower gravitational potentials (into a gravity well). Also, there is a reduction in the frequency of light when the source or emitter is nearer the body than the receiver. The frequency of light will decrease (shifting visible light towards the red end of the spectrum) as it moves into higher gravitational potentials (out of a gravity well). This was experimentally confirmed in the laboratory by the Pound-Rebka experiment in 1959 (they used the Mossbauer effect to measure the change in frequency in gamma rays as they travelled from the ground to the top of Jefferson Labs at Havard University) [2]. This gravitational phenomenon was later confirmed by astronomical observations [3]. In this article, we verify the validity of our metric tensor exterior to a massive homogeneous oblate spheroid by studying gravitational spectral shift in the vicinity of the Sun, Earth and other oblate spheroidal planets. Basically, we assume that these gravitational sources are time independent and homogeneous distributions of mass within spheroids, characterized by at most two typical integrals of geodesic motion, namely, energy and angular momentum. From an astrophysical point of view, such an assumption, although not necessary, could, however, prove useful, because it is equivalent to the assumption that the gravitational source is changing slowly in time so that partial time derivatives are negligible compared to the spatial ones. We stress that the mass source considered is not the most arbitrary one from a theoretical point of view, but on the other hand, many astrophysically interesting systems are usually assumed to be time independent (or static from another point of view) and axially symmetric continuous sources.

2 Covariant metric tensor exterior to a massive homogeneous oblate spheroid

The covariant metric tensor in the gravitational field of a homogeneous oblate spheroid in oblate spheroidal coordinates (η, ξ, ϕ) has been obtained [4, 5] as;

$$g_{00} = \left(1 + \frac{2}{c^2} f(\eta,\xi)\right), \tag{2.1}$$

$$g_{11} = -\frac{a^2}{1+\xi^2-\eta^2}\left[\eta^2\left(1+\frac{2}{c^2} f(\eta,\xi)\right)^{-1} + \frac{\xi^2(1+\xi^2)}{(1-\eta^2)}\right], \tag{2.2}$$

$$g_{12} \equiv g_{21} = -\frac{a^2\eta\xi}{1+\xi^2-\eta^2}\left[1-\left(1+\frac{2}{c^2} f(\eta,\xi)\right)^{-1}\right], \tag{2.3}$$

$$g_{22} = -\frac{a^2}{1+\xi^2-\eta^2}\left[\xi^2\left(1+\frac{2}{c^2} f(\eta,\xi)\right)^{-1} + \frac{\eta^2(1-\eta^2)}{(1+\xi^2)}\right], \tag{2.4}$$

$$g_{33} = -a^2(1+\xi^2)(1-\eta^2), \tag{2.5}$$

$f(\eta,\xi)$ is an arbitrary function determined by the mass or pressure distribution and hence possesses all the symmetries of the latter, a priori. Let us now recall that for any gravitational field [4–7]

$$g_{00} \cong 1 + \frac{2}{c^2}\Phi \tag{2.6}$$

where Φ is Newton's gravitational scalar potential for the field under consideration. Thus we can then deduce that the unknown function in our field equation can be given approximately as

$$f(\eta,\xi) \cong \Phi(\eta,\xi)\ , \tag{2.7}$$

where $\Phi(\eta,\xi)$ is Newton's gravitational scalar potential exterior to a homogeneous oblate spheroidal mass. It has been shown that [8];

$$\Phi(\eta,\xi) = B_0 Q_0(-i\xi) P_0(\eta) + B_2 Q_2(-i\xi) P_2(\eta)\ , \tag{2.8}$$

where Q_0 and Q_2 are the Legendre functions linearly independent to the Legendre polynomials P_0 and P_2 respectively; B_0 and B_2 are constants given by

$$B_0 = \frac{4\pi G\rho_0 a^2\xi_0}{3\Delta_1}$$

and

$$B_2 = \frac{4\pi G\rho_0 a^2\xi_0}{9\Delta_2}\left[\frac{d}{d\xi}P_2(-i\xi)\right]_{\xi=\xi_0},$$

where Δ_1 and Δ_2 are defined as

$$\Delta_1 = \left[\frac{d}{d\xi}Q_0(-i\xi)\right]_{\xi=\xi_0}$$

and

$$\Delta_2 = Q_0\left[\frac{d}{d\xi}P_2(-i\xi)\right]_{\xi=\xi_0} - P_2(-i\xi)\left[\frac{d}{d\xi}Q_2(-i\xi)\right]_{\xi=\xi_0},$$

G is the universal gravitational constant, ρ_0 is the uniform density of the oblate spheroid and a is a constant parameter.

In a recent article [9], we obtained a satisfactory approximate expression for equation (2.8) as;

$$\Phi(\eta,\xi) \approx \frac{B_0}{3\xi^3}\left(1+3\xi^2\right)i - \frac{B_2}{30\xi^3}\left(7+15\xi^2\right)\left(3\eta^2-1\right)i \tag{2.9}$$

with

$$\Phi(\eta,\xi) \approx \frac{B_0}{3\xi^3}\left(1+3\xi^2\right)i + \frac{B_2}{30\xi^3}\left(7+15\xi^2\right)i$$

and

$$\Phi(\eta,\xi) \approx \frac{B_0}{3\xi^3}\left(1+3\xi^2\right)i - \frac{B_2}{15\xi^3}\left(7+15\xi^2\right)i$$

as the respective approximate expressions for the gravitational scalar potential along the equator and pole exterior to homogeneous oblate spheroidal bodies. These equations were used to compute approximate values for the gravitational scalar potential exterior to the Sun, Earth and other oblate spheroidal planets [9].

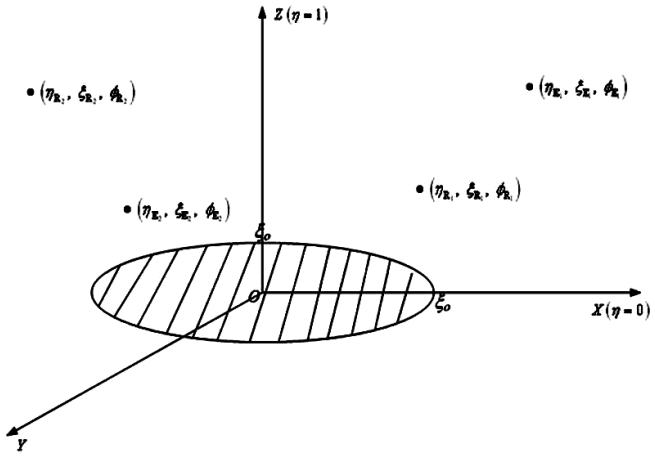

Fig. 1: Emission and reception space points of light (photon).

3 Gravitational spectral shift exterior to oblate spheroidal distributions of mass

Here, we consider a beam of light moving from a source or emitter at a fixed point in the gravitational field of the oblate spheroidal body to an observer or receiver at a fixed point in the same gravitational field. Einstein's equation of motion for a photon is used to derive an expression for the shift in frequency of a photon moving in the gravitational field of an oblate spheroidal mass.

Now, consider a beam of light moving from a source or emitter (E) at a fixed point in the gravitational field of an oblate spheroidal body to an observer or receiver (R) at a fixed point in the field as shown in Fig. 1.

Let the space time coordinates of the emitter and receiver be $(t_E,\ \eta_E,\ \xi_E, \phi_E)$ and $(t_R,\ \eta_R,\ \xi_R, \phi_R)$ respectively. It is well known that light moves along a null geodesic given by

$$d\tau = 0\,. \tag{3.1}$$

Thus, the world line element for a photon (light) takes the form

$$c^2 g_{00}\,dt^2 = g_{11}\,d\eta^2 + 2g_{12}\,d\eta\,d\xi + g_{22}\,d\xi^2 + g_{33}\,d\phi^2. \tag{3.2}$$

Substituting the covariant metric tensor for this gravitational field in equation (3.2) gives

$$\begin{aligned} c^2\left(1+\frac{2}{c^2}f(\eta,\xi)\right)dt^2 &= -\frac{a^2}{1+\xi^2-\eta^2}\times \\ &\times\left[\eta^2\left(1+\frac{2}{c^2}f(\eta,\xi)\right)^{-1} + \frac{\xi^2\left(1+\xi^2\right)}{\left(1-\eta^2\right)}\right]d\eta^2 - \\ &- \frac{2a^2\eta\xi}{1+\xi^2-\eta^2}\left[1-\left(1+\frac{2}{c^2}f(\eta,\xi)\right)^{-1}\right]d\eta\,d\xi - \\ &- \frac{a^2}{1+\xi^2-\eta^2}\left[\xi^2\left(1+\frac{2}{c^2}f(\eta,\xi)\right)^{-1} + \frac{\eta^2\left(1-\eta^2\right)}{\left(1+\xi^2\right)}\right]d\xi^2 - \\ &- a^2\left(1+\xi^2\right)\left(1-\eta^2\right)d\phi^2. \end{aligned} \tag{3.3}$$

Now, let u be a suitable parameter that can be used to study the motion of a photon in this gravitational field. Then equation (3.3) can be written as

$$c^2\left(1+\frac{2}{c^2}f(\eta,\xi)\right)\left(\frac{dt}{du}\right)^2 = -\frac{a^2}{1+\xi^2-\eta^2}\times$$
$$\times\left[\eta^2\left(1+\frac{2}{c^2}f(\eta,\xi)\right)^{-1}+\frac{\xi^2\left(1+\xi^2\right)}{(1-\eta^2)}\right]d\eta^2 -$$
$$-\frac{2a^2\eta\xi}{1+\xi^2-\eta^2}\left[1-\left(1+\frac{2}{c^2}f(\eta,\xi)\right)^{-1}\right]\left(\frac{d\eta}{du}\frac{d\xi}{du}\right) -$$
$$-\frac{a^2}{1+\xi^2-\eta^2}\left[\xi^2\left(1+\frac{2}{c^2}f(\eta,\xi)\right)^{-1}+\frac{\eta^2\left(1-\eta^2\right)}{(1+\xi^2)}\right]\times$$
$$\times\left(\frac{d\xi}{du}\right)^2 - a^2\left(1+\xi^2\right)\left(1-\eta^2\right)\left(\frac{d\phi}{du}\right)^2. \quad (3.4)$$

Equation (3.4) can be equally written as

$$\frac{dt}{du} = \frac{1}{c}\left(1+\frac{2}{c^2}f(\eta,\xi)\right)^{-\frac{1}{2}}ds, \quad (3.5)$$

where ds is defined as

$$ds^2 = -\frac{a^2}{1+\xi^2-\eta^2}\times$$
$$\times\left[\eta^2\left(1+\frac{2}{c^2}f(\eta,\xi)\right)^{-1}+\frac{\xi^2\left(1+\xi^2\right)}{(1-\eta^2)}\right]d\eta^2 -$$
$$-\frac{2a^2\eta\xi}{1+\xi^2-\eta^2}\left[1-\left(1+\frac{2}{c^2}f(\eta,\xi)\right)^{-1}\right]\left(\frac{d\eta}{du}\frac{d\xi}{du}\right) -$$
$$-\frac{a^2}{1+\xi^2-\eta^2}\left[\xi^2\left(1+\frac{2}{c^2}f(\eta,\xi)\right)^{-1}+\frac{\eta^2\left(1-\eta^2\right)}{(1+\xi^2)}\right]\times$$
$$\times\left(\frac{d\xi}{du}\right)^2 - a^2\left(1+\xi^2\right)\left(1-\eta^2\right)\left(\frac{d\phi}{du}\right)^2. \quad (3.6)$$

Integrating equation (3.5) for a signal of light moving from emitter E to receiver R gives

$$t_R - t_E = \frac{1}{c}\int_{u_E}^{u_R}\left[\left(1+\frac{2}{c^2}f(\eta,\xi)\right)^{-\frac{1}{2}}ds\right]du. \quad (3.7)$$

The time interval between emission and reception of all light signals is well known to be the same for all light signals in relativistic mechanics (constancy of the speed of light) and thus the integral on the right hand side is the same for all light signals. Consider two light signals designated 1 and 2 then

$$t_R^1 - t_E^1 = t_R^2 - t_E^2 \quad (3.8)$$

or

$$t_R^2 - t_R^1 = t_E^2 - t_E^1. \quad (3.9)$$

Thus,

$$\Delta t_R = \Delta t_E. \quad (3.10)$$

Hence, coordinate time difference of two signals at the point of emission equals that at the point of reception. From our expression for gravitational time dilation in this gravitational field [10], we can write

$$\Delta\tau_R = \left(1+\frac{2}{c^2}f_R(\eta,\xi)\right)^{\frac{1}{2}}\Delta t_R. \quad (3.11)$$

Equations (3.9), (3.10) and (3.11) can be combined to give

$$\frac{\Delta\tau_R}{\Delta\tau_E} = \left(\frac{1+\frac{2}{c^2}f_R(\eta,\xi)}{1+\frac{2}{c^2}f_E(\eta,\xi)}\right)^{\frac{1}{2}}. \quad (3.12)$$

Now, consider the emission of a peak or crest of light wave as one event. Let n be the number of peaks emitted in a proper time interval $\Delta\tau_E$, then, by definition, the frequency of the light relative to the emitter, ν_E, is given as

$$\nu_E = \frac{n}{\Delta\tau_E}. \quad (3.13)$$

Similarly, since the number of cycles is invariant, the frequency of light relative to the receiver, ν_R, is given as

$$\nu_R = \frac{n}{\Delta\tau_R}. \quad (3.14)$$

Consequently,

$$\frac{\nu_R}{\nu_E} = \frac{\Delta\tau_E}{\Delta\tau_R} = \left(1+\frac{2}{c^2}f_E(\eta,\xi)\right)^{\frac{1}{2}}\left(1+\frac{2}{c^2}f_R(\eta,\xi)\right)^{-\frac{1}{2}} \quad (3.15)$$

or

$$\frac{\nu_R}{\nu_E} \approx \left(1+\frac{2}{c^2}f_E(\eta,\xi)\right)\left(1-\frac{2}{c^2}f_R(\eta,\xi)\right) \quad (3.16)$$

or

$$\frac{\nu_R}{\nu_E} - 1 \approx \frac{1}{c^2}\left[f_E(\eta,\xi) - f_R(\eta,\xi)\right] \quad (3.17)$$

to the order of c^{-2}. Alternatively, equation (3.17) can be written as

$$z \equiv \frac{\Delta\nu}{\nu_E} \equiv \frac{\nu_R-\nu_E}{\nu_E} \approx \frac{1}{c^2}\left[f_E(\eta,\xi) - f_R(\eta,\xi)\right]. \quad (3.18)$$

It follows from equation (3.18) that if the source is nearer the body than the receiver then $f_E(\eta,\xi) < f_R(\eta,\xi)$ and hence $\Delta\nu < 0$. This indicates that there is a reduction in the frequency of light when the source or emitter is nearer the body than the receiver. The light is said to have undergone a red shift (that is the light moves toward red in the visible spectrum). Otherwise (source further away from body than receiver), the light undergoes a blue shift. Now, consider a signal of light emitted and received along the equator of the homogeneous oblate spheroidal Earth (approximate gravitational field where $f(\eta,\xi) \approx \Phi(\eta,\xi)$. The ratio of the shift

Emi Pt	Recep pt	$z\,(\times 10^{-10})$	Type of shift
ξ_0	ξ_0	0	none
$2\xi_0$	ξ_0	3.454804	blue
$3\xi_0$	ξ_0	4.603165	blue
$4\xi_0$	ξ_0	5.176987	blue
$5\xi_0$	ξ_0	5.521197	blue
$6\xi_0$	ξ_0	5.750643	blue
$7\xi_0$	ξ_0	5.914522	blue
$8\xi_0$	ξ_0	6.037426	blue
$9\xi_0$	ξ_0	6.133016	blue
$10\xi_0$	ξ_0	6.209486	blue

Fig. 2: Ratio of the shift in frequency of light to the frequency of the emitted light at points along equator and received on the surface of the Earth on the equator.

Emi Pt	Recep pt	$z\,(\times 10^{-10})$	Type of shift
ξ_0	ξ_0	0	none
ξ_0	$2\xi_0$	−3.454804	red
ξ_0	$3\xi_0$	−4.603165	red
ξ_0	$4\xi_0$	−5.176987	red
ξ_0	$5\xi_0$	−5.521197	red
ξ_0	$6\xi_0$	−5.750643	red
ξ_0	$7\xi_0$	−5.914522	red
ξ_0	$8\xi_0$	−6.037426	red
ξ_0	$9\xi_0$	−6.133016	red
ξ_0	$10\xi_0$	−6.209486	red

Fig. 3: Ratio of the shift in frequency of light to the frequency of the emitted light at points along equator and received on the surface of the Earth on the equator.

Body	Radial dist. (km)	ξ at pt	Φ_E ($\mathrm{N\,m\,kg^{-1}}$)	Φ_R ($\mathrm{N\,m\,kg^{-1}}$)	Predicted shift
Sun	700,022.5	241.527	-1.9375791×10^{11}	-1.9373218×10^{11}	-2.85889×10^{-21}
Earth	6,378.023	12.010	-6.2079113×10^{7}	-6.2078881×10^{7}	-2.57800×10^{-15}
Mars	3,418.5	9.231	-1.2401149×10^{7}	-1.2317966×10^{7}	-9.24256×10^{-20}
Jupiter	71,512.5	2.641	-1.4968068×10^{9}	-1.4958977×10^{9}	-1.010111×10^{-20}
Saturn	60,292.5	1.971	-4.8486581×10^{8}	-4.8484869×10^{8}	-1.902222×10^{-21}
Uranus	25,582.5	3.994	-2.1563913×10^{8}	-2.1522082×10^{8}	-4.647889×10^{-20}
Neptune	24,782.5	4.304	-2.5243240×10^{8}	-2.5196722×10^{8}	-5.168667×10^{-20}

Fig. 4: Predicted Pound-Rebka shift in frequency along the equator for the Sun, Earth and the other oblate spheroidal planets.

in frequency to the frequency of the emitted light at various points along the equator and received on the equator at the surface of the homogeneous oblate spheroidal Earth can be computed using equation (3.18). This yields Table 1. Also, the ratio of the shift in frequency of light to the frequency of the emitted light on the equator at the surface and received at various points along the equator of the homogeneous oblate spheroidal Earth can be computed. This gives Table 2.

Tables 1, thus confirms our assertion above that there is an increase in the frequency of light when the source or emitter is further away from the body than the receiver. The frequency of light will increase (shifting visible light toward the blue end of the spectrum) as it moves to lower gravitational potentials (into a gravity well). Table 2, also confirms our assertion above that there is a reduction in the frequency of light when the source or emitter is nearer the body than the receiver. The frequency of light will decrease (shifting visible light toward the red end of the spectrum) as it moves to higher gravitational potentials (out of a gravity well). Also, notice that the shift in both cases increases with increase in the distance of separation between the emitter and receiver. The value of the shift is equal in magnitude at the same separation distances for both cases depicted in Tables 1 and 2.

Now, suppose the Pound-Rebka experiment is performed at the surface of the Sun, Earth and other oblate spheroidal planets on the equator. Then, since the gamma ray frequency shift was observed at a height of 22.5m above the surface, we model our theoretical computation and calculate the theoretical value for this shift. This computation yields Table 3.

With these predictions, experimental astrophysicists and astronomers can now attempt carrying out similar experiments on these bodies. Although, the prospects of carrying out such experiments on the surface of some of the planets and Sun are less likely (due to temperatures on their surfaces and other factors); theoretical studies of this type helps us to understand the behavior of photons as they leave or approach these astrophysical bodies. This will thus aid in the development of future instruments that can be used to study these heavenly bodies.

4 Conclusion

The practicability of the findings in this work is an encouraging factor. More so, that in this age of computational precision, the applications of these results is another factor.

Submitted on June 01, 2010 / Accepted on June 05, 2010

References

1. Matolcsi T. and Matolcsi M. GPS revisited: the relation of proper time and coordinate time. arXiv: math-ph/0611086.
2. Pound R.V. and Rebka G.A. Jr. Gravitational red shift in nuclear resonance. *Physical Review Letters*, 1959, v. 3(9), 439–441.
3. Ohanian H.C. and Remo R. Gravitation and space-time. W.W. Norton and Company, 1994.

4. Howusu S.X.K. The 210 astrophysical solutions plus 210 cosmological solutions of Einstein's gravitational field equations. Natural Philosophy Society, Jos, 2007, 47–79.
5. Chifu E.N., Usman A. and Meludu O.C. Orbits in homogeneous oblate spheroidal gravitational space-time. *Progress in Physics*, 2009, v.3, 49–53.
6. Chifu E.N. and Howusu S.X.K. Gravitational radiation and propagation field equation exterior to astrophysically real or hypothetical time varying distributions of mass within regions of spherical geometry. *Physics Essays*, 2009, v.22(1), 73–77.
7. Chifu E.N. and Howusu S.X.K. Solution of Einstein's geometrical field equations exterior to astrophysically real or hypothetical time varying distributions of mass within regions of spherical geometry. *Progress in Physics*, 2009, v.3, 45–48.
8. Howusu S.X.K. Gravitational fields of spheroidal bodies-extension of gravitational fields of spherical bodies. *Galilean Electrodynamics*, 2005, v.16(5), 98–100.
9. Chifu E.N., Usman A., and Meludu O.C. Gravitational scalar potential values exterior to the Sun and planets. *Pacific Journal of Science and Technology*, 2009, v.10(1), 663–673.
10. Chifu E.N., Usman A., and Meludu O.C. Gravitational time dilation and length contraction in fields exterior to static oblate spheroidal mass distributions. *Journal of the Nigerian Association of Mathematical Physics*, 2009, v.15, 247–252.

Microwave Spectroscopy of Carbon Nanotube Field Effect Transistor

Aziz N. Mina*, Attia A. Awadalla*, Adel H. Phillips†, and Riham R. Ahmed*

*Faculty of Science, Beni-Suef University, Beni-Suef, Egypt. E-mail: attiamd2005@yahoo.com
†Faculty of Engineering, Ain-Shams University, Cairo, Egypt. E-mail: adel_phillips@yahoo.com

The quantum transport property of a carbon nanotube field effect transistor (CNTFET) is investigated under the effect of microwave radiation and magnetic field. The photon-assisted tunneling probability is deduced by solving Dirac equation. Then the current is deduced according to Landauer-Buttiker formula. Oscillatory behavior of the current is observed which is due to the Coulomb blockade oscillations. It was found, also, that the peak heights of the dependence of the current on the parameters under study are strongly affected by the interplay between the tunneled electrons and the photon energy. This interplay affects on the sidebands resonance. The results obtained in the present paper are found to be in concordant with those in the literature, which confirms the correctness of the proposed model. This study is valuable for nanotechnology applications, e.g., photo-detector devices and solid state quantum computing systems and quantum information processes.

5 Introduction

Carbon Nanotubes (CNTs) have been discovered by Sumio Iijim of the NEC Tsukuba Laboratory in HRTEM study of carbon filaments [1]. Carbon-based materials, clusters and molecules are unique in many ways [2]. One distinction related to the many possible configurations of the electronic states of carbon atom, which is known as the hybridization of atomic orbital. Electrical conductivity of carbon nanotube depending on their chiral vector carbon nanotube with a small diameter is metallic or semiconducting [2,3]. The differences in conducting properties are caused by the molecular structure that results in a difference band structure and thus a different band gap. The quantum electronic transport properties of carbon nanotubes have received much attention in recent years [4,5]. This is due to the very nice features of the band structure of these quasi-one dimensional quantum systems. The quantum mechanical behavior of the electronic transport in carbon nanotubes has been experimentally and theoretically investigated by many authors [6,7]. According to these investigations, the authors showed that carbon nanotube sandwiched between two contacts behaves as coherent quantum device. A microwave field with frequency, ω, can induce additional tunneling process when electrons exchange energy by absorbing or emitting photons of energy, $\hbar\omega$. This kind of tunneling is known as the photon-assisted tunneling [8]. The aim of the present paper is to investigate the quantum transport characteristics of a CNTFET under the microwave irradiation and the effect magnetic field.

6 CNTFET

A carbon nanotube field effect transistor (CNTFET) is modeled as: two metal contacts are deposited on the carbon nanotube quantum dot to serve as source and drain electrodes. The conducting substance is the gate electrode in this three-terminal device. Another metallic gate is used to govern the electrostatics and the switching of the carbon nanotube channel. The substrates at the nanotube quantum dot /metal contacts are controlled by the back gate. The tunneling through such device is induced by an external microwave field of different frequencies of the form $V = V_{ac}\cos(\omega t)$ where V_{ac} is the amplitude of the field and ω is its angular frequency, that is the photon-assisted tunneling process is achieved. One of the measurable quantities of the transport characteristic is the current which may be expressed in terms of the tunneling probability by the following Landauer-Buttiker formula [9]:

$$I=\left(\frac{4e}{h}\right)\int\left[f_{FD(s)}(E)-f_{FD(d)}(E-eV_{sd})\right]\Gamma_n(E)dE \qquad (1)$$

where $\Gamma(E)$ is the photon-assisted tunneling probability, $f_{FD(s/d)}$ are the Fermi-Dirac distribution function corresponding to the source (s) and drain (d) electrodes, while e and h are electronic charge and Planck's constant respectively. The tunneling probability $\Gamma_n(E)$ might be calculated by solving the following Dirac equation [7]

$$\left[i\upsilon_{F\hbar}\begin{pmatrix}0 & \partial_x-\partial_y\\ \partial_x-\partial_y & 0\end{pmatrix}-eV_{sd}+\right. \qquad (2)$$
$$\left.+(e\hbar B)(2m)^{-1}+eV_B+eV_{sd}\cos(\omega t)\right]\psi_{\frac{e}{\hbar}}=i\hbar\frac{\partial\psi_{\frac{e}{\hbar}}}{\partial E}$$

where υ_F is the Fermi velocity corresponding to Fermi-energy E_F, V_g is the gate voltage, V_{sd} is source-drain voltage, B is the applied magnetic field, m^* is the effective mass of the charge carrier, $\hbar$ is the reduced Planck ı́s constant, ω is the frequency of the applied microwave field with amplitude V_{ac} and V_b is the barrier height. The index e/h refers to electron like (with the energy > 0 with respect to the Dirac point) and hole-like (with energy < 0 with respect to the Dirac point) solutions to the eigenvalue differential equation (2).

The solution of equation (2) is given by [7]:

$$\Psi^{(ac)}_{+,n}(x,t) = \sum J_n\left(\frac{eV_{ac}}{\hbar\omega}\right)\Psi^{ac}_{0,e/h}(x,t)\, e^{(-in\omega t)} \tag{3}$$

where

$$\Psi^{(in)}_{0,e/h}(x,t) = \Psi^{(ac)}_{0,e/h}(x)\, e^{\mp iEt/h}. \tag{4}$$

Accordingly equation (2) will take the following form.

$$\left[i\nu_{F\hbar}\begin{pmatrix} 0 & \partial_x-\partial_y \\ \partial_x-\partial_y & 0 \end{pmatrix}-\varepsilon\right]\Psi^{ac}_{0.e/h} = \pm E\Psi_{0.e/h} \tag{5}$$

where the letter ε denotes the following

$$\varepsilon = E_F + eV_g + eV_{sd} + \left(\frac{e\hbar B}{2m^*}\right) + V_b + eV_{ac}\cos\omega t\,. \tag{6}$$

In Eq. (3), J_n is the n^{th} order Bessel function. Since in ballistic transport from one region of quantum dot to another one, charge carriers with a fixed energy (which can be either positive or negative with respect to the Dirac point) are transmitted and their energy is conserved. The desired state represents a superposition of positive and negative solution to the eigenvalue problem Eq. (5). The solution must be generated by the presence of the different side-bands, n, which come with phase factors $\exp(-in\omega t)$ that shift the center energy of the transmitted electrons by integer multiples of $\hbar\omega$ [8]. The complete solution of Eq. (5) is given by [7]:

(i) The incoming eigenfunction

$$\Psi^{(ac)}_{icome}(x,t) = \sum_{n=-\infty}^{\infty} J_n\left(\frac{eV_{ac}}{\hbar\omega}\right)\times \\ \times\Psi^{ac}_{0,+}\exp\left(i\left(\varepsilon + E + n\hbar\omega\right)t/h\right) \tag{7}$$

(ii) The reflected eigenfunction

$$\Psi^{\alpha}_{r}(x,t) = \sum_{n=-\infty}^{\infty} R_n(E)\, J_n\left(\frac{eV_{ac}}{\hbar\omega}\right)\times \\ \times\Psi^{ac}_{0,-}\exp\left(i\left(\varepsilon + E + n\hbar\omega\right)t/h\right) \tag{8}$$

where $R_n(E)$ is the energy-dependent reflection coefficient.

(iii) The transmitted eigenfunction

$$\Psi^{ac}_{tr}(x,t) = \sum_{n=-\infty}^{\infty} \Gamma_n(E)\, J_n\left(\frac{eV_{ac}}{\hbar\omega}\right)\times \\ \times\Psi^{in}_{+,n}\exp\left(i\left(\varepsilon + E + n\hbar\omega\right)t/h\right) \tag{9}$$

where $\Psi^{(ac)}_{0,+}, \Psi^{(ac)}_{0,-}$ are respectively given by

$$\Psi^{(ac)}_{0,+} = \frac{e^{iq_n y + ik_n x}}{\sqrt{\cos\alpha_{ac}}}\begin{pmatrix} \exp\left(-\frac{\alpha_{ac}}{2}\right) \\ -\exp\left(\frac{\alpha_{ac}}{2}\right) \end{pmatrix} \tag{10}$$

and

$$\Psi^{(ac)}_{0,-} = \frac{e^{iq_n y - ik_n x}}{\sqrt{\cos\alpha_{ac}}}\begin{pmatrix} \exp\left(\frac{\alpha_{ac}}{2}\right) \\ -\exp\left(-\frac{\alpha_{ac}}{2}\right) \end{pmatrix} \tag{11}$$

$\Psi^{(in)}_{+,n}$ in Eq. (9) is expressed as

$$\Psi^{(in)}_{+,n} = \frac{e^{iq,y-ik,x}}{\sqrt{\cos\alpha_{in,n}}}\begin{pmatrix} \exp\left(-\frac{\alpha_{in,n}}{2}\right) \\ \exp\left(\frac{\alpha_{in,n}}{2}\right) \end{pmatrix}. \tag{12}$$

In equations (10, 11, 12), the symbols α_{ac}, $\alpha_{in,n}$ are

$$\alpha_{ac} = \sin^{-1}\left(\frac{\hbar\nu q_n}{\varepsilon}\right) \tag{13}$$

and

$$\alpha_{in,n} = \sin^{-1}\left(\frac{\hbar\nu q_n}{\varepsilon + n\hbar\omega}\right) \tag{14}$$

where

$$q_n = \frac{n\pi}{W} \quad (n = 1, 2, 3, \ldots) \tag{15}$$

where W is the dimension of the nanotube quantum dot. The parameter k_n in Eqs. (10, 11, 12) is given by

$$k_n^2 = \left[\frac{V_b + eV_g + eV_{sd} + \frac{\hbar eB}{m^*}}{\hbar\omega}\right]^2 - q_n^2. \tag{16}$$

In order to get an explicit expression for the tunneling probability $\Gamma_n(E + n\hbar\omega)$ this can be achieved by applying the matching condition for the spatial eigenfunctions at the boundaries $x = 0$ and $x = L$. So, the tunneling probability $\Gamma_n(E+n\hbar\omega)$ will take the following form after some algebraic procedures, as

$$\Gamma_n(E + n\hbar\omega) = \\ = \left|\frac{k_n}{k_n\cos(k_nL) + i\left(\frac{eV_g + eV_{sd} + (\hbar eB/2m^*)}{\hbar\omega}\right)\sin(k_nL)}\right|^2. \tag{17}$$

The complete expression for the tunneling probability with the influence of the microwave field is given by [8]:

$$\Gamma_{withphoton}(E) = \sum J_n^2\left(\frac{eV_{ac}}{\hbar\omega}\right)\times \\ \times f_{FD}\left(E - \frac{C_g}{C}eV_g - n\hbar\omega - eV_{cd}\right)\Gamma(E - n\hbar\omega) \tag{18}$$

where C_g is the quantum capacitance of the nanotube quantum dot and C is the coupling capacitance between the nanotube quantum dot and the leads.

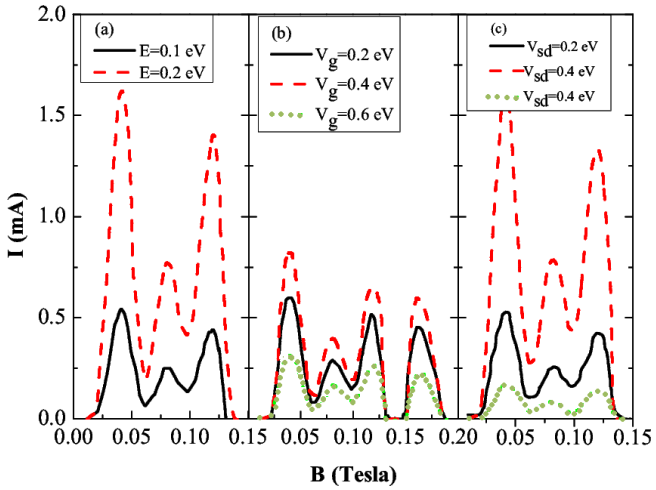

Fig. 1: The current as a function of the applied magnetic field (a) photon energy (b) gate voltage in energy units(c) source drain voltage in energy units.

7 Results and Discussions

Numerical calculations were performed according to the following:

(i) The electron transport through the present investigated device is treated as a stochastic process, so that the tunneled electron energy has been taken as a random number relative to the Fermi-energy of the carbon nanotube. The calculations had been conducted previously by the authors [9, 11].

(ii) The value of the quantum capacitance, C_g, is 0.25 nF.

(iii) The coupling capacitance between carbon nanotube quantum dot and the leads is calculated in the Coulomb blockade regime and in the charging energy of the quantum dot [9, 11]. Its value is found to be approximately equals $\sim$ 0.4 nF. The value of the Fermi energy, E_F is calculated using the values of the Fermi velocity, ν_F, and it was found to be approximately equals $\sim$ 0.125 eV. This value of the Fermi energy, E_F, was found to be consisted with those found in the literature [12, 13]. The effective mass of the charge carrier was taken as 0.054 m_e [12, 13].

The variation of the current, I, with the applied magnetic field, B, at difference values of the photon energy, E, gate voltage, V_g, and different values of the bias voltage, V_{sd}, is shown in Figs. (1a,b,c). It is known that the influence of an external magnetic field, B, will lead to a change in the energy level separation between the ground state and the first excited state [14] in the carbon nanotube quantum dot. We notice that the current dependence on the magnetic field oscillates with a periodicity of approximately equals $\sim$ 0.037 T. This value corresponds roughly to the addition of an extra flux quantum to the quantum dot. These results have been observed by the authors [12, 15]. The peak heights are different due the interplay between the tunneled electrons and the applied photons of the microwave field and also this flux quantum will affect on the photon–assisted tunneling rates between electronic states of the carbon nanotube quantum dot. The results obtained in the present paper are, in general, found to be in concordant with those in the literature [12–20].

8 Conclusion

We conclude from the present analysis of the proposed ccc theoretically and numerically that the present device could be used as photo-detector device for very wide range of frequencies. Some authors suggested that such mesoscopic device, i.e. cccc could be used for a solid state quantum computing system. Recently the investigation of the authors [20] shows that such carbon nanotubes (CNT's) could find applications in microwave communications and imaging systems.

Submitted on June 27, 2010 / Accepted on July 10, 2010

References

1. Iijma S. *Nature*, v.354, 1991, 56.
2. Harris F. Carbon nanotubes and related structures. Cambridge University Press, 1999.
3. Dresselhaus M. S. Dresselhaus G.,Eklund P. C., Science of fullerenes and carbon nanotubes. Academic Press, NY, 1996.
4. Javey A. and Keng Jing. Carbon nanotube electronics. Springer Science + Business Media LLC, 2009.
5. Dai Liming. Carbon nanotechnology Recent developments in chemistry, Physics, Materials Science and Device Applications. Elsevier, Amsterdam, 2006.
6. Saito R., Fujita M., Dresselhaus G., and Dresselhaus M. S. *Appl. Phys. Lett.*, v.60, 1992, 2204.
7. Tworzydlo J., Trauzett B, Titov M., Rycerz A., and Beenakker C. W. J. *Phys. Rev.Lett.*, v.96, 2006, 246802.
8. Platero G. and Aguado R. *Physics Reports*, v.395, 2004, 1.
9. Atallah A. S., Phillips A. H., Amin A. F. Semary M. A., *Nano 2006*, v.1, no. 3, 2006, 259 .
10. Phillips A. H., Mina A. N., Sobhy M. S., and Fouad E. A. *J. of Computational and theoretical nanoscience*, v.4 (1), 2007, 174 .
11. Phillips A. H., Aly N. A. I., Kirah K., El-Sayes H. E. *Chinese Physics Letters*, v.25, no. 1, 2008, 250.
12. Anantram M. P., Leonard F. *Rep. Prog. Phys.*, v.69, 2006, 507.
13. Durkop T., Getty S. A., Cobas E., Fuhrer M. S. *Nano Lett.*, v.4, 2004, 35.
14. Oosterkamp T. H., Kouwenhoven L. P., Koolen A. E. A., van der Vaart N. C. and Harmans C. J. P. M. *Semicond. Sci. Technol.*, v.11, 1996, 1512.
15. Meyer C., Elzerman J. M., and Kouwenhoven L. P. *Nano Lett.*, v.7, no. 2, 2007, 295.
16. Orellana P. A., Pacheco M. *Phys. Rev.*, v.B75, 2007, 115427.
17. Kim J., Hye–Miso, Kim Nam, Kim Ju–Ji, and Kicheon Kang. *Phys. Rev.*, v.B70, 2004, 153402.
18. Zhao Li–Na and Zhao Hong–Kang. *Phys. Lett.*, v.A325, 2004, 156.
19. Pan Hui, Li Tsung–Han, and Ya Dapeng. *Physica B*, v.369, 2005, 33.
20. Lin Y. M., Dimitrakpoulos C., Jenkins K. A., Farmer D. B., Chiu H. Y., Grill A., Avouris Ph. *Science, 2010*, v.327, no. 5966, 2010, 662.

On the Geometry of the Periodic Table of Elements

Albert Khazan
E-mail: albkhazan@gmail.com

The presented analytical research manifests a geometrical connexion existing among the elements of the Periodic Table of Elements, in addition to the known physical chemical connexion.

Despite the spectacular versions of the periodic tables of elements were suggested by the scientists, no one person did not state the following problem: how the elements are geometrically connected among each other in the groups and periods? As is known, the element are located in the cells, which are joined into 18 groups along the vertical axis in the Table of Elements, and into 7 periods (I suggested recently that 8 periods, see [1] and references therein) along the horizontal axis. Number of the elements rises from left to right in the periods, and from up to down in the groups. The periods begin with the elements of Group 1, and end with the elements of Group 18. Each column determines the main physical chemical properties of the elements, which change both from up to down and from left to right. For example, the elements of Group 1 are alkaline metals (the very active chemical elements), while Group 18 consists of inert gases which manifest a very low chemical activity under the regular physical conditions. In the end of the 20th century, IUPAC suggested a long period form of the Table of Elements, where Period 1 consists of 2 elements, Periods 2 and 3 consist of 8 elements in each, Periods 4 and 5 consist of 18 elements in each, while Periods 6 and 7 consist of 32 elements in each. Finally, Period 8 consisting of 37 elements was suggested on the basis of my theoretical studies [1].

This short study targets a search for the geometrical connexion among the elements of the Periodic Table.

Figure 1 in Page 65 shows that the elements of Group 18 are concentrated along the upper broken line, which is split into three straight lines joining three elements (four elements in the end) in each. The numbers indicate the periods and elements. Period 8, containing element No.155, is also shown here. Each straight section of these can easily be described by a straight line equation.

The lower broken line presents Group 1 (as seen according to the numbers of the elements). The space between the upper and lower straight lines is filled with the straight line of Group 13. It consists of Periods 2–4, 4–6, and 6–8 (Period 1 was omitted from the graph for simplicity). Besides, the points 6,67; 6,81; and 7, 99 which are related to actinides and lanthanides are shown inside the boundaries. Hence, we can suppose that the plane bounded by the lines of Group 1 and Group 18, and also by the points 8,155 and 8,119 on right and the points 1,2; 1,1 on left (and 2,3 of course) contains all known and unknown elements of the Periodic Table. Thus, this figure obtained as a result of the purely geometrical constructions, allows us to make the following conclusions:

- The Periodic Table should necessary contain Period 8, which begins with No.119 and ends by No.155;
- No elements can exists outside this figure;
- A strong geometrical connexion exists among the groups and periods.

Thus, this short study hints at a geometrical connection among the elements of the Table of Elements, which exists in addition to the known physical chemical properties of the elements. Note that the geometrical connexion manifests itself per se in the study, without any additional suggestions or constructions. Therefore, this does not change the form of the Periodic Table of Elements, which remains the same.

Submitted on June 29, 2010 / Accepted on July 12, 2010

References

1. Khazan A. Upper limit in Mendeleev's Periodic Table — Element No.155. 2nd expanded edition, Svenska fysikarkivet, Stockholm, 2010.

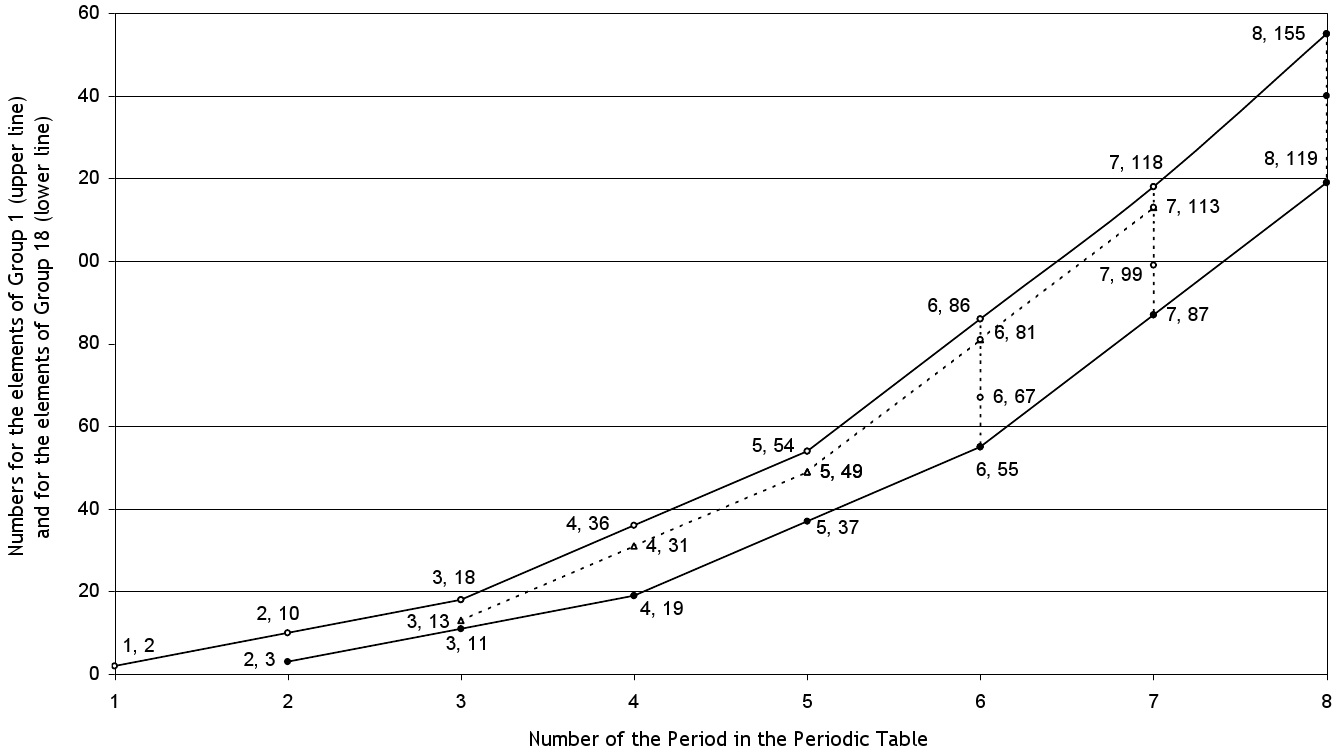

Fig. 1: Locations of the elements opening the Periods (the lower line) and those closing the Periods (the upper line).

On the Source of the Systematic Errors in the Quatum Mechanical Calculation of the Superheavy Elements

Albert Khazan
E-mail: albkhazan@gmail.com

It is shown that only the hyperbolic law of the Periodic Table of Elements allows the exact calculation for the atomic masses. The reference data of Periods 8 and 9 manifest a systematic error in the computer software applied to such a calculation (this systematic error increases with the number of the elements in the Table).

Most scientists who worked on the problems of the Periodic Table of Elements (G. T. Seaborg, J. T. Bloom, V. I. Goldanskii, F. W. Giacobbe, M. R. Kibler, J. A. Rihani et al.) attempted to construct new models of the Table with the use of quantum mechanical calculations. In this process, they used a complicate mathematical apparatus of Quantum Mechanics, and introduced additional conditions such as the periods, the number of the elements, and so on. In other word, they first set up a problem of introducing Periods 8 and 9 into the Table of Elements (50 elements in each), and predict the respective interior of the cells of the Table and the interior of the atoms. Only then, on the basis of the above data, they calculate the atomic mass and the number of the neutrons. However the main task — obtaining the exact numerical values of the atomic mass, corresponding to the numbers of the elements higher than period 8 — remains unsolved.

The core of my method for the calculation is the law of hyperbolas discovered in the Periodic Table [1]. Using the law, we first calculated the atomic mass of the upper (heaviest) element allowed in the Periodic Table (411.663243), then its number (155) was also calculated. According to the study [1], this element should be located in Group 1 of Period 8. The main parameters of the chemical elements were obtained in our study proceeding from the known data about the elements, not from the suggestions and the use of the laws specific to the microscale.

Figure 1 in Page 67 shows two dependencies. The first is based on the IUPAC 2007 data for elements 80–118 (line 1). The second continues upto element 224 (line 2). As is seen, there is a large deviation of the data in the section of the numbers 104–118. This is obviously due to the artificial synthesis of the elements, where the products o the nuclear reactions were not measured with necessary precision. Line 2 is strictly straight in all its length except those braking sections where it is shifted up along the ordinate axis. Is is easy to see that at the end of line 1, in the numbers 116–118, the atomic mass experiences a shift for 17 units. These shifts increase their value with the number of the elements: the next shift rises the line up for 20 units, and the last shift — for 25 units. In order to find the numerical values of the shifts more precisely, Figure 2 was created (see Page 67): this is the same broken line (the initially data) compared to itself being averaged by the equation of the line of trend (whose data were compared to the initial data). Hence, the difference between these lines should give the truly deviation of the numerical values f the atomic masses between the FLW Inc. data and our data (our data deviate from the equation of the line of trend for nothing but only one hundredth of 1 atomic mass unit). Figure 3 in Page 68 shows a shift of the atomic mass just element 104, before Period 8: in element 118 the atomic mass is shifted for 11 units; in Period 9 the shift exceeds 15 units, and then it increases upto 21 units. The respective data for Period 8 are shown in Figure 4.

These data lead to only a single conclusion. Any software application, which targets the quantum mechanical calculation for the atomic mass of the elements, and is constructed according to the suggested law specific to the microscale, not the known data about the chemical elements, will make errors in the calculation. The theory [1] referred herein manifested its correctness in many publications, and met no one negative review.

Submitted on July 06, 2010 / Accepted on July 12, 2010

References

1. Khazan A. Upper limit in Mendeleev's Periodic Table — Element No.155. 2nd expanded edition, Svenska fysikarkivet, Stockholm, 2010.

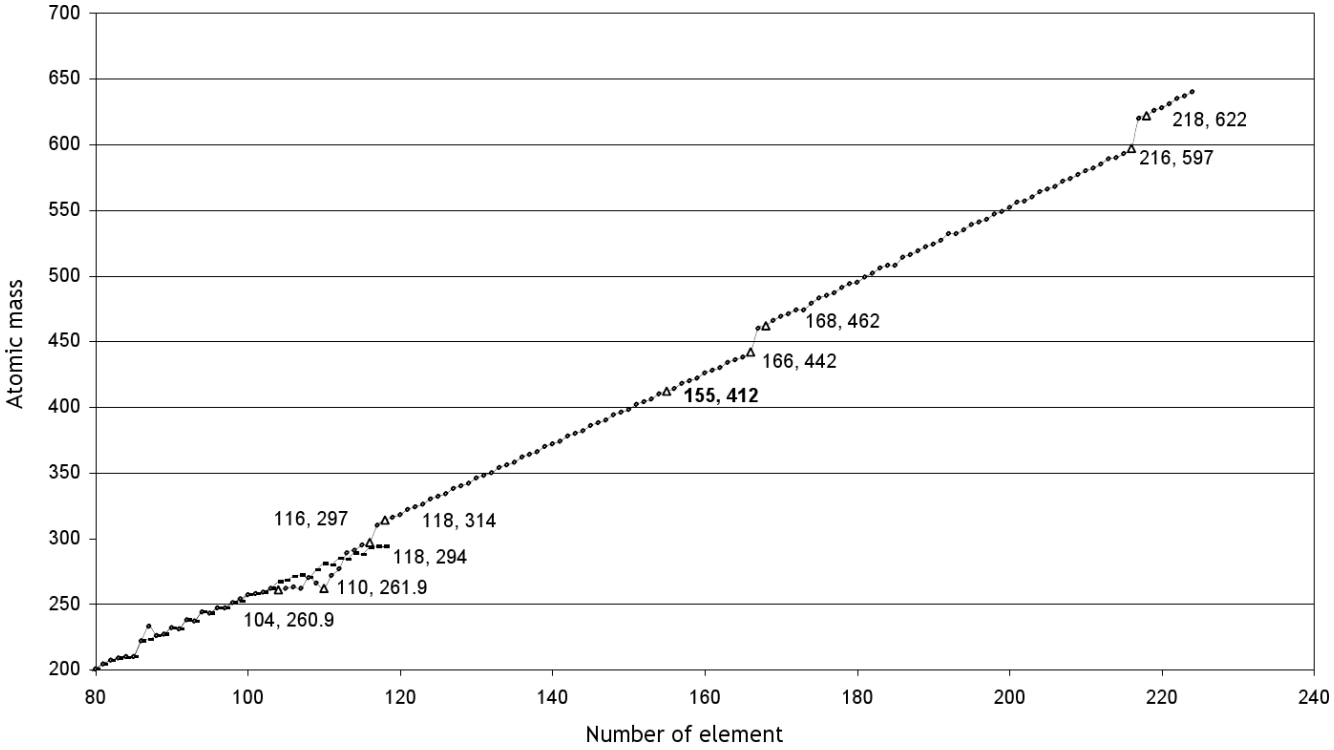

Fig. 1: Dependency between the atomic mass of the elements and their number in the Table of Elements. The IUPAC data and the FLW Inc. data begin from number 80, for more visibility of the dependency.

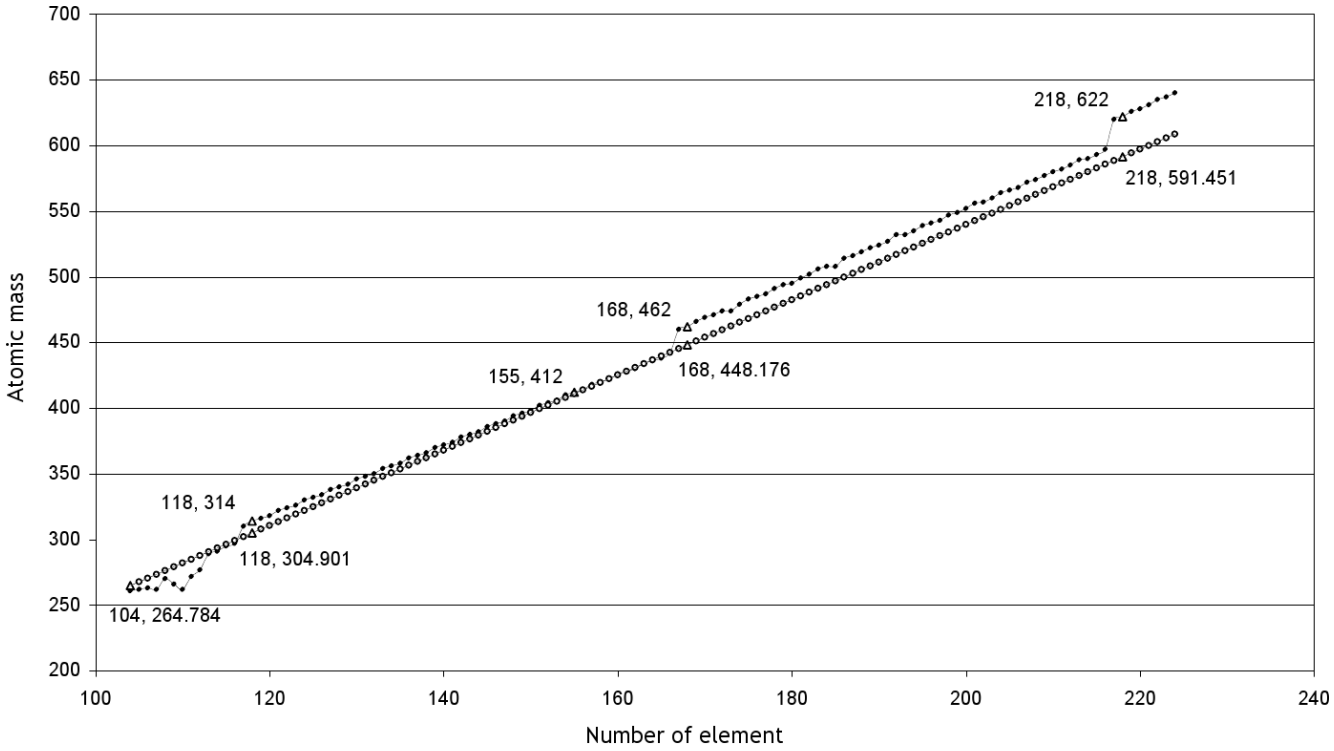

Fig. 2: Dependency between the atomic mass of the elements and their number in the Table of Elements. Black dots are the FLW Inc. data. Small circles — the averaged results according to the FLW Inc. data.

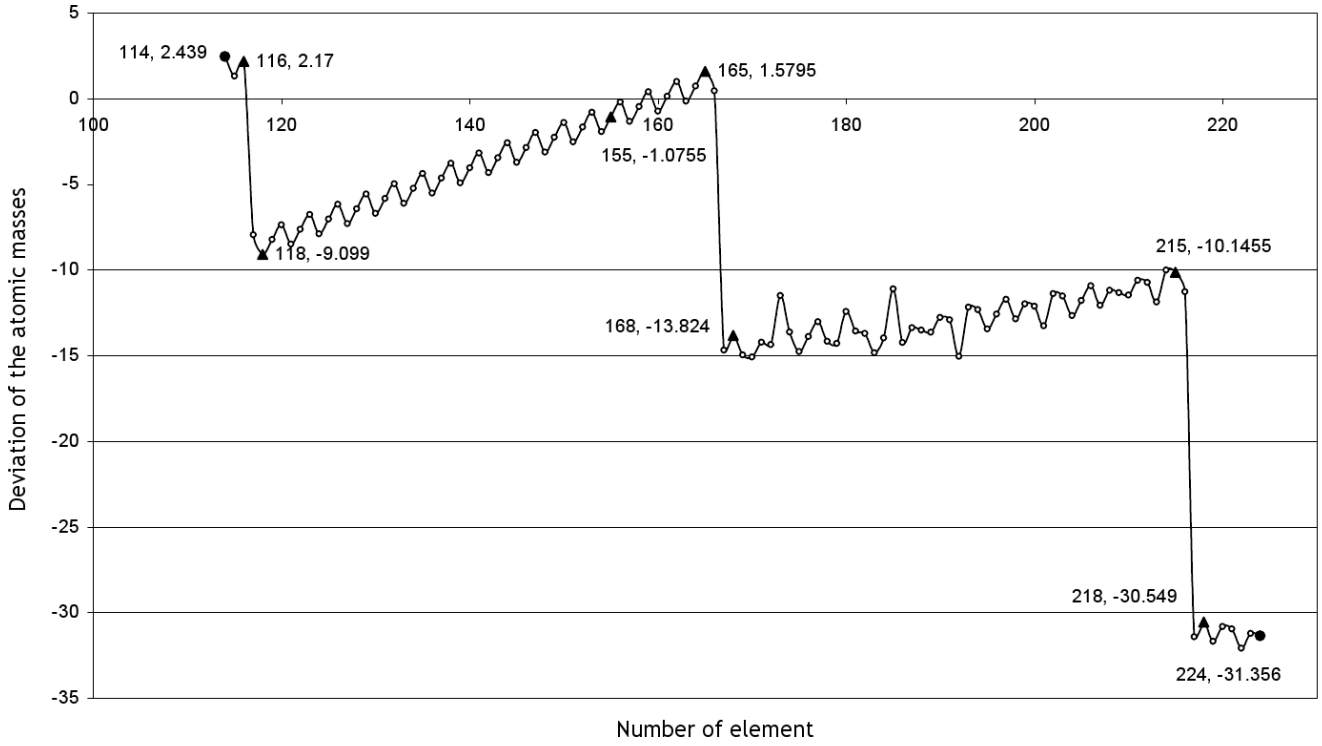

Fig. 3: Dependency between the atomic mass, calculated according to our theory and the FLW Inc. data, and their number in the Table of Elements.

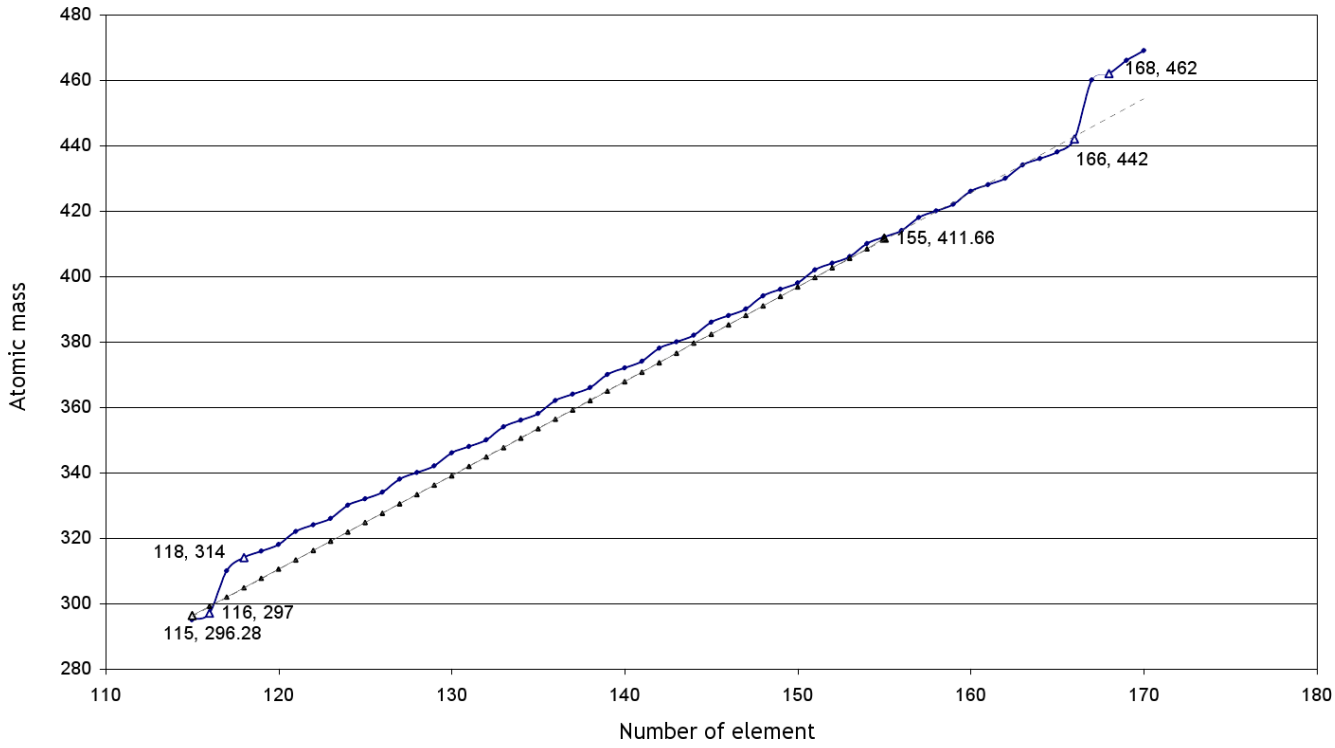

Fig. 4: Dependency between the atomic mass of the elements and their number in the Table of Elements, shown for Period 8. Black dots are the FLW Inc. data. Small triangles — the data according to our calculations.

The Dirac Electron in the Planck Vacuum Theory

William C. Daywitt

National Institute for Standards and Technology (retired), Boulder, Colorado, USA.
E-mail: wcdaywitt@earthlink.net

The nature of the Dirac electron (a massive point charge) and its negative-energy solutions are examined heuristically from the point of view of the Planck vacuum (PV) theory [1,2]. At the end of the paper the concept of the vacuum state as previously viewed by the PV theory is expanded to include the massive-particle quantum vacuum [3,4].

1 The Dirac equation

When a free, massless, bare charge travels in a straight line at a uniform velocity v, its bare Coulomb field e_*/r^2 perturbs (polarizes) the PV. If there were no PV, the bare field would propagate as a frozen pattern with the same velocity. However, the PV responds to the perturbation by producing magnetic and Faraday fields [1,5] that interact with the bare charge in a iterative fashion that leads to the well-known relativistic electric and magnetic fields [6] that are ascribed to the charge as a single entity. The corresponding force perturbing the PV is e_*^2/r^2, where one of the charges e_* in the product e_*^2 belongs to the free charge and the other to the individual Planck particles making up the degenerate negative-energy PV. By contrast, the force between two free elementary charges observed in the laboratory is $e^2/r^2\,(=\alpha e_*^2/r^2)$, where e is the observed electronic charge and α is the fine structure constant.

In the Dirac electron, where the bare charge has a mass m, the response of the PV to the electron's uniform motion is much more complicated as now the massive charge perturbs the PV with *two* forces, the polarization force e_*^2/r^2 and the attractive curvature force mc^2/r [1]. The radius at which the magnitudes of these two forces are equal

$$\frac{mc^2}{r} = \frac{e_*^2}{r^2} \qquad \text{at } r = r_c \tag{1}$$

is the electron's Compton radius $r_c\,(= e_*^2/mc^2)$. The string of Compton relations [4]

$$r_c\, mc^2 = r_*\, m_*\, c^2 = e_*^2 = c\hbar \tag{2}$$

tie the electron $(r_c mc^2)$ to the Planck particles $(r_* m_* c^2)$ within the PV, where r_* and m_* are the Compton radius and mass of those particles. The charges in the product e_*^2 of (2) are assumed to be massless point charges.

The Dirac equation for the electron is [3,7]

$$\left(c\,\widehat{\alpha}\,\widehat{p} + \beta mc^2\right)\psi = E\psi\,, \tag{3}$$

where the momentum operator and energy are given by

$$\widehat{p} = \hbar\,\nabla/i \qquad \text{and} \qquad E = \pm(m^2c^4 + c^2p^2)^{1/2} \tag{4}$$

and where $\widehat{\alpha}$ and β are defined in the references. The relativistic momentum is $p\,(= mv/\sqrt{1 - v^2/c^2})$.

As expressed in (3), the physics of the Dirac equation is difficult to understand. Using (2) to replace $\hbar$ in the momentum operator and inserting the result into (3), reduces (3) to

$$\left(\widehat{\alpha}\,\frac{e_*^2\nabla}{imc^2} + \beta\right)\psi = \frac{E}{mc^2}\,\psi\,, \tag{5}$$

where the charge product e_*^2 suggests the connection in (2) between the free electron and the PV. It is significant that neither the fine structure constant nor the observed electronic charge appear in the Dirac equation, for it further suggests that the bare charge of the electron interacts *directly* with the bare charges on the individual Planck particles within the PV, without the fine-structure-constant screening that leads to the Coulomb force e^2/r^2 in the first paragraph. Equation (5) leads immediately to the equation

$$\left(\widehat{\alpha}\,\frac{r_c\nabla}{i} + \beta\right)\psi = \frac{E}{mc^2}\,\psi \tag{6}$$

with its Del operator

$$r_c\,\nabla = \sum_{n=1}^{3} \widehat{x}_n\,\frac{\partial}{\partial x_n/r_c} \tag{7}$$

being scaled to the electron's Compton radius.

Through (2), (5), and (6), then, the connection of the Dirac equation to the PV is self evident — the Dirac equation represents the response of the PV to the two perturbations from the uniformly propagating electron. As an extension of this thinking, the quantum-field and Feynman-propagator formalisms of quantum electrodynamics are also associated with the PV response.

2 The Klein paradox

The "hole" theory of Dirac [7] that leads to the Dirac vacuum will be presented here along with the Klein paradox as the two are intimately related. Consider an electrostatic potential of the form

$$e\phi = \begin{cases} 0 & \text{for } z < 0 \ \text{(Region I)} \\ V_0 & \text{for } z > 0 \ \text{(Region II)} \end{cases} \tag{8}$$

acting on the negative-energy vacuum state (corresponding to the negative E in (4)) with a free electron from $z < 0$ being

scattered off the potential step at $z = 0$, beyond which $V_0 > E + mc^2 > 2mc^2$. This scattering problem leads to the Klein paradox that is reviewed below.

The scattering problem is readily solved [8, pp.127–131]. For the free electron in Region I, $E^2 = m^2c^4 + c^2p^2$; and for Region II, $(E - V_0)^2 = m^2c^4 + (cp')^2$, where E is the total electron energy in Region I, and p and p' are the z-directed electron momenta in Regions I and II respectively.

The Dirac equation (with motion in the z-direction) for $z < 0$ is

$$\left(c\,\alpha_z\,\widehat{p_z} + \beta mc^2\right)\psi = E\psi \tag{9}$$

and for $z > 0$ is

$$\left(c\,\alpha_z\,\widehat{p_z} + \beta mc^2\right)\psi = (E - V_0)\psi\,. \tag{10}$$

The resulting incident and reflected electron wavefunctions are

$$\psi_{\mathrm{I}} = A \begin{pmatrix} 1 \\ 0 \\ \frac{cp}{E+mc^2} \\ 0 \end{pmatrix} e^{ipz/\hbar} \tag{11}$$

and

$$\psi_{\mathrm{R}} = B \begin{pmatrix} 1 \\ 0 \\ \frac{-cp}{E+mc^2} \\ 0 \end{pmatrix} e^{-ipz/\hbar} \tag{12}$$

respectively, where $cp = \sqrt{E^2 - m^2c^4}$. The transmitted wave turns out to be

$$\psi_{\mathrm{T}} = D \begin{pmatrix} 1 \\ 0 \\ \frac{cp'}{V_0-E-mc^2} \\ 0 \end{pmatrix} e^{ip'z/\hbar}\,, \tag{13}$$

where $cp' = \sqrt{(V_0 - E)^2 - m^2c^4}$. It should be noted that the imaginary exponent in (13) represents a propagating wave which results from $V_0 > E + mc^2$; in particular, the particle motion in Region II is not damped as expected classically and quantum-mechanically when $V_0 < E + mc^2$.

The constants A, B, and D are determined from the continuity condition

$$\psi_{\mathrm{I}} + \psi_{\mathrm{R}} = \psi_{\mathrm{T}} \tag{14}$$

at $z = 0$ and lead to the parameter

$$\Gamma \equiv \left(\frac{V_0 - E + mc^2}{V_0 - E - mc^2}\,\frac{E + mc^2}{E - mc^2}\right)^{1/2} > 1\,. \tag{15}$$

The particle currents are calculated from the expectation values of

$$j_z(x) = c\,\psi^{\dagger}(x)\,\alpha_z\psi(x) \tag{16}$$

and yield j_I, j_R, and j_T for the incident, reflected, and transmitted currents respectively. The resulting normalized reflection and transmission currents become

$$\frac{j_R}{j_I} = -\left(\frac{1+\Gamma}{1-\Gamma}\right)^2\,, \tag{17}$$

$$\frac{j_T}{j_I} = -\frac{4\Gamma}{(1-\Gamma)^2}\,. \tag{18}$$

Since Γ is positive, (17) gives

$$\left|\frac{j_R}{j_I}\right| - 1 > 0 \tag{19}$$

for the excess reflected current; i.e., the reflected current is *greater* than the incident current! This seemingly irrational result is known as the Klein paradox.

The most natural and Occam's-razor-consistent conclusion to be drawn from (19), however, is that the excess electron (or electrons) in the reflected current is (are) coming from the right ($z > 0$) of the step at $z = 0$ and proceeding in the negative z direction away from the step. Furthermore, the minus sign on the normalized transmission current in (18) implies that no electrons are entering Region II — the total electron current (reflected plus "transmitted") travels in the negative z direction away from the step. Then, given the experimental fact of electron-positron pair creation, it is reasonable to conclude that the incident free electron creates such pairs when it "collides" with the stressed portion of the vacuum ($z > 0$), the positrons (Dirac "holes") proceeding to the right *into the vacuum* after the collision [8, fig. 5.6]. That is, positrons (like neutrinos [9]) travel within the vacuum, not free space!

The evidence of the created positrons is felt in free space as the positron fields, analogous to the zero-point fields whose source is the zero-point agitation of the Planck particles within the PV. The curving of the positrons in a laboratory magnetic field is due to that field permeating the PV and acting on the "holes" within. (In the PV-theory view of things, the free electron is not seen as propagating *within* the vacuum state — only the electron force-fields (e_*^2/r^2 and mc^2/r) permeate that vacuum; consequently, the electron is not colliding with the negative-energy Planck particles making up the vacuum.)

3 Summary and comments

The total r-directed perturbing force the electron exerts on the PV is

$$F_e = \frac{e_*^2}{r^2} - \frac{mc^2}{r} = \frac{e_*^2}{r^2}\left(1 - \frac{r}{r_c}\right), \tag{20}$$

where the force vanishes at the electron's Compton radius r_c. For $r > r_c$ the force compresses the vacuum and for $r < r_c$ the vacuum is forced to expand. Ignoring the second term in (20) for convenience and concentrating on the region $r < r_c$, the lessons from the preceding section can be applied to the internal electron dynamics.

Recalling that the bare charge of the free electron interacts directly with the individual Planck particles in the PV, the electron-Planck-particle potential (e_*^2/r) in the inequality $e_*^2/r > E + mc^2$ leads to

$$r < \frac{e_*^2}{E + mc^2} = \frac{r_c}{1 + E/mc^2} < \frac{r_c}{2}\,, \tag{21}$$

where the positive and negative energy levels in (4) now *overlap*, and where any small perturbation to the PV can result in an electron-positron pair being created (the electron traveling in free space and the positron in the PV). The smaller the radius r, the more sensitive the PV is to such disruption.

The electron mass results from the massless bare charge being driven by ultra-high-frequency photons of the zero-point electromagnetic vacuum [4, 10]; so the bear charge of the electron exhibits a small random motion about its center-of-motion. The resulting massive-charge collisions with the sensitized PV produce a cloud of electron-positron pairs around that charge. The massive free charge then exhibits an exchange type of scattering [3, p.323] with some of the electrons in the pairs, increasing the free electron's apparent size in the process.

In the current PV theory it is assumed that the total quantum vacuum, which consists of the electromagnetic vacuum and the massive-particle vacuum [3, 4], exists in free space as virtual particles. However, the simple picture presented in the previous paragraphs and in Section 2 concerning pair creation modifies that view significantly. It is the massive-particle quantum vacuum that overlaps the positive energy levels of the free-space electron in the previous discussion. Thus, as the appearance of this latter vacuum in free space requires a sufficiently stressed vacuum state (in the above region $r < r_c/2$ e.g.), it is more reasonable to assume that the massive-particle component of the quantum vacuum does not exist in free space except under stressful conditions.

Consequently, it seems reasonable to conclude that the PV is a composite state patterned, perhaps, after the hierarchy of Compton relations

$$r_e m_e c^2 = r_p m_p c^2 = \cdots = r_* m_* c^2 = e_*^2 , \qquad (22)$$

where the products $r_e m_e$, $r_p m_p$, and $r_* m_*$ refer to the electron, proton, and Planck particle respectively. The dots between the proton and Planck-particle products represent any number of heaver intermediate-particle states. The components of this expanded vacuum state correspond to the sub-vacua associated with these particles; e.g., the electron-positron Dirac vacuum ($r_e m_e c^2$) in the electron case. If these assumptions are correct, then the negative-energy states in (4) no longer end in a negative-energy infinity — as the energy decreases it passes through the succession of sub-vacuum states, finally ending its increasingly negative-energy descent at the Planck-particle stage $r_* m_* c^2$. In summary, the PV model now includes the massive-particle quantum vacuum which corresponds to the collection of sub-vacuum states in (22).

Submitted on July 13, 2010 /Accepted on July 16, 2010

References

1. Daywitt W.C. The Planck vacuum, *Progress in Physics*, v. 1, 20, 2009.
2. Daywitt W.C. A paradigm shift from quantum fields to the Planck vacuum. To be published in *Galilean Electrodynamics*. See also http://www.planckvacuum.com
3. Milonni P.W. The quantum vacuum — an introduction to Quantum Electrodynamics. Academic Press, New York, 1994.
4. Daywitt W.C. The source of the quantum vacuum. *Progress in Physics*, 2009, v. 1, 27.
5. Pemper R.R. A classical foundation for electrodynamics. Master Dissertation, U. of Texas, El Paso, 1977. Barnes T.G. Physics of the future — a classical unification of physics. Institute for Creation Research, California, 1983, 81.
6. Jackson J.D. Classical Electrodynamics. John Wiley & Sons, 1st ed., 2nd printing, NY, 1962.
7. Dirac P.A.M. A theory of electrons and protons. *Proc. Roy. Soc. Lond. A*, 1930, v.126, 360.
8. Gingrich D.M. Practical Quantum Electrodynamics. CRC, The Taylor & Francis Group, Boca Raton, London, New York, 2006.
9. Daywitt W.C. The neutrino: evidence of a negative-energy vacuum state. *Progress in Physics*, 2009, v. 2, 3.
10. Puthoff H.E. Gravity as a zero-point-fluctuation force. *Phys. Rev. A*, 1989, v. 39, no. 5, 2333–2342.

IN MEMORIAM OF NIKIAS STAVROULAKIS

On the Field of a Spherical Charged Pulsating Distribution of Matter

Nikias Stavroulakis*

In the theory of the gravitational field generated by an isotropic spherical mass, the spheres centered at the origin of $\mathbb{R}^3$ are non-Euclidean objects, so that each of them possesses a curvature radius distinct from its Euclidean radius. The classical theory suppresses this distinction and consequently leads to inadmissible errors. Specifically, it leads to the false idea that the field of a pulsating source is static. In a number of our previous publications (see references), we have exposed the inevitable role that the curvature radius plays and demonstrated that the field generated by a pulsating not charged spherical course is dynamical. In the present paper we prove that the curvature radius plays also the main role in the description of the gravitational field generated by a charged pulsating source.

1 Introduction

The manifold underlying the field generated by an isolated spherical distribution of matter is the space $\mathbb{R}\times\mathbb{R}^3$, considered with the product topology of four real lines. In fact, the distribution of matter is assumed to be located in a system represented topologically by the space $\mathbb{R}^3$ and moreover to every point of $\mathbb{R}^3$ there corresponds the real line described by the time coordinate t (or rather ct). In the general case, the investigation of the gravitational field by means of the Einstein equations is tied up with great mathematical difficulty. In order to simplify the problem, we confine ourselves to the case when the spherical distribution of matter is isotropic. The term "*isotropic*" refers classically to the action of the rotation group SO(3) on $\mathbb{R}^3$ and the corresponding invariance of a class of metrics on $\mathbb{R}^3$. But in our case we have to deal with a *space-time* metric on $\mathbb{R}\times\mathbb{R}^3$, so that its invariance must be conceived with respect to another group defined by means of SO(3) and acting on $\mathbb{R}\times\mathbb{R}^3$. This necessity leads to the introduction of the group SΘ(4), which consist of the matrices

$$\begin{pmatrix} 1 & 0_H \\ 0_V & A \end{pmatrix}$$

with $0_H = (0,0,0)$, $0_V = \begin{pmatrix} 0 \\ 0 \\ 0 \end{pmatrix}$ and $A \in \mathrm{SO}(3)$. It is also convenient to introduce the larger group $\Theta(4)$ consisting of the matrices of the same form for which $A \in \mathrm{O}(3)$.

From the general theory [10] of the SΘ(4)-invariant and $\Theta(4)$-invariant tensor fields on $\mathbb{R}\times\mathbb{R}^3$, we deduce the explicit form of an SΘ(4)-invariant space-time metric to be

$$ds^2 = [f(t,\|x\|)\,dt + f_1(t,\|x\|)\,(xdx)]^2 - l_1^2(t,\|x\|)dx^2 -$$

$$-\frac{l^2(t,\|x\|) - l_1^2(t,\|x\|)}{\|x\|^2}\,(xdx)^2$$

and the condition $l(t,0) = l_1(t,0)$ is satisfied, which is also $\Theta(4)$-invariant. The functions that appear in it, result from the functions of two variables

$$f(t,u)\,,\quad f_1(t,u)\,,\quad l(t,u)\,,\quad l_1(t,u)\,,$$

assumed to be C^∞ on $\mathbb{R}\times[0,+\infty[$, if we replace u by the norm

$$\|x\| = \sqrt{x_1^2 + x_2^2 + x_3^2}.$$

However, since the norm $\|x\|$ is not differentiable at the origin of $\mathbb{R}^3$, the functions

$$f(t,\|x\|)\,,\quad f_1(t,\|x\|)\,,\quad l(t,\|x\|)\,,\quad l_1(t,\|x\|)$$

are not either. So, without appropriate conditions on these functions in a neighborhood of the origin, the curvature tensor and hence the gravitational field, will present a singularity at the origin of $\mathbb{R}^3$, which would not have any physical meaning. In order to avoid the singularity, our functions must be **smooth functions of the norm** in the sense of the following definition:

*Professor Dr. Nikias Stavroulakis, born on the island of Crete on October 6, 1921, passed away in Athens, Greece, on December 20, 2009. A handwritten manuscript of this paper was found on his desk by his daughter Eleni, who gave it to Dr. Ioannis M. Roussos, Professor of Mathematics at Hamline University, Saint Paul, Minnesota, compatriot scientific collaborator and closed friend of her father, to fill in some gaps, rectify some imperfections existing in the manuscript and submit it for publication to *Progress in Physics*. At this point Dr. I. M. Roussos wishes to express that he considers it a great honor to himself the fact that his name will remain connected with this great and original scientist. This is a continuation of the 5 most recent research papers that have appeared in this journal since 2006, but as we shall see at the end of this paper, very unfortunately Professor Stavroulakis has left it unfinished. Some of the claimed final conclusions are still pending. We believe that an expert on this subject matter and familiar with the extensive work of Professor Stavroulakis, on the basis of the material provided here and in some of his previous papers, will be able to establish these claims easily. No matter what, these 6 papers make up his swan-song on his pioneering research on gravitation and relativity.

Definition 1. Let $\phi(t,u)$ be a function C^∞ on $\mathbb{R}\times[0,\infty[$. (This implies that the function $\phi(t,\|x\|)$ is C^∞ with respect to the coordinates $t,\ x_1,\ x_2,\ x_3$ on $\mathbb{R}\times\Big[\mathbb{R}^3\times\Big(\mathbb{R}^3-\{(0,\,0,\,0)\}\Big)\Big]$.) Then the function $\phi(t,u)$ will be called **smooth function of the norm**, if every derivative

$$\frac{\partial^{p_0+p_1+p_2+p_3}\,\phi\,(t,\|x\|)}{\partial t^{p_0}\partial x_1^{p_1}\partial x_2^{p_2}\partial x_3^{p_3}}$$

at the point $(t,\ x)\in\mathbb{R}^3\times\Big(\mathbb{R}^3-\{(0,\,0,\,0)\}\Big)$ tends to a definite value, as $(x_1,\ x_2,\ x_3)\to(0,\,0,\,0)$.

The following Theorem characterizes the smooth functions of the norm:

Theorem 1. Let $\phi(t,u)$ be a C^∞ function on $\mathbb{R}\times[0,\infty[$. Then $\phi\,(t,\|x\|)$ is a smooth function of the norm if and only if the right derivatives of odd order

$$\frac{\partial^{2s+1}\phi\,(t,u)}{\partial u^{2s+1}}\bigg|_{u=0}$$

vanish for every value of t.

We will not need this theorem in the sequel, because we confine ourselves to the gravitational field outside the spherical source, so that we have to do exclusively with functions whose restrictions to a compact neighborhood of the origin of $\mathbb{R}^3$ are not taken into account.

This is why we also introduce two important functions on account of their geometrical and physical significance. Namely:

$$h\,(t,\|x\|)=\|x\|\ f_1\,(t,\|x\|)$$

and

$$g\,(t,\|x\|)=\|x\|\ l_1\,(t,\|x\|)\ ,$$

although, considered globally on $\mathbb{R}\times\mathbb{R}^3$, they are not smooth functions of the norm. Then if we set $\|x\|=\rho$, we can conveniently rewrite the space-time metric in the form

$$ds^2=\left[fdt+\frac{h}{\rho}(xdx)\right]^2-\left(\frac{g}{\rho}\right)^2dx^2-\frac{1}{\rho^2}\left[l^2-\left(\frac{g}{\rho}\right)^2\right](xdx)^2 \quad (1)$$

under the condition $|h|\leqslant l$, as explained in [4]. We recall, [2], that with this metric, the field generated by a spherical charged, pulsating in general, distribution of matter, is determined by the system of equations

$$Q_{00}+\frac{v^2}{g^4}f^2=0\,, \quad (2)$$

$$Q_{01}+\frac{v^2}{g^4}\frac{fh}{\rho}=0\,, \quad (3)$$

$$Q_{11}+\frac{v^2}{g^2\rho^2}=0\,, \quad (4)$$

$$Q_{11}+\rho^2Q_{22}+\frac{v^2}{g^4}(-l^2+h^2)=0\,, \quad (5)$$

where $v^2=\frac{k}{c^4}\,\varepsilon^2$, ε being the charge of the source.

Regarding the function $Q_{00}\,,\ Q_{01}\,,\ Q_{11}\,,\ Q_{22}\,$, they occur in the definition of the Ricci tensor $R_{\alpha\beta}$ related to (1) and are given by:

$$R_{00}=Q_{00}\,,\quad R_{0i}=R_{i0}=Q_{01}x_i\,,$$
$$R_{ii}=Q_{11}+Q_{22}x_i^2\,,\quad R_{ij}=Q_{22}x_ix_j\,,$$

where $i,\ j=1,2,3$ and $i\neq j$.

This been said, before dealing with the solutions of the equations of gravitation, we have to clarify the questions related to the boundary conditions at finite distance.

Let S_m be the sphere be the sphere bounding the matter. S_m is an isotropic non-Euclidean sphere, characterized therefore by its radius and its curvature-radius, which, in the present situation, are both time dependent. Let us denote them by $\sigma(t)$ and $\zeta(t)$ respectively. Since the internal field extends to the external one through the sphere S_m, the non-stationary (dynamical) states outside the pulsating source are brought about by the radial deformations of S_m, which are defined by the motions induced by the functions $\sigma(t)$ and $\zeta(t)$. Consequently these functions are to be identified with the boundary conditions at finite distance.

How is the time occurring in the functions $\sigma(t)$ and $\zeta(t)$ defined? Since the sphere S_m is observed in a system of reference defined topologically by the space $\mathbb{R}^3$, the time t must be conceived in the same system. But the latter is not known *metrically* in advance (i.e., before solving the equations of gravitation) and moreover it is time dependent. Consequently the classical method of special relativity is not applicable to the present situation. It follows that the first principles related to the notion of time must be introduced axiomatically in accordance to the very definition of SΘ(4)-invariant metric. Their physical justification will be sought a-posteriori on the basis of results provided by the theory itself.

This been said, the introduction of the functions $\sigma(t)$ and $\zeta(t)$ is implicitly related to another significant notion, namely the notion of synchronization in S_m. If S_1 denotes the unit sphere

$$S_1=\{\ \alpha\in\mathbb{R}^3\quad|\quad\|\alpha\|=1\}\,,$$

the equation of S_m *at each distance* t is written as

$$x=\alpha\sigma(t)\,.$$

So the assignment of the value t at every point of S_m defines both the radius $\sigma(t)$ and the "*simultaneous events*"

$$\{\,[t,\ \alpha\sigma(t)]\quad|\quad\alpha\in S_1\,\}\,.$$

What do we mean exactly by saying that two events A and B in S_m are simultaneous? The identity of values of time at A and B does not imply by itself that we have to do with simultaneous events. The simultaneity is ascertained by the fact that the value of time in question corresponds to a definite

position of the advancing spherical gravitational disturbance which is propagated radially and isotropically according to the very definition of the SΘ(4)-invariant metric.

If $\sigma'(t) = \zeta'(t) = 0$ on a compact interval of time $[t_1, t_2]$, no propagation of gravitational disturbances takes place in the external space during $[t_1, t_2]$ (at least there is no diffusion of disturbances), so that the gravitational radiation outside the matter depends on the derivatives $\sigma'(t)$ and $\zeta'(t)$. It follows that we may identify the pair $[\sigma'(t)\,,\,\zeta'(t)]$ with the gravitational disturbance emitted radially from the totality of the points of S_m at the instant t. We assume that this gravitational disturbance is propagated as a spherical wave and reaches the totality of any of the spheres

$$S_\rho = \{\, x \in \mathbb{R}^3 \quad | \quad \|x\| = \rho > \sigma(t) \,\}$$

outside the matter, in consideration, at another instant.

2 Propagation function and canonical metric

A detailed study of the propagation process appears in the paper [2]. It is shown that the propagation of gravitation from a spherical pulsating source is governed by a function $\pi(t,\rho)$, termed **propagation function**, such that

$$\frac{\partial\pi(t,\rho)}{\partial t} > 0\,, \quad \frac{\partial\pi(t,\rho)}{\partial\rho} \leqslant 0\,, \quad \rho \geqslant \sigma(t)\,, \quad \pi[t,\sigma(t)] = t\,.$$

If the gravitational disturbance reaches the sphere

$$S_\rho = \{\, x \in \mathbb{R}^3 \quad | \quad \|x\| = \rho > \sigma(t) \,\}$$

at the instant t, then

$$\tau = \pi(t,\rho)$$

is the instant of its radial emission from the totality of the sphere S_m.

Among the infinity of possible choices for $\pi(t,\rho)$, we distinguish principally the one obtained in the limit case where $h = l$. Then $\pi(t,\rho)$ reduces to the time coordinate, denoted by τ, in the sphere that bounds the matter and the space-time metric takes the so-called **canonical form**

$$ds^2 = \left[f(t,\rho)d\tau + l(\tau,\rho)\frac{(xdx)}{\rho}\right]^2 - \tag{6}$$
$$-\left[\left[\frac{g(\tau,\rho)}{\rho}\right]^2 dx^2 + \left[l^2(\tau,\rho) - \left[\frac{g(\tau,\rho)}{\rho}\right]^2\right]\frac{(xdx)^2}{\rho^2}\right].$$

Any other Θ(4)-invariant metric is derived from (6) if we replace τ by a conveniently chosen propagation function $\pi(t,\rho)$. It follows that the general form of a Θ(4)-invariant metric outside the matter can be written as follows:

$$ds^2 = \left[f\,[\pi(t,\rho),\rho]\,\frac{\partial\pi(t,\rho)}{\partial t}\,dt + \right.$$
$$+\left.\left(f\,[\pi(t,\rho),\rho]\,\frac{\partial\pi(t,\rho)}{\partial t} + l\,[\pi(t,\rho),\rho]\right)\frac{(xdx)}{\rho}\right]^2 - \tag{7}$$
$$-\left[\left(\frac{g[\pi(t,\rho),\rho]}{\rho}\right)^2 dx^2 + \right.$$
$$+\left.\left(l^2[\pi(t,\rho),\rho] - \left(\frac{g[\pi(t,\rho),\rho]}{\rho}\right)^2\right)\frac{(xdx)^2}{\rho^2}\right].$$

We do not need to deal with the equations of gravitation related to (7). Their solution follows from that of the equations of gravitation related to (6), if we replace in it τ by the general propagation function $\pi(t,\rho)$. Each permissible propagation function is connected with a certain conception of time, so that, the infinity of possible propagation functions introduces an infinity of definitions of time with respect to (7). So, the notion of time involved in (7) is not quite clear.

Our study of the gravitational field must begin necessarily with the canonical form (6). Although the conception of time related to (6) is unusual, it is easily definable and understandable. The time in the bounding the matter sphere S_m as well as in any other sphere S_ρ outside the matter is considered as a time synchronization according to what has been said previously. But of course this synchronization cannot be extended radially. Regarding the time along the rays, it is defined by the radial motion of photons. The motion of a photon emitted radially at the instant τ_0 from the sphere S_m will be defined by the equation $\tau = \tau_0$. If we label this photon with indication τ_0, then as it travels to infinity, it assigns the value of time τ_0 to every point of the corresponding ray. **The identity values of τ along this ray does not mean "synchronous events"**. This conception of time differs radically from the one encountered in special relativity.

3 The equations related to (2.1)

Since $h = l$ the equations (2), (3), (4) and (5) are greatly simplified to:

$$Q_{00} + \frac{v^2}{g^4}f^2 = 0\,, \tag{8}$$

$$\rho\,Q_{01} + \frac{v^2}{g^4}fl = 0\,, \tag{9}$$

$$\rho^2 Q_{11} + \frac{v^2}{g^2} = 0\,, \tag{10}$$

$$Q_{11} + \rho^2 Q_{22} = 0\,. \tag{11}$$

Regarding the functions Q_{00}, Q_{01}, Q_{11} and Q_{22}, they are

already known, [3], to be:

$$Q_{00} = \frac{1}{l}\frac{\partial^2 f}{\partial\tau\partial\rho} - \frac{f}{l^2}\frac{\partial^2 f}{\partial\rho^2} + \frac{f}{l^2}\frac{\partial^2 l}{\partial\tau\partial\rho} + \frac{2}{g}\frac{\partial^2 g}{\partial\tau^2} -$$
$$- \frac{f}{l^3}\frac{\partial l}{\partial\tau}\frac{\partial l}{\partial\rho} + \frac{f}{l^3}\frac{\partial f}{\partial\rho}\frac{\partial l}{\partial\rho} + \frac{2f}{l^2 g}\frac{\partial l}{\partial\tau}\frac{\partial g}{\partial\rho} - \frac{2f}{l^2 g}\frac{\partial f}{\partial\rho}\frac{\partial g}{\partial\rho} - \quad (12)$$
$$- \frac{2}{fg}\frac{\partial f}{\partial\tau}\frac{\partial g}{\partial\tau} - \frac{2}{lg}\frac{\partial l}{\partial\tau}\frac{\partial g}{\partial\tau} + \frac{2}{lg}\frac{\partial f}{\partial\rho}\frac{\partial g}{\partial\tau} - \frac{1}{fl}\frac{\partial f}{\partial\tau}\frac{\partial f}{\partial\rho},$$

$$\rho Q_{01} = \frac{\partial}{\partial\tau}\left[\frac{1}{fl}\frac{\partial(fl)}{\partial\rho}\right] - \frac{\partial}{\partial\rho}\left(\frac{1}{l}\frac{\partial f}{\partial\rho}\right) + \frac{2}{g}\frac{\partial^2 g}{\partial\tau\partial\rho} - \frac{2}{lg}\frac{\partial f}{\partial\rho}\frac{\partial g}{\partial\rho}, \quad (13)$$

$$\rho^2 Q_{11} = -1 - \frac{2g}{fl}\frac{\partial^2 g}{\partial\tau\partial\rho} + \frac{g}{l^2}\frac{\partial^2 g}{\partial\rho^2} - \frac{2}{fl}\frac{\partial g}{\partial\tau}\frac{\partial g}{\partial\rho} -$$
$$- \frac{g}{l^3}\frac{\partial l}{\partial\rho}\frac{\partial g}{\partial\rho} + \frac{1}{l^2}\left(\frac{\partial g}{\partial\rho}\right)^2 + \frac{g}{fl^2}\frac{\partial f}{\partial\rho}\frac{\partial g}{\partial\rho}, \quad (14)$$

$$Q_{11} + \rho^2 Q_{22} = \frac{2}{g}\left[\frac{\partial^2 g}{\partial\rho^2} - \frac{\partial g}{\partial\rho}\frac{1}{fl}\frac{\partial(fl)}{\partial\rho}\right]. \quad (15)$$

From (8) and (9) we deduce the equation

$$lQ_{00} - f\rho\, Q_{01} = 0, \quad (16)$$

which is easier to deal with than (8) on account of the identity

$$lQ_{00} - f\rho\, Q_{01} = \frac{2l}{g}\frac{\partial^2 g}{\partial\tau^2} + \frac{2f}{lg}\frac{\partial l}{\partial\tau}\frac{\partial g}{\partial\rho} - \frac{2l}{fg}\frac{\partial f}{\partial\tau}\frac{\partial g}{\partial\tau} - \quad (17)$$
$$- \frac{2}{g}\frac{\partial l}{\partial\tau}\frac{\partial g}{\partial\tau} + \frac{2}{g}\frac{\partial f}{\partial\rho}\frac{\partial g}{\partial\tau} - \frac{2f}{g}\frac{\partial^2 g}{\partial\tau\partial\rho}$$

which follows from (12) and (13).

On account of (15), the equation (11) gives

$$\frac{\partial}{\partial\rho}\left(\frac{1}{fl}\frac{\partial g}{\partial\rho}\right) = 0$$

whence

$$\frac{1}{fl}\frac{\partial g}{\partial\rho} = \beta = \text{function of } \tau$$

and, more explicitly,

$$\frac{\partial g(\tau,\rho)}{\partial\rho} = \beta(\tau)\, f(\tau,\rho)\, l(\tau,\rho).$$

We contend that the function $\beta(\tau)$ cannot vanish. In fact, if $\beta(\tau_0) = 0$ for some value τ_0 of τ, then

$$\frac{\partial g(\tau_0,\rho)}{\partial\rho} = 0$$

from which it follows that

$$g(\tau_0,\rho) = \text{constant}.$$

This condition is un-physical: Since a photon traveling radially to infinity, assigns the values of time τ_0 to every point of a ray, this condition implies that the curvature radius $g(\tau_0,\rho)$ is constant outside the matter at the instant τ_0. Consequently $\beta(\tau) \neq 0$, so that

$$\text{either} \quad \beta(\tau) > 0 \quad \text{or} \quad \beta(\tau) < 0 \quad \text{for every value of} \quad \tau.$$

But, since $f(\tau,\rho) > 0$ and $l(\tau,\rho) > 0$, the condition $\beta(\tau) < 0$ implies

$$\frac{\partial g(\tau,\rho)}{\partial\rho} < 0$$

and so the curvature radius $g(\tau,\rho)$ is a strictly decreasing function of ρ. **This last conclusion is also un-physical**.

Consequently $\beta(\tau) > 0$ for every τ, so that we can define the positive function

$$\alpha = \alpha(\tau) = \frac{1}{\beta(\tau)}$$

and write

$$fl = \alpha\frac{\partial g}{\partial\rho}$$

and so

$$f = \frac{\alpha}{l}\frac{\partial g}{\partial\rho}. \quad (18)$$

Consequently

$$\frac{\partial f}{\partial\rho} = -\frac{\alpha}{l^2}\frac{\partial l}{\partial\rho}\frac{\partial g}{\partial\rho} + \frac{\alpha}{l}\frac{\partial^2 g}{\partial\rho^2} \quad (19)$$

and inserting this expression into (14) we obtain

$$\rho^2 Q_{11} = -1 - \frac{2g}{\alpha\frac{\partial g}{\partial\rho}}\frac{\partial^2 g}{\partial\tau\partial\rho} + \frac{2g}{l^2}\frac{\partial^2 g}{\partial\rho^2} -$$
$$- \frac{2}{\alpha}\frac{\partial g}{\partial\tau} - \frac{2g}{l^3}\frac{\partial l}{\partial\rho}\frac{\partial g}{\partial\rho} + \frac{1}{l^2}\left(\frac{\partial g}{\partial\rho}\right)^2.$$

On account of (10), we can deduce that

$$0 = \left(\rho^2 Q_{11} + \frac{v^2}{g^2}\right)\frac{\partial g}{\partial\rho} =$$
$$= -\frac{\partial g}{\partial\rho} - \frac{2g}{\alpha}\frac{\partial g^2}{\partial\tau\partial\rho} + \frac{2g}{l^2}\frac{\partial^2 g}{\partial\rho^2}\frac{\partial g}{\partial\rho} - \frac{2}{\alpha}\frac{\partial g}{\partial\tau}\frac{\partial g}{\partial\rho} -$$
$$- \frac{2g}{l^3}\frac{\partial l}{\partial\rho}\left(\frac{\partial g}{\partial\rho}\right)^2 + \frac{1}{l^2}\left(\frac{\partial g}{\partial\rho}\right)^3 + \frac{v^2}{g^2}\frac{\partial g}{\partial\rho} =$$
$$= \frac{\partial}{\partial\rho}\left[-g - \frac{2g}{\alpha}\frac{\partial g}{\partial\tau} + \frac{g}{l^2}\left(\frac{\partial g}{\partial\rho}\right)^2 - \frac{v^2}{g}\right],$$

whence

$$-g-\frac{2g}{\alpha}\frac{\partial g}{\partial\tau}+\frac{g}{l^2}\left(\frac{\partial g}{\partial\rho}\right)^2-\frac{v^2}{g}=-2\mu=\text{function of }\tau$$

and so

$$\frac{\partial g}{\partial\tau}=\frac{\alpha}{2}\left[-1+\frac{2\mu}{g}-\frac{v^2}{g^2}+\frac{1}{l^2}\left(\frac{\partial g}{\partial\rho}\right)^2\right]. \tag{20}$$

To continue our discussion we need the following derivatives obtained by direct computation:

$$\frac{\partial^2 g}{\partial\tau\partial\rho}=\alpha\left[-\frac{\mu}{g^2}\frac{\partial g}{\partial\rho}+\frac{v^2}{g^3}\frac{\partial g}{\partial\rho}-\frac{1}{l^3}\frac{\partial l}{\partial\rho}\left(\frac{\partial g}{\partial\rho}\right)^2+\frac{1}{l^2}\frac{\partial g}{\partial\rho}\frac{\partial^2 g}{\partial\rho^2}\right], \tag{21}$$

$$\begin{aligned}\frac{\partial^3 g}{\partial\tau\partial\rho^2}=&\alpha\left[\frac{2\mu}{g^3}\left(\frac{\partial g}{\partial\rho}\right)^2-\frac{\mu}{g^2}\frac{\partial^2 g}{\partial\rho^2}-\frac{3v^2}{g^4}\left(\frac{\partial g}{\partial\rho}\right)^2+\frac{v^2}{g^3}\frac{\partial^2 g}{\partial\rho^2}+\right.\\&+\frac{3}{l^4}\left(\frac{\partial l}{\partial\rho}\right)^2\left(\frac{\partial g}{\partial\rho}\right)^2-\frac{1}{l^3}\frac{\partial^2 l}{\partial\rho^2}\left(\frac{\partial g}{\partial\rho}\right)^2-\frac{4}{l^3}\frac{\partial l}{\partial\rho}\frac{\partial l}{\partial\rho}\frac{\partial^2 g}{\partial\rho^2}+\\&\left.+\frac{1}{l^2}\left(\frac{\partial^2 g}{\partial\rho^2}\right)^2+\frac{1}{l^2}\frac{\partial g}{\partial\rho}\frac{\partial^3 g}{\partial\rho^3}\right].\end{aligned} \tag{22}$$

Consider now the equation (9). Since

$$\frac{\partial}{\partial\tau}\left[\frac{1}{fl}\frac{\partial(fl)}{\partial\rho}\right]=\frac{\partial}{\partial\tau}\left(\frac{\frac{\partial^2 g}{\partial\rho^2}}{\frac{\partial g}{\partial\rho}}\right)=\frac{\frac{\partial g}{\partial\rho}\frac{\partial^3 g}{\partial\tau\partial\rho^2}-\frac{\partial^2 g}{\partial\rho^2}\frac{\partial^2 g}{\partial\tau\partial\rho}}{\left(\frac{\partial g}{\partial\rho}\right)^2}$$

by taking into account (21) and (22), we find after some computations

$$\begin{aligned}\frac{\partial}{\partial\tau}\left[\frac{1}{fl}\frac{\partial(fl)}{\partial\rho}\right]=&\alpha\left[\frac{2\mu}{g^3}\frac{\partial g}{\partial\rho}-\frac{3v^2}{g^4}\frac{\partial g}{\partial\rho}+\frac{3}{l^4}\left(\frac{\partial l}{\partial\rho}\right)^2\frac{\partial g}{\partial\rho}-\right.\\&\left.-\frac{3}{l^3}\frac{\partial l}{\partial\rho}\frac{\partial^2 g}{\partial\rho^2}-\frac{1}{l^3}\frac{\partial^2 l}{\partial\rho^2}\frac{\partial g}{\partial\rho}+\frac{1}{l^2}\frac{\partial g^3}{\partial\rho^3}\right].\end{aligned}$$

On the other hand (19) leads to the relation

$$\frac{\partial}{\partial\rho}\left[\frac{1}{l}\frac{\partial f}{\partial\rho}\right]=\alpha\left[\frac{3}{l^4}\left(\frac{\partial l}{\partial\rho}\right)^2\frac{\partial g}{\partial\rho}-\frac{1}{l^3}\frac{\partial^2 l}{\partial\rho^2}\frac{\partial g}{\partial\rho}-\frac{3}{l^3}\frac{\partial l}{\partial\rho}\frac{\partial^2 g}{\partial\rho^2}+\frac{1}{l^2}\frac{\partial^3 g}{\partial\rho^3}\right].$$

Moreover by (21)

$$\frac{2}{g}\frac{\partial^2 g}{\partial\tau\partial\rho}=\alpha\left[-\frac{2\mu}{g^3}\frac{\partial g}{\partial\rho}+\frac{2v^2}{g^4}\frac{\partial g}{\partial\rho}-\frac{2}{l^3 g}\frac{\partial l}{\partial\rho}\left(\frac{\partial g}{\partial\rho}\right)^2+\frac{2}{l^2 g}\frac{\partial g}{\partial\rho}\frac{\partial^2 g}{\partial\rho^2}\right]$$

and

$$\frac{2}{lg}\frac{\partial f}{\partial\rho}\frac{\partial g}{\partial\rho}=\alpha\left[-\frac{2}{l^3 g}\frac{\partial l}{\partial\rho}\left(\frac{\partial g}{\partial\rho}\right)^2+\frac{2}{l^2 g}\frac{\partial g}{\partial\rho}\frac{\partial^2 g}{\partial\rho^2}\right].$$

Inserting these expressions into (13) we find, after cancelations,

$$\rho Q_{01}=-\alpha\frac{v^2}{g^4}\frac{\partial g}{\partial\rho}$$

so that

$$\rho\,Q_{01}+\frac{v^2}{g^4}fl=-\alpha\frac{v^2}{g^4}\frac{\partial g}{\partial\rho}+\frac{v^2}{g^4}\alpha\frac{\partial g}{\partial\rho}=0\,.$$

Consequently the equation (9) is verified.

It remains to examine the equation (16), which amounts to transform the expression (17). In principle, we need the derivatives

$$\frac{\partial^2 g}{\partial\tau^2}\quad\text{and}\quad\frac{\partial f}{\partial\tau}$$

expressed by means of l and g.

First we consider the expression of $\frac{\partial^2 g}{\partial\tau^2}$ resulting from the derivative of (20) with respect to τ and then replace in it the $\frac{\partial g}{\partial\tau}$ and $\frac{\partial^2 g}{\partial\tau\partial\rho}$, given by their expressions (20) and (21). We get:

$$\begin{aligned}2\frac{\partial^2 g}{\partial\tau^2}=&\frac{d\alpha}{d\tau}\left[-1+\frac{2\mu}{g}-\frac{v^2}{g^2}+\frac{1}{l^2}\left(\frac{\partial g}{\partial\rho}\right)^2\right]+\\&+\alpha\left[-\frac{2}{l^3}\frac{\partial l}{\partial\tau}\left(\frac{\partial g}{\partial\rho}\right)^2+\frac{2}{g}\frac{d\mu}{d\tau}\right]+\\&+\alpha^2\left[\frac{\mu}{g^2}-\frac{2\mu^2}{g^3}+\frac{3\mu v^2}{g^4}-\frac{3\mu}{l^2 g^2}\left(\frac{\partial g}{\partial\rho}\right)^2-\frac{v^2}{g^3}-\frac{v^4}{g^5}+\right.\\&\left.+\frac{3v^2}{l^2 g^3}\left(\frac{\partial g}{\partial\rho}\right)^2-\frac{2}{l^5}\left(\frac{\partial g}{\partial\rho}\right)^3\frac{\partial l}{\partial\rho}+\frac{2}{l^4}\left(\frac{\partial g}{\partial\rho}\right)^2\frac{\partial^2 g}{\partial\rho^2}\right].\end{aligned}$$

On the other hand taking the derivative of

$$f=\frac{\alpha}{l}\frac{\partial g}{\partial\rho}$$

with respect to τ and then, in the resulting expression, replace the expression of $\frac{\partial^2 g}{\partial\tau\partial\rho}$ given by equation (21) , we obtain

$$\begin{aligned}\frac{\partial f}{\partial\tau}=&\frac{d\alpha}{d\tau}\frac{1}{l}\frac{\partial g}{\partial\rho}-\frac{\alpha}{l^2}\frac{\partial l}{\partial\tau}\frac{\partial g}{\partial\rho}+\\&+\frac{\alpha^2}{l}\left[-\frac{\mu}{g^2}\frac{\partial g}{\partial\rho}+\frac{v^2}{g^3}\frac{\partial g}{\partial\rho}-\frac{1}{l^3}\frac{\partial l}{\partial\rho}\left(\frac{\partial g}{\partial\rho}\right)^2+\frac{1}{l^2}\frac{\partial g}{\partial\rho}\frac{\partial^2 g}{\partial\rho^2}\right].\end{aligned}$$

So, we have already obtained f, $\frac{\partial f}{\partial\tau}$, $\frac{\partial f}{\partial\rho}$, $\frac{\partial^2 g}{\partial\tau\partial\rho}$, $\frac{\partial^2 g}{\partial\tau^2}$, by means of l and g. Inserting them into (21), we get after some computations and several cancelations the relation

$$lQ_{00}-f\rho Q_{01}=\frac{2\alpha l}{g^2}\frac{d\mu}{d\tau}\,,$$

so that the equation (16) is written as

$$\frac{2\alpha l}{g^2}\frac{d\mu}{d\tau}=0$$

which implies

$$\frac{d\mu}{d\tau}=0$$

and so μ is a constant.

Later on we will prove that this constant is identified with the mass that produces the gravitational field. . . *

Submitted on July 12, 2010 / Accepted on July 14, 2010

References

1. Stavroulakis, N. On the stationary charged spherical source. *Progress in Physics*, 2009, v.2, 66–71.
2. Stavroulakis, N. Gravitation and electricity. *Progress in Physics*, 2008, v.2, 91–96.
3. Stavroulakis, N. On the gravitational field of a pulsating source. *Progress in Physics*, 2007, v.4, 3–8.
4. Stavroulakis, N. On the propagation of gravitation from a pulsating source. *Progress in Physics*, 2007, v.2, 75–82.
5. Stavroulakis, N. Non-Euclidean geometry and gravitation. *Progress in Physics*, 2006, v.2, 68–75.
6. Stavroulakis, N. On a paper by J. Smoller and B. Temple. *Annales de la Fondation Louis de Broglie*, 2002, v.27, no.3, 511–521.
7. Stavroulakis, N. Matière cache et relatitité générale. *Annales de la Fondation Louis de Broglie*, 2001, v.26, no. spécial, 411–427.
8. Stavroulakis, N. Vérité scientifique et trous noirs (quatrième partie). Determination de métriques $\Theta(4)$-invariantes. *Annales de la Fondation Louis de Broglie*, 2001, v.26, no.4, 743–764.
9. Stavroulakis, N. Vérité scientifique et trous noirs (troisième partie). Équations de gravitation relatives à une métrique $\Theta(4)$-invariante. *Annales de la Fondation Louis de Broglie*, 2001, v.26, no.4, 605–631.
10. Stavroulakis, N. Vérité scientifique et trous noirs (deuxmième partie). Symétries relatives au groupe des rotations. *Annales de la Fondation Louis de Broglie*, 2000, v.25, no.2, 223–266.
11. Stavroulakis, N. Vérité scientifique et trous noirs (premième partie). Les abus du formalisme. *Annales de la Fondation Louis de Broglie*, 1999, v.24, no.1, 67–109.
12. Stavroulakis, N. On the principles of general relativity and the $S\Theta(4)$-invariant metrics. *Proceedings of the 3rd Panhellenic Congress of Geometry*, Athens, Greece, 1997, 169–182.
13. Stavroulakis, N. Sur la function de propagation des ébranlements gravitationnels. *Annales de la Fondation Louis de Broglie*, 1995, v.20, no.1, 1–31.

*At this point, Professor Dr Nikias Stavroulakis laid the pen down for good, before writing the proofs of this latter important assertion and some of the claims found in the abstract and thus completing this very interesting work. — I. M. Roussos.

Spin-Dependent Transport through Aharonov-Casher Ring Irradiated by an Electromagnetic Field

Walid A. Zein*, Nabil A. Ibrahim†, and Adel H. Phillips*

*Faculty of Engineering, Ain-Shams University, Cairo, Egypt
†Higher Technological Institute, Ramadan Tenth City, Egypt
E-mail: adel_phillips@yahoo.com

The spin dependent conductance of mesoscopic device is investigated under the effect of infrared and ultraviolet radiation and magnetic field. This device is modeled as Aharonov-Casher semiconducting ring and a quantum dot is embedded in one arm of the ring. An expression for the conductance is deduced. The results show oscillatory behavior of the conductance. These oscillations might be due to Coulomb blockade effect and the interplay of Rashba spin orbit coupling strength with the induced photons of the electromagnetic field. The present device could find applications in quantum information processing (qubit).

1 Introduction

Advances in nanotechnology opened the way for the synthesis of artificial nanostructures with sizes smaller than the phase coherence length of the carriers [1]. The electronic properties of these systems are dominated by quantum effects and interferences [2]. One of the goals of semiconductor spintronics [3,4] is to realize quantum information processing based on electron spin. In the last decades, much attention is attracted by many scientists to study the spin-dependent transport in diverse mesoscopic systems, e.g., junctions with ferromagnetic layers, magnetic semiconductors, and low-dimensional semiconducting nanostructures [5, 6]. Coherent oscillations of spin state driven by a microwave field have been studied extensively [7–11].

Many authors investigated the spin transport through quantum rings [12–18]. These rings are fabricated out of two dimensional electron gas formed between heterojunction of III–V and II–VI semiconductors. Spin-orbit interaction (SOI) is crucial in these materials. The purpose of the present paper is to investigate the quantum spin transport in ring made of semiconductor heterostructure under the effect of infrared and ultraviolet radiations.

2 Theoretical treatment

In order to study the quantum spin characteristics of a mesoscopic device under the effect of both infrared (IR) and ultraviolet (UV) radiation, we propose the following model:

A semiconductor quantum dot is embedded in one arm of the Aharonov-Casher ring with radius comparable with the Fermi-wavelength of semiconductor heterostructure. This ring is connected to two conducting leads. The form of the confining potential is modulated by an external gate electrode allowing for direct control of the electron spin-orbit interaction. By introducing an external magnetic field, we also calculate the combined Aharonov-Casher, and Aharonov-Bohm conductance modulations. The conductance G for the present investigated device will be calculated using Landauer formula [17–19] as:

$$G = \frac{2e^2}{h} \sin\phi \sum_{\mu=1,2} dE \left(-\frac{\partial j_{FD}}{\partial E} \right) \left| \Gamma_{\mu,with\ photon}(E) \right|^2 , \quad (1)$$

where f_{FD} is the Fermi-Dirac distribution function, e is the electron charge, h is Planck's constant, ϕ is the electron phase difference propagating through the upper and lower arms of the ring, and $\left|\Gamma_{\mu,with\ photon}(E)\right|^2$ is the tunneling probability induced by the external photons.

Now, we can find an expression for the tunneling probability $\left|\Gamma_{\mu,with\ photon}(E)\right|^2$ by solving the following Schrodinger equation and finding the eigenfunctions for this system as follows:

$$\left(\frac{P^2}{2m^*} + V_d + eV_g + E_F + eV_{ac}\cos(\omega t) + \right.$$
$$\left. + \frac{\hbar eB}{2m^*} + \widehat{H}_{Soc} + eV_{Sd} \right) \psi = E\psi , \quad (2)$$

where V_d is the barrier height, V_g is the gate voltage, m^* is the effective mass of electrons, E_F is the Fermi-energy, B is the applied magnetic field, and V_{ac} is the amplitude of the applied infrared, and ultraviolet electromagnetic field with frequency ω. In (2) $\widehat{H}_{Soc}$ is the Hamiltonian due to the spin-orbit coupling which is expressed as:

$$\widehat{H}_{Soc} = \frac{\hbar^2}{2m^*a^2} \left(-i\frac{\partial}{\partial\phi} - \frac{\Phi_{AB}}{2\pi} - \frac{\omega_{Soc} m^* a^2}{\hbar}\, \sigma_r \right), \quad (3)$$

where $\omega_{Soc} = \alpha/(\hbar a)$ and it is called the frequency associated with the spin-orbit coupling,α is the strength of the spin-orbit coupling, a is the radius of the Aharonov-Casher ring, and σ_r is the radial part of the Pauli matrices which expressed in the components of Pauli matrices σ_x, σ_y as:

$$\begin{aligned} \sigma_r &= \sigma_x \cos\phi + \sigma_y \sin\phi, \\ \sigma_\phi &= \sigma_y \cos\phi - \sigma_x \sin\phi . \end{aligned} \quad (4)$$

Due to the application of magnetic field B, normal to the plane of the device, the Aharonov-Bohm phase will be picked up by an electron which encircling the following magnetic flux Φ_{AB}, see Eq. (3), as:

$$\Phi_{AB} = \frac{\pi e B a^2}{\hbar} . \tag{5}$$

Now, the solution of Eq. (2) will consist of four eigenfunctions [17, 18, 20], where $\psi_L(x)$ is the eigenfunction for transmission through the left lead, $\psi_R(x)$ for the right lead, $\psi_{up}(\theta)$ for the upper arm of the ring, and $\psi_{low}(\theta)$ for the lower arm of the ring. Their expressions are:

$$\psi_L(x,t) = \sum_{\sigma} \sum_{n=-\infty}^{\infty} J_n\left(\frac{eV_{ac}}{\hbar\omega}\right)\left[Ae^{ikx} + Be^{-ikx}\right]\chi^{\sigma}(\pi)\, e^{-in\omega t}, \tag{6}$$

$\chi \in [-\infty, 0]$

$$\psi_R(x,t) = \sum_{\sigma} \sum_{n=-\infty}^{\infty} J_n\left(\frac{eV_{ac}}{\hbar\omega}\right)\left[Ce^{ik'x} + De^{-ik'x}\right]\chi^{\sigma}(0)\, e^{-in\omega t}, \tag{7}$$

$\chi \in [0, \infty]$,

$$\psi_{up}(\theta,t) = \sum_{\sigma,\mu} \sum_{n=-\infty}^{\infty} J_n\left(\frac{eV_{ac}}{\hbar\omega}\right) F_{\mu} e^{in'^{\sigma}_{\mu}\phi} e^{-in\omega t}\chi^{\sigma}(\phi), \tag{8}$$

$\phi \in [0, \pi]$,

$$\psi_{low}(\theta,t) = \sum_{\sigma,\mu} \sum_{n=-\infty}^{\infty} J_n\left(\frac{eV_{ac}}{\hbar\omega}\right) G_{\mu} e^{in^{\sigma}_{\mu}\phi} e^{-in\omega t}\chi^{\sigma}(\phi), \tag{9}$$

$\phi \in [\pi, 2\pi]$

were $J_n(eV_{ac}/(\hbar\omega))$, Eqs. (6–9), is the n^{th} order Bessel function. The solutions, Eqs. (6–9), must be generated by the presence of the different side-bands n, which come with phase factor $\exp(-in\omega t)$. The parameter $\chi^{\sigma}(\phi)$ is expressed as:

$$\chi^1_n(\phi) = \begin{pmatrix} \cos(\theta/2) \\ e^{i\phi}\sin(\theta/2) \end{pmatrix} \tag{10}$$

and

$$\chi^2_n(\phi) = \begin{pmatrix} \sin(\theta/2) \\ -e^{i\phi}\cos(\theta/2) \end{pmatrix} \tag{11}$$

where the angle θ [17, 18, 21] is given by

$$\theta = 2\tan^{-1}\left(\frac{\Omega - \sqrt{\Omega^2 + \omega^2_{Soc}}}{\omega_{Soc}}\right) \tag{12}$$

in which Ω is given by

$$\Omega = \frac{\hbar}{2m^* a^2}. \tag{13}$$

Also, the parameters n'^{σ}_{μ} and n^{σ}_{μ} expressed respectively as:

$$n'^{\sigma}_{\mu} = \mu k' a - \phi + \frac{\Phi_{AB}}{2\pi} + \frac{\Phi^{\sigma}_{AC}}{2\pi} , \tag{14}$$

$$n^{\sigma}_{\mu} = \mu k a - \phi + \frac{\Phi_{AB}}{2\pi} + \frac{\Phi^{\mu}_{AC}}{2\pi} , \tag{15}$$

in which $\mu = \pm 1$ corresponding to the spin-up, and spin-down of the transmitted phase, expressed as [17, 18, 20]:

$$\Phi^{\mu}_{AC} = \pi\left[1 + \frac{(-1)^{\mu}\left(\omega^2_{Soc} + \Omega^2\right)^{1/2}}{\Omega}\right] . \tag{16}$$

The wave numbers k' and k are given respectively by

$$k' = \sqrt{\frac{2m^*(E + n\hbar\omega)}{\hbar^2}} , \tag{17}$$

and

$$k = \sqrt{\frac{2m^*}{\hbar^2}\left(V_d + eV_g + \frac{N^2e^2}{2C} + E_F + n\hbar\omega - E\right)}, \tag{18}$$

where V_d is the barrier height, V_g is the gate voltage, N is the number of electrons entering the quantum dot, C is the total capacitance of the quantum dot, e is the electron charge, E_F is the Fermi energy, m^* is the effective mass of electrons with energy E, and $\hbar\omega$ is the photon energy of both infrared and ultraviolet electromagnetic field.

Now, the tunneling probability $\left|\Gamma_{\mu,with\ photon}(E)\right|^2$ could be obtained by applying the Griffith boundary condition [15, 17, 18, 20, 21] to Eqs. (6–9). The Griffith boundary condition states that the eigenfunctions, Eqs. (6–9), are continuous and their current density is conserved at each intersection. Accordingly therefore, the expression for the tunneling probability is given by:

$$\left|\Gamma_{\mu\ with\ photons}(E)\right|^2 = \tag{19}$$

$$= \sum_n J^2_n \left[\frac{8i\cos\left(\frac{\Phi_{AB}+\Phi^{\mu}_{AC}}{2}\right)\sin(\pi k a)}{4\cos(2\pi k' a) + 4\cos\left(\Phi_{AB} + \Phi^{\mu}_{AC}\right) + 4\sin(2\pi k' a)}\right]^2 .$$

Now, substituting $\left|\Gamma_{\mu\ with\ photons}(E)\right|^2$, into Eq. (1), we get a full expression for the conductance G, which will be solved numerically as will be seen in the next section.

3 Result and discussion

Numerical calculations are performed for the conductance G as function of the gate voltage V_g, magnetic field B, and function of ω_{Soc} frequency due to spin-orbit coupling at specific values of photon energies, e.g., energies of infrared and ultraviolet radiations. The values of the following parameters

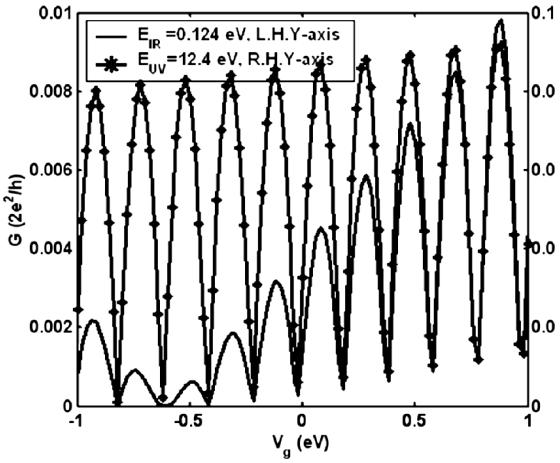

Fig. 1: The variation of the conductance G with the gate voltage V_g at different photon energy E_{IR} and E_{UV}.

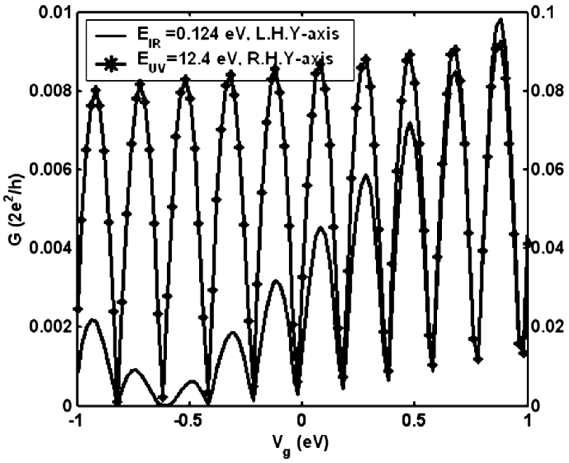

Fig. 3: The variation of the conductance G with the frequency ω_{Soc} at different photon energy E_{IR} and E_{UV}.

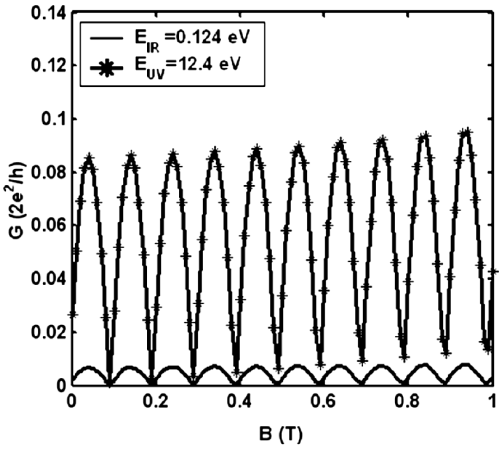

Fig. 2: The variation of the conductance G with the magnetic field B at different photon energy E_{IR} and E_{UV}.

have been found previous by the authors [22–24]. The values of $C \sim 10^{-16}$ F and $V_d \sim 0.47$ eV. The value of the number of electrons entering the quantum dot was varied as random number.

We use the semiconductor heterostructures as In Ga As/ In Al As. The main features of our obtained results are:

1. Fig. (1), shows the dependence of the conductance G, on the gate voltage V_g, at both photon energy of infrared (IR), and ultraviolet (UV) radiations. Oscillatory behavior is shown. For the case of infrared radiation, the peak height strongly increases as gate voltage increases from –0.5 to 1. But for the case ultraviolet, this increase in peak height is so small.
2. Fig. (2), shows the dependence of the conductance G, on the applied magnetic field B, at both the photon energies considered (IR and UV). A periodic oscillation is shown for the two cases, the periodicity equals the quantum flux h/e.
3. The dependence of the conductance G, on the frequency associated with the spin-orbit coupling, ω_{Soc}. at different values of the investigated applied photon energies is shown in Fig. 3.

The obtained results might be explained as follows: The oscillatory behavior of the conductance is due to spin-sensitive quantum interference effects caused by the difference in the Aharonov-Casher phase accumulated by the opposite spin states. The Aharonov-Casher phase arises from the propagation of the electron in the spin-orbit coupling. The quantum interference effect appears due to photon spin-up, and spin-down subbands coupling. Our results are found concordant with these in the literature [15, 16, 25].

4 Conclusion

The Aharonov-Casher, and Aharonov-Bohm effects are studied, taking into consideration the influence of both infrared (IR), and ultraviolet (UV) electromagnetic field. This could be realized by proposing a semiconducting quantum dot embedded in one arm of semiconducting ring. Spin filtering, and spin pumping due to the effect of photons are studied by deducing the spin transport conductance. The present results are valuable for the application in the field of quantum information processing (qubit) quantum bit read out, and writing.

Submitted on August 08, 2010 / Accepted on August 12, 2010

References

1. Heinzel T. Mesoscopic electronics in solid state nanostructures. Wiley-VCH Verlag Weinheim, 2003.
2. Mitin V.V., Sementsov D.I., and Vagidov N.Z. Quantum Mechanics for nanostructures. Cambridge University Press, Cambridge, 2010.
3. Awschalom D.D., Loss D., and Samart N., editors. Semiconductor spintronics and quantum computation. Spinger, New York, 2000.
4. Sahoo S., Kantos T., et al. *Nature Physics*, v.1, 2005, 99.
5. Zutic I., Fabian J., and Das Sarma S. *Rev. Mod. Phys.*, v.76, 2004, 323.

6. Parkin S.S.P. Applications of magnetic nanostructures. Taylor and Francis, NY, 2002.
7. Rashba E.J. and Efros A.L. *Phys. Rev. Lett.*, v.91, 2003, 126405.
8. Cheng J.L., Wu M.W. *Appl. Phys. Lett.*, v.86, 2005, 032107.
9. Jiang J.H., Weng M.Q., and Wu M.W. *J. Appl. Phys.*, v.100, 2006, 063709.
10. Tokura Y., van der Wiel W.G., Obata T., and Tarucha S, *Phys. Rev. Lett.*, v.96, 2006, 047202.
11. Duckheim M., and Loss D. *Nature Physics*, v.2, 2006, 195.
12. Meijer F.E., Morpurgo A.F., and Klapwijk T.M. *Phys. Rev. B*, v.66, 2002, 033107.
13. Frustaglia D. and Richter K. *Phys. Rev. B*, v.69, 2004, 235310.
14. Nitta J., Meijer F.E., and Takayanagi H. *Appl. Phys. Lett.*, v.75, 1999, 695.
15. Molnar B., Peeters F.M., and Vasilopoulos P. *Phys. Rev. B*, v.69, 2004, 155335.
16. Kovalev A.A., Borunda M.F., Jungwirth T., Molenkamp L.W., and Sinov J. *Phys. Rev. B*, v.76, 2007, 125307.
17. Zein W.A., Phillips A.H., and Omar O.A. *Progress in Physics*, v.4, 2007, 18.
18. Zein W. A., Phillips A.H. and Omar O.A. *NANO*, v.2, no.6, 2007, 389.
19. Datta S. Electronic transport in mesoscopic systems. Cambridge University Press, Cambridge, 1997.
20. Hentschel M., Schomerus H., Frustaglia D., and Richter K. *Phys. Rev. B*, v.69, 2004, 155326.
21. Goiffith S. *Trans. Faraday Soc.*, v.49, 1953, 345.
22. Phillips A.H., Mina A.N., Sobhy M.S., and Fouad E.A. *J. Computational and Theoretical Nanoscience*, v.4, 2007, 174.
23. Aly A.H., Hong J., and Phillips A.H. *International J. of Modern Phys. B*, v.20, no.16, 2006, 2305.
24. Aly A.H., and Phillips A.H. *Phys. Stat. Sol. B*, v.232, no.2, 2002, 283.
25. Moskalenko A.S., Matos-Abiague A., and Berakdar J. *Europhys. Lett.*, v.78, 2007, 57001.

Fractal Structure of Nature's Preferred Masses: Application of the Model of Oscillations in a Chain System

Andreas Ries and Marcus Vinicius Lia Fook

Universidade Federal de Campina Grande, Unidade Acadêmica de Engenharia de Materiais, Rua Aprígio Veloso 882, 58429-140 Campina Grande — PB, Brazil
E-mail: andreasries@yahoo.com, marcusvinicius@dema.ufcg.edu.br

A numerical analysis of elementary particle masses on the logarithmic number line revealed systematic mass gaps of $2e$, e, $\frac{e}{2}$, $\frac{e}{4}$, $\frac{e}{8}$ and $\frac{e}{16}$. Also in abundance data of the chemical elements, a repeated abundance gap of $\frac{e}{2}$ could be detected. This lead us to modify a fractal scaling model originally published by Müller in this journal, interpreting elementary particles as proton resonances. We express a set of 78 accurately determined particle masses on the logarithmic scale in a continued fraction form where all numerators are Euler's number.

1 Introduction

Recently in three papers of this journal, Müller [1–3] has proposed a chain of similar harmonic oscillators as a new model to describe the fractal properties of nature. For a specific process or data set, this model treats observables such as energies, frequencies, lengths and masses as resonance oscillation modes and aims at predicting naturally preferred values for these parameters. The starting point of the model is the fact that hydrogen is the most abundant element in the universe and therefore the dominant oscillation state. Consequently, Müller calculates the spectrum of eigenfrequencies of a chain system of many proton harmonic oscillators according to a continued fraction equation [2]

$$f = f_p \exp S \,, \tag{1}$$

where f is any natural oscillation frequency of the chain system, f_p the oscillation frequency of one proton and S the continued fraction corresponding to f. S was suggested to be in the canonical form with all partial numerators equal 1 and the partial denominators are positive or negative integer values

$$S = n_0 + \cfrac{1}{n_1 + \cfrac{1}{n_2 + \cfrac{1}{n_3 + \ldots}}} \,. \tag{2}$$

Particularly interesting properties arise when the nominator equals 2 and all denominators are divisible by 3. Such fractions divide the logarithmic scale in allowed values and empty gaps, i.e. ranges of numbers which cannot be expressed with this type of continued fractions. He showed that these continuous fractions generate a self-similar and discrete spectrum of eigenvalues [1], that is also logarithmically invariant. Maximum spectral density areas arise when the free link n_0 and the partial denominators n_i are divisible by 3.

This model was applied to the mass distribution of celestial bodies in our solar system [2] as well as to the mass distribution of elementary particles such as baryons, mesons, leptons and gauge bosons [3]. The masses were found to be located at or close to spectral nodes and definitively not random.

In this article we investigated the properties of masses in the micro-cosmos on the logarithmic scale by a graphical analysis with particular interest in detection of periodic trends. We analyzed abundance data of the chemical elements, atomic masses and the masses of elementary particles. Then we applied a slightly modified version of Müller's fractal model and demonstrate that there is a hidden structure in the masses of elementary particles.

2 Data sources and computational details

Solar system abundance data of chemical elements (with uncertainties of around 10%) were taken from reference [4]. High accuracy nuclide masses are given in an evaluation by Audi [5]. Relative isotope abundances for a selected chemical element can be found in the CRC Handbook of Chemistry and Physics [6]. Accurate masses of elementary particles are given in Müller's article [3] and were used for the calculation of continued fractions. In order to avoid machine based rounding errors, numerical values of continued fractions were always calculated using the the Lenz algorithm as indicated in reference [7].

3 Results

Figure 1 shows the relative abundance of the chemical elements in a less usual form. In textbooks or articles these data are normally presented as $log_{10}(abundance)$ versus atomic number on a linear scale. Here we adopted Müller's formalism and present the abundance data as a function of the natural logarithm of the atomic masses (here mean values from a periodic table were used) which were previously divided by the lowest atomic weight available (hydrogen). As can be seen, there is a general trend of decreasing abundance with increasing atomic mass, but the plot has a few remarkable extremities.

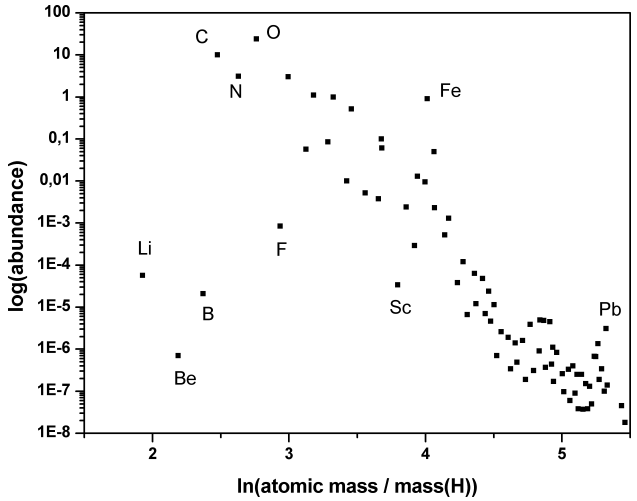

Fig. 1: Solar system abundance data of the chemical elements on a logarithmic scale. H and He omitted for clarity.

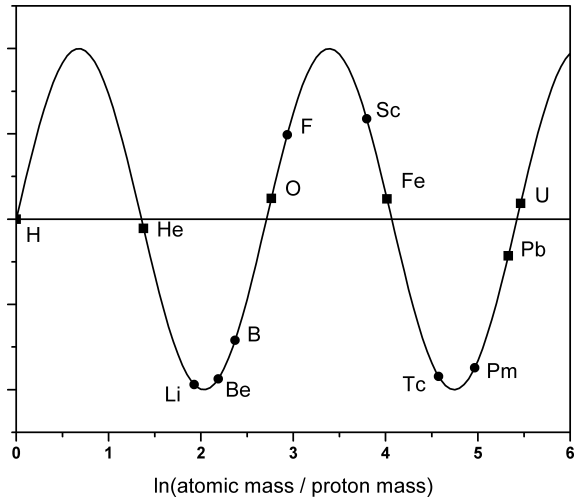

Fig. 2: Abundance maxima and minima of chemical elements on the logarithmic number line.

Nuclide	$\ln \frac{m(nuclide)}{m(\mathrm{H})}$	multiples of $\frac{e}{2}$
$^{1}_{1}$H	0.0	$0.0 \times \frac{e}{2}$
$^{4}_{2}$He	1.379	$1.015 \times \frac{e}{2}$
$^{16}_{8}$O	2.764	$2.034 \times \frac{e}{2}$
$^{56}_{26}$Fe	4.016	$2.955 \times \frac{e}{2}$
$^{208}_{82}$Pb	5.330	$3.921 \times \frac{e}{2}$

Table 1: $\ln \frac{m(nuclide)}{m(\mathrm{H})}$ of element abundance maxima expressed in multiples of $\frac{e}{2}$.

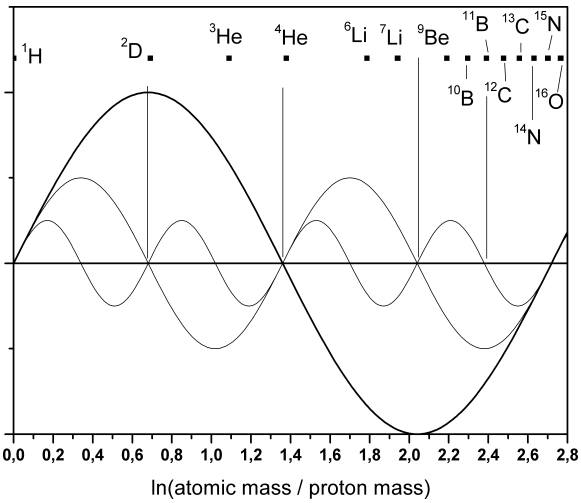

Fig. 3: Stable isotopes on the logarithmic scale in the range 0 to e.

Elements marking very clear maxima or minima are labeled with symbols. The most relevant maxima in graph are elements O, Fe and Pb. Of course, H and He, the most abundant elements in the universe (not shown in Fig. 1) must also be interpreted as maxima in the figure. From Figure 2 it becomes directly clear that these abundance maxima occur in almost equal distances on the logarithmic number line. The simple calculation $\ln \frac{m(^4_2\mathrm{He})}{m(^1_1\mathrm{H})} - \ln \frac{m(^1_1\mathrm{H})}{m(^1_1\mathrm{H})} = 1.37$ reveals that these distance seems to be $\frac{e}{2}$, where e is Euler's number. When drawing a sine function with period e, $f(x) = \sin(\frac{2\pi x}{e})$ on the logarithmic number line, the abundance maxima are closely located to the zeros of this function.

Table 1 summarizes the numerical deviations from multiples of $\frac{e}{2}$. The calculations were performed for the naturally most abundant isotope of the considered element.

Figure 2 has some analogy to Kundt's famous experiment with standing sound waves in a tube. It seems as a standing wave on the logarithmic number line supporting an accumulation of naturally preferred mass particles in the nodes, which are multiples of $\frac{e}{2}$. On the other hand these preferred masses are not exactly located in the notes, more evidently the less abundant chemical elements (Li, Be, B, F) are more distant from the bulges than H, He, O, Fe and U from the nodes. Pm and Tc are even completely absent in the abundance data due to their radioactivity.

Within the first period of the sine function in Fig. 2, very few stable isotopes are found. So it is possible to analyze the location of their isotope masses in relation to nodes of the previously constructed sine function including higher harmonics. Figure 3 displays the logarithmic axis from zero to e with a sine function of period e and two corresponding (2nd and 4th) higher harmonics defined through repeated frequency doubling. The location ($= \ln \frac{m_{nuclide}}{m_{proton}}$) of all existing stable isotopes in that range is indicated. From this, similar wave stabilizations regarding these light isotopes can be obtained:

1. Deuterium is a stable, but hardly abundant hydrogen isotope. It seems to be stabilized by the second harmonics with period $\frac{e}{2}$ due to location in the node (tritium does not fit in a node of this wave). Possibly hy-

drogen isotopes are principally governed by the basic wave with period e and the influence of higher harmonics is greatly reduced, which explains the low abundance.

2. Why is the isotope ^{4}He (99.999%) much more abundant than ^{3}He (0.0001%)? Assuming that He is principally governed as H by the wave with period e, the isotope ^{4}He is closer to the node than ^{3}He. In this case the higher stability of ^{4}He can also explained with the magic numbers for both, protons and neutrons.
3. Lithium is composed of 92.5% ^{7}Li and 7.5% ^{6}Li. The isotope ^{7}Li is more abundant and clearly closer to a node of the second harmonic (it has also a little higher bonding energy per nucleon than ^{6}Li).
4. The isotope ^{11}B is exactly located in the node of the third harmonic with period $\frac{e}{4}$. It is much more abundant (80.1%) than ^{10}B (19.9%).
5. The isotope ^{12}C is closer to the node of the fourth harmonics than ^{13}C. This is in agreement with the abundances of 98.0% for ^{12}C and 1.1% for ^{13}C.
6. Nitrogen is composed of 99.63% ^{14}N and 0.36% ^{15}N. The isotope ^{15}N is almost in the node of the basic wave and all higher harmonics. Here the model fails to predict the correct abundance order, but the isotope ^{15}N has the higher stability, which can be readily confirmed by the magic number of 8 neutrons in this nuclide. For a certain reason, the nuclide stability does not go along with the corresponding abundance. For an explanation of this fact must be considered that elements heavier than He cannot be built up in our sun or similar present-day (second generation) stars [8]. This is due to the fact that for all nuclei lighter than carbon, a nuclear reaction with a proton leads to the emission of an alpha particle disintegrating the original nucleus. So the heavier elements in stars must already have existed prior to the second generation star formation. Bethe [8] investigated possible nuclear reactions of both nitrogen isotopes and found that ^{15}N can give a $p-\alpha$ reaction

$$^{15}\mathrm{N} + {}^{1}\mathrm{H} \rightarrow {}^{4}\mathrm{He} + {}^{12}\mathrm{C}$$

while ^{14}N can only capture a proton

$$^{14}\mathrm{N} + {}^{1}\mathrm{H} \rightarrow {}^{15}\mathrm{O} + \gamma.$$

According to Bethe, such a $p-\alpha$ reaction is always more probable than a radiative capture. So we theorize that without existence of the above mentioned nuclear reaction, the abundance data would show an excess of ^{15}N.

A nuclear reaction also explains why lead is the element with the highest deviation from such a node (Fig. 2). We believe that Pb does actually not present its true abundance value as existed through stellar element formation, its abundance is increased since it is the end product of the 3 most important decay chains (thorium series, uranium series, actinium series). There are no stable isotopes between Pb and ^{238}U, which has a long half-life. The element uranium lies much more close to a node than Pb, and also because of its long half-life, we believe that this nuclide could be a former abundance maximum.

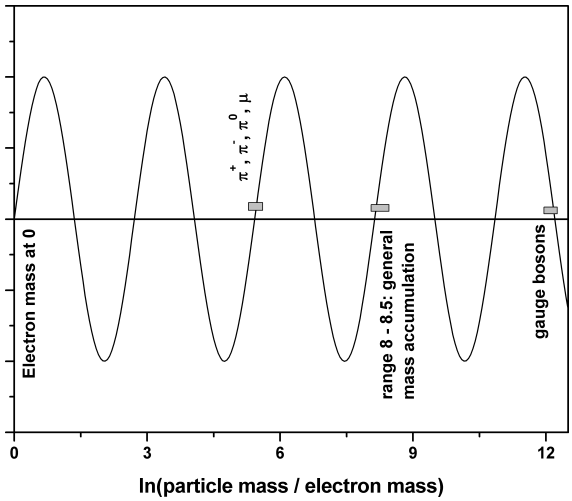

Fig. 4: Accumulation of particle masses on the logarithmic scale.

In order to find similar regularities for elementary particles we selected according to some physics textbooks a set of commonly discussed particles. Their importance was mainly justified by the relatively long lifetimes ($> 10^{-19}$ s). We believe that nature's preferred masses are the more stable particles and particularly for these masses some regularities could be expected. Table 2 presents the considered set of particles, their rest masses and positions on the logarithmic scale. It was found that the particles produce an interesting set of mass distances on the logarithmic number line: $2e$, e, $\frac{e}{2}$, $\frac{e}{4}$, $\frac{e}{8}$ and $\frac{e}{16}$. These mass gaps are listed in Table 3. There is, however, no standing wave analogy on the logarithmic scale that can be applied to all particles, consequently here, another model must be applied, which lead us to modify Müller's continued fraction term in an empirical way. However, the standing wave analogy is not completely absent. Müller [3] has shown that the majority of baryon and meson masses is in the range of 1300–8600 MeV/c^2. When scaling according to $\ln \frac{m_{particle}}{m_{electron}}$, this range translates to 8–8.5 on the logarithmic scale and it becomes clear that this range and as well as the masses of the electron, muon, pion and gauge bosons are in proximity of the zeros of the above considered sine function (see Figure 4).

Considering the framework of Müller's fractal scaling model, we interpret these numerical regularities as follows: Masses in nature are in relation to proton resonance states. Nature can realize various masses, only when they are close to proton resonance states, they are preferred masses. For stable particles such as nuclides, the term "preferred mass" translates to more abundance. For unstable particles, "preferred mass" translates to more realization probability. Un-

Particle	Rest mass m [MeV/c^2]	$\ln \frac{m(particle)}{m(proton)}$
Leptons:		
Electron	0.511	−7.515
μ	105.658	−2.183
τ	1776.84	0.638
Mesons:		
$\pi^{\pm}$	139.57	−1.905
π^0	134.9766	−1.939
$K^{\pm}$	493.677	−0.642
K^0_S, K^0_L	497.614	−0.634
η	547.853	−0.538
$\rho^{\pm}$	770	−0.198
ρ^0	775.5	−0.191
ω	782.6	−0.181
η^0	957.8	0.021
$K^{*\pm}$	891.7	−0.051
K^{*0}	896.0	−0.046
ϕ	1019.5	0.083
$D^{\pm}, D^0$	1869.6	0.689
$D^{\pm}_s$	1968.5	0.741
J/Ψ	3096.9	1.194
$B^{\pm}, B^0$	5279.2	1.727
Y	9460.3	2.311
Baryons:		
p	938.272	0
n	939.56	0.001
Λ^0	1115.6	0.173
Σ^+	1189.4	0.237
Σ^0	1192.5	0.240
Σ^-	1197.3	0.244
$\Delta^{\pm}, \Delta^{++}, \Delta^0$	1232	0.272
Ξ^0	1314.9	0.337
Ξ^-	1321.3	0.342
Ω	1672	0.578
Λ^+_C	2281	0.888
Λ^0_b	5624	1.791
Ξ_b	5774	1.817
Ξ^{-*}, Ξ^{0*}	15300	2.792

Table 2: Selected particles with rest masses and values on the logarithmic number line.

Particle mass step	Rest mass difference on logarithmic scale	Numerical result
Mass gap 2*e* (= 5.436):		
Electron → μ	$\lvert -7.515 - -2.183\rvert$	5.332
Mass gap *e* (= 2.718):		
$p \to \Xi^{-*}, \Xi^{0*}$	$\lvert 0 - 2.792\rvert$	2.792
Mass gap $\frac{e}{2}$ (= 1.359):		
$\pi^0 \to K^{\pm}$	$\lvert -1.939 - -0.642\rvert$	1.297
$\Xi^0 \to B^{\pm}, B^0$	$\lvert 0.337 - 1.727\rvert$	1.390
$\Lambda^+_C \to Y$	$\lvert 0.888 - 2.311\rvert$	1.423
Mass gap $\frac{e}{4}$ (= 0.68):		
$K^0_S, K^0_L \to p$	$\lvert -0.634 - 0\rvert$	0.634
$\Lambda^0 \to \Lambda^+_C$	$\lvert 0.173 - 0.888\rvert$	0.715
$p \to D^{\pm}, D^0$	$\lvert 0 - 0.689\rvert$	0.689
$p \to D^{\pm}_s$	$\lvert 0 - 0.741\rvert$	0.741
$p \to \tau$	$\lvert 0 - 0.638\rvert$	0.638
Mass gap $\frac{e}{8}$ (= 0.34):		
$\eta \to \rho^{\pm}$	$\lvert -0.538 - -0.198\rvert$	0.340
$p \to \Xi^0$	$\lvert 0 - 0.337\rvert$	0.337
$p \to \Xi^-$	$\lvert 0 - 0.342\rvert$	0.342
$\eta \to \rho^0$	$\lvert -0.538 - -0.191\rvert$	0.347
$\eta \to \rho^{\pm}$	$\lvert -0.538 - -0.198\rvert$	0.340
$\Sigma^+ \to \Omega$	$\lvert 0.237 - 0.578\rvert$	0.341
$\Sigma^0 \to \Omega$	$\lvert 0.240 - 0.578\rvert$	0.338
$\Sigma^- \to \Omega$	$\lvert 0.244 - 0.578\rvert$	0.334
$\Lambda^+_C \to J/\Psi$	$\lvert 0.888 - 1.194\rvert$	0.306
$\Omega \to \Lambda^+_C$	$\lvert 0.578 - 0.888\rvert$	0.310
Mass gap $\frac{e}{16}$ (= 0.17):		
$\omega \to p$	$\lvert -0.181 - 0\rvert$	0.181
$\rho^{\pm} \to p$	$\lvert -0.198 - 0\rvert$	0.198
$\rho^0 \to p$	$\lvert -0.191 - 0\rvert$	0.191
$p \to \Lambda^0$	$\lvert 0 - 0.173\rvert$	0.173
$\Lambda^0 \to \Xi^0$	$\lvert 0.173 - 0.337\rvert$	0.164
$\Lambda^0 \to \Xi^-$	$\lvert 0.173 - 0.342\rvert$	0.169
$\Omega \to D^{\pm}_s$	$\lvert 0.578 - 0.741\rvert$	0.163
$D^{\pm}_s \to \Lambda^+_C$	$\lvert 0.741 - 0.888\rvert$	0.147
$D^{\pm}, D^0 \to \Lambda^+_C$	$\lvert 0.689 - 0.888\rvert$	0.199

Table 3: Mass gaps between elementary particles on the logarithmic scale.

Particle	Particle mass with standard deviation. Continued fraction representation
N-baryons (S=0, I=1/2):	
p	938.27203 ±0.00008 [0; 0]
n	939.565346 ±0.000023 [0; 0 | 1973]
Λ-baryons (S=−1, I=0):	
Λ	1115.683 ±0.006 [0; 0 | 15, $e+1$, 15, −6]
$\Lambda(1520)$	1519.5 ±1.0 [0; 0 | 6, −9, $e+1$, $-e-1$, ***]
Σ-baryons (S=−1, I=1):	
Σ^+	1189.37 ±0.07 [0; 0 | 12, −6, $e+1$, $-e-1$, 6]
Σ^0	1192.642 ±0.024 [0; 0 | 12, $-e-1$, −9, $e+1$, $-e-1$, ***]
Σ^-	1197.449 ±0.03 [0; 0 | 12, $-e-1$, 6, $-e-1$, $e+1$, $-e-1$]
$\Sigma(1385)^+$	1382.8 ±0.4 [0; 0 | 6, $e+1$, $-e-1$, ***]
$\Sigma(1385)^0$	1383.7 ±1.0 [0; 0 | 6, $e+1$, $-e-1$, $e+1$, $-e-1$]
$\Sigma(1385)^-$	1387.2 ±0.5 [0; 0 | 6, $e+1$, $-e-1$, $e+1$, $e+1$]
Ξ-baryons (S=−2, I=1/2):	
Ξ^0	1314.86 ±0.2 [0; 0 | 9, $-e-1$, $e+1$, −6]
Ξ^-	1321.71 ±0.07 [0; 0 | 9, $-e-1$, $e+1$, ***]
$\Xi(1530)^0$	1531.8 ±0.32 [0; 0 | 6, −6]
$\Xi(1530)^-$	1535.0 ±0.6 [0; 0 | 6, −6, 9]
Ω-baryons (S=−3, I=0):	
Ω^-	1672.45 ±0.29 [0; 0 | $e+1$, $e+1$, $-e-1$, $e+1$, $-e-1$, $-e-1$] [1.5; 0 | $-e-1$, $e+1$, −15, 6]
charmed baryons (C = +1):	
Λ_C^+	2286.46 ±0.14 [1.5; 0 | $-e-1$, $-e-1$, 45, −15]
$\Lambda_C(2595)^+$	2595.4 ±0.6 [1.5; 0 | −6, 6, $e+1$, $-e-1$, ***]
$\Lambda_C(2625)^+$	2628.1 ±0.6 [1.5; 0 | −6, 12, 6]
$\Lambda_C(2880)^+$	2881.53 ±0.35 [1.5; 0 | −6, $-e-1$, $e+1$, ***]

Table 4: Continued fraction representation of particle masses according to equation (4).

Particle	Particle mass with standard deviation. Continued fraction representation
charmed baryons (C = +1):	
$\Sigma_C(2455)^{++}$	2454.02 ±0.18 [1.5; 0 | −6, $e+1$, $-e-1$, $e+1$, $e+1$, $-e-1$, $e+1$]
$\Sigma_C(2455)^+$	2452.9 ±0.4 [1.5; 0 | −6, $e+1$, $-e-1$, $e+1$, $e+1$]
$\Sigma_C(2455)^0$	2453.76 ±0.18 [1.5; 0 | −6, $e+1$, $-e-1$, $e+1$, $e+1$, $-e-1$]
Ξ_c^+	2467.8 ±0.6 [0; 0 | $e+1$, $-e-1$, $e+1$, 60] [1.5; 0 | −6, $e+1$, $-e-1$, −15]
Ξ_c^0	2470.88 ±0.8 [0; 0 | $e+1$, $-e-1$, $e+1$, −162] [1.5; 0 | −6, $e+1$, $-e-1$, −6]
$\Xi_c(2645)^+$	2645.9 ±0.6 [1.5; 0 | −6, 21, −6]
$\Xi_c(2645)^0$	2645.9 ±0.5 [1.5; 0 | −6, 21, −6]
$\Xi_c(2815)^+$	2816.6 ±0.9 [1.5; 0 | −6, $-e-1$, 12]
$\Xi_c(3080)^+$	3077.0 ±0.4 [1.5; 0 | −9, 9, 18]
light unflavored mesons (S = C = B = 0):	
$\pi^\pm$	139.57018 ±0.00035 [1.5; −3 | −6, $-e-1$, 18, $-e-1$, $e+1$, $-e-1$, $e+1$]
π^0	134.9766 ±0.0006 [1.5; −3 | −6, −15, $e+1$, $-e-1$, −33]
η	547.853 ±0.024 [0; 0 | −6, $e+1$, $-e-1$, 6, $-e-1$, 12] [1.5; −3 | $e+1$, $-e-1$, $e+1$, 9, $-e-1$, $-e-1$]
$\rho(770)$	775.49 ±0.34 [0; 0 | −15, $-e-1$]
$\omega(782)$	782.65 ±0.12 [0; 0 | −15]
$\rho'(958)$	957.78 ±0.06 [0; 0 | 132]
$\phi(1020)$	1019.455 ±0.02 [0; 0 | 33, −12, $e+1$]
$f_1(1285)$	1281.8 ±0.6 [0; 0 | 9, −9, −6]
$a_2(1320)$	1318.3 ±0.6 [0; 0 | 9, $-e-1$, $e+1$, $-e-1$, $e+1$, $-e-1$]
$f_1(1420)$	1426.4 ±0.9 [0; 0 | 6, 6, −6]
strange mesons (S =±1, C = B = 0):	
$K^\pm$	493.667 ±0.016 [0; 0 | $-e-1$, −6, $e+1$, 39]
K^0	497.614 ±0.024 [1.5; −3 | $e+1$, $-e-1$, $-e-1$, $e+1$, $-e-1$]

Particle	Particle mass with standard deviation. Continued fraction representation
strange mesons (S =±1, C = B = 0):	
$K^*(892)^{\pm}$	891.66 ±0.26 [0; 0 | −54, e+1]
$K^*(892)^0$	896.00 ±0.25 [0; 0 | −60, e+1]
charmed mesons (S =±1):	
$D^{\pm}$	1869.62 ±0.2 [0; 0 | e+1, 12, 24]
D^0	1864.84 ±0.17 [0; 0 | e+1, 12, −e−1, −e−1]
$D^*(2007)^0$	2006.97 ±0.19 [0; 0 | e+1, −18, −e−1, e+1, −e−1] [1.5; 0 | −e−1, 63]
$D^*(2010)^{\pm}$	2010.27 ±0.17 [0; 0 | e+1, −18, −216] [1.5; 0 | −e−1, 78]
charmed, strange mesons (C = S =±1):	
$D_s^{\pm}$	1968.49 ±0.34 [0; 0 | e+1, −54]
$D_s^{*\pm}$	2112.3 ±0.5 [1.5; 0 | −e−1, −12, 15]
$D_{S0}^*(2317)^{\pm}$	2317.8 ±0.6 [0; 0 | e+1, −e−1, −27] [1.5; 0 | −e−1, −e−1, 6, −e−1, −e−1]
$D_{S1}(2460)^{\pm}$	2459.6 ±0.6 [0; 0 | e+1, −e−1, e+1, 12] [1.5; 0 | −6, e+1, −e−1, 9]
$D_{S1}(2536)^{\pm}$	2535.35 ±0.34 [0; 0 | e+1, −e−1, e+1, −e−1, e+1, e+1] [1.5; 0 | −6, e+1, e+1, e+1]
$D_{S2}(2573)^{\pm}$	2572.6 ±0.9 [1.5; 0 | −6, 6, −15]
bottom mesons (B =±1):	
$B^{\pm}$	5279.17 ±0.29 [1.5; 0 | 12, −54]
B^0	5279.5 ±0.3 [1.5; 0 | 12, −51]
B^*	5325.1 ±0.5 [1.5; 0 | 12, −6, 6]
bottom, strange mesons (S = B =±1):	
B_S^0	5366.3 ±0.6 [1.5; 0 | 12, −e−1, 6, −e−1]
cc-mesons (S = B =±1):	
$J/\Psi(1S)$	3096.916 ±0.011 [1.5; 0 | −9, 24]
$X_{c0}(1P)$	3414.75 ±0.31 [1.5; 0 | 12, −e−1, e+1, ***]
$X_{c1}(1P)$	3510.66 ±0.07 [1.5; 0 | −15, −45]
$h_c(1P)$	3525.67 ±0.32 [1.5; 0 | −15, −6, −6]

Particle	Particle mass with standard deviation. Continued fraction representation
cc-mesons (S = B =±1):	
$X_{c2}(1P)$	3556.20 ±0.09 [1.5; 0 | −15, −e−1, e+1, ***]
$\Psi(2S)$	3686.09 ±0.04 [1.5; 0 | −21, 9, −e−1, e+1, ***]
$\Psi(3770)$	3772.92 ±0.35 [1.5; 0 | −24, −e−1, e+1, ***]
$X(3872)$	3872.3 ±0.8 [1.5; 0 | −33]
$Y(1S)$	9460.3 ±0.26 [0; 3 | −e−1, −12, −87]
$X_{b0}(1P)$	9859.44 ±0.42 [0; 3 | −e−1, −6, 9, −15] [1.5; 0 | e+1, −6, e+1, −6, e+1, −e−1]
$X_{b1}(1P)$	9892.78 ±0.26 [1.5; 0 | e+1, −6, e+1, −e−1, e+1, −9]
$X_{b2}(1P)$	9912.21 ±0.26 [0; 3 | −e−1, −6, e+1, 15, −e−1]
$Y(2S)$	10023.76 ±0.31 [0; 3 | −e−1, −e−1, −e−1, −e−1] [1.5; 0 | e+1, −e−1, −e−1, e+1, 12, −e−1]
$X_{b0}(2P)$	10232.5 ±0.4 [0; 3 | −e−1, −e−1, 327] [1.5; 0 | e+1, −e−1, −6, −e−1, e+1, −e−1]
$X_{b1}(2P)$	10255.46 ±0.22 [0; 3 | −e−1, −e−1, 30, 6]
$X_{b2}(2P)$	10268.65 ±0.22 [0; 3 | −e−1, −e−1, 21, −e−1] [1.5; 0 | e+1, −e−1, −9, 6, 6]
$Y(3S)$	10355.2 ±0.5 [0; 3 | −e−1, −e−1, 6, e+1, 6] [1.5; 0 | e+1, −e−1, −18, 9]
leptons:	
Electron	0.510998910 ±0.000000013 [1.5; −9 | −177]
μ	105.658367 ±0.000004 [0; −3 | e+1, −6, −e−1, e+1, ***]
τ	1776.84 ±0.17 [0; 0 | e+1, 6, −e−1, e+1, −e−1, −e−1]
gauge bosons:	
W	80398 ±25 [1.5; 3 | −54, −e−1, e+1]
Z	91187.6 ±2.1 [1.5; 3 | 36, −6, e+1]

fortunately, these simple graphs do not provide information to distinguish between stable and unstable particles. The repeatedly occurring mass gaps from $2e$ to $\frac{e}{16}$ strongly support the idea that masses in the micro-cosmos are not random and have a self-similar, fractal structure. However, we emphasize that this fractal behavior is only a statistical influence with low priority, since we know for instance that nature realizes with the chemical elements easily the whole logarithmic mass range from 0 to $2e$ without significant mass gaps. Also it should be noted that the logarithmic mass differences in Table 3 are always approximately multiples of the fractions of e. This means the fractal property provides only a signature of regularities, becoming visible only on the logarithmic number line.

Due to the fact that frequently mass distances occur which are close, but not exactly a fraction of e, we decided to modify Müller's continued fractions (given in equation(2)). Specifically we abandon the canonical form and change all partial numerators to Euler's number. Furthermore we follow results published by Müller in one of his patents [9] and introduce a phase shift p in equation (2). According to [9] the phase shift can only have the values 0 or ± 1.5. So we write

$$\ln \frac{particle\ mass}{proton\ mass} = p + S\ , \tag{3}$$

where S is the continued fraction

$$S = n_0 + \cfrac{e}{n_1 + \cfrac{e}{n_2 + \cfrac{e}{n_3 + \dots}}}\ . \tag{4}$$

We abbreviate $p + S$ as $[p; n_0 \mid n_1, n_2, n_3, \dots]$. Provided that our initial assumption is correct, and the particles are resonance states, their masses should be located in the maximum spectral density areas. Consequently we must require that the free link n_0 and the partial denominators n_i are integers divisible by 3. For convergence reason, we have to include $|e + 1|$ as allowed partial denominator. This means the free link n_0 is allowed to be $0, \pm 3, \pm 6, \pm 9 \dots$ and all partial denominators n_i can take the values $e + 1, -e - 1, \pm 6, \pm 9, \pm 12 \dots$ In order to test the model very critically for a more extended set of particles we followed Müller's article [3] and selected all elementary particles which have their masses determined with a standard deviation $\leqslant 1$ MeV/c^2 and included additionally the gauge bosons due to their special importance (78 particles altogether). For the calculation of the continued fractions we assumed first that the mass values were without any measurement error. This means, equation (3) does not hold and one ideally obtains a continued fraction with an infinite number of partial denominators. For practical reasons we determined only 18 partial denominators. Next we calculated repeatedly the particle mass from the continued fraction, every time considering one more partial denominator. As soon as the calculated mass value (on the linear scale) was in the interval "*mass* $\pm$ *standard deviation*", we stopped considering further denominators and gave the resulting fraction in Table 4. In special cases, where the particle mass is much more accurately determined than the proton mass (e.g. electron) the standard deviation was set to that of the proton.

It was found that the great majority of the particle masses could be expressed by a continued fraction, which means that they are localized in nodes or sub-nodes. Only 10 particles were found to be localized in a gap. In such a case the continued fraction turns into an alternating sequence of $-e-1$ and $e+1$ without any further significant approximation to the mass value. In Table 4, this sequence was then abbreviated by three stars. It should be noted that the particle mass calculated from such a fraction is still close to the experimental value, but has a difference from the experimental value higher than the standard deviation. For around 50% of the particles, it was required to set the phase shift to 1.5 in order to get the masses located in a node or sub-node. For 14 particles, their masses can even be located in sub-nodes for both phase shifts (0 and 1.5). If so, both continued fractions were indicated in Table 4. As can be seen, the continued fractions have seldom more than 5 partial denominators, they can be even shortened abandoning the standard deviation requirement and accepting a small percentage error on the logarithmic scale as it was done in Müller's article [2].

There are, however some general questions open. It is clear that the continued fraction analysis provides a new system to put the particles in groups regarding the length of the fraction (fractal layers), the phase shift, value of the free link and the value of the numerator. Which of these parameters have physical meaning and which ones are just mathematics?

Especially regarding the physical significance of the nominator, more research must be done. We believe that is not coincidence that most of the masses become localized in nodes or sub-nodes when calculating the fractal spectrum with nominator e, similar calculations have shown that the numerators 2 or the golden ratio do not work in this manner. This however, was here found empirically, to the best of our knowledge there is no way to calculate directly which nominator reproduces best the fractal distribution. It must still be done by trial and error combined with intuition. Anyway, we suggest to abandon the canonical form of the continued fractions whenever possible, since with numerator 1, actually some physical information of the fractal distribution is lost. It is known that continued fractions with arbitrary numerator $\neq 1$ can be transformed into fractions with numerator equal to 1, via Euler equivalent transformation.

From the presented numerical results, some ideas can be derived:

1. The three most stable here considered particles are the electron, proton and neutron with half-life of around 11 minutes. Their continued fraction representations are quite short, consisting only of the free link and one

partial denominator. Possibly short continued fractions indicate stability. Furthermore the very high values of the first partial denominators n_1 indicate two facts: a proximity to the node n_0 and an irrelevance of any further partial denominator which can change the value of the fraction only insignificantly. This means a high value of n_1 might also be considered as a criterion for stability.

2. According to reference [1], in a node, there is a change from spectral compression to spectral decompression, which means that with a certain probability a change in process trend can be observed. This statement is in agreement with the continued fraction representations of the electron and the neutron. The electron [1.5; −9 | −177] lies with a negative first partial denominator closely before the principal node [1.5; −9], whereas the neutron [0; 0 | 1973] is positioned right after the principal node [0; 0] due to its positive denominator. This means the electron in the compression range is stable whereas the neutron is in a decompression range and already exhibits decay property.

4 Resume

Numerical investigation of particle masses revealed that 87% of the considered elementary particles can be interpreted as proton resonance states. We cannot expect that all particle masses are only governed by proton resonance properties, other natural laws apply as well. The here presented mathematical model can be modified in various ways and future research should concentrate on identifying fractal properties in other data sets such as half-lifes of radioactive nuclides or mass defects, utilizing either our or similarly modified continued fractions. Only when multiple fractal data sets are known, the possible numerical values of the numerator or the phase shift can be adequately interpreted and maybe attributed to a physical property.

Acknowledgements

The authors greatly acknowledge the financial support from the Brazilian governmental funding agencies FAPESQ and CNPq.

Submitted on July 21, 2010 / Accepted on August 11, 2010

References

1. Müller H. Fractal scaling Models of resonant oscillations in chain systems of harmonic oscillators. *Progress in Physics*, 2009, v. 2, 72–76.
2. Müller H. Fractal scaling models of natural oscillations in chain systems and the mass distribution of the celestial bodies in the solar system. *Progress in Physics*, 2010, v. 1, 62–66.
3. Müller H. Fractal scaling models of natural oscillations in chain systems and the mass distribution of particles. *Progress in Physics*, 2010, v. 3, 61–66.
4. Anders E., Grevesse N. Abundances of the elements — meteoritic and solar. *Geochimica et Cosmochimica Acta*, 1989, v. 53, 197–214.
5. Audi G., Wapstra A. H., Thibault C. The AME2003 atomic mass evaluation (II). Tables, graphs and references. *Nuclear Physics A*, 2003, v. 729, 337–676.
6. Lide D. R. (Editor) CRC Handbook of Chemistry and Physics. CRC Press, Boca Raton, 2005.
7. Press W. H., Teukolsky S. A., Vetterling W. T., Flannery B. P. Numerical recipes in C. Cambridge University Press, Cambridge, 1992.
8. Bethe H. A. Energy production in stars. *Physical Review*, 1939, v. 55, 434–456.
9. Otte R., Müller H. German patent No. DE102004003753A1, date: 11.08.2005.

Charge of the Electron, and the Constants of Radiation According to J. A. Wheeler's Geometrodynamic Model

Anatoly V. Belyakov
E-mail: belyakov.lih@gmail.com

This study suggests a mechanical interpretation of Wheller's model of the charge. According to the suggested interpretation, the oppositely charged particles are connected through the vortical lines of the current thus create a close contour "input-output" whose parameters determine the properties of the charge and spin. Depending on the energetic state of the system, the contour can be structurized into the units of the second and thirs order (photons). It is found that, in the framework of this interpretation, the charge is equivalent to the momentum. The numerical value of the unit charge has also been calculated proceeding from this basis. A system of the relations, connecting the charge to the constants of radiation (the Boltzmann, Wien, and Stefan-Boltzmann constants, and the fine structure constant) has been obtained: this give a possibility for calculating all these constants through the unit charge.

William Thomson (Baron Kelvin), the prominent physicist of the 19th century, said: "we can mean a phenomenon to be clearly understood only if a mechanical model of it has been constructed". It would be fine if the famous phrase would be actual in the nowadays as well. This however meets some difficulties, in particular — in the case of the electron, despite its spin has the dimension of mechanical angular momentum, and the charge is not (at least) a special "entity" or "electric substance".

In order to explain the properties of the electric charge, John A. Wheeler suggested his own concept of geometrodynamics. According to the concept, the charged microparticles are special points in the three-dimensional spatial surface of our world, connected to each other through "wormholes" — vortical tubes analogous to the lines of current working according to the "input-output" ("source-drain") principle, but in an additional dimension of space.

Is the fourth dimension still necessary in this case?

Suppose that the world, being an entity in the limits of the three-dimensional continuum, is a really *surface* which is *topologically non-unitary coherent* and *fractalized* upto the parameters of the micro-world bearing a fraction dimension of the numerical value upto three. In this case, it is easy to see that the Wheeler vortical tube is located "under the surface" of our world, thus is "invisible" to us, the fragments of the fractalized surface.

Meanwhile numerous specific properties of the microworld do not manifest themselves into it, or are manifested being *distorted*, as if they were projected into our world from an "additional" dimension. In particular, this should be true in the charge and spin of the electron, which can be considered according to the mechanistic scheme as the respective momentum of the vortical tube and the angular momentum with respect to its longitudinal axis. So forth we will consider, for brevity, the close contour crossing the surface X of the our world in the points, say, p^+ and e^-. In the framework of this scheme, a free charged particle is presented as a section of the open contour, or as a single-pole curl directed along the "additional" direction; the electron can be presented as an object activating the motion of the medium (electric current).

Let S be the sinus of an angle determining the projection of the momentum onto the surface X, and also the projection of the circulation velocity v (this is also, in the same time, the velocity of the rotation around the longitudinal axis of the contour) onto the chosen direction, say the axis $p^+ - e^-$. In this case, S^i characterizes the ratio of the projection of the velocity to the velocity itself ($i = 1, 2, 3$ depending on the orientation of the velocity vector).

Let, according to our initially suggestion, the charge be equivalent to the momentum, thus be Coulomb = kg×m/sec. Replace the elementary charge with the ultimate momentum of the electron, $m_e c$, in the formulae of Coulomb and Ampere. With taking this into account, in order to arrive at the numerical coincidence with the electric and magnetic forces (determined by the classical formulae), it is sufficient to introduce new formulae for the electric and magnetic contants, ε_0 and μ_0, as follows

$$\varepsilon_0 = \frac{m_e}{r_e} = 3.233{\times}10^{-16}\ \left[\mathrm{kg/m}\right], \tag{1}$$

$$\mu_0 = \frac{1}{c^2\,\varepsilon_0} = 0.0344\ \left[\mathrm{N}^{-1}\right], \tag{2}$$

where m_e is the mass of the electron, while c is the velocity of light. The quantity r_e means the classical radius of the electron, which is, in SI units,

$$r_e = \frac{10^{-7}\,e_0^2}{m_e}, \tag{3}$$

where e_0 is the charge of the electron.

Thus, these constants get a clear physical meaning now. They characterize the vortical tube, because ε_0 has a dimen-

sion of its density per meter, while μ_0 is the quantity reciprocal to the centrifugal force which appears when the element of the vortical tube, whose mass is m_e, rotates with the radius r_e with the linear velocity c.

The contour's length can vary, depending on the energetic state of the system. Assume that its increase, according to the well-known analogy to hydrodynamics, results the decrease of the tube's radius upto an arbitrary numerical value r, and also the creation of the secondary and tertiary spiral structures, which fill the toroidal volume (the section of the torus is the same as the classical radius of the electron r_e).

Thus, the charge of a particle can be characterized by the projection of the longitudinal component of the momentum Mv onto the surface X, where the mass of the vortical tube (contour) is proportional to the tube's length, and is

$$M = \varepsilon_0 R = \varepsilon n^2 R_b \,, \tag{4}$$

where n is the leading quantum number, $R_b = \alpha^2 r_e$ is the Bohr 1st radius, while α is the reciprocal fine structure constant which is 137.036 (it will be shown below that α is also determined according to the suggested model).

Among the possible contours characterized by different masses and velocities, there is such a contour in which the energy of the unit charge (electron) reaches the maximal numerical value. We take into account that a potential, in the framework of the mechanistic "coulombless" system, corresponds to a velocity. Thus, in the case of this contour, we can write down

$$e\,v = m_e c^2 = E_{max} \,, \tag{5}$$

where e is the common charge, which is identical to the momentum (in contrast to its projection, the observed charge e_0). In this contour, we determine the standard unit of the potential (velocity) as follows

$$\mathrm{v} = \frac{m_e v^2}{e} = 1 \ \text{[m/sec]} \,. \tag{6}$$

Thus we obtain, from (5) and (6),

$$v = c_p^{2/3}\,\mathrm{v} \,, \tag{7}$$

where the dimensionless velocity of light $c_p = \frac{c}{\mathrm{v}}$ has been introduced, and also

$$e = M v = m_e c_p^{2/3} c_p^{2/3}\,\mathrm{v} \,. \tag{8}$$

In other word, we see that the mass M of the contour is the same as $m_e c_p^{2/3} = 4.48{\times}10^5\, m_e$ that is close to the *summary mass of the bosons* W^+, W^-, Z^0.

We will refer to the contour as the *standard contour*. In it, the maximal energy of the "point-like" electron, $m_e c^2$, is the same as that of the current tube, $M v^2$. The numerical values of the charge and spin remain unchanged for any contour, and have a common component — the contour's momentum Mv. It should be noted that, despite the dimension of electric charge corresponds to the dimension of momentum, it is not common to both entities, thus cannot be divided by the dimensions of mass and velocity.

The projection of the momentum, which is the *observed charge*, is

$$e_0 = m_e c_p^{4/3} S^i \mathrm{v} \,, \tag{9}$$

where, as is obvious, $i = 1$, while the complete momentum of the vortical tube (the Planck constant h) reduced to the radius of the electron can be determined as the vector recovered, on the basis of the projection, in the general way where $i = 3$. Thus

$$\frac{h}{r_e} = 2\pi\alpha\, m_e c = \frac{e_0}{S^3} \,. \tag{10}$$

Taking e_0 from (9), we obtain, through (10),

$$S = \frac{c_p^{1/6}}{\sqrt{2\pi\alpha}} = 0.881, \tag{11}$$

thus the *projective angle* is 61.82°, while the obtained numerical value of the observed charge $e_0 = 1.61{\times}10^{-19}$ kg/m×sec differs from the exact value (standard numerical value obtained in the experiments) for doles of the percent.

The charge of the "point-like" electron in the region X, we will denote as e_x, is substituted into the formulae of Coulomb and Ampere: under ε_0 and μ_0 assumed in the model, it consist a very small part of e_0, which is

$$e_x = m_e c = \frac{e_0}{c_p^{1/3} S} = \frac{e_0}{590} \,. \tag{12}$$

The *main standard quantum number* can be expressed through the mass M of the contour and its density per one meter (the electric constant ε_0)

$$n_s = \sqrt{\frac{m_e c_p^{2/3}}{\varepsilon_0 R_b}} = \frac{c_p^{1/3}}{\alpha} = 4.884; \tag{13}$$

the contour's size is $R_s = n_s^2 R_b = 1.26{\times}10^{-9}$ m.

The *number of the ordered structural units* z of the contour (we will refer to them as *photons*, for brevity) is determined, for an arbitrary quantum number, by the ratio between the full length of the contour and the length of the wave λ

$$z = \frac{n^2 R_b \left(\frac{r_e}{r}\right)}{\lambda} \,, \tag{14}$$

where

$$\lambda = \frac{W}{R_\infty} \,, \tag{15}$$

Rydberg's constant is expressed as

$$R_\infty = \frac{1}{4\pi\alpha^3 r_e} \,, \tag{16}$$

while Balmer's formula is

$$W = \frac{m^2 n^2}{m^2 - n^2}\,, \tag{17}$$

where $n, m = 1, 2, \ldots$ Here the ratio of the radii $\frac{r_e}{r}$ takes into account the increase of the length of the "stretched" contour in the case where the spiral structures of the second and third orders are created. Because $\varepsilon_0 = const$ and $\mu_0 = const$, in the case of arbitrary r and v the formulae (1) and (2) lead to

$$\frac{r_e}{r} = \left(\frac{c}{v}\right)^2. \tag{18}$$

We obtain the *velocity v* and *radius r of the vortical tube of the contour*, in the general case, from the condition of constancy of the momentum which is true for any contour having an arbitrary quantum number n. We obtain

$$M v = m_e c_p^{4/3} \mathrm{v} = n^2 R_b \varepsilon_0 v\,, \tag{19}$$

wherefrom, substituting the extended formulae of R_b and ε_0, and taking (18) into account, we obtain

$$v = \frac{c_p^{1/3} c}{(\alpha n)^2}\,, \tag{20}$$

$$r = \frac{c_p^{2/3} r_e}{(\alpha n)^4}\,. \tag{21}$$

As a result, with (15) and (16) taken into account, and having the velocity v replaced with its projection $v S^i$, we obtain the number of the photons in the arbitrary contour

$$z = \frac{n^6 \alpha^3}{4\pi W c_p^{2/3} S^{2i}}\,. \tag{22}$$

In particular, consider the standard contour (denote it by the index s). In the unitary transfer in it from n_s to $n_s + 1$, we obtain: $W_s = 76.7$, $\lambda_s = 7.0{\times}10^{-6}$ m, $v_s = 4.48{\times}10^5$ m/sec, $r_s = 6.3{\times}10^{-21}$ m, while the number of the photos z_s being calculated under $i = 2$ is close to $\alpha = 137$.

Thus, given a "standard" photon, the following relation

$$\frac{R_s}{r_e} = \frac{r_e}{r_s} = c_p^{2/3} = 448000 \tag{23}$$

is reproduced (that is specific to an atom).

The *Boltzmann, Wien, and Stefan-Boltzmann constants*, k, b, and σ, can be determined connecting the energy of the section of the contour in the region X taken per one photon, E_z, i.e. the energy of the structural unit, with the energy of the heat motion E_t (the average energy of the radiating oscillator) in the case of a specific particular conditions.

We express E_z and E_t as follows

$$E_z = \frac{e_x v S}{z}\,, \tag{24}$$

$$E_t = k\,T\,. \tag{25}$$

The numerical value of E_z decreases with the increase of the quantum number so that, with a numerical value of n, it becomes equal E_t taken with the wavelength λ of the photon emitted by a black body whose temperature is that of the scale unit

$$E_z = E_t \quad \text{under} \quad T = 1^\circ\ [\mathrm{K}]\,. \tag{26}$$

With decreasing n, the numerical value of E_z increases faster than E_t. Assume that, with taking (23) into account, the following ratio

$$(E_z)_s = z E_t \quad \text{under} \quad T = T_s \tag{27}$$

is true for the standard contour.

Using (12), (20), and (22), we modify (24) then re-write (26) and (27) for n and n_s assuming that the most large contour has been contracted into a tertiary structure

$$\frac{A W}{n^8} = k\,T\,, \qquad i = 3, \quad T = 1^\circ\ [\mathrm{K}]\,, \tag{28}$$

$$\frac{A_s W_s}{n_s^8} = k\,T_s\,z\,, \qquad i = 2. \tag{29}$$

where $A = 4\pi S^{2i} n_s^5 e_0 \mathrm{v}$. Taking into account that $\frac{A}{A_s} = S^2$ and also

$$1^\circ\ [\mathrm{K}] = \frac{b R_\infty}{W}\,, \tag{30}$$

$$T_s = \frac{b R_\infty}{W_s} \tag{31}$$

where Wien's constant is

$$b = T\lambda\,, \tag{32}$$

we obtain, from the common solution of (28) and (29),

$$\frac{n^4}{W} = \frac{S\,z^{1/2} n_s^4}{W_s}\,. \tag{33}$$

Assume $z = z_s = 137$. Taking (17) into account, we calculate, for the transfer from n to $n+1$: $n = 39.7$, $W = 32470$, $\lambda = 0.0030$ m, *Wien's constant* $b = 0.0030$ m×K. From (28), we obtain *Boltzmann's constant* $k = 1.38{\times}10^{-23}$ J/K. According (22), we obtain the *number of the photons* of the contour: $z = 117840$ under $i = 3$.

The number of the photons z of the given contour is very close to the numerical value of $2\pi\alpha^2$. This result does not follow from the initially assumptions, thus is absolutely independent. So, the presence of the secondary and tertiary structures has been confirmed. That is, there are three specific contours: the contour of the 1st order (the Bohr 1st radius, $n = 1$; the contour of the 2nd order (the standard contour, $n = 4.884$, containing α structural units, the photons); and the contour of the 3rd order ($n \approx 40$, containing $2\pi\alpha^2$ photons).

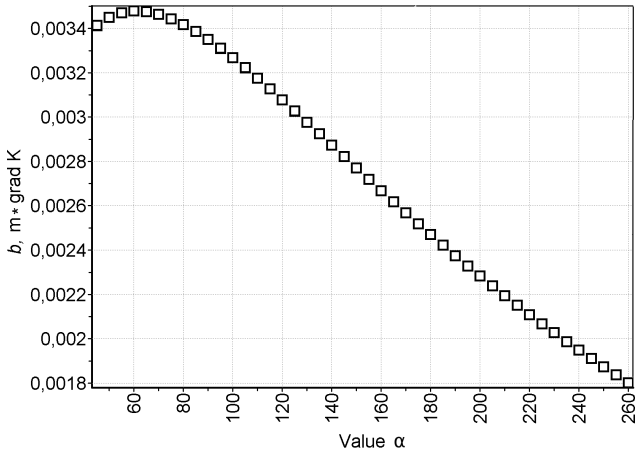

Fig. 1: Dependency of Wien's constant b on the reciprocal value of the fine structure constant α.

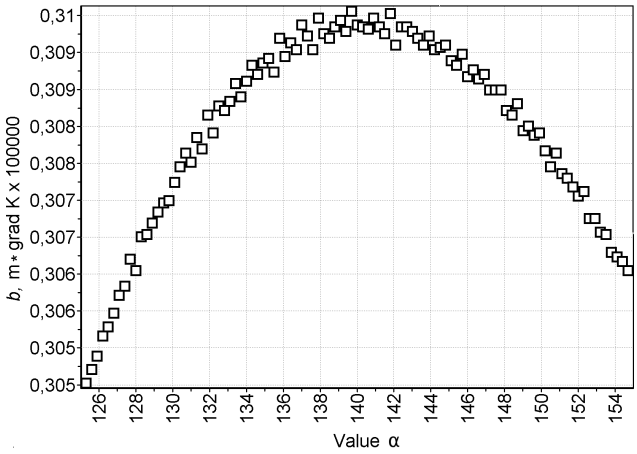

Fig. 2: Results of the numerical differentiation of the function $b(\alpha)$ in the region of the second singular point (inflection of the $b(\alpha)$ arc). The ordinate axis means the speed of the change of the parameter b.

Boltzmann's constant can be expressed also through the parameters of the standard contour

$$k = \frac{n_s e_0 \mathrm{v}}{\alpha T_s} = 1.38{\times}10^{-23} \text{ [J/K]} , \qquad (34)$$

where $T_s = \frac{b}{\lambda_s} = 414.7^\circ$ K.

Formula (34) can be transformed so that

$$\frac{kT}{n_s} = m_e \left(c_p^{2/3} \mathrm{v}\right)^2 \frac{S}{\alpha} , \qquad (35)$$

i.e. *given the standard contour, the energy of the radiating oscillator per the contour's quantum number is equal to the energy of the internal rotation of the "point-like" electron taken per the number of the structural units of the contour.*

It is interesting to compare the Planck entropy of the photon, S_h, to the entropy of the part of the contour related to the single photon, S_z, within the region X. The Planck entropy remains constant

$$S_h = \frac{E_h}{T} = \frac{hc}{\lambda T} = \frac{hc}{b} = 6.855{\times}10^{-23} \text{ [J/K]} , \qquad (36)$$

while S_z decreases rapidly with the increase of the leading quantum number

$$S_z = \frac{E_z}{T} = \frac{AW}{n^8 T} = \frac{AW^2}{n^8 b R_\infty} . \qquad (37)$$

Equalizing S_h to S_z, and expanding the formulae for h, R_∞, and A for the case of the ionization of the atom (that means the transfer from n to $m \to \infty$ under $W \to \infty$), we obtain, under $i = 1 \ldots 3$,

$$n_\infty = \sqrt[4]{8\pi n_s^3 S^{2i+1}} = 6.7 \ldots 5.9 . \qquad (38)$$

Because the common direction of the physical processes to the increase of entropy, thermodynamics prefers, with $n > 6.7$, that the structural units of the contour exist separately from each other, i.e. are the photons. It is probably, this result verifies the identity of the contour's structural units to the photons, and also manifests one of the causes of that the stable atoms have no more electronic shells than 6 or 7.

The *Stefan-Boltzmann constant* can be expressed as the projection of the unit energy of the heat motion per one photon and the unit square of the standard contour, i.e. as $k\Delta T S/(\alpha n_s^4 R_b^2)$, where $\Delta T = 1^\circ$K, and reduced to the unit of time and the unit of temperature (in the respective exponent). As a result, we obtain $\sigma = 5.56{\times}10^{-8}$ [W/m^{2}K^4].

The obtained formulae (34), (35), and (39) are actually definitions. They completely confirm the existence of the special standard contour.

Despite the fine structure constant was used in the calculation (the constant itself is meant to be derived from e_0 and h), the calculation was processed in independent way. Besides, assuming that α and all other quantities dependent on it (r_e, S, e_0, n_s, z, k, b) are variables, we can determine the numerical value of α according to the location of the second singular point (inflection of the $b(\alpha)$ arc in Fig. 1), where the change of b is proportional to the quantum number. Numerical differentiation, Fig. 2, manifest the numerical value of α within the boundaries 137–140 and, hence, it manifests the numerical values of all other parameters (for instance, k and z in Fig. 3 and Fig. 4 respectively). That is, finally, in order to calculate all the parameters we only need: the *mass of the electron*, the *velocity of light*, the *units of velocity and temperature*, and the *assumption that E_z is proportional to E_t in the standard contour*.

It is interesting that more precise numerical value of α arrives under the condition that m and n approach to infinity in the function $b(\alpha)$ and Balmer's formula (17). Thus Balmer's formula becomes $W = \frac{n^3}{2}$ under infinite large distance between the charges, that meets the determination of the textbook nu-

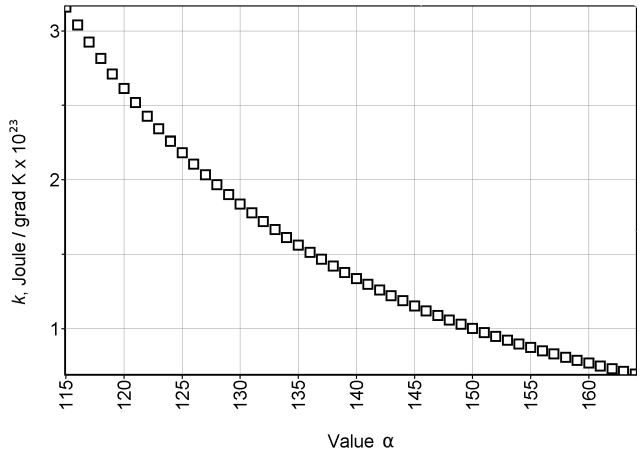

Fig. 3: Dependency of Boltzmann's constant k on the reciprocal value of the fine structure constant α.

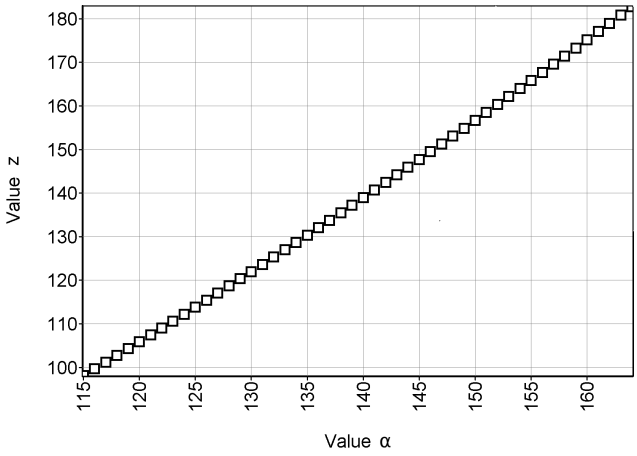

Fig. 4: Dependency of the number of the photons z of the standard contour on the reciprocal value of the fine structure constant α.

merical value of α. In the same time, we can obtain the exact numerical value of the charge from formula (1), by substituting α determined from the function $b(\alpha)$, Fig. 2.

Note that the validity of the suggested model is confirmed by that significant fact that the quantity kT, which is the unit of the work done by the structural unit of an ideal gas (this quantity is also interpreted, in the theory of heat radiation, as the energy of an elementary oscillator), is connected here with the charge of the electron. A connexion between Planck's constant and the quantity kT was found, as is known, in already a century ago by Max Planck, through the formula of the blackbody radiation. This formula is proportional to

$$\frac{1}{\lambda}\,\frac{1}{\lambda}\,\frac{1}{\lambda\,(e^{C/\lambda}-1)}\,,$$

where C is a constant. Taking all that has been obtained in our study, we understand follows. The first term here manifests the decrease of the intensity of the radiation with the increase of the wavelength of the photon. The second term manifests the decrease of the number of the photons per the unit of the full length of the contour. The third term manifests the change of the length of the contour itself, which reaches a contant with the increase of λ thus the Planck formula transforms into the Rayleigh-Jeans formula. With small numerical values of λ, the contour compresses upto the size of the photon. This gives an explanation to the decrease of the radiation power on high frequencies.

In the end, it should be noted that the properties of the charge are, of course, not limited by Wheeler's model in its mechanistic interpretation suggested here. Meanwhile, the unexpected relation between the charge of the electron and the molecular kinetic properties of the atoms and molecules manifests additional connexions between the elementary particles and macro-particles, thus this fact needs to be more studied in the future.

Submitted on July 24, 2010 / Accepted on August 17, 2010

LETTERS TO PROGRESS IN PHYSICS

Scientific Community of Valentin N. Samoilov

(On the Occasion of His 65th Birthday Anniversary)

Dmitri Rabounski
E-mail: rabounski@ptep-online.com

In this letter we celebrate the 65th birthday anniversary of Prof. Valentin N. Samoilov, a man of the Soviet scientific ancestry in the nuclear and space research, who is a pupil and follower of the famous Soviet engineer Sergey P. Korolev and the prominent Soviet nuclear physicist Michael G. Mescheryakov.

Prof. Valentin N. Samoilov. The back wall of his cabinet is curtained with photo portrait of Michael G. Mescheryakov.

On behalf of the Editorial Board of *Progress in Physics*, in April 25, 2010, I am pleased to celebrate the 65th birthday anniversary of Professor Valentin Nikolaevich Samoilov, ScD, Director of Scientific Centre of Applied Research, Joint Institute for Nuclear Research (JINR), Dubna, Russia. His more than 45 years of the successful work on science rose from that fact that he started his scientific activity being of a pupil of two famous persons of the Soviet scientific ancestry: Sergey P. Korolev, the engineer and rocket designer who headed the pioneering cosmic flights in the USSR, and Prof. Michail G. Mescheryakov, the nuclear physicist an close co-labour of Igor V. Kurchatov in the construction and launch of the first cyclotronic accelerator of particles in Leningrad, 1938–1940. According to the testament of his teachers, Prof. Samolilov spends his life in scentific research. He is still full of energy and creative scentific ideas until the present day.

In the row of Prof. Samoilov's scientific achievements, which are many, I would like to emphasize four fundamental discoveries in physics of solids and particles he did in common with Dr. Vahan N. Minasyan (reportas about these were published recently in *Progress in Physics* [4–7]). In these papers, they presented a new and very original approach to investigation of the excitation processes of electromagnetic surface shape resonances in lamellar metallic gratings by light, from the visible to near-infrared scale, based on the surface plasmon–polaritons, where they first argued that the smooth metal-air interface should be regarded as a distinct dielectric medium, the skin of the metal. They predicted the existence of light quasi-particles bearing spin equal to 1, and a finite effective mass $m = 2.5{\times}10^{-5}\, m_e$ (where m_e is the mass of the electron); these light quasi-particles should excite two type surface polaritons in the nanoholes in metal films. They also found, theoretically, that a transverse electromagnetic field should exist being formed by supersonic longitudinal and transverse waves in solids which acquire the frequency and the speed of sound. According to their theory, the transverse electromagnetic field should propagate along the direction the forming supersonic wave travels. In this context, another very interesting result obained in the paper [6] should also be noted: there they first proved that the property of the lambda-point of superliquid helium is determined by registering the single neutron modes or neutron pair modes in the neutron-spectrometer.

In addition to his scientific research, Prof. Valentin N. Samoilov is known as a successful organizer of science, and also as a designer of the space flight complexes and their segregate components. He was granted by the honorary title Merit Creator of Cosmical Techniques (2006) and by the international order Tsciolkovski Star (2002). He also was conferred with the order Beneficence, Honor and Glory (2006), Tsiolkovski Medal (2004), and Korolev Medal (2005). Due to his activity in astro-biology research, in 2005 he was elected to the International Academy of Information, Communica-

tion, Control, in Engineering, Nature, and Society (Pasadena, California, USA). Aside for these, during the last 15 years Prof. Samoilov governs numerous common scientific projects on the nuclear safety between JINR and DOE, which include close communications with the US National Laboratories such as BNL, SNL and PNNL. Also, during the last 20 years he governs communications between JINR and European Scientific Nuclear Research Centre in Geneva (CERN), in the framework of the scientific projects LHC, CMS, ATLAS, COMPASS, and CLIC. By governing of him, a joint scientific community is working amongst JINR, Institute of Particle and Nuclear Studies, and High Energy Accelerator Research Organization (Japan). Due to his international activity, connecting research scientists throughout the world, Prof. Samoilov was conferred with Order of People Friendship which was decorated upon him in 2006 by Vladimir V. Putin, President of Russia.

Prof. Valentin N. Samoilov authored two scientific monographs, *Technology Modeling of the Complicated Processes* [1] and *Theoretical Informational Analysis of the Complicated Systems* [2], and co-authored seven other scientific books. During his long term and successful scientific carrier, he also authored about 300 scientific publications, 20 registered inventions certified by patents, and 30 software application [3]. For several of these achievements, he was confered wth A. S. Popov Silver Medal (2006).

The decades of distinguished leadership and mutual cooperation in the field of nuclear material protection control and accountability between Russia and the USA are greatly recognized as his contribution to the global security. In the present time, Prof. Valentin N. Samoilov is still engaged for the nuclear and cosmic safety as an experienced veteran of the atomic industry.

I would like to wish Prof. Samoilov for long life and success in the future.

Submitted on April 29, 2010 / Accepted on April 30, 2010

References

1. Samoilov V.N. Technology modeling of the complicated processes. *Joint Institute for Nuclear Research*, Dubna, Russia, 2000.
2. Samoilov V.N. Theoretical informational analysis of the complicated systems. *Joint Institute for Nuclear Research*, 2000, Dubna, Russia.
3. Interacademic Information Bulletin, Saint Petersburg, *International Academia*, 2006, v. 22 anniversary, 316–325.
4. Minasyan V.N. and Samoilov V.N. Two type surface polaritons excited into nanoholes in metal films. *Progress in Physics*, 2010, v. 2, 3.
5. Minasyan V.N. and Samoilov V.N. The intensity of the light diffraction by supersonic longitudinal waves in solid. *Progress in Physics*, 2010, v. 2, 63.
6. Minasyan V.N. and Samoilov V.N. Formation of singlet fermion pairs in the dilute gas of boson-fermion mixture. *Progress in Physics*, 2010, v. 4, 3.
7. Minasyan V.N. and Samoilov V.N. Dispersion of own frequency of ion-dipole by supersonic transverse wave in solid. *Progress in Physics*, 2010, v. 4, 10.

LETTERS TO PROGRESS IN PHYSICS

Nikias Stavroulakis (1921–2009). In Memoriam

Ioannis M. Roussos

Dept. of Mathematics, Hamline University, 1536 Hewitt Avenue, Saint Paul, Minnesota 55104-1284, USA
E-mail: iroussos@gw.hamline.edu

This paper was written by Dr. Ioannis M. Roussos, Professor of Mathematics, Hamline University at Saint Paul, Minnesota, in honor and memoriam of the late Dr. Nikias Stavroulakis, Professor of Mathematical Physics. The included information is particularly based on the publications of the late professor, and was particularly collected through the various types of communication (personal visits with lengthy and extensive discussions, professional meetings, letters, telephone-calls, words of relatives and friends, etc.) Dr. Roussos had with and about him in the last 14 years. Dr. Roussos first met Dr. Stavroulakis in the 3rd Panhellenic Congress of Geometry, University of Athens, Greece, May 1996, and they became friends ever since.

Prof. Nikias Stavroulakis, Limoges, France, 1980.

Nikias Stavroulakis was born at the village Thronos Rethymnes of the Island of Crete, Greece, on October 2, 1921. In 1938 he finished high school (Lyceum) and then entered the National Technical University (E. M. Polytechnion), Athens, Greece, where he studied Civil Engineering.

Although World War II interrupted the smooth course of his studies, destroyed his country, and he escaped execution by the Nazis on account of their defeat and hasty retreat for a time-span of just a few days, he managed to continue his studies after the war was over, in 1945. He graduated from the National Technical University (E. M. Polytechnion), Athens, Greece, in 1947.

During the years 1949–1963 he worked as a civil engineer in Greece. His work, as civil engineer, was done under extremely trying and bad conditions, civil war, imprisonment, great difficulties and political turmoil, struggle and pressure.

The year 1963, he was released from a Greek prison in which he was kept because of ideological believes and political reasons, and went to Paris, France, to pursue graduate studies in mathematics. He eventually received Doctorat d'Etat from Faculté des Sciences of Paris in 1969. His advisor was the famous professor Charles Ehresmann. His dissertation was entitled *Substructure of Differentiable Manifolds and Riemannian Spaces with Singularities*.

Then, he was immediately hired as a professor of mathematics by the University of Limoges, France, from which he retired the year 1990. On his retirement he returned to Athens, Greece, where he mainly stayed and continued his research until the end of his life.

He is the author of numerous papers related to the subjects of: Geometry, algebraic topology, differential geometry, optimization problems, mathematical physics and general relativity. His scientific work and contributions were recognized internationally from the beginning.

Although he had retired for several years, he continued his scientific and mathematical research up to the end of his life in December 2009 at the ages of 88. His main purpose was to restore the theory of gravitational field by pointing out the misunderstandings and correcting the mathematical errors committed by relativists since the inception of general relativity and thus rejecting them right from the beginning of his carrier.

Unfortunately he died on the 20th of December 2009, due a chronic aneurism in the abdominal area. At that time he was working on several papers, but his untimely death left them unfinished. As he had told me, among other things, he was planning to write a few things about the use of the polar coordinates beyond those he had already exposed in his already published papers, write some expository papers and above all to finish especially the important paper *On the Filed of a Spherical Charged Pulsating Distribution of Matter*, which will appear (as he left it unfinished), as his sixth publication in the journal *Progress in Physics*. He will be greatly missed from his friends and scientific collaborators.

Nikias Stavroulakis at the age of 4 years, outside his house at the village Thronos, Crete, Greece, 1925.

Nikias Stavroulakis (center, 6th from the left in the middle row), with his classmates and teachers of the last grade of Lyceum of Rethymno, Crete, Greece, 1938.

Nikias Stavroulakis and Salomi in their wedding, Athens, Greece, 1958.

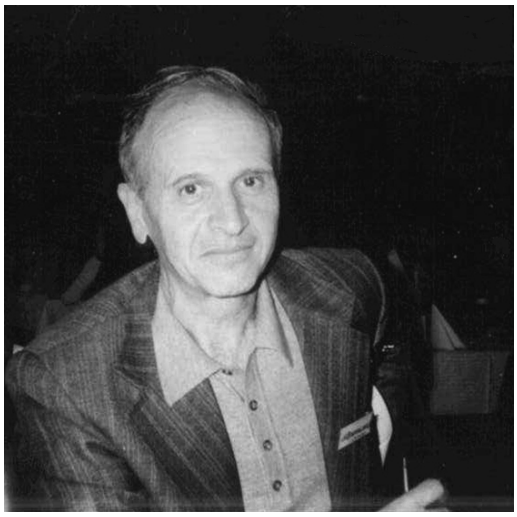

Prof. Nikias Stavroulakis on the 10th International Conference on General Relativity and Gravitation in Padova, Italy, July 4–9, 1983.

He was married to Salomi, who died four years earlier, with whom he had a daughter, Eleni.

Besides being a great, well published, voluminous and original scientist, Nikias Stavroulakis was always the polite man of principle and humility; seeking the truth and never being afraid to say "*we do not know yet*", when something was unknown, elusive or simply surmised.

Dr. Nikias Stavroulakis was Professor at Université de Limoges, Département de Mathématique, France, and Member of Faculté des Sciences de Limoges, U. E. R. des Sciences de Limoges and then Emeritus during his time of research in relativity and gravitation. He made an extensive and advanced contribution in:

1) the Birkhoff theorem in General Relativity;
2) the indiscriminate use of the polar coordinates, before knowing what the manifold in which we work is;
3) the static and dynamical field of a pulsating spherical mass;
4) the theory of black holes and the Big Bang theory.

Nikias Stavroulakis' publications on mathematical physics and General Relativity

1. A statical smooth extension of Schwarzschild's metric. *Lettere al Nuono Cimento*, 1974, v. 11, no. 8, 427–430.
2. Paramètres cachés dans les potentials des champs statiques. *Annales de la Fondation Louis de Broglie*, 1981, v. 6, no. 4, 287–327.
3. Mathématiques et trous noirs. *Gazette des mathematiciens*, Juillet 1986, no. 31, 119–132.
4. Solitons et propagation d'actions suivat la relativité générale. (Premième partie). *Annales de la Fondation Louis de Broglie*, 1987, v. 12, no. 4, 443–473.
5. Solitons et propagation d' actions suivat la relativité générale. (Deuxième partie). *Annales de la Fondation Louis de Broglie*, 1988, v. 13, no. 1, 7–42.
6. Sur quelques points de la theorie gravitationnelle d'Einstein. *Tiré à part de Sinsularité*, Lyon, France, Aout–Septembre 1991, v. 2, no. 7, 4–20.
7. Particules et particules test en relativité générale. *Annales de la Fondation Louis de Broglie*, 1991, v. 16, no. 2, 129–175.
8. Sur la function de propagation des ébranlements gravitationnels. *Annales de la Fondation Louis de Broglie*, 1995, v. 20, no. 1, 1–31.
9. On the principles of general relativity and the SΘ(4)-invariant metrics. *Proceedings of the 3rd Panhellenic Congress of Geometry*, Athens, Greece, 1997, 169–182.
10. Vérité scientifique et trous noirs (première partie). Les abus du formalisme. *Annales de la Fondation Louis de Broglie*, 1999, v. 24, no. 1, 67–109.
11. Vérité scientifique et trous noirs (deuxmième partie). Symétries relatives au groupe des rotations. *Annales de la Fondation Louis de Broglie*, 2000, v. 25, no. 2, 223–266.
12. Vérité scientifique et trous noirs (troisième partie). Équations de gravitation relatives à une métrique Θ(4)-invariante. *Annales de la Fondation Louis de Broglie*, 2001, v. 26, no. 4, 605–631.
13. Vérité scientifique et trous noirs (quatrième partie). Determination de métriques Θ(4)-invariantes. *Annales de la Fondation Louis de Broglie*, 2001, v. 26, no. 4, 743–764.
14. Matière cachée et relatitité générale. *Annales de la Fondation Louis de Broglie*, 2001, v. 26, no. spécial, 411–427.
15. On a paper by J. Smoller and B. Temple. *Annales de la Fondation Louis de Broglie*, 2002, v. 27, no. 3, 511–521.
16. Non-Euclidean geometry and gravitation. *Progress in Physics*, 2006, v. 2, 68–75.
17. On the propagation of gravitation from a pulsating source. *Progress in Physics*, 2007, v. 2, 75–82.
18. On the gravitational field of a pulsating source. *Progress in Physics*, 2007, v. 4, 3–8.
19. Gravitation and electricity. *Progress in Physics*, 2008, v. 2, 91–96.
20. On the stationary charged spherical source. *Progress in Physics*, 2009, v. 2, 66–71.
21. General Relativity and black holes. *The Hellenic Mathematical Review*, January–June 2009, no. 71, 43–83 (*in Greek*).
22. On the field of a spherical charged pulsating distribution of matter. *Progress in Physics*, 2010, v. 4, 72–77.

Submitted on July 20, 2010 / Accepted on August 22, 2010

Progress in Physics **is an American scientific journal on advanced studies in physics, registered with the Library of Congress (DC, USA): ISSN 1555-5534 (print version) and ISSN 1555-5615 (online version). The journal is peer reviewed and listed in the abstracting and indexing coverage of: Mathematical Reviews of the AMS (USA), DOAJ of Lund University (Sweden), Zentralblatt MATH (Germany), Scientific Commons of the University of St. Gallen (Switzerland), Open-J-Gate (India), Referential Journal of VINITI (Russia), etc.** ***Progress in Physics*** **is an open-access journal published and distributed in accordance with the Budapest Open Initiative: this means that the electronic copies of both full-size version of the journal and the individual papers published therein will always be acessed for reading, download, and copying for any user free of charge. The journal is issued quarterly (four volumes per year).**

Electronic version of this journal:
http://www.ptep-online.com

Postal address: Department of Mathematics and Science, University of New Mexico, 200 College Road, Gallup, NM 87301, USA

Printed in the United States of America

ISSN 1555-5534

9 771555 553907 >